Hydroformylation of High Temperature Fischer -Tropsch Synthol Products for the Production of Detergent Alcohols

By

Mark Justin Betts

Thesis Presented for the Degree of

DOCTOR OF PHILOSOPHY

in the Department of Chemical Engineering

UNIVERSITY OF CAPE TOWN

September 1996

Hydroformylation of High Temperature Fischer -Tropsch Synthol Products for the Production of Detergent Alcohols

By

Mark Justin Betts

Thesis Presented for the Degree of

DOCTOR OF PHILOSOPHY

in the Department of Chemical Engineering

UNIVERSITY OF CAPE TOWN

August 1996

Acknowledgements

I would like to thank the following persons and institutions:

Thanks to my supervisor, Professor Mark Dry originally from Sasol and now from the University of Cape Town for initiating this project. This study would not have been possible without him. His time and effort, insights, attention to detail and guidance are greatly appreciated.

The project would also not have been possible without the support of Sasol. In this regard, my sincerest gratitude to the management of Sastech Research and Development under the leadership of Dr Arie Geertsema for the opportunity to undertake this study. I especially appreciate your confidence in me.

A special thanks to Dr Leon Ferreira of Sastech who facilitated this study. He and Dr Keith Lawson were particulary supportive throughout this exercise.

Thanks also to my work colleagues under the leadership of Dr Keith Lawson for their inputs in technical discussions. These persons include Dr Jannie Scholtz, Dr Sybren Kindermans, Judith du Toit, Morgan Naidoo, and Marina Hop. Special thanks go to Sybren and Judith for help with various analyses. Jannie's thoughts and inputs were especially helpful with regards to modelling of various experimental data. His combination of mathematical, engineering and computer skills are a big asset to Sasol.

It should be mentioned at the outset that the continuous reactor is in fact a mini pilot plant, and was not all my own work. Special acknowledgements with regard to the continuous unit go to Dr Keith Lawson and Marina Hop who were instrumental in its design and commissioning. Alan Mather co-ordinated the construction of the system. A combined effort was often required to keep the unit operating 24 hours a day and to generate the necessary data. Apart from my collegues already mentioned, Kobus van Eeden spent many hours "running" the unit, and his efforts are appreciated.

Thanks also to Dr Gerrie Rall, Ignus Potgieter, Karel Kriel, Dr Raphael Espinoza, Dr Peter van Berge and Dr Hein Strauss for useful technical exchanges.

Thanks to the "Sastech Library Ladies", especially Stephanie Roux, for their help in sourcing various literature. Although not always convinced that my requests were "not for private purposes", your efforts are appreciated.

Mohammed Rawat proved to have enormous powers of patience when it came to assigning "best hits" and provided invaluable assistance with MS peak identifications.

Thanks to Dr Klaus Möller of UCT for help with Biosym® representations of various catalyst complexes, and to Karien Coetzee of Sastech for help in generating the 3-D graphs.

Finally to my wife Adrienne, thank you for your patience and moral support. You inspired me to undertake this study. I therefore dedicate this thesis to you.

SYNOPSIS

The use of Synthol High Temperature Fischer-Tropsch (HTF-T) products as an inexpensive and alternative hydroformylation feedstock for producing Oxo alcohols has been investigated. These alcohols are precursors for biodegradable detergents.

The HTF-T product targeted as a feedstock source was Synthol Light Oil (SLO), in the C_8 to C_{12} range.

The aim of the work was to identify a suitable hydroformylation catalyst system for use with SLO feeds. Process variables such as feed composition, temperature, pressure and contact time were investigated. Emphasis was placed on the determination of feed-catalyst compatibility; the development of a "working" kinetic model on a batch micro-reactor scale; and extrapolation of the results to a continuous catalyst testing unit. An integral part of the work therefore involved characterization and quantification of these complex hydroformylation systems, as well as the development of methods to achieve this goal.

Hydroformylation of various SLO fractions in the C_8 to C_{12} range was undertaken. As a yardstick, the results were compared with those generated using pure 1-decene feed. The results obtained with pure feeds were duplicated, and in some cases improved upon when using SLO.

The C_{8-9}, C_9, C_{10} and C_{11-12} single and double carbon number SLO fractions tested were prepared by distillation. This, apart from caustic washing to remove carboxylic acids, was demonstrated as the only step required to produce suitable hydroformylation feeds. Minimal cleanup of the feed was facilitated by the apparent "inertness" of non-olefinic components in SLO. These consist of various aromatics, oxygenates and paraffins.

The olefins in SLO consist mainly of linear α-olefins, mono-methyl α-olefins and smaller quantities of internal olefins. Different olefin isomer distributions could be obtained by refractionation of the SLO. Feed, as well as resultant product compositions, could therefore be tailored according to the distillation procedures employed.

Phosphine modified hydrocarbonyl rhodium and cobalt hydroformylation catalysts were screened. These experiments were undertaken with a view to maximizing product linearity and establishing feed - catalyst compatibility. In this regard, TriPhenylPhospine (TPP) ligand was tested with Rh and Tri-n-ButylPhosphine (TBP) as well as TPP ligands were tested with Co. Various so called heterogeneous catalysts based on Co were unsuccessfully evaluated. The Rh/TPP and Co/TBP experiments were successful, but the Rh catalysts appeared more susceptible to poisoning.

It was demonstrated that the unique character of the olefin composition and distribution in the HTF-T fractions could be exploited in n-alkylphosphine modified Co systems. These catalyst systems facilitate isomerization of α-olefins to internal olefins and interchange between internal and α-olefins occurs rapidly. Despite this however, the aldehydes and alcohols produced are predominantly linear because of the higher rate of hydroformylation of the α-olefins. It was shown that more internal olefins undergo hydroformylation in pure linear feeds compared with SLO feeds. This may be explained due to the methyl-branched internal olefins in SLO being thermodynamically favoured, but also being less reactive for hydroformylation compared with linear internal olefins.

Because of the screening results, and the perceived difficulties in efficient recycling of Rh catalysts, further work concentrated on phosphine modified Co catalysts for the hydroformylation of SLO. This involved constant pressure "batch" experiments, and development of a system for quantifying olefins in the complex feeds.

Emphasis was placed on testing and comparing results obtained with a "conventional" n-alkylphosphine ligand and a bi-cyclic alkylphosphine ligand. The specific ligands under consideration were Tri-n-OctylPhosphine (TOP) and 9-Eicosyl-9-Phosphabicyclonane (EP).

The following "standard" reaction conditions were selected based on the screening experiment results, and using reports in the literature as a guideline:

Reaction temperature = 170°C; Pressure = 75 bar (g) constant; Syngas composition = 2:1 pure H_2:CO; Molar ratio of phosphine:Co = 2:1; Stirrer speed = 500rpm.

The kinetics of olefin consumption for both pure linear and HTF-T product feed olefins of a single carbon number were shown to be approximately first order with respect to the olefin concentration. The rate was directly proportional to the cobalt concentration. This first order relationship was relatively independent of the (methyl branched) : (linear) olefin ratio in the F-T feed. It was however demonstrated that longer olefins (for example C_{12}) reacted more slowly than shorter olefins (for example C_{11}).

A kinetic expression describing the effect of carbon number and catalyst concentration on the rate of olefin consumption was derived for the Co/EP catalyst system. This expression was expanded to include the effect of temperature as well as syngas composition and pressure.

Similar results were obtained with pure 2:1 H_2:CO syngas, commercial syngas from an existing F-T facility, as well as syngas that had a 14% CO_2 content. On varying the H_2:CO ratio in the syngas from 2:1 to 1:2 and the total pressure from

45 to 90 bar (g), it was evident that reactions undertaken at 75 bar(g) with a H_2:CO ratio of 2:1 were suitable for achieving high reaction rates coupled with satisfactory product linearity and catalyst stability.

The catalyst systems were shown to be sensitive to temperature. Temperatures of around 185°C and higher resulted in Co/EP catalyst deactivation with concomitant precipitation of cobalt. This was ascribed to disintegration of the catalyst complex. The selected "standard" operating conditions therefore appeared to be in the correct regime. Based on the results in this study, coupled to the reported results of other workers, a theory on the effect of temperature in Co hydroformylation systems was proposed. The onset of catalyst deactivation was linked to the reaction rate and temperature and this was quantified.

The hydroformylation activation energy (E_a) was calculated as being 99 kJ per mole for C_{10}, C_{11} and C_{12} olefins in SLO with the Co/EP catalyst. This value is similar to values reported by other workers, who used different feeds and catalysts. The high value of E_a indicates that the system was free of diffusion constraints.

The effect of an alkali modifier - namely potassium hydroxide (KOH) - was investigated for pure and HTF-T feeds. Contrary to reports in the literature, KOH did not appear to catalyse aldol condensation reactions with resultant heavy oxygenate formation at "standard" reaction conditions. Instead, the predominant heavier oxygenates were esters. These in turn were mostly formates formed as a result of CO incorporation into adsorbed aldehyde intermediates.

The effect of KOH on Co/EP systems was more marked compared with Co/TOP. For the Co/EP systems, the KOH resulted in slower rates of reaction and appeared to have a similar effect to that of increasing the EP:Co ratio.

A significant quantity of water (10%) in SLO was not deleterious to hydroformylation with a Co/TOP catalyst. Indeed, an improvement in the reaction kinetics was observed. Given the beneficial effects of caustic on phosphine modified hydroformylation systems, aqueous caustic washing of the feed with minimal drying of the feed may be facilitated.

Overall, the micro-reactor results indicated that the phosphine modified Co catalyst systems were relatively insensitive to the process changes. This is indicative of robust catalyst systems and good F-T feed-catalyst compatibilities. This "robustness" appeared to be more marked in the Co/TOP system compared with Co/EP. However, the Co/EP catalyst gave markedly better results in terms of rates and selectivities. This was achieved without sacrificing product linearities.

In order to quantify the performance in a continuous reactor system, a kinetic model was developed based on proposed reaction pathways. Micro-reactor data was used to develop and test the model. The model incorporated not only an expression for olefin consumption but also reactions occurring in sequence and in parallel to hydroformylation. These reactions are hydrogenation of olefins, hydrogenation of aldehydes and formation of esters.

The model could be successfully applied to all the micro-reactor experimental data for the phosphine modified Co experiments undertaken at constant pressure.

A continuous reactor run with Co/EP and a C_{11-12} SLO feed was performed. The kinetic model was successful in predicting the performance of the larger continuous reactor system with respect to conversions and quantities of components in the various streams. Furthermore, continuous operation was performed for extended periods of time (up to 60 days) which further demonstrated satisfactory feed-catalyst compatibility.

In addition to the above findings, the following general points regarding the suitability of Synthol products, and specifically SLO, became evident during the course of the work:

- By combining the F-T and Oxo Syntheses, syngas is the only raw material required for producing higher aldehydes and alcohols.
- The fact that sulphur containing compounds are strongly adsorbed onto F-T catalysts, means that hydroformylation feedstocks are essentially sulphur free.
- Unique hydroformylation products are obtained, based on the characteristics of olefins in F-T products. These are linear and mono-methyl α-olefins. The methyl groups are attached at any one position along the linear backbone of the α-olefin molecule.
- In contrast, when using conventional feedstocks for hydroformylation, the only mono-methyl products that can form, are of the 2-methyl variety.
- The inert components present in the F-T feed can act as combination of a built-in solvent and coolant. This so called solvent does not require recycling since it has alternative synthetic fuel value.
- Hydroformylation of the olefins in the F-T fractions is an efficient way of both separating them from other F-T components, which may otherwise be difficult, whilst at the same time converting them to a still more valuable product.
- The higher and lower molecular weight alcohol products obtained from HTF-T feeds may be suitable for the production of biodegradable surfactants and plasticizers.

The feasibility of combining the F-T and Oxo Syntheses has been demonstrated, and may be suitable for industrial application. Given the large synfuels industry in South Africa, the work demonstrates a process and an opportunity to further beneficiate natural gas and coal reserves in this country.

TABLE OF CONTENTS

APPENDICES

LIST OF FIGURES

LIST OF TABLES

NOMENCLATURE

AE	Alcohol Ethoxylates
alc.	alcohol
ald.	aldehyde
APE	Alkyl PhenolEthoxylate
AS	Alcohol Sulphate
ASCII	American Standard Code for Information Interchange
ASF	Anderson-Schulz-Flory (polymerization model)
atm.	Atmosheres (unit of pressure)
bis-PPB	bis-diPhenylPhosphinoButane $(C_6H_5)_2P(CH_2)_4P(C_6H_5)_2$
br.	branched
C	Fractional conversion
CFB	Circulating Fluidized Bed
conv.	conversion
Co/P	General term describing phosphine modified Co hydrocarbonyl catalysts.
Co/TBP	TBP modified Co hydrocarbonyl catalyst
Co/TPP	TPP modified Co hydrocarbonyl catalyst
Co/EP	EP modified Co hydrocarbonyl catalyst
Co/TOP	Tri-n-OctylPhosphine modified Co hydrocarbonyl catalyst
Conv.	Conversion
C_x	Carbon number = x
EDAX	Energy Dispersive Analysis of X-rays
E_a	Activation Energy
EP	a mixture of: 9-Eicosyl-9-Phospha (3,3,1) bicyclononane (60%)and 9-Eicosyl-9-Phospha (4,2,1) bicyclononane (40%). $C_8H_{14}P(CH_2)_{19}CH_3$
f	Dilution Factor
F-T	Fischer-Tropsch

FAM	Fatty Alkanolamide
FAO	Fatty Amine Oxides
FID	Flame Ionization Detector
(g)	gauge
GC	Gas Chromatogram / Gas Chromatography
HOF	Heavy Oxo Fraction
HTF-T	High Temperature Fischer-Tropsch
ICP	Inductively Coupled Plasma
int.	internal
k	First order rate constant describing olefin consumption
k'	First order rate constant (k) corrected for cobalt concentration
L	Ligand
LAS	Linear Akylbenzene Sulphonate
M	Metal
M:L	Metal:Ligand molar ratio
M_x	Mass fraction of component x
MS	Mass Spectrometry
MW	Molecular Weight
ole.	olefin
Oxo	Hydroformylation
P	Phosphine
$P\text{-i-}Pr_3$	Triisopropylphosphine $P(CCH_3)_3)_3$
$P\text{-n-}Pr_3$	Tri-n-propylphospine $P((CH_2)_2CH_3)_3$
$P\text{-n-}Oct_3$	Tri-n-octylphosphine (=TOP $P((CH_2)_7CH_3)_3$)
PPh_3	Triphenylphosphine (=TPP $P(C_6H_5)_3$)
PPh_2Et	Diphenylethylphospine $P(C_6H_5)_2(CH_2CH_3)$
$PPhEt_2$	Monophenyldiethylphosphine $P(C_6H_5)(CH_2CH_3)_2$
PBu_3	Tri-n-butylphosphine (=TBP $P((CH_2)_3CH_3)_3$).
P_f	Final Pressure
P_i	Initial Pressure

$PØ_3$	Triarylphosphine (=triphenylphosphine)
ppb	parts per billion (or milligrams per 1000 liters)
ppm	parts per million (or milligrams per liter)
PR_3	Linear Alkylphosphine
Rh/TPP	TriPhenylPhosphine modified Rh hydrocarbonyl catalyst
RHO	Aldehyde
ROH	Alcohol
rpm	revolutions per minute
SAS	Sasol Advanced Synthol (reactor)
Sel.	Selectivity
SEM	Scanning Electron Microscopy
SLO	Synthol Light Oil
t	Reaction time (hours)
TBP	Tri-n-ButylPhosphine $P((CH_2)_3CH_3)_3$
TCD	Thermal Conductivity Detector
TOP	Tri-n-OctylPhosphine $P((CH_2)_7CH_3)_3$
TOS	Time On Stream
TPP	TriPhenylPhosphine $P(C_6H_5)_3$
TPPite	TriPhenylPhosphite $P(OC_6H_5)_3$
TPPMS	TriPhenylPhosphine MonoSulphonate
(tr.)	trace amount
UV-VIS	Ultra-Violet Visible

CHAPTER 1

INTRODUCTION

1 INTRODUCTION

1.1 LINEAR ALCOHOLS FOR THE PRODUCTION OF DETERGENTS

1.1.1 The Current World Detergent Business

Today, most petrochemical based alcohols, also known as synthetic alcohols are produced by hydroformylation of olefins. This process is also termed the "oxo synthesis". These "oxo alcohols" are used as precursors for various plasticizers and detergents. Typically, $C_{4\text{-}10}$ oxo alcohols are used in plasticizers, and oxo alcohols with carbon numbers in the $C_{11\text{-}15}$ range are used in detergents. The estimated world production capacity (based on 1995 figures) of these synthetic alcohols is approximately 6600 kilotonnes per annum (kt/a) [Beller et al., 1995] of which detergent range alcohols constitute around 20%. Around 75% of these detergent range alcohols are manufactured by hydroformylation which represents about 1000 kt/a. The balance (25%) are manufactured using modified Ziegler polymerization technology. Prices for synthetic detergent alcohols range between 1100 to 1250 US$ per ton. This represents an approximate annual turnover of between 1020 and 1160 million US$ for these products. It is therefore obvious that hydroformylation technology and hydroformylation feedstocks for detergent range alcohols are of great industrial and commercial significance.

The estimated traded volumes of around 90kt/a for α-olefins (C_{10} and higher) used as detergent range alcohol precursors compares with a value of 1000 kt/a for synthetic detergent alcohols. It is therefore evident that traded higher alpha olefins constitute a small portion of current detergent range alcohol feedstocks. This may be ascribed to the fact that most producers of higher synthetic alcohols use ethylene or paraffins as starting materials and produce their own higher olefins. In addition, oleochemical based alcohols constitute a significant portion of the detergent alcohol market ($\geq$50%). Existing commercial routes to detergents are illustrated by way of a flow diagram in Figure 1.1.

Figure 1.1 Current commercial routes to surfactants: Tracing detergent components back to their raw materials.

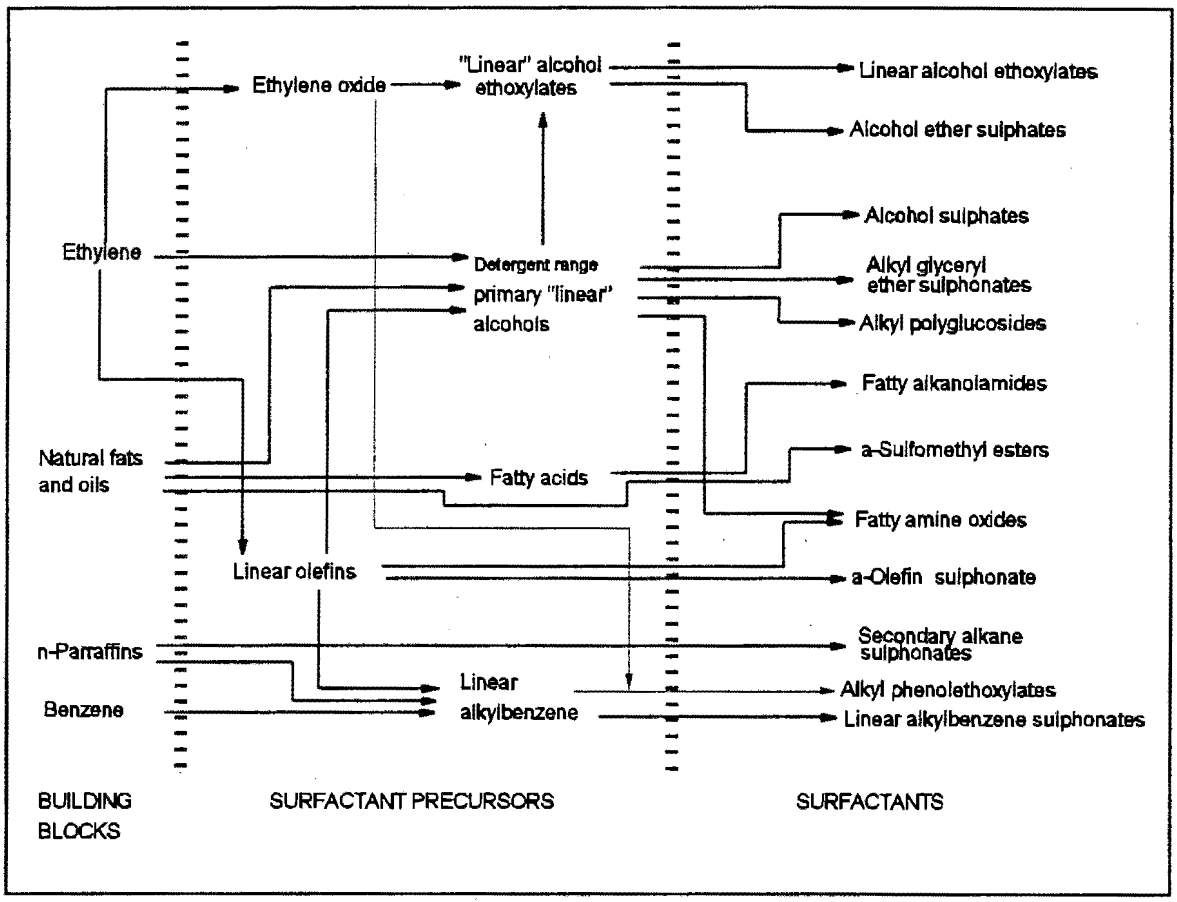

Source: C&EN [Thayer, 1993]

The current state of affairs in the detergent business has been outlined recently in a product report on soaps and detergents in "Chemical and Engineering News" [Ainsworth, 1995].

The report indicates that producers of surfactant intermediates (see Figure 1.1) are under pressure due to the current trend of increasing cost of key raw materials such as ethylene ,coconut oil and palm oil. This has occurred in the face of continued demand for low prices by their customers, namely the soap and detergent formulators and manufacturers, as well as consumers. Ways in which surfactant suppliers can stay ahead is by developing new technologies, products and by process improvements. An important new consideration in the detergent scenario is the potential move by the Department of Energy in the US to require the use of more energy efficient technology in washing machines. According to the C&EN report, the new washing machines will most likely favour the substitution of anionic surfactants such as Linear Alkylbenzene Sulphonate (LAS) with nonionic surfactants such as linear alcohol ethoxylates which produce less foam.

The report goes on to state that although earnings in the surfactant manufacturing sector are currently weak, there will be continued growth in the demand for nonionic surfactants, based on US forecasts. In household detergents, this growth is expected to be in the region of 3.4% per annum from 1993 through to 2005. Anionics are expected to maintain their market share for this period.

An additional important factor that may influence the detergent markets in future is the way that aromatic containing surfactants derived from linear alkylbenzene are viewed by consumers. Benzene and "environmentally friendly" are generally viewed as incompatible terms. Since Linear Alkylbenzene Sulphonates (LAS) and Alkyl Phenol Ethoxylates (APE) constitute the major segments of the detergent market, as indicated in Figure 1.2, it is conceivable that a change in attitude by consumers resulting in a preference for alternative nonaromatic products would result in enormous growth of α-olefin and oxo-alcohol derived products. APE, especially has been regarded as being troublesome to the environment as it interferes with fish breeding patterns [Vines, 1995]. New and alternative sources of raw materials for these products would have to be sought.

Heavy duty surfactants account for the largest portion of use by industrial, oil field, institutional and industrial cleaners, and household end users. A breakdown of how households in the USA use surfactants in Figure 1.3 shows that heavy duty detergents do take up the largest share of the surfactants business.

Figure 1.2 A breakdown of surfactant consumption in North America: Comparison between market segment allocation of heavy duty surfactants and total surfactant end use application.

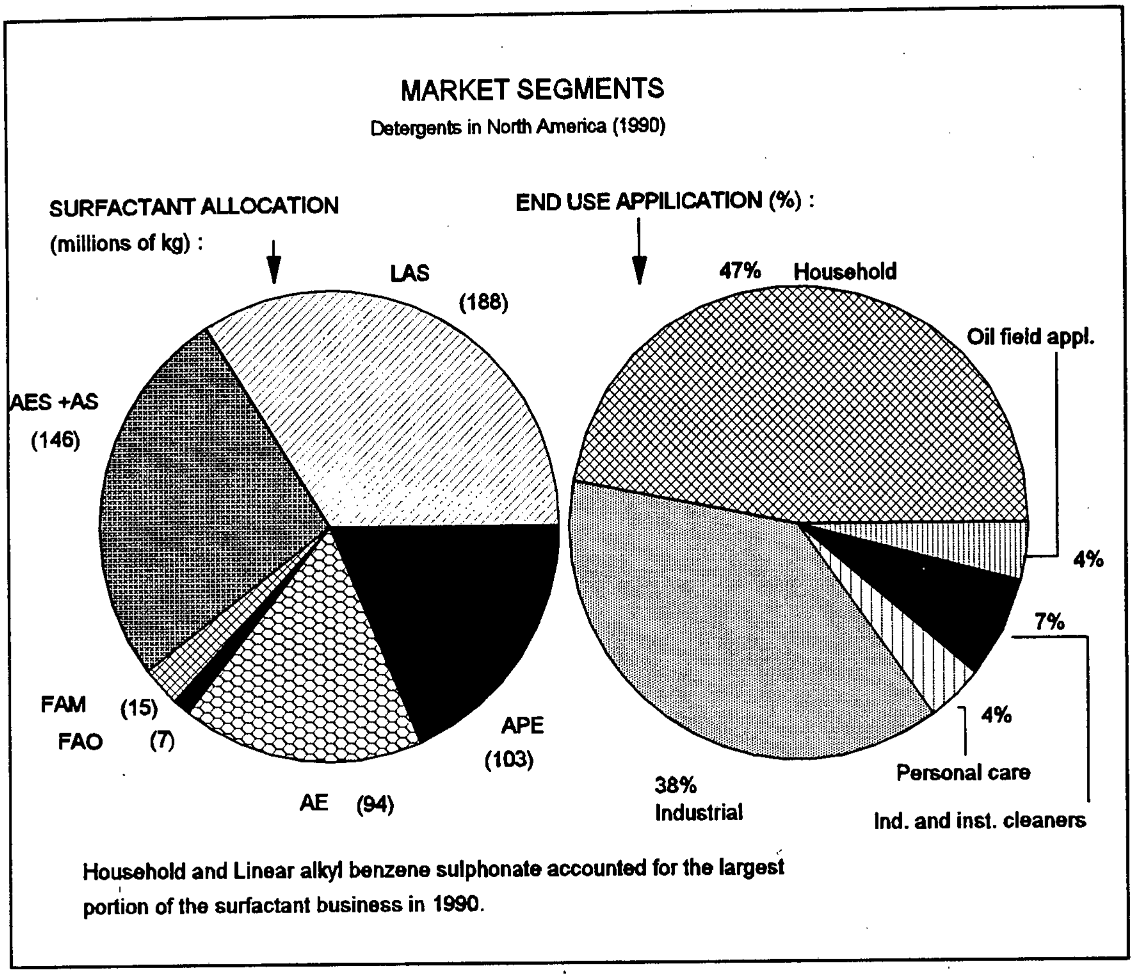

Source: *C&EN* [Thayer, 1993]

The following list of abbreviations apply to the heavy duty surfactant allocation in Figure 1.2 above.

LAS: Linear alkylbenzene sulphonate

APE: Alkyl phenol ethoxylates

FAM: Fatty Alkanolamides

FAO: Fatty amine oxides

AES: Alcohol ether sulphates

AS: Alcohol sulphates

AE: Alcohol ethoxylates

Figure 1.3 A breakdown of US household detergent consumption.

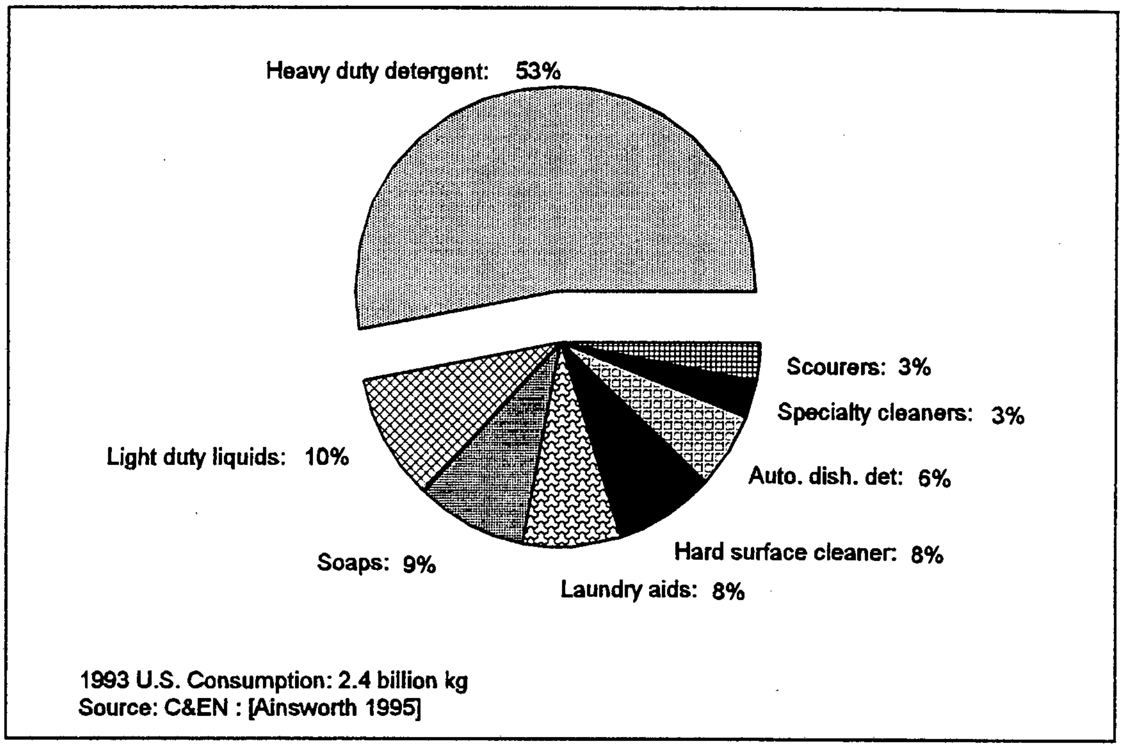

1993 U.S. Consumption: 2.4 billion kg
Source: C&EN : [Ainsworth 1995]

An important topic in the detergent business is the ongoing and often emotional debate surrounding petrochemical versus oleochemical raw material feedstocks. Manufacturers of products based on oleochemicals have argued that their products are more environmentally friendly than products derived from petrochemical feedstocks. They claim this is because their products are more linear in hydrocarbon structure and they are based on renewable fats and oils. The often emotive use of the word "natural" has been associated with oleochemical based detergents and soaps in advertisements to consumers. However, improvements in the analysis and tracing of detergents, and their decomposition products or the so called science of "life cycle analysis" is shedding more light on the environmentally friendliness of raw materials used in soaps and detergents [Ainsworth, 1995]. It may be argued that large scale farming for the production of oleochemicals, with the associated use of fertilizers, possible soil erosion, as well as natural vegetation and habitat destruction is environmentally unfriendly. The natural based oleochemicals are subjected to chemical processing as are petrochemical based raw materials. The above considerations have probably resulted in a shift in the move towards favouring oleochemical feedstocks in 1992 and 1993, with an equilibrium being reached in 1994. The current split between oleochemical and petrochemical derived fatty alcohol capacity is approximately 50:50, but with a premium still being paid for linear products.

From the above discussion it is obvious that trends in the surfactant market do warrant a look at an alternative route to production of biodegradable and predominantly linear alcohol derived surfactants. Fisher-Tropsch (F-T) products obtained from coal and natural gas are currently not utilized for this purpose. A detailed investigation for using predominantly linear F-T products as a feedstock, and specifically a hydroformylation feedstock for this purpose, is hence of commercial interest.

1.1.2 Conventional Olefin Feedstocks for Producing Linear Alcohols.

The commercial processes used for the production of predominantly linear oxo olefin feedstocks are outlined below [Demianiw, 1981]. Higher olefins manufactured by oligomerizing propylene and/or butenes are highly branched which results in highly branched oxo alcohols. These are undesirable from an environmental point of view as they in turn give rise to products having poor biodegradability.

1. Thermal and catalytic cracking of petroleum wax or n-paraffins: This results in a wide range of carbon numbers being produced.

2. Oligomerization of ethylene: Companies such as Exxon, Ethyl, Gulf and Shell have oligomerization processes for manufacturing even numbered linear alpha

olefins in the C_{6-20} range. These technologies are primarily based on the use of Ziegler-Natta type catalyst systems. The exception is Shell, which use a process based on non-Ziegler chemistry [Freitas and Gum, 1979].

3. Chlorination followed by dechlorination of n-paraffins: This process results in linear internal olefins . It was originally employed by Shell, but is not believed to be commercial at present.

4. Catalytic dehydrogenation of n-paraffins: The Universal Oil Products company (UOP) markets technology for the production of detergent range linear internal olefins known as the PACOL-OLEX ® process.

5. Shell Higher Olefins Process (SHOP). This involves using C_4 and C_{16+} α-olefins from ethylene oligomerization, isomerizing them to internal olefins and subsequently disproportionating them to internal olefins of different chainlengths using the metathesis reaction. The desired detergent range olefins, typically in the range C_{11-14}, are recovered by distillation. The light and heavy ends are recycled to extinction in the process. Aspects of ethylene polymerization and oligomerization and the SHOP have been patented and reported by Keim *et al.* [1971, 1972, 1984], Morris *et al.* [1971], Glockner *et al.* [1971], Singleton *et al.* [1972] and Bauer *et al.* [1972] and reviewed by others [Spitzer, 1981][Nieuwenhuis, 1980].

1.1.3 Fischer Tropsch Products : An Alternative Hydroformylation Feedstock

Since the cost of the olefin feedstock is probably the single most important factor in determining the cost of producing oxo alcohols, any improvement in this area would be advantageous.

The price of gasoline and diesel fuel payed by consumers at filling stations in the Republic of South Africa currently (November 1995) is approximately R2.51 and

2.29 per kg whilst the price of detergent alcohols is about R4.38 per kg. Since a large portion of fuels in South Africa are obtained from hydrogenated olefinic Fischer-Tropsch product, an opportunity exists to add significant value to F-T products if they could be used directly as a hydroformylation feedstock.

The way in which F-T products can be incorporated into existing pathways to detergent and plasticizer alcohols is illustrated in Figure 1.4. Olefins which are conventionally used as hydroformylation feedstocks for predominantly linear higher alcohols, are obtained by processing of a primary product which involve additional step/s compared with using F-T products directly.

An additional advantage when using F-T products directly has to do with sulphur. Sulphur containing compounds are poisons of expensive oxo catalysts [Macho, 1961][Tummes *et al.*, 1976, 1981][Cornils and Förster, 1973][Falbe, 1970, 1980]. Sulphur compounds are absent in F-T products because F-T catalysts based on iron, or cobalt, are poisoned by S-compounds and are therefore removed from the F-T syngas. In the case of iron catalyzed F-T processes using syngas obtained by coal gasification, as practised by Sasol, this is achieved by scrubbing the syngas in a Rectisol process [Dry, 1981]. Any residual sulphur would be trapped by the F-T catalyst. Depending on the source of the primary syngas, F-T product streams may therefore represent primary products to be used directly in an oxo process.

In the review of the literature, there have been references that olefins produced by F-T synthesis <u>may</u> be suitable as a hydroformylation feedstock [Falbe, 1977] [Hargis, 1981] [Schulze, 1977]. However, no work has been reported on the direct use of F-T products, and specifically not F-T products produced over an iron catalyst, as a hydroformylation feedstock. This forms the basis of this study, and is expanded upon to include the selection and investigation of a suitable catalytic process for the hydroformylation of these feeds.

Figure 1.4 Cascaded flow diagram of existing commercial process routes to higher alcohols: **F-T from coal** (and natural gas) is **superimposed**.

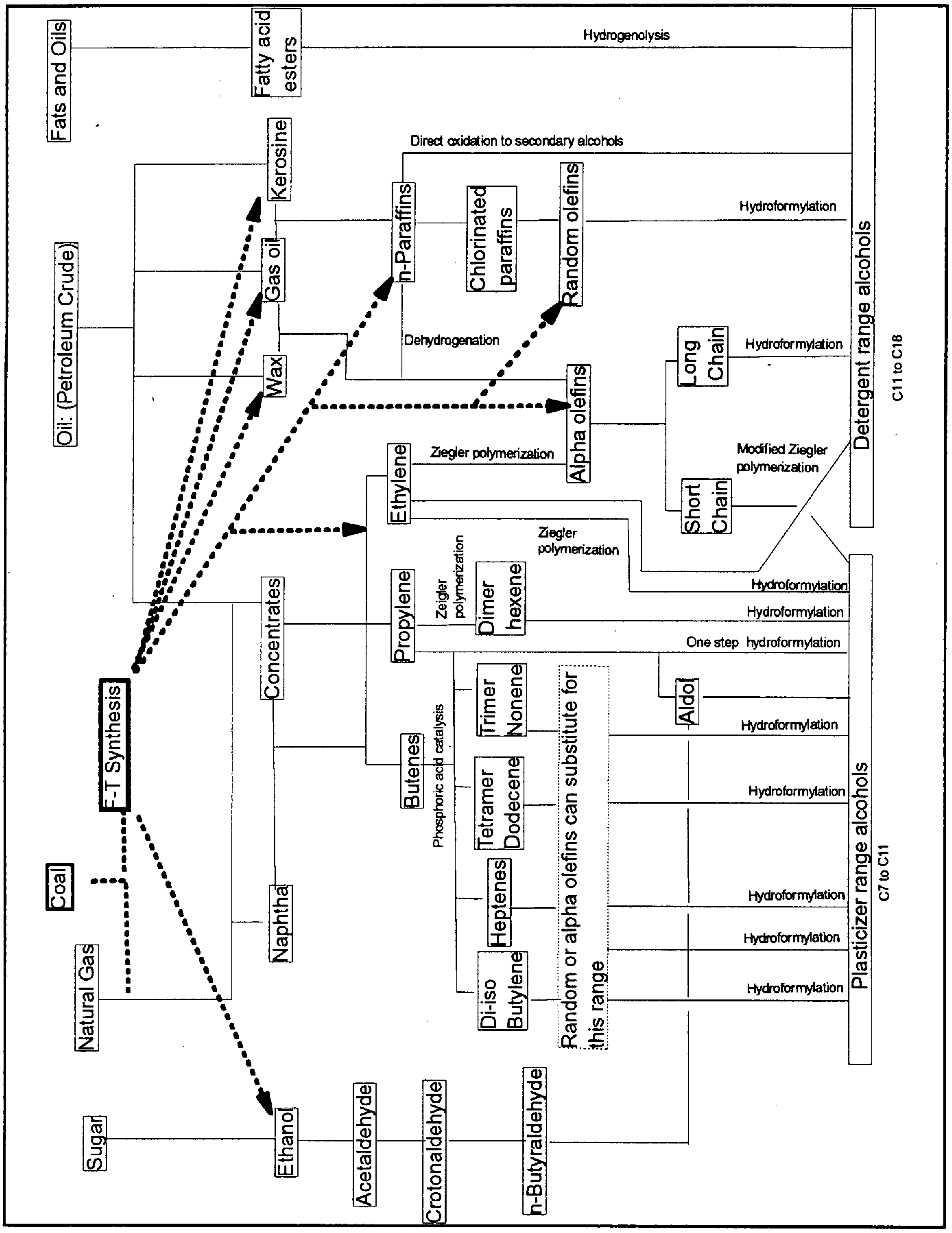

As far back as 1977, Schulze [Schulze, 1977] considered the economic possibility for the production of chemical feedstocks from coal. He argued that the F-T synthesis may be advantageously employed for the production of detergent feedstocks. Specific emphasis was placed on the production of the component in the surfactant business then occupying the largest market share, namely alkyl benzenesulphonates . According to Schulze, in the early 1970's this surfactant constituted two thirds of the anion active detergent market, which in turn constituted two thirds of all surfactant production. These alkyl benzenesulphonates were originally manufactured from "kogasin" F-T products which was the term then used to describe the $C_{10\text{-}18}$ F-T fraction. According to Schulze, these initial surfactants were biodegradable. However, closure of the German F-T plants resulted in their replacement with cheaper but less biodegradable branched dodecylbenzene produced via the tetramerization of propene. These highly branched surfactants, were subsequently phased out due to their environmentally unfriendly label. n-Paraffins, obtained from molecular sieving of oil, were then used as an olefin feedstock for benzene alkylation to produce linear alkylbenzene sulphonates (LAS). According to Schulze, the production of other surfactants namely α-olefin sulphonates, paraffin sulphonates, and fatty alcohols could be possible from F-T products, although this was not as an attractive option as LAS, because of limiting market factors at the time, such as areas of application and unsatisfactory feedstock situations.

Following Roelen's discovery of hydroformylation while he was researching the F-T reaction [Falbe, 1970], no follow up work on combining F-T and Oxo processes has been reported. This may largely be due to the fact that the use of F-T technology to produce hydrocarbon feedstocks as an alternative to oil waned in the 1950's following the discoveries of large oil deposits in the Middle East [Dry, 1981]. For many years Sasol in South Africa was the only company to operate large scale F-T plants based on iron catalysts. A license was sold to Mossgas to use Sasol Synthol technology for beneficiating natural gas to higher hydrocarbons in the early 1990's. More recently, Shell constructed a F-T plant in Malaysia for producing diesel fuel and waxes using a cobalt catalyst [Sie *et al.*, 1991]. However, F-T catalysts based on cobalt give rise to hydrocarbons having a lower olefinicity compared to iron [Dry, 1981] [Jager and Espinoza, 1995]. For this reason, direct use of olefin streams obtained from Co F-T systems are probably less attractive hydroformylation feedstocks. Although cracked wax is often referred to as an olefin feedstock for hydroformylation [Slaugh and Mullineaux, 1966, 1969], this may be construed as an indirect method of using F-T products as a hydroformylation feedstock. Apart from a recent report [Dry, 1993], the use of Synthol F-T products as a hydroformylation feedstock, has not been investigated by others.

Gregor [1990] stated that: "Unfortunately, there is no commercial process for separating a F-T product stream into distinct hydrocarbon and oxygenated components". However, UOP [Johnson and Raghuram, 1987] did propose a process whereby olefins may be beneficiated once oxygenates are removed using Olex® technology. The use of hydroformylation technology as a method of "beneficiating" these olefins is not mentioned.

1.2 FISCHER-TROPSCH (F-T) SYNTHESIS: GENERAL INTRODUCTION

Due to the industrial significance of the F-T process various reviews, on this topic exist [Storch *et al.* 1951][Anderson, 1953, 1956][Pichler, 1952][Dry, 1981,1996][Frohning *et al.*, 1982]. It was nevertheless considered appropriate to give a brief overview of this topic.

The Fischer-Tropsch Synthesis (abbreviated as F-T synthesis) is the general term describing the reaction of carbon monoxide and hydrogen or synthesis gas (syngas) to form a range of hydrocarbons and water. These hydrocarbons are characterized by the fact that they typically range from methane to solid products at room temperature; they may be olefinic and/ or paraffinic and/ or oxygenated to a degree.

The first CO hydrogenation reaction was reported in 1902 by Sabatier and Sendersons [1902] who produced methane from CO and H_2 over cobalt and nickel. BASF later used high pressures of syngas over a cobalt catalyst to produce liquid products in 1913 [BASF patent 1913].

It was not until the early 1920's when further work into the CO-hydrogenation was undertaken by two Germans, Franz Fischer and Hans Tropsch and interest in the subject was rekindled resulting in the F-T process. Fischer and Tropsch's [1923] initial work reported the production of hydrocarbons and oxygenated derivatives (then referred to as Synthol) using alkali treated iron shavings at around 400°C and >100 atm. Because of the high tendency toward oxygenate formation and rapid deactivation observed with this catalyst, further work in order to find a more viable catalyst was pursued. Zinc oxide was added to Fischer and Tropsch's original catalyst [Fischer and Tropsch, 1926], and lower reaction pressures were found to favour lower oxygenated hydrocarbon selectivity, but short catalyst lifetimes were still a problem. This led to the use of more expensive cobalt type catalysts which consisted mainly of Co, ThO_2, MgO and Kieselghur [Dry, 1981] (with relative mass units in the order of 100:5:8:200 respectively). Industrialization of the process followed in 1936 and found large scale application during World War II. The discovery by Pichler in 1936 [Pichler, 1939] that the lifetime of iron F-T catalysts is largely improved by the use of higher pressures contrasted with Fischer and Tropsch's findings and was not followed up by German firms during World War II. It was not until after the war that iron catalysts were used in commercial F-T plants.

Of the F-T plants in operation today, those owned and licensed by Sasol use iron-based catalysts. The Sasol High Temperature (HT) fluidized bed process for making synthetic fuels is known as the "Synthol Process". This should not be confused with the term "Synthol" first used by Fischer and Tropsch. Subsequently, the term "Synthol" has generally associated with, and accepted as describing, Sasol's High Temperature commercial F-T process. In order to clear up any discrepancy, hereinafter (and in the Thesis Title) the Synthol term is used only in the context of the Sasol HTF-T process.

1.2.1 Alpha olefins and Chemicals from F-T

Since F-T products, depending on the reaction conditions, may contain a variety of oxygenates, aromatics, paraffins (including paraffinic wax) and olefins, this technology is an alternative to oil based processes for producing chemicals and chemical feedstocks. A recent article by Ross [1995] indicates current perceptions in this regard. Selected portions of the article are rewritten in the following paragraph.

"Ever since the pioneering work of Fischer, Tropsch and Pichler on the indirect liquefication of coal, there has been a perception that a synfuels industry will compete with petroleum. This competition appears to be materializing, however not as much in the area of petroleum, but rather in the production of chemicals. Examples of this are that Sasol has become a major supplier of waxes by modifying some of their existing facilities in order to maximize wax production and quality. In the past this product was obtained from petroleum. In addition, Sasol has begun to supply polymerization grade 1-hexene and 1-pentene α-olefins to world markets. A major factor contributing to this has been the development of suitable separation technology to obtain the needed purity for these α-olefins. Although initial reports of these developments were met with scepticism by producers of similar products using ethylene based technology, it now appears that these "new" products appear to be displacing ones derived from petroleum based products. It is reported that the trend of beneficiating olefins from synfuels has extended to the olefins higher than C_6. This, however, will have to utilize sophisticated technology to separate internal and branched olefins from the linear α-olefins."

Mention is made that for the production of α-olefins, iron based catalysts appear to be favoured over cobalt and ruthenium containing catalysts which give rise to lower olefin content products. Ross goes on to say that "it appears that 65% or more of the products in the $C_{5\text{-}12}$ carbon number range are olefins, and the dominant fraction of these are α-olefins".

The use of iron and iron based F-T catalysts for manufacturing synfuels giving rise to high yields of α-olefins in the F-T process has been reported [Hargis, 1981][Soled, *et al.*, 1992][Fiato *et al.*, 1986, 1987]. Although there may be significant differences in the method of catalyst preparation and final composition of some of these catalysts, the general observation is that the olefin distribution and composition and yields reported do not constitute an improvement upon those obtained using the Sasol Synthol catalyst. Hargis [1981] of the Ethyl Corporation patented an iron titanate-alkali metal hydroxide F-T "catalyst for olefin production", in which it is stated that the olefins thus produced, and specifically those in the C_6 to C_{12} range "may be particularly useful in the synthetic chemical industry finding uses, for example as intermediates for alcohol synthesis and as detergents in lube oil and fuel compositions". No mention as to direct hydroformylation of the products is made by the author.

The work undertaken by Roelen [1938, 1943] may be construed as having been performed on a F-T feedstock, but this material would have been prepared over a cobalt based F-T catalyst. A literature survey undertaken for this study revealed that with the exception of a report by Dry [1993], no work has been undertaken on the direct hydroformylation of F-T products; and specifically on an iron based catalyst such as that used in the Sasol Synthol Process.

1.2.2 The Sasol Synthol Process

The Sasol Synthol process has been reviewed in some detail by Dry [Dry, 1981]. This description contains aspects of Dry's review as well as Schulz's description of the "Entrained Bed Synthesis" [Schulz, 1982] which is in essence also a description of the Sasol Synthol process.

A basic flow diagram of the Sasol F-T plant layout and description thereof may be useful in illustrating how the Synthol process is incorporated into the Sasol 2 and 3 plants - this is shown in Figure 1.5.

Raw syngas derived from coal gasification is cooled to remove water and heavier tar oils. These streams are processed further to yield valuable materials as indicated. Further cooling of the syngas removes the light naphtha. The raw syngas is then scrubbed with cold methanol (Lurgi Rectisol Process) which removes the sulphur compounds as well as the bulk of the CO_2. The purified syngas passes to a F-T process comprising Synthol reactors. The reactor products are cooled in the second separation stage to remove, by condensation, the oil, water and water soluble products from the reactor outlet gases. Light hydrocarbons (C_1 to C_6), methane, H_2 and CO_2 are separated in the gas separation stage. The methane may be reformed into synthesis gas and recycled to the Synthol process. Various oxygenates as indicated are recovered from the aqueous stream. The oil stream can be worked up to separate selected α-olefins as well as petroleum and diesel fuel.

1.2.3 Synthol Reactors

The Synthol Process utilizes Circulating Fluidized Bed (CFB) reactor technology. More recently, the CFB reactor technology has been improved upon at Sasol with the development of the Sasol Advanced Synthol (SAS) process [Jager *et al.*, 1990, 1991]. The MW Kellogg Company developed the first CFB reactors [McGrath, 1951]. Several modifications and process improvements led to commissioning of 3 scaled up versions (± 46m high) of the Kellogg CFB reactors at Sasol 1, and the development of the Sasol Synthol process. Further scale up of the reactors (with an approximate three-fold increase in capacity of the original CBF's at Sasol 1) and additional improvements to them superseded the commissioning of the Sasol 2 and Sasol 3 plants at Secunda, with each plant having 8 CFB reactors. A simplified schematic of a CFB reactor is shown in Figure 1.6.

Figure 1.5 Flow-scheme illustrating a Sasol plant incorporating the Synthol Process

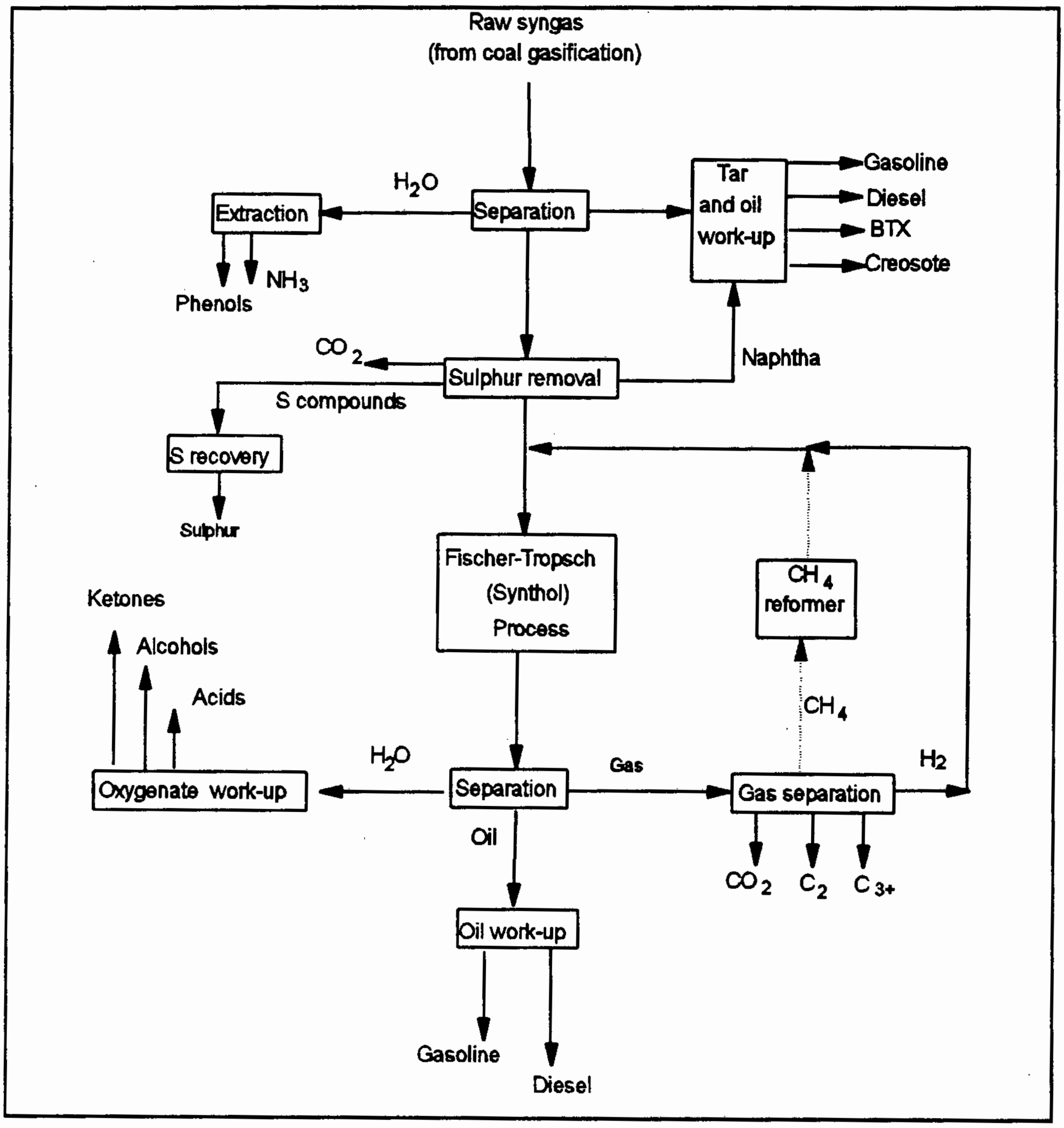

The fresh syngas and recycle gases are fed in at the bottom and come into contact with the finely divided catalyst. The catalyst becomes fluidized and moves up into the reaction zone. Between 30% and 40% of the heat of reaction is removed by heat exchangers in the reaction zone, the balance is absorbed by the product and recycle gases. Subsequent separation of the fine catalyst and gas occurs in cyclones designed for this purpose. The solid catalyst particles settle in a catalyst hopper before moving down a standpipe from which they are returned to the reaction zone. A slide valve regulates the amount of catalyst being re-introduced. Because the catalyst used is relatively cheap (iron based), it is normally replaced after about 1000 hours of use as a result of a decrease in the syngas conversion.

Typical ranges of operating condition in the Synthol reactors are as follows:
Temperature: Between 300 and 340°C.
Inlet syngas pressure: Between 22 and 30 bar (g).
H_2:CO ratio in the fresh feed: Between 1.8 and 2.2.

Figure 1.6 Schematic of a Sasol Circulating Fluidized Bed (CFB) reactor.

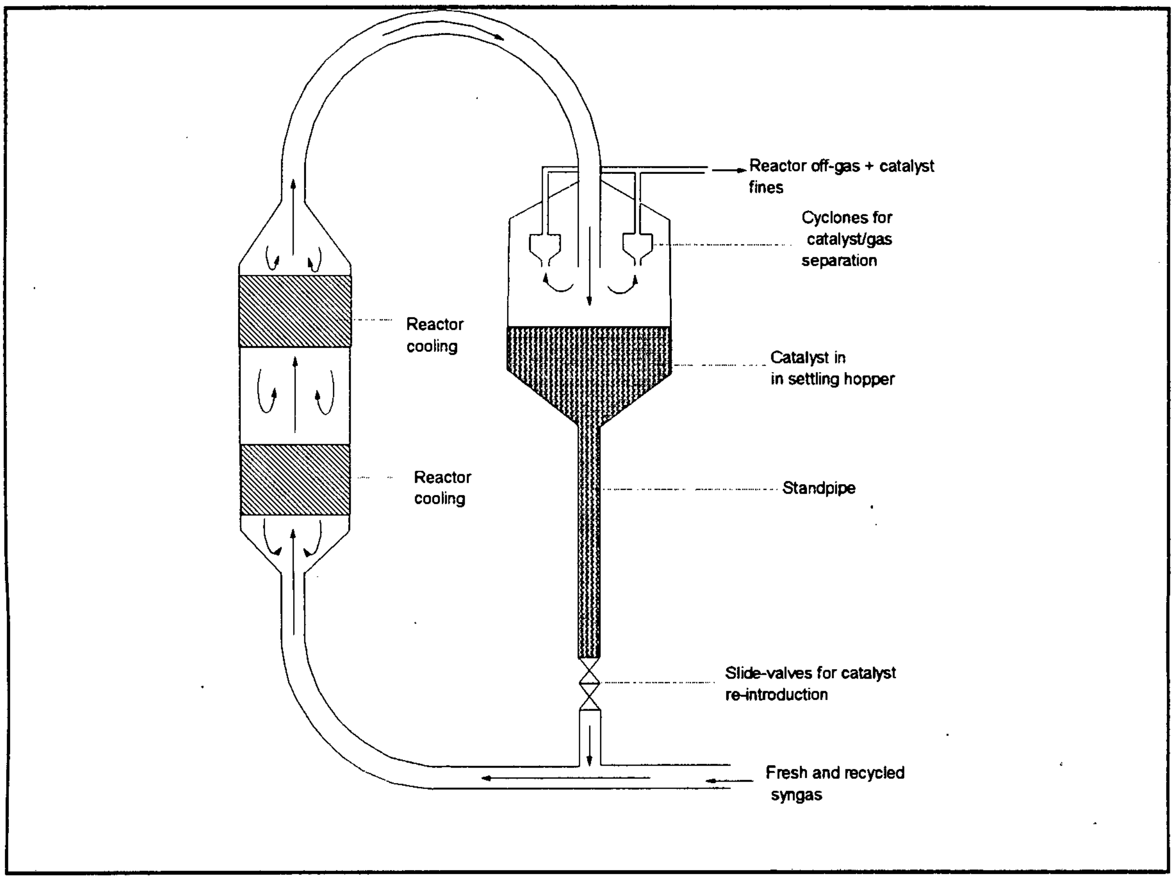

1.2.4 Synthol Catalyst

Exact details of the Synthol catalyst composition, and preparation are of a proprietary nature and therefore cannot be fully disclosed. However, the catalyst may be described in general terms as is the case in Dry's review [1981].

The catalyst of choice is based on fused iron prepared from iron oxide/s, preferably magnetite. The iron oxide is fused together in an electric arc furnace, with the desired amount of structural and chemical oxide promoters, into ingots. These ingots are crushed to give a desired particle size distribution which is suitable for fluidization and operability of the Synthol reactor catalyst-gas separation system. The crushed material is reduced in fluidized bed reduction units before being introduced into the Synthol reactors. Typical chemical promoters include oxides of potassium and sodium. These have a high "basicity" which result in the catalyst surface having a higher electron density which has important consequences on the surface intermediates and therefore product distribution. Structural promoters such as alumina increase the active iron surface area by incorporation into the solid-state structure and by inhibition of iron crystal growth. Various promoters fulfill both roles, for example Al_2O_3 has acidic characteristics and can offset some of the effect of the alkali, whilst Na_2O can go into solid solution with Fe-oxides. The ratio as well as content of the various promoters is therefore crucial.

1.2.5 Synthol Products

A typical GC trace of HTF-T reactor product is shown in Figure 1.7.

Figure 1.7 Gas chromatogram of HTF-T products .

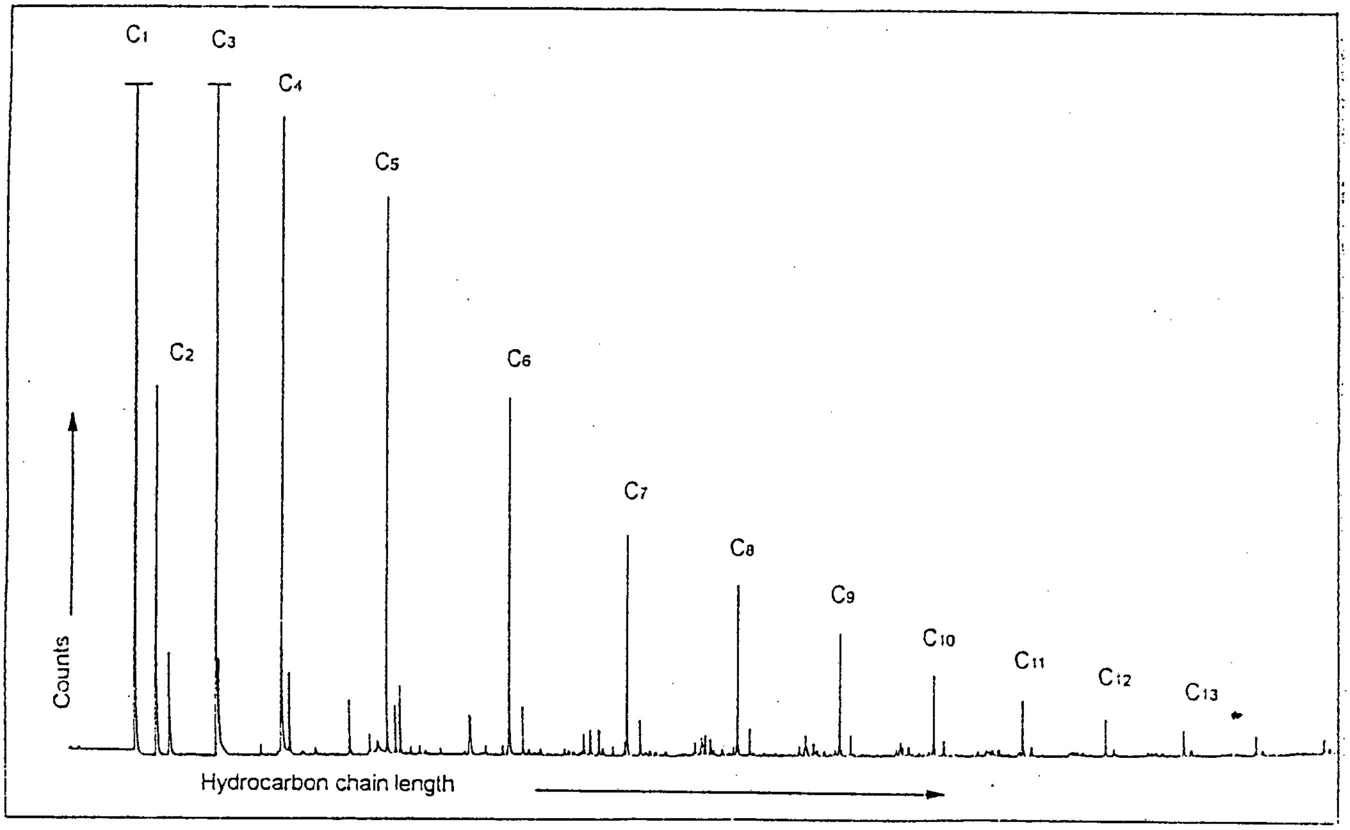

The predominant Fischer-Tropsch products from Synthol reactors are olefins. The higher olefins are predominantly linear and mono-methyl alpha olefins, with lesser quantities of linear and mono-methyl branched internal olefins. The balance of the F-T products consist of a range of aromatics and cyclic compounds, paraffins and oxygenates such as ketones, aldehydes, alcohols and carboxylic acids. The aldehydes and alcohols are predominantly primary and linear. The ketones are predominantly methyl ketones. These "non-olefinic" compounds are more evident in the region of "higher" carbon numbers. The increased complexity of the products for higher C_{number} or hydrocarbon chainlength fractions is demonstrated by Figure 1.8, which is a magnification of the diesel fraction.

Figure 1.8 Gas chromatogram of diesel containing fraction of HTF-T products.

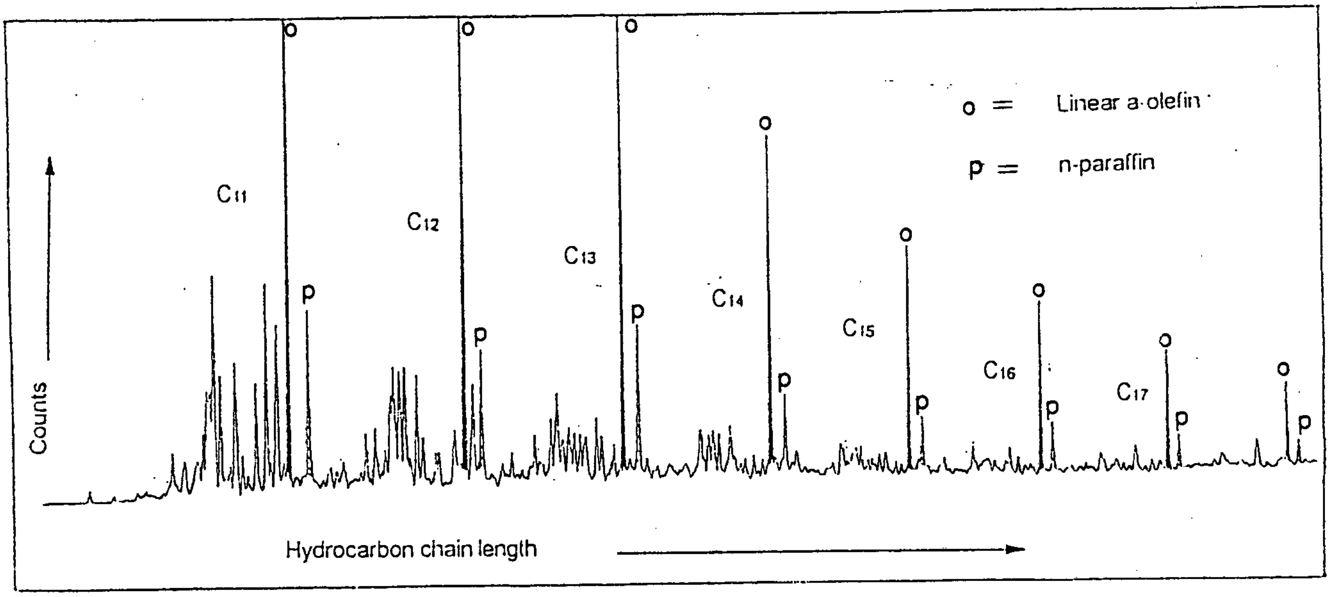

Table 1.1 Product Selectivities of Synthol Commercial Reactors [Dry, 1981]

Product	Product composition / % carbon atom Synthol at 325°C
CH_4	10
C_2H_4	4
C_2H_6	4
C_3H_6	12
C_3H_8	2
C_4H_8	9
C_4H_{10}	2
C_5 to C_{11} (gasoline)	40
C_{12} to C_{18} (diesel)	7
C_{19}+	4
Water soluble non-acid chemicals	5
Water soluble acid	1

Table 1.2 Synthol products: Breakdown of gasoline and diesel Synthol fractions by functional group [Dry, 1981, 1993].

Functional group	Approx. wt in product cut %	
	Gasoline: (C_5-C_{11})	Diesel: (C_{12}-C_{18})
Olefins	65	60
Paraffins	14	17
Aromatics	7	16
Alcohols	6	4
Ketones	6	2
Carboxylic acids	2	1

Examples of product selectivities of Sasol commercial reactors, as well as selected properties of the liquid and solid products have been reported [Dry, 1981], [Schulz, 1982]. These are listed in Tables 1.1 to 1.3. The gasoline and diesel fractions are particularly relevant as they represent the portion of the F-T product spectrum from whence hydroformylation feeds are derived in this study. The majority of olefinic and paraffinic and oxygenated products in both fractions are linear or are based on a linear hydrocarbon "backbone". Of the olefins, most of the branched olefins are mono-methyl branched α-olefins [Schulz, 1982], the balance are linear α-olefins with a smaller amounts of linear internals.

Pichler *et al.* [1968] analysed the C_4 to C_{17} F-T products obtained with cobalt and iron catalysts. The iron catalyst products were obtained from fixed and fluidized bed reactors at Sasol. The methodology employed by Pichler *et al.* was to hydrogenate the F-T products, thereby simplifying the GC spectra. Comparisons of F-T product spectra before and after hydrogenation facilitated quantification and identification of F-T components. More specifically, an improvement in differentiating between olefins and paraffins was facilitated. Dry [1981] summarized Pichler *et al.*'s findings in his F-T review, as shown in Table 1.3. In Table 1.3 the balance of the components in each carbon number fraction comprises a mixture of oxygenates and aromatics. From the olefin distribution in each of the carbon numbers in Table 1.3, it is evident that the olefins from the fixed bed iron catalyst could be the most suitable for use as a hydroformylation feedstock if linear products are the main objective. However, hydroformylation yield maximization is also important. The fixed bed iron reactor is geared to wax production and therefore makes less olefins in the detergent range.

Table 1.3 Summary of F-T product components for various carbon numbers (weight%) using various F-T processes. [Pichler *et al.*, 1968][Dry, 1981].

Carbon number	Compound type	Process		
		Cobalt catalyst: 190°, 1 bar	Iron catalyst Fixed bed 220°C, 27 bar	Iron Catalyst **Synthol** 320°C, 22 bar
6	n- paraffin	56	45	18
	n- α-olefin	4	25	42
	n- internal olefin	21	26	19
	br. paraffins	13	2.4	6
	br. olefins	6.1	1.5	14
	aromatics		< 0.01	0.2
	Total olefins (%)	31.1	52.5	75
	Olefin linearity (%)	80	97	81
8	n- paraffin	54	41	11
	n- α-olefin	3	35	33
	n- internal olefin	4	19	11
	br. paraffins	16	1.5	7
	br. olefins	11	3	21
	aromatics		0.17	5.2
	Balance	12	0.33	
	Total olefins (%)	18	57	65
	Olefin linearity (%)	39	95	68
10	n- paraffin	51	42	10
	n- α-olefin	3	37	26
	n- internal olefin	3	15	9
	br. paraffins	25	2	10
	br. olefins	1	3	22
	Balance	17	1	23
	Total olefins (%)	7	55	57
	Olefin linearity (%)	86	95	61

1.2.6 F-T Mechanisms: To Explain Product Distribution.

Product distributions in the F-T synthesis can be quantified using the Anderson-Schulz-Flory (ASF) polymerization model. The ASF distribution is a combination of Schulz's equation for radical polymerization of vinyl monomers [Schulz, 1975], and Flory's linear condensation polymerization expression [Flory, 1936]. The resulting equation is widely used in F-T catalysis for predicting hydrocarbon distributions. Various F-T hydrocarbon product distribution models have been proposed, based in turn on different reaction mechanisms. However, due to the diversity of products encountered, few of these models satisfactorily explain all aspects of the observed product spectra [Dry, 1981].

Although the possibility exists that they are closely related mechanistically [Dry, 1981], the hydroformylation reaction chemistry and F-T synthesis have been treated as separate topics. It may therefore be of interest to briefly review aspects of the F-T mechanism.

The mechanism of the F-T reaction is still a topic of debate, and various mechanisms have been proposed. To generalize, most are based on either one, or a combination of, the carbide, hydroxycarbene and CO insertion mechanisms.

The carbide mechanism.

Fischer and Tropsch [1926] proposed a mechanism proceeding via hydrogenation of a metal carbide followed by polymerization of these metal methylene complexes to form hydrocarbons. Product formation is via beta-elimination or hydrogenation. This mechanism has been extensively reviewed by Muetterties and Stein [1979], Brady and Petit [1980, 1981], Herrmann [1982], Roder and Werner [1982] as well as Henrici-Olivé and Olivé [1984]. Although there is considerable evidence for this mechanism, it does not fully explain all the products observed during F-T synthesis, especially the oxygenated hydrocarbons, and aromatics.

Figure 1.9 Schematic of the carbide mechanism.

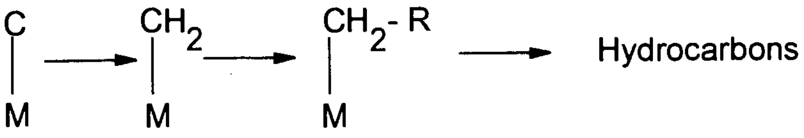

The hydroxycarbene mechanism.

This involves CO adsorption onto the metal to form an M=C=O species which interacts with M-H units to form the M-CHOH (or hydroxycarbene) intermediate. C-C bond formation then takes place via a condensation reaction involving two M-CHOH and two M-H units to produce $M{=}CCH_3OH$ and H_2O. F-T product formation is facilitated by dehydration, along with hydrogenation, resulting in the formation of a hydrocarbon. Alternatively, desorption of the products is facilitated by hydrogenation of the intermediate to form an alcohol. The mechanism was developed by Storch, Golumbic and Anderson [1951].

Figure 1.10 Schematic of the hydroxycarbene mechanism

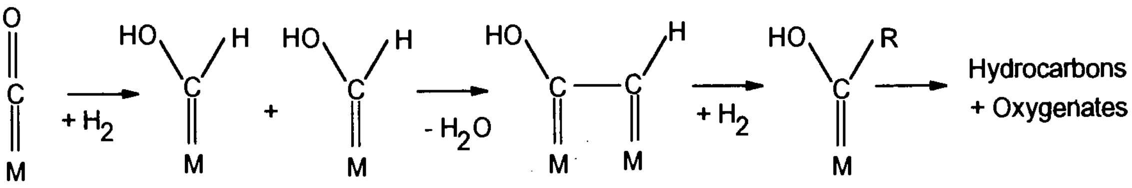

The CO insertion mechanism.

This involves CO insertion into the M-H bond of a $HM(CO)_x$ unit derived from the interaction of syngas and the F-T catalyst metal. CO insertion is coupled to hydrogenation and results in a $MCH_3(CO)_{x-1}$ unit [Pichler and Schultz, 1970]. Another carbonyl then attaches to the metal site resulting in a $M\text{-}CH_3(CO)_x$ species. Hydrocarbon chain propagation then proceeds via further CO insertion into the M-C bond, resulting in $MCOR(CO)_{x-1}$ which can undergo a number of desorption reactions to form various oxygenates and hydrocarbons. A common variation of this mechanism is the formyl mechanism whereby CO groups do not necessarily have to be on the same metal atom. This mechanism is closely linked to the hydroformylation mechanism. It has been extensively reviewed [Muetteries and Stein, 1979], [Rofer -De Poorter, 1970], [Henrici-Olivé and Olivé, 1984, 1985].

Figure 1.11 Schematic of the CO insertion mechanism.

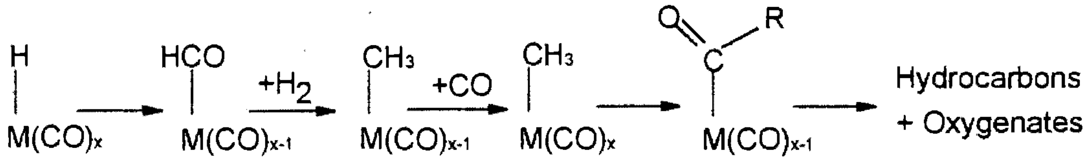

The above three basic mechanisms all argue on the type of C_1 species present, and no one can be discounted completely. Indeed, it is possible that a combination of these mechanisms (as well as others, including hydroformylation type reactions) all occur. Numerous other mechanisms, some of which combine more than one of the above general schemes have been proposed and reviewed in the past [Dry, 1981] [Schulz *et al.*, 1990], with more recent evaluations and interpretations presented [van Berge, 1993][Dry, 1993][Maitlis *et al.*, 1994]. Maitlis *et al.* [1994] used homogeneous model compounds decomposition products as a means of identifying F-T intermediates. van Berge's [1993] critical evaluation of Schulz's "Non-trivial-surface-polymerization Model" has led to more accurate prediction of the F-T product distribution/s.

Mechanism describing HTF-T products.

A method of describing the observed Synthol products has been proposed recently by Dry [1993] which makes use of three and four membered "cyclic ring" intermediates as postulated in Ziegler-Natta polymerization as well as olefin metathesis type reactions. The mechanism/s incorporate accepted principles of hydroformylation and carbonylation reactions, namely CO insertion (or alkyl migration) resulting in chain growth from the metal centre and/or hydrogenation. The mechanisms represented in Figures 1.12 and 1.13 for olefin, paraffin and oxygenate formation were proposed.

Although aromatics and cyclic compounds are present in Synthol products (see Table 1.2), the above mechanisms do not make allowance for these compounds. Aromatics are claimed to form as a result of secondary reactions as they are only observed at high temperatures [Dry, 1993]. It is however, not inconceivable that they may form from cyclic intermediates, albeit larger ones, as drawn in the mechanisms. Alternatively, or in addition to this, aromatics may form as a result of conjugated dienes undergoing a cycloaddition or Diels-Alder reaction to form cyclohexenes and related compounds which take place under conditions of heat and pressure [Streitweiser and Heathcock, 1981].

Figure 1.12 Mechanism for olefin and paraffin formation [Dry, 1993]

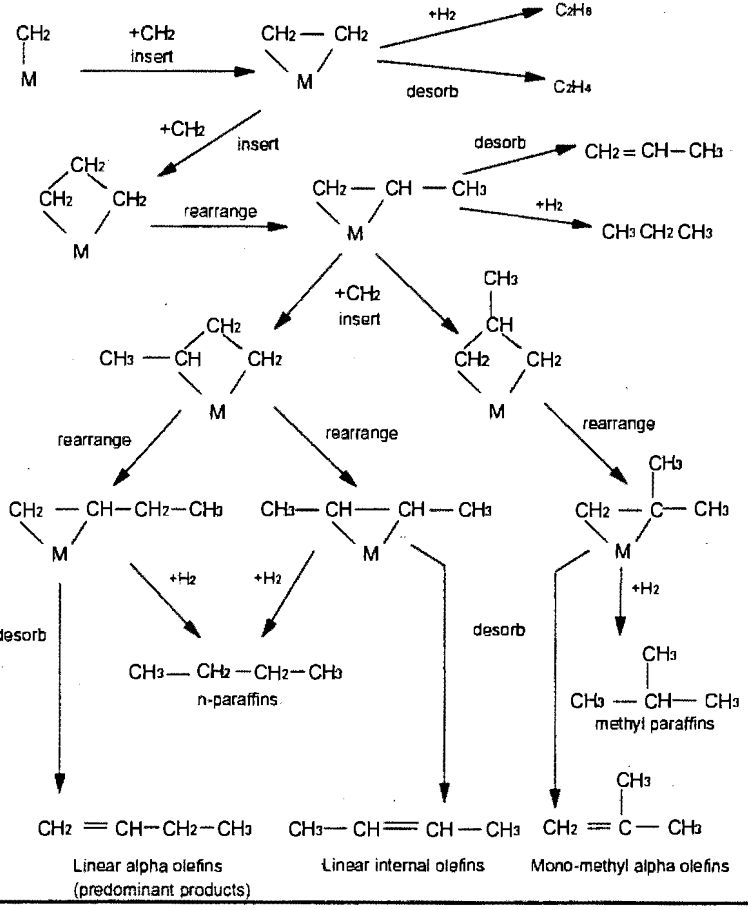

In HTF-T products, the ketones observed are mainly methyl ketones, and oxygenates are predominantly linear. This is consistent with the scheme in Figure 1.13.

Figure 1.13 Mechanism for oxygenate formation [Dry, 1993]

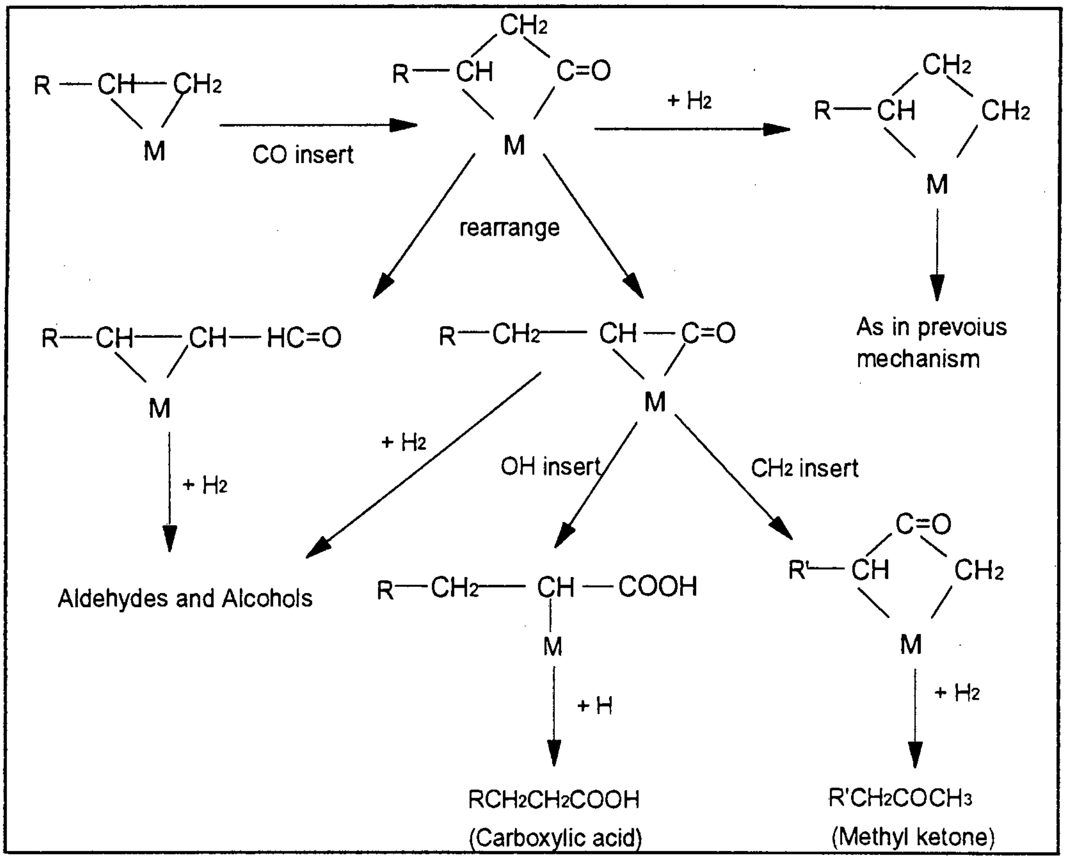

1.2.7 Higher Alcohols Directly from F-T

This topic is different to the synthesis of higher alcohols by hydroformylation of F-T products. F-T variants for higher alcohol synthesis include the manufacture of primary monohydric alcohols [Cornils and Rottig, 1982] via Fischer and Tropsch's "old Synthol" as well as the **Synol** [Wenzel, 1948] and **Oxyl** [Heckel *et al.*, 1943][Rottig, 1943] syntheses. The Oxyl and Synol syntheses manipulate F-T reaction conditions so that a large share of the synthesis product comprises primary aliphatic alcohols.

The Synol synthesis first carried out by Wenzel employs iron catalysts in fixed bed reactors (preferably two stage, with interstage cooling) under selected reaction conditions of between 180-200°C and 18-25 bar of 1:1 H_2:CO synthesis gas at a space velocity 100-200 hr^{-1} .

Table 1.4 Typical composition of Liquid Products from the Synol Synthesis [Cornils and Rottig, 1982] *

Boiling point at normal pressure. (°C)	Content (wt. %)	Primary aliphatic alcohols (wt. %)
0-100	27	35
100-140	16	45
140-180	12	48
180-220	9	50
220-260	7	55
260-300	6	55
300-350	5	45
350-385	4	35
385-420	2.5	15
>420	11.5	7

* Synthesis conditions: 187°C; 20 bar.

The Oxyl synthesis is similar in many respects to the Synol synthesis. Precipitated iron catalysts, originally with cerium and vanadium promoters/activators [Heckel *et al.*, 1943], and later with copper and alkali [Rottig, 1943] were shown to give high yields of oxygen rich products under F-T conditions similar to those employed in the Synol synthesis. The notable difference in conditions pertains to the preferred use of syngas with a H_2:CO ratio of 1:1.2 to 1:2

Table 1.5 Typical composition of Products from the Oxyl Synthesis [Falbe, 1977].

Oxygenates	Content (wt. %)
Alcohols ≤C18	55.3
Alcohols>C18	0.5
Aldehydes + Ketones	2.0
Esters < 320°C	2.0
Esters > 320°C	1.2
Free carboxylic acids	1.0
Hydrocarbons	38

The Synol and Oxyl syntheses yield significant quantities of higher alcohols which still need to be beneficiated. This appears to be a potential drawback of these processes for producing higher alcohols. The recognized way of achieving this alcohol beneficiation is by their esterification with boric acid to form the corresponding triesters. These are high-boilers which can then be separated from the balance of the material using distillation techniques. Saponification techniques may be used to recover the alcohols from the triesters. Depending on the economics of reactor efficiency and beneficiation as well as the linearities and other characteristics of the alcohol products, the Synol and Oxyl processes may be considered as alternative routes for the manufacture of detergent (and plasticizer) alcohols. Their commercial application for this purpose has, however, not materialized. Although it has more in common with the methanol synthesis than with the F-T reaction, the isobutyl oil synthesis [Winnacker and Weingärtner, 1952][Winnacker and Küchler, 1959] was the only commercially operated process for the production of "higher" aliphatic alcohols directly from syngas.

1.3 HYDROFORMYLATION OR OXO SYNTHESIS: GENERAL INTRODUCTION

Hydroformylation is the general term applied to the reaction of an olefin with carbon monoxide and hydrogen to form an aldehyde [Pruett, 1979]. This term was first proposed by Adkins and Krsek [1949] as an alternative and probably more technically descriptive term to the one more commonly used in industry, namely the "Oxo Synthesis" [Pruett, 1979]. The reaction has also been referred to by some (especially those having links with Ruhrchemie) as the "Roelen Reaction" named after the first person to identify this synthesis.

Due to its industrial importance, hydroformylation has been the topic of several reviews [Falbe, 1970, 1980][Cornils, 1980][Orchin and Rupilius, 1972][Paulik, 1972], [Pino *et al.*, 1977][Pruett, 1979][Rylander, 1973][Davidson *et al.*, 1977][Beller *et al.*, 1995]. A brief review of hydroformylation is however appropriate in this, the introductory chapter. Additional hydroformylation detail from the literature is interwoven into the text of subsequent chapters describing results.

It is noteworthy and to a degree expected that the CO-hydrogenation and hydroformylation reactions were discovered by scientists working in similar fields and on similar catalysts. Indeed, the production of oxygenated products first observed by Fischer and Tropsch at high syngas pressures were possibly the result of CO insertions / migration into olefinic hydrocarbon intermediates.
The hydroformylation reaction was discovered by Otto Roelen in 1938 [Roelen, 1938, 1943]. Although the commercial hydroformylation catalysts used today are almost exclusively based on homogeneous organometallic complexes, and specifically carbonyl derivatives of the Group VIII metals [Kirshenbaum and Inchalik, 1981], the first reported hydroformylation catalyst was a solid [Pruett, 1979]. This is because Roelen discovered hydroformylation whilst he was undertaking experiments on the effect of recycling olefins, specifically ethylene [Cornils *et al.*,

1994] to the Fischer-Tropsch reaction [Falbe, 1970]. As he was using a contemporary heterogenous cobalt Fischer-Tropsch catalyst consisting of 66% silica, 30% cobalt, 2% thorium oxide and 2% magnesium oxide [Roelen, 1948][Pruett, 1979], Roelen's work indicated that the Oxo and Fischer-Tropsch syntheses may be combined. Although he did not actually undertake hydroformylation on a pure F-T feed, his work is the only reference obtained wherein actual hydroformylation of a "F-T feed" is reported. In Pruett's review [1979], Wender *et al.* [1950] are credited with proving the homogenous nature of the hydroformylation catalyst and it is claimed that Roelen probably did not realize at the time that his active catalyst was a homogenous derivative of the F-T catalyst. However, in Falbe's review [Falbe, 1970], Roelen is credited as being the first to assume that hydrocarbonyls are the active catalysts in hydroformylation but Falbe goes on to say that this was only clarified much later from 1946-1948 [Roelen, 1948][Hecht and Kröper, 1948][Kröper, 1955][Adkins and Krsek, 1948]. It does however appear that the subject of the homogenous nature of the first hydroformylation catalysts was a somewhat controversial topic at the time.

It is however generally accepted that hydroformylation catalysts are metal hydrocarbonyls or derivatives thereof. The general structure is of the form

$$H_xM_y(CO)_zL_n$$

where L represents an optional modification with a ligand [Beller *et al.*, 1995].

Iron carbonyl (and cobalt carbonyl) formation occurs at high syngas pressures [Anderson, 1956]. It may theferore be speculated that the rapid deactivation of the first F-T catalyst may have been due to iron carbonyl formation, which also catalyzed the first "homogenous" hydroformylation reaction in the gas phase. This can explain the high levels of oxygenated products observed by Fischer and Tropsch. Alternatively, isosynthesis, which occurs at high temperatures and pressures of syngas over oxide catalysts (oxidation of the Fe in a F-T catalyst also results in deactivation) may have taken place. Either way, the mechanisms of the isosynthesis, F-T and hydroformylation reactions are all expected to be similar.

1.3.1 Hydroformylation Mechanisms

Once the homogenous nature of the hydrocarbonyl complex had been ascertained, detailed studies of the hydroformylation reaction mechanism followed [Falbe, 1970]. Although the basic steps of the mechanism are generally accepted, the hydroformylation mechanism is still a topic of debate [Beller *et al.*, 1995]. Recent presentations by Markó *et.al* [1994] and Tannenbaum [1994] are confirmation of this. Pioneers as regards elucidation of a mechanism were Wender *et al.* [1953], Orchin *et al.* [1956, 1958, 1959,1960], Pino *et al.* [1963, 1968] Markó *et al.* [1963] as well as Heck and Breslow [1960-1966]. These workers were the first to carry out experiments to arrive at a reaction sequence for producing aldehydes involving a number of organometallic intermediates. The mechanism by Heck and Breslow is generally accepted as a tool to describe the sequence of reactions in hydroformylation and is illustrated by means of a cyclic diagram in Figure 1.14 wherein the linear aldehyde is produced via co-ordination of the α carbon atom of the olefin.

Figure 1.14 incorporates the Heck-Breslow mechanism as well as the theories of Pino and Piancenti and is redrawn by Cornils [1980] in Falbe's review [Falbe, 1980]. Co-ordination via the β carbon also occurs to produce 2-methyl branched aldehydes. This is illustrated in Figure 1.15. The same basic set of steps occur if internal olefin reactants are used, but the intermediates and products would be more highly branched.

Figure 1.14 The multistep hydroformylation reaction pathways using an unmodified Co catalyst.

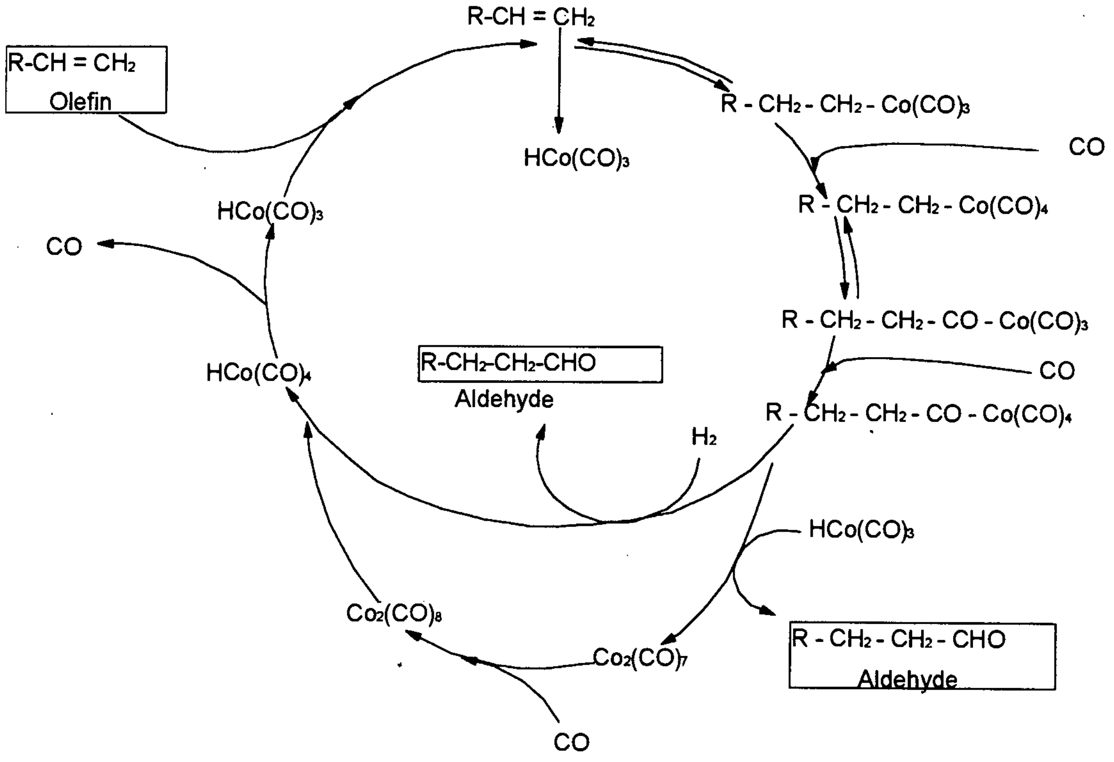

Note: A ligand can replace one of the carbonyl groups in the mono-cobalt catalyst complexes; for the di-cobalt complexes, two ligands may be present (*ie*. 1 ligand per Co atom).

As described previously in Section 1.1.2, linear alcohols are desirable. The hydroformylation catalyst system should therefore be operated so as to maximize "pathway 1" in Figure 1.15.

Figure 1.15 Hydroformylation reaction steps to linear and 2-methyl products.

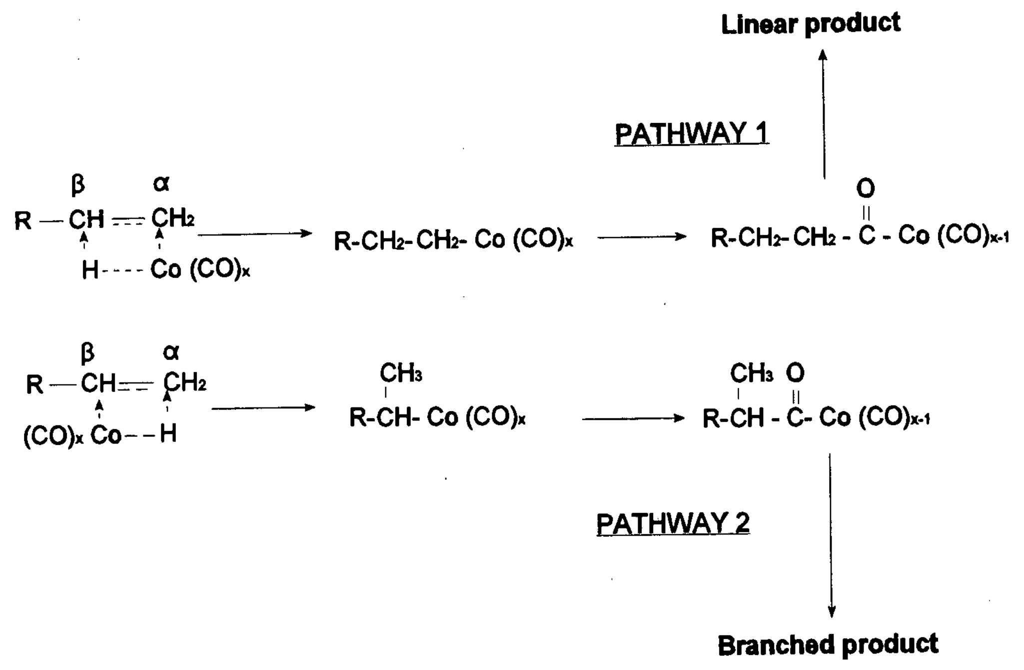

1.3.2 Side Reactions Occurring During Hydroformylation

Apart from the obvious requirement of a suitable olefin content, distribution and linearity in an olefinic feedstock for hydroformylation; an additional and important factor in ascertaining the suitability of an olefinic feed is the possibility of unwanted side reactions during hydroformylation. These side reactions are undesirable since they represent a loss of the valuable olefin starting material. They also incur additional costs in purification of the products in the downstream workup. The odd exception occurs when the system is tailored to yield a specific product. For example, the production of 2 ethylhexanal from aldol condensation products of butryaldehyde produced by hydroformylation of propylene as shown in Figure 1.4.

Figure 1.14 does not include the possibility of various side reactions that can occur during hydroformylation. These include: Olefin isomerization; olefin hydrogenation; aldehyde hydrogenation; and reactions to form heavier oxygenates.

Of the side reactions, those producing higher boiling materials such as aldols, esters, ethers, ketones and acetals are particularly undesirable. These high boilers have been collectively termed the Heavy Oxo Fraction (HOF) [van Vliet, 1987]. The HOF should be kept to a minimum, and especially so in a system in which the catalyst is recycled via the residue leg of a distillation unit. The HOF buildup in such a process is regulated by purging the recycle stream, which results in losses of the homogeneous catalyst.

Numerous reports on the side reactions, mechanisms and products of reactions giving rise to species comprising the HOF have been reported and these have been reviewed by Cornils and Falbe [Falbe, 1970, 1980].

The non-olefinic components in HTF-T products, and specifically the oxygenate and aromatic containing component groups, would be expected to have an effect on the systems to be tested. Paraffins would be inert in the hydroformylation reaction. Apart from being possible poisons, the effects of additional oxygenates (and possibly aromatics) could lead to undesirable secondary reactions, thereby causing unwanted by-product formation. If one considers the layout of existing hydroformylation plants, it is clear that apart from distillation procedures in the work-up, chemical treatment of the product is also necessary, regardless of the olefin feed purity.

Possible reactions in parallel or in series accompanying the desired reactions of "olefin + CO + H_2 → aldehyde (for Rh/P catalysts) + H_2 → alcohol (for Co/P catalysts)" are shown schematically in Figure 1.16 [Cornils, 1980] with the possible effect of oxygenates in a F-T feed superimposed.

Figure 1.16 Possible reactions occurring in series or parallel during hydroformylation (using a F-T feed).

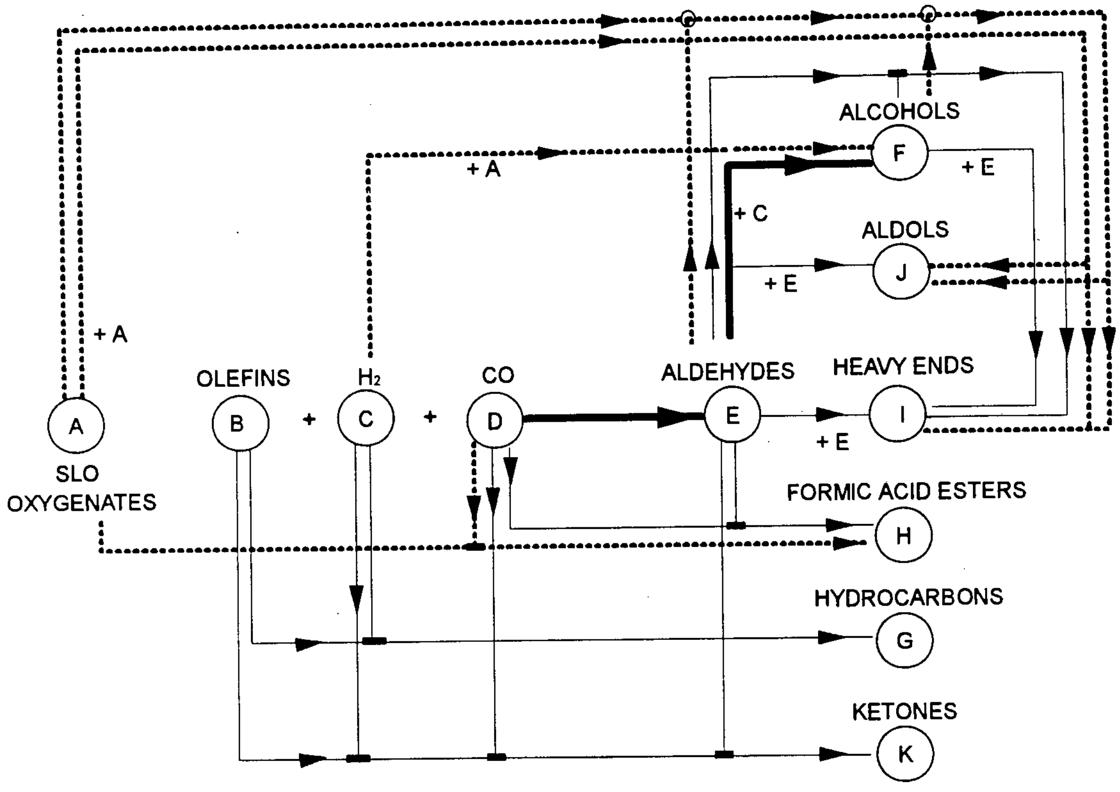

Key and explanation of Figure 1.16:

Letters refer to components;

A = SLO oxygenates, B = olefins, C = H_2, D = CO; E = aldehydes; F = alcohols; G = hydrocarbons; H = formic acid esters; J = aldols; K = ketones; I = heavy ends (acetals *etc*.).

Bold broken lines indicate the possible complications or additional reactions attributed to the presence of SLO oxygenate (A) components.

Bold solid lines indicate the desired reaction pathway *ie*., olefins (B) + H_2 (C) + CO (D) to give an aldehyde (E) + H_2 (C) to give an alcohol (F).

+ / ▬ are the symbols indicating a combination. For example: SLO oxygenate (A) combining with CO (D) to give a formic acid ester (H).

○ indicates more than one reaction possibility. For example: SLO oxygenates (A) may combine with aldehydes (E) or alcohols to form aldols (J) and/or heavy ends (I). Alternatively, SLO oxygenates (A) may combine with each other to form aldols or heavy ends.

1.3.3 Hydroformylation Catalysts: Striving for Linear Products

A variety of transition metals catalyze the hydroformylation reaction, with the following generally accepted [Beller *et al.*, 1995] order of activity:

Rh >> Co >> Ir, Ru > Os > Pt > Pd > Fe > Ni.

However only cobalt and rhodium complexes are used in commercial oxo plants [Kirshenbaum and Inchalik, 1981][Beller *et al.*, 1995]. Few metals, apart from those based on Co and Rh warrant investigation as they are generally considered too inactive or expensive for use in hydroformylation catalysis. A comparative study by Alvila *et al.* [1992] of the homogeneous hydroformylation catalytic activity of various complexes of Group 8-9 metals, Fe, Co, Rh, Ru, and Ir, confirms this. However, although not applied commercially, a significant amount of work has been carried out with Ru complexes [Evans *et al.*, 1965][Schultz and Bellstedt, 1973][Braca *et al.*, 1970][Sanchez-Delgado *et al.*, 1976].

The use of "conventional" homogeneous Co hydrocarbonyl catalysts as illustrated in Figure 1.14 in industrial oxo facilities is still widespread. Although unmodified Rh hydrocarbonyl catalysts are very active for hydroformylation, they are generally not used commercially due to problems associated with their recovery as discussed below.

A considerable amount of hydroformylation research has been directed at improving reaction selectivity to linear products. The use of organophosphines as ligands to replace one or more CO molecules on the Rh or Co hydrocarbonyl complex significantly improves the product linearity [Slaugh and Mullineaux, 1966, 1968][Tucci, 1968][Pruett, 1969, 1970][Bryant, 1979] as well as the thermal stability of the catalyst complex. According to Beller *et al.* [1995], the most active research areas in hydroformylation over the last 15 years (1980 to 1995) are ligand synthesis and their coordination chemistry. Beller *et al.*, however state that there is a lack of consistency in the relationship between ligand structure and activity and that "very often the catalytic results of sometimes costly synthesized ligands are disappointing".

Phosphine ligands are the most widely used and accepted ligands [Beller *et al.*, 1995] in hydroformylation. The other major class of ligands is based on nitrogen containing compounds such as amines, amides and isonitriles [Beller *et al.*, 1995]. These ligands give rise to less active hydroformylation catalysts due to their strong coordination to the metal centre [Beller *et al.*, 1995]. Beller *et al.* [1995] claim that a significant breakthrough in the replacement of phosphines was recently achieved by Herrmann *et al.* [1995]. Rh-carbene complexes synthesized by Herrmann *et al.*, are said to be surprisingly stable and catalyze the hydroformylation of 1-hexene. Beller *et al.*, go on to state that "it remains to be seen what this new class of ligands will contribute to the hydroformylation reaction in particular and to catalysis in general".

Replacement of one or more of the carbonyls in conventional $HM(CO)_x$ type complexes (where x = 3 or 4) with phosphines typically results in complexes of the form:

$HRh(CO)(P\O_3)_3$ for rhodium catalysts (where $P\O_3$ represents a triphenylphosphine ligand = TPP) and;

$HCo(CO)_3PR_3$ for cobalt catalysts (where PR_3 represents a trialkylphosphine group) [Falbe, 1970].

The Rh atomic radius is larger than that of Co (134 $\times 10^{-12}$m versus 125$\times 10^{-12}$m, [Lof, 1987]) which lessens the steric crowding of ligands surrounding the central atom [Falbe, 1967][Heil and Marko, 1969]. This can explain higher reaction rates observed with Rh as well as the larger amount of branched products observed when using unmodified Rh compared with Co if the reactions are undertaken at the <u>same</u> conditions.

Trivalent phosphine ligands are better σ (sigma) electron donors than CO, but poorer π (pi) electron acceptors. In P-modified catalysts, this results in the remaining CO's being more strongly bonded to the central metal atom. This is due to the increased negative charge on the metal atom being transferred to the CO atom through π electron donation. The increased stability of the complex results in lower hydroformylation activity. The ligand basicity (or capability to "donate" electrons to the metal atom) therefore has important consequences for the catalyst activity. The selectivity is also affected, as some of this negative charge may be transferred to the hydrogen atom. This in turn results in the complex having a more hydridic character which may facilitate hydrogenation of the aldehyde and some of the olefins.

The improved thermal stability of modified catalysts may enable the use of lower reaction pressures, as well as distillation as a method of recycling the homogeneous catalyst instead of more cumbersome chemical extraction techniques.

The higher product linearities of alcohols used as surfactant precursors result in improved biodegradation of the products. Linear hydroformylation products are more desirable than the corresponding branched products. Linearity is therefore associated with the terms "high value" and "environmentally friendly". However, there is a trade-off in terms of the process; the ligand modified complexes are less reactive and require higher reaction temperatures. Even then, the reaction rates are typically between a fifth and sixth of those obtained with the corresponding conventional catalysts [Falbe, 1970]. An additional trade-off in modified Co systems is the loss of 10 and 15% of the olefin to paraffin through hydrogenation compared with 2 to 3% in conventional hydroformylation processes [Falbe, 1970].

The most common catalysts used for the production of predominantly linear products are generally based on phosphine and or phosphite ligand modified Rh, Co and Ru homogeneous systems. Pioneers in this regard were Slaugh and Mullineaux [1966, 1969] whose work resulted in numerous patents on alkyl phosphine modified oxo catalysts being granted to Shell Oil Company. Modified Rh systems were first patented by Pruett and Smith [1970] of Union Carbide Corporation (UCC). The industrial significance of phosphines in order to improve reaction selectivities and catalyst stability, compared with the corresponding unmodified hydrocarbonyl catalysts, is evidenced by the fact that most, if not all, the initial literature in this regard appears in patents. Of these systems, it appears that triaryl phosphorous derivatives are favoured for use as ligands with Rh, and that alkyl phosphorous derivatives are favoured for use as ligands with Co.

Specific examples commonly cited in the literature are triphenylphosphine (TPP) [Pruett and Smith, 1970] as well as tri and bisphenylphosphites patented by UCC [Billing *et al.*, 1987, 1988,1989], both of which are used with rhodium.

Of the alkyl phosphines (used with cobalt), examples include various tri-alkyl phosphines [Slaugh and Mullineaux, 1966]. Of these, tri-n-butyl phosphine (TBP) is the most commonly referred to in the literature [Beller *et al.*, 1995]. Other alkyl phosphines suitable for use with Co reported in the patent literature are those with a cyclic character [van Winkle et al., 1969, 1971] [Mason and van Winkle, 1968,1970]. Examples of these are a combination of the isomers: 9-phosphabicyclo [4,2,1] nonane and 9-phosphabicyclo [3,3,1] nonane , and derivatives thereof. Work undertaken by others using these particular ligands does not appear in the open scientific literature. A more detailed description of the various ligands used in this study is presented in Chapter 2. (See Figure 2.12 in Section 2.2.3.2).

A comparison of the phosphine modified and conventional Co and Rh catalyst systems, typical conditions under which they operate, and expected product characteristics is shown in Table 1.6.

Table 1.6 A comparison of commercial hydroformylation catalysts summarized by Cornils in Falbe's [1980] review.

Variables	Most common catalysts used in industrial hydroformylation			
	Co-hydrocarbonyl	Co-PR_3 modified	Rh-hydrocarbonyl	Rh-PPh_3 modified
Structure	$HCo(CO)_4$	$HCo(CO)_3PR_3$	$HRh(CO)_4$	$HCo(CO)(PØ_3)_3$
Temperature (°C)	110 -180	160 -200	100 -140	80-130
Preferred syngas composition: (H2/CO ratio)	1	2	1	1-2
Typical syngas pressure (bar)	200 - 300	20 - 100	200 - 300	4 - 50
Common Ligands (L)	CO, H	CO, H, PR_3	CO, H	CO, H, $PØ_3$
L/Metal (molar ratio)	-	2/1	-	> 50/1
Metal/olefin (mass%)	0.1 - 1	0.5 - 1	10^{-4} - 0.01	10^{-3} - 0.1
Reactor throughput (LHSV) hr^{-1}	0.5 - 2.0	0.1 - 0.2	0.3 - 0.6	0.1 - 0.25
Product linearity (%)	60 - 80%	$\geq$80%	± 50%	$\geq$ 90%
Preferred feed	Range of olefins	Higher olefins	$\leq C_6$	$\leq C_6$
% Alcohol selectivity	±10	±75	±10	±0
% Aldehyde selectivity	±80	±5	±80	±96
% Paraffin selectivity	±2	±15	±2	±2
% HOF selectivity *	±8	±5	±8	±2
Sensitivity towards poisons	Low	Low	High	High
Notes	"Conventional oxo"; unselective to linear products	Can feed internal olefins and get linear products	"Conventional oxo"; unselective to linear products	Cannot feed internal olefins and get linear products

* HOF denotes Heavy Oxo Fraction (from side reactions).

On consideration of Table 1.6, it is evident that ligand modification results in numerous changes in hydroformylation performance. These changes include lower operating pressures, lower activity and higher product linearities. Lower reaction pressures and lower activity has been associated with increased catalyst stability [Falbe, 1970]. This lower activity coupled to the increased steric crowding of the central atom may be cited as reasons for the increased selectivity to linear products when ligands are used.

1.3.4 Separation and Recovery of Homogeneous Hydroformylation Catalysts

Because of the homogeneous nature of the catalysts, their separation from products and recycle is an important part of an Oxo process. Carbonyls of the type $HCo(CO)_x$ and $Co(CO)_8$ are very volatile and only weakly soluble in organic solvents [Falbe, 1970]. These complexes are thus often taken out of solution with gas streams resulting in metallic deposits in parts of the plant downstream to the hydroformylation reactors. Catalyst residues that may be carried over to the raw hydroformylation reactor product cause condensation and oxidation reactions in the subsequent work-up (purification) of these products, and specifically during product distillations. This typically results in coloured products (unsaturated oxygenates) in the work-up. Quantitative recovery of the catalyst from an economic and process point of view is therefore important. To date, there are five general methods employed by industry.

1. Distillation:

Although a convenient method for catalyst separation on lab-scale, flash distillation is only used industrially to separate low boiling aldehydes such as propionaldehyde and butryaldehyde from catalysts with a low volatility, such as P-modified ones. The Shell hydroformylation process which utilizes phosphine modified Co catalysts to hydroformylate linear internal olefins to produce predominantly linear detergent range alcohols, makes use of falling film evaporation as a means of recycling catalyst.

2. Thermal Decomposition:

Carbonyls are decomposed by high temperature treatment at low pressures and the solid metallic decomposition product is recovered from the remaining organic material.

3. Decomposition by Hydrogenation:

This is similar to thermal decomposition, but here the carbonyls are decomposed by reduction with H_2.

4. Chemical Treatment of reaction products:

Various options exist in this regard. The most common involves reacting the metal to form a water-soluble salt followed by precipitation and recovery. Extra care is necessary with Rh complexes as losses can be very costly. Special methods for this have been developed [Weber, 1968][Falbe *et al.*, 1969].

A more recent approach is the Exxon hydroformylation process [Beller *et al.*, 1995]. This entails treating the crude reactor product with dilute aqueous caustic to form water soluble $NaCo(CO)_4$ under conditions of temperature and pressure. Addition of H_2SO_4 in the presence of syngas results in $HCo(CO)_4$ which is recovered from the aqueous phase with an olefin rich stream.

5. Phase Separation

"Heterogenizing" the catalyst on or inside a support is a way in which the catalyst can be "recovered" from the liquid or gaseous reaction media and products. Alternatively, modification of the ligand structure so as to make the ligand and catalyst complex water soluble for subsequent downstream organic-aqueous phase separation is also a method of recovering the catalyst. A more detailed review of these approaches is given subsequently in Section 1.3.5.3.

1.3.5 Selecting a Catalyst for Higher Olefin Hydroformylation

Various factors need to be taken into account when selecting a catalyst system for hydroformylation of detergent range olefins. The choice may be divided into three categories: a) using cobalt-based homogenous technology, b) using rhodium-based homogeneous technology and c) using so called "heterogenous" catalyst technology which may incorporate aspects of b) and c).

1.3.5.1 Cobalt-Based Homogeneous

Industrial hydroformylation of higher olefins is still largely undertaken with the less selective and less active cobalt catalysts. The factors in Table 1.6 need to be weighed up against each other in selecting either a phosphine modified or conventional catalyst for a process.

The following list of advantages that phosphine modified Co systems hold over conventional Co ones have been claimed by Slaugh and Mullineaux [1969]:

1. Higher catalyst stability enables the use of lower reaction pressures thereby saving on capital expenditure and operating costs.
2. The higher stability enables the catalyst to be recycled directly to the reactor system after crude product separation, thereby eliminating the need for catalyst decomposition and redissolving steps and the associated losses, as well as a reduction in operating costs and some capital investment.
3. Equilibrium isomerization (internal to α-olefins) occurs readily and the α-olefin hydroformylates to form an alcohol. The α-olefin reacts preferentially to the internal olefin and thus linear alcohols are formed in preference to branched alcohols.
4. If the catalyst utilizes synthesis gas with a H_2:CO ratio of 2:1; it has a high hydrogenation activity so that the main products are alcohols and not aldehydes. This assures low make of heavy by-products and reduces

additional hydrogenation requirements. However, loss of some of the olefin by direct hydrogenation to the paraffin can occur.

5. The catalyst gives a high ratio of linear to iso-alcohol products (>80% linear) thereby providing desirable detergent properties and rapid biodegradability.

Given these advantages, it is noteworthy that Shell is the only company apparently operating oxo plants using this technology. Until recently (1993) Shell have held the patent rights for the relevant catalysts and technology. The possible reluctance of higher oxo alcohol producers to purchase the technology, or a reluctance on the part of Shell to sell it, may in part explain why it is not applied by the other producers. Economic considerations, such as markets, existing capacities and the cost of changing the technology may have played a role.

1.3.5.2 Rhodium-Based Homogeneous

There is no doubt that Rh-based hydroformylation catalysts are technically superior to Co-based ones. Although Rh-based catalysts are more active and selective to linear products than Co-based ones, the use of Rh has largely been limited to the hydroformylation of low boiling alkenes such as propene [Falbe, 1980]. The reason for this is the fact that catalyst losses occur during the catalyst-product separation procedures. These typically involve extraction and in phosphine modified systems, distillation. The use of higher olefin feeds necessitates that these recovery procedures be more severe. In distillation, this can lead to catalyst complex degradation and loss of the metal. On average, the cost of Rh has been in the order of 1000 times higher than Co over the last 10 years. Rh and Co price trends are shown in Figure 1.17. The relatively high price of Rh makes even very small losses unacceptable. It has been reported that a loss of > 0.1ppm of Rh in the reaction products cannot be tolerated [Kuntz, 1987]. This may, however, vary depending on Rh price fluctuations. Development of Rh catalyst for higher olefin hydroformylation has therefore been linked to attempts to "heterogenize" the catalyst complex in order to overcome problems associated with recycle and recovery (see Section 1.3.5.3).

Development of Rh hydroformylation technology has also gone hand in hand with ways of producing cleaner feeds [Kosswig, 1994]. This is because poisons represent an area whereby catalyst losses in a process can occur. The price of Rh versus Co is therefore not the only consideration in selecting a catalyst system. Various factors that increase the cost of a process such as additional feed purification, and measures to ensure the absence of any poisons, must be taken into account.

Figure 1.17 Co and Rh world traded metal prices .

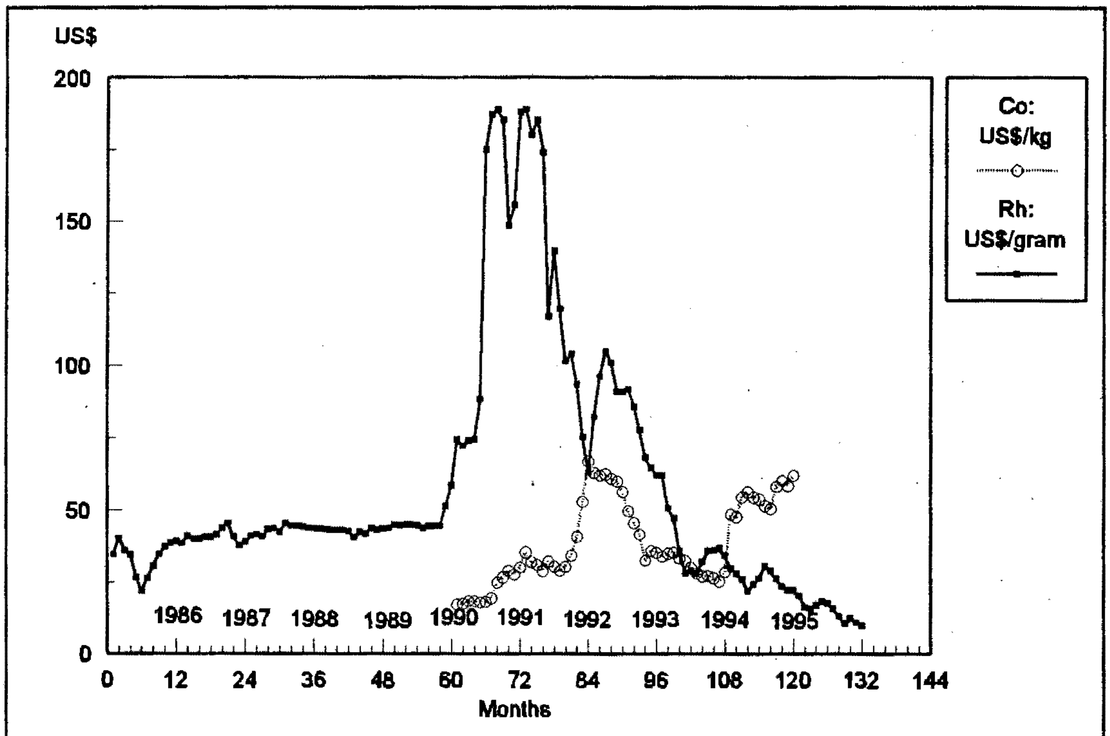

Source: Minerals Bureau (Metals bulletin Prices)
MJB: 12-12-1995

A possible exception to the use of Rh-based technology for hydroformylation of higher olefins was reported by Onoda [1983] in which recycling TPP=O (triphenylphosphine oxide) with Rh/TPP recovered by distillation results in an "increase in activity of the system" for hydroformylation of 1-octene.

1.3.5.3 "Heterogeneous"

In addition to the conventional and ligand modified hydrocarbonyl Co and Rh catalysts, numerous derivatives or modifications to the catalysts mentioned above have been reported. Most of these relate to the so-called heterogenous hydroformylation catalysts. Investigating the possibility of "heterogenizing" homogenous hydroformylation catalysts has been an area of continuing investigation since the homogenous nature of hydroformylation catalysis was ascertained. This area of hydroformylation catalysis is the most widely researched as evidenced by the number of journal articles [Beller *et al.*, 1995] that appear regularly on the topic. The aim of the work involves variation of the reaction phase by "separating" or "fixing" the catalytically active centres and by so doing combine the benefits of homogeneous and heterogenous catalysis. This has led to various, supported, water soluble, two-phase and bimetallic systems being investigated. The "ship in the bottle" concept wherein the homogeneous catalyst is encapsulated in zeolite structures [Hölderich, 1993] can represent a significant area of academic research. This may be facilitated by the continual improvement in computer technology and related molecular modelling and design packages. The use of membrane technology [Grosser *et al.*, 1977][Bahrmann *et al.*, 1989][Healy *et al.*, 1993] as a way of separating homogeneous catalysts and by so doing overcoming the problems associated with catalyst recycle and the concomitant losses of catalyst may also be a field that will enjoy more attention in the future.

Because of the superior nature of Rh-based catalysts over Co-based ones, most of the work in this field has concentrated on "heterogenizing" Rh hydroformylation catalysts. Two general approaches have been followed in order to achieve this [Buhling *et al.*, 1995]. The first involves anchoring the homogeneous catalyst to or inside a solid support such as silica/zeolites, polymers and resins. No industrial success in this area has however been reported. This is probably due to difficulties associated with leaching, stability, and complicated synthesis [Buhling *et al.*, 1995]. The other approach involves maintaining the catalyst in an aqueous phase by derivatizing the ligands so as to make the catalyst complex water-soluble. This facilitates catalyst separation and recovery from the organic reagents and products by means of phase separation. The first ligands used for this purpose were triphenylphosphines (TPP's) containing sulphonate groups for use with Rh [Kuntz, 1981, 1987]. Functional groups, other than sulphonates, reported as being suitable for this purpose include ammonium [Nagel and Kinzel, 1986], phosphonium [Renaud *et al.*, 1991], and carboxyl [Avey *et al.*, 1993] groups.

The use of these bi-phasic systems has been limited industrially to propene hydroformylation [Kuntz, 1981] because the reaction takes place at the organic-aqueous interface. Poor solubility of the reactants (especially higher olefins) in the aqueous media results in slow reaction rates as a result of phase transfer limitations. The use of additional surfactants and "phase transfer agents" (which can result in micelle formation) [Fell and Papadogianakis, 1991] as a means of speeding up the process has been investigated. No industrial application of these systems has been reported. However, the use of quaternary ammonium or phosphonium salts and "alternative" ligand structures which improve the solubility of the catalyst complex in the organic media at the phase interface are reported to be suitable for industrial hydroformylation of higher olefins [Kühlein, 1994][Weibus and Cornils, 1994]. In addition, researchers at Union Carbide [Abatjoglou *et al.*, 1995] have recently claimed a process whereby a Rh-TPPMS (tri-phenylphosphine mono-sulphate) catalyst used for higher olefin (octene, dodecene, styrene and dienes) hydroformylation in conjunction with solubilizing agents such as n-methylpyrrolidone can be effectively recycled by making use of excess water and/or methanol in the extraction stage [Haggin, 1995]. The process was reported to have been demonstrated on a "small experimental unit" wherein the Rh content in the product recovery stream was less than 20 ppb.

1.3.6 Hydroformylation Catalyst Poisons

Various compounds have been reported as hydroformylation catalyst poisons. An extensive amount of work has been undertaken in this regard. The most commonly cited catalyst poisons are dienes/ acetylenes, sulphur and sulphur-compounds, halogens, carboxylic acids, and iron-carbonyls [Falbe, 1970,1980]. The presence of small quantities of dienes in HTF-T products [Dry, 1981] may therefore be a cause for concern when including these compounds in a hydroformylation feedstock. Reports on the effects of dienes as a poison are however not consistent. Fell *et al.* [1975], reported that hydroformylation of butadiene with cobalt, modified cobalt or with rhodium alone, yielded only monoaldehydes or monoalcohols. These workers showed that the reaction proceeds via a semi-hydrogenation of the diene to the monoolefin.

Various sulphur compounds such as saturated thioethers and thiophene have been reported not to harm hydroformylation catalysts [Falbe, 1970][Macho, 1961][Weibus and Cornils, 1994], but other S compounds such as COS, H_2S unsaturated thioethers, mercaptans, mercaptals, disulphides CS_2 and S all inhibit the hydroformylation reaction by forming inactive S-containing carbonyls which also have a lower solubility in the organic reaction media [Falbe, 1980]. NH_3 and amines were originally thought to retard hydroformylation, but it was subsequently shown [Falbe, 1970][Ungvary and Markó, 1969] that small amounts of amines, including pyridine, accelerate the reaction. In addition, water, CO_2 and oxygen have also been referred to as poisons, but are also said to effect an increase in conversion and selectivity if present at low concentrations [Falbe, 1980]. The effects of these components are discussed in more detail with the results in subsequent chapters. Depending on the type of hydroformylation catalyst, the presence of some of these compounds does not necessarily result in a direct attack on the catalyst. Instead, they cause the formation of unwanted by-products by means of secondary reactions. This causes process difficulties in product purification or the catalyst recycle stages of a continuous process. The continued reference to sulphur as a hydroformylation catalyst poison is significant in the context of this investigation. As sulphur is a recognized F-T catalyst poison, much effort goes into removing it from the syngas to F-T reactors. If a sulphur "breakthrough" occurs, F-T catalysts would be most effective in "capturing" all of the unwanted sulphurous gas. Hence, the products, *ie.* the hydroformylation feed, would be sulphur free.

1.3.7 Hydroformylation Solvents

The fact that a HTF-T feed, depending on the manner in which it is prepared, may contain significant quantities of non-olefinic material necessitates that one considers the effect of solvents on hydroformylation. Cornils in Falbe's review [1980] has reviewed work undertaken on these effects. The fact that no industrial processes employ solvents implies that the potential advantages are outweighed by the disadvantages. According to the review, the following general advantages and disadvantages apply regarding the use of solvents:

<u>Advantages:</u>

- Improved reaction control by varying the concentration of reactants, intermediates and final products and by so doing influencing the reaction selectivity.
- The solubility of the syngas improves in various solvents thereby improving gas to liquid mass transfer.
- Process engineering benefits, such as the solvent behaving as an additional coolant, catalyst carrier, or a selective solvent for the feedstock or product.
- Improving the reaction selectivity in causing a shift in the equilibrium to a desired product by using an undesired product as a solvent.
- "Reactive" solvents may be employed to react selectively with intermediates to give a desired product.
- Several solvents may exert electronic effects and by so-doing function as

activators or modifiers.

Disadvantages:

- The outlay necessary for a solvent recycle coupled to a catalyst recovery section is considered prohibitive.
- The additional reactor volume taken up by the inert solvent is not available for oxo synthesis thereby decreasing reactor efficiency and increasing costs.

These disadvantages are of an economic nature, but factors such as the cost of the feedstock, as well as the alternative value of the solvent if it were not necessary to recycle it, could result in a paradigm shift.

The reference to benzene and various oxygenated compounds such as aldehydes and alcohols as solvents exerting a beneficial effect [Falbe, 1980] is relevant. Apart from the olefins and paraffins in a C_8 to C_{12} HTF-T product fraction, there may be >20% by mass of aromatic and oxygenated compounds present. (See Section 1.2.5). The F-T products in this carbon number range have for the purposes of this work been collectively termed Synthol Light Oil (SLO).

Studying the use of SLO fractions as hydroformylation feeds wherein the feed contains a possible "built in" solvent may therefore be of interest.

1.4 OBJECTIVES OF THIS STUDY

To ascertain the feasibility, and investigate catalytic aspects of hydroformylation of SLO. The objective being to propose a suitable method for beneficiating the higher olefins in this material. This topic has not been reported previously.

This subject was tackled using the following approach.

i) To perform initial screening experiments with phosphine modified Rh and Co catalysts in order to ascertain feed-catalyst compatibilities. The aim of these experiments being to identify a suitable catalyst or catalyst system for the hydroformylation of these feeds whilst at the same time maximizing alcohol product linearity.

ii) Characterisation and quantification of such hydroformylation systems, with particular attention to feed and product characterization.

iii) Testing the effect of reaction conditions, including feed composition and ligand effects.

iv) A kinetic investigation of the selected hydroformylation system incorporating modelling of the results.

v) Scale up of the selected system to a continuous unit incorporating catalyst recycle. An additional objective of this experiment being to check feed-catalyst compatibility as well as the predicted kinetics.

CHAPTER 2

EXPERIMENTAL PROCEDURES

2 EXPERIMENTAL PROCEDURES

2.1 REACTORS AND REACTOR PROCEDURES

2.1.1 Screening (Work in Chapter 3)

Initial hydroformylation catalyst evaluations were undertaken in a "1 litre" Andreas Hofer autoclave.

A description of the "1 litre" screening autoclave is best achieved by means of Figure 2.1. The high pressure reactor had an approximate volume of 1.3 litres. The stirrer mechanism was of the plunger type wherein a magnet lifted and dropped a shaft fitted with conical fixtures in order to promote efficient mixing of the syngas and liquids. The heater was connected to a temperature controller. Temperature and pressure outputs were monitored via type "J" thermocouples and Rosemount pressure transducers respectively, and logged on a chart recorder.

Procedures

The reactor was operated in a "batch mode" (closed system).

The following procedure was employed:

- The desired quantities of phosphine ligand, metal precursor and liquid feed were loaded under a N_2 atmosphere into the autoclave reactor.
- Sealing and pressure testing (with N_2) of the reactor.
- The reactor contents were heated to the desired temperature under a 1 bar(g) N_2 atmosphere.
- The stirrer was switched on, and the stirrer speed maintained at a fixed

arbitrary plunger speed setting "= max."

- Syngas was introduced to the desired pressure once the desired temperature was attained at time = zero, and the reactor sealed.
- The pressure was monitored with time. Once the pressure drop ceased, the reaction was considered "complete".
- After "completion" of the reaction/s, the reactor was cooled, flushed with N_2, and opened.
- The heavier catalyst and/or catalyst component in the reactor product was allowed to "segregate" to the bottom of the samples before the liquids were analysed. This was occasionally speeded up by centrifuging.
- The liquid composition of the reactor was analyzed by GC and GC-MS techniques.

The same procedure for screening was used from time to time on the Parr micro-reactor system described for reaction studies in Section 2.1.2. The screening reactions undertaken are described in Chapter 3.

Key to Figure 2.1.

1	Magnet (for magnetic plunger)
2	Stirrer/plunger housing
3	Nut (for sealing reactor)
4	Spacer
5	Bomb/reactor cover
6	Screw
7	Flange
8	Inlet gas line (from cylinder)
9	Thermowell
10	Heating body
11	Agitator
12	Reactor vessel (± 1 litre)
13	Compressed air sprinkler
14	Electrical connection with plug
15	Electrical connection with plug
16	Thermocouple guide
17	Safety release valve
18	Gas outlet (with valve)
19	Line to pressure transducer

Figure 2.1 Diagram of the "1 litre" reactor used in screening experiments.

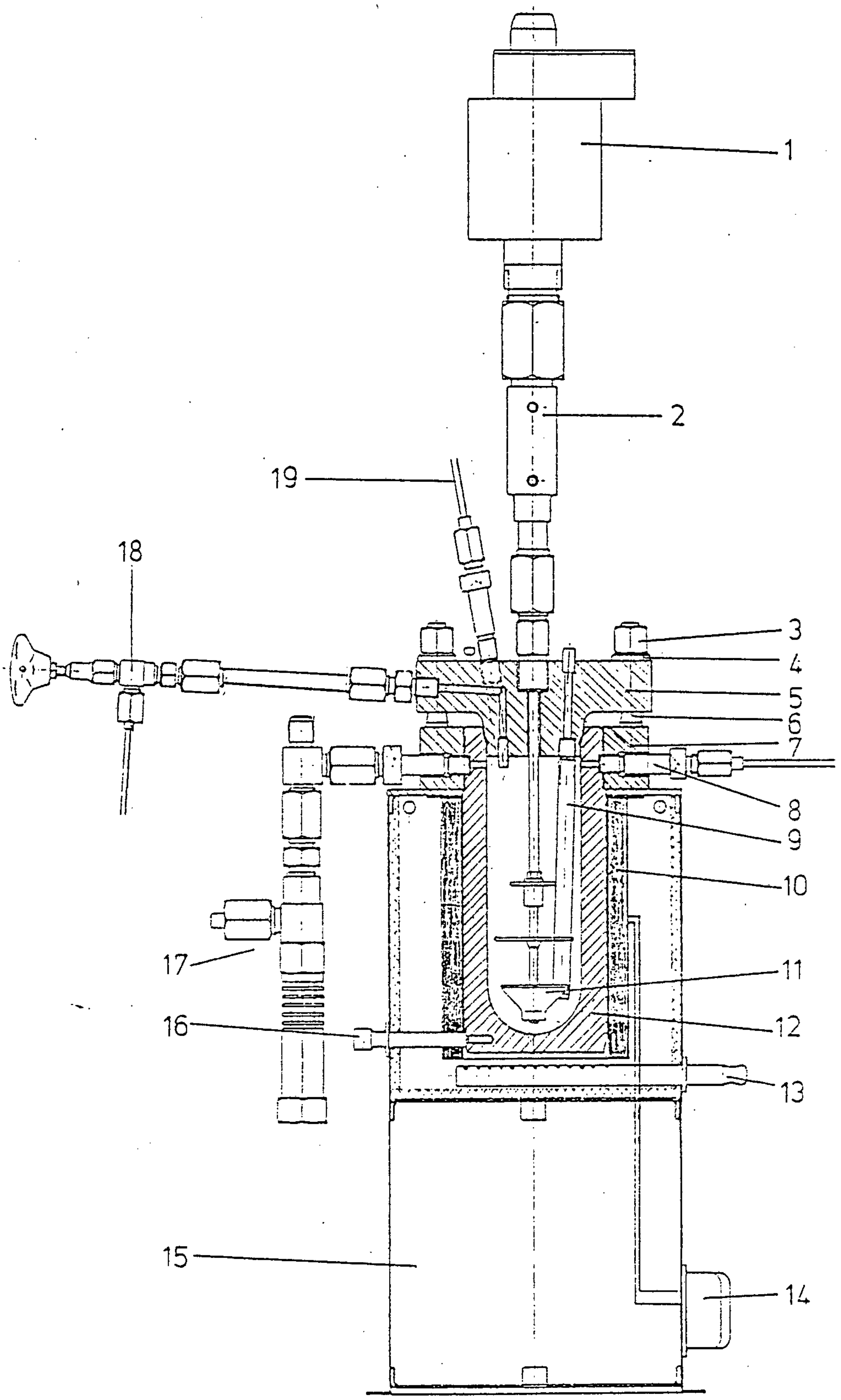

2.1.2 Constant Pressure Reaction Studies (Work in Chapters 4-6)

Reaction studies on selected hydroformylation catalyst systems were undertaken in a micro-reactor system incorporating a 450ml 316 stainless steel Parr reactor, which is illustrated in Figures 2.2 to 2.5.

Hydroformylation reaction rate and selectivity data were obtained by undertaking batch reactions under fixed pressures of syngas. The following approach was used:

Since the ratio of H_2:CO of 2:1 was shown not to change significantly during the course of the experiments, reactions under "constant gas pressure and composition" were undertaken using a 2:1 H_2:CO syngas composition. The reason being that approximately 2 moles of H_2 are consumed for every mole of CO used in the nett reaction olefin to alcohol. Monitoring the progress of the various reactions was thus simplified and achieved by sampling of the reactor contents at regular intervals. Details of the reactor configuration used in the constant pressure experiments are illustrated in Figures 2.3 to 2.5. When syngas in which the H_2:CO ratio was not equal to 2:1 was used, gas was continually fed through the system so that the syngas composition inside the reactor remained approximately constant.

The micro-reactor was equipped with a magnetically driven gas entrainment impeller. Use was made of gas intake ports situated near the top of the hollow stirrer shaft. Gas was sucked in through these ports and expelled into the vigorously stirred liquids. This ensured efficient mixing and good liquid-gas contact. Stirrer speed was monitored by a digital read-out on the Parr Series 4842 controller. Stirrer speeds $\geq$500 rpm were used.

Gas inlet and liquid sample take-off was facilitated by means of a dip/sample tube fitted with appropriate valves as demonstrated by Figures 2.2 to 2.4. Continual replacement of gas consumed by the reaction, as well as gas lost during sampling of the reactor contents, occurred through the dip tube and ensured that no contamination of liquid samples by previous samples took place.

For various experiments in which solid "heterogeneous" catalyst particles were tested, a modification which involved fitting a 5µm filter to the bottom of the dip tube was used. This ensured that solids remained in the reactor.

Syngas pressure to the reactor was maintained by a high pressure Dr'a'ger Tescom stainless steel regulator connected to syngas cylinders with downstream connection to an in-line Brooks pressure controller and a suitable valving arrangement (see Figure 2.5). The reactor gas inlet was kept open so that the gas consumed could be replaced, and so that the reactor pressure remained constant. The gas pressure in the reactor was monitored by means of an Aschcroft pressure transducer connected to the Series 4842 controller with digital pressure readout, as well as by a pressure gauge connected directly to the reactor as demonstrated in Figure 2.4.

Gas sampling of the reactor off-gas was facilitated by making use of the gas-ampule technique [Schulz and Geertsema, 1977]. A gas ampule sample collection device (see Figure 2.6) with a suitable valving arrangement was fitted to the reactor outlet for this purpose as illustrated in Figure 2.5. This technique involves capturing gas in a previously evacuated glass ampule by placing it in the gas stream, followed by breaking of one end which allows the gas to enter, and then sealing the ampule by means of a flame. The gas-containing ampule can then be analyzed by Gas Chromatography (GC) - See the description of GC procedures in Section 2.3.2.

Temperature control and measurement was facilitated by a LFE Series 200 controller connected to a type "J" thermocouple inserted into the reactor and an external heating jacket. An additional thermocouple inserted into the reactor was connected to a Westronics series 1500 chart recorder. Pressure and stirrer speed readout signals were also connected to the chart recorder.

Procedures

The following procedure was employed:

- The desired quantities of phosphine ligand, metal precursor and liquid feed were loaded under a N_2 or Ar atmosphere into the autoclave reactor.
- Sealing and pressure testing (with N_2) of the reactor.
- The reactor contents were heated to the desired temperature at 1 bar (g) N_2 atmosphere.
- The stirrer was switched on, and the stirrer speed maintained above 500 rpm.
- Syngas was introduced to the desired pressure once the desired temperature was attained at time = zero.
- Gas consumed by the reactions was replaced so as to maintain a constant reaction pressure.
- The liquid composition inside the reactor was measured by sampling the reactor contents at regular time intervals and analysing the liquids with GC and GC-MS techniques. (Analysis of gas samples taken at the end of the runs confirmed that the H_2:CO ratio was not altered significantly during the course of these experiments).
- Care was taken to ensure that no contamination from previous samples took place during liquid sampling of the reactor contents.
- GC (and GC-MS) analysis of liquids (as well as gases).

Reaction studies undertaken at constant pressure are described in Chapters 4 and 5.

Figure 2.2 Diagram of the Parr (450ml) micro-reactor (side view)

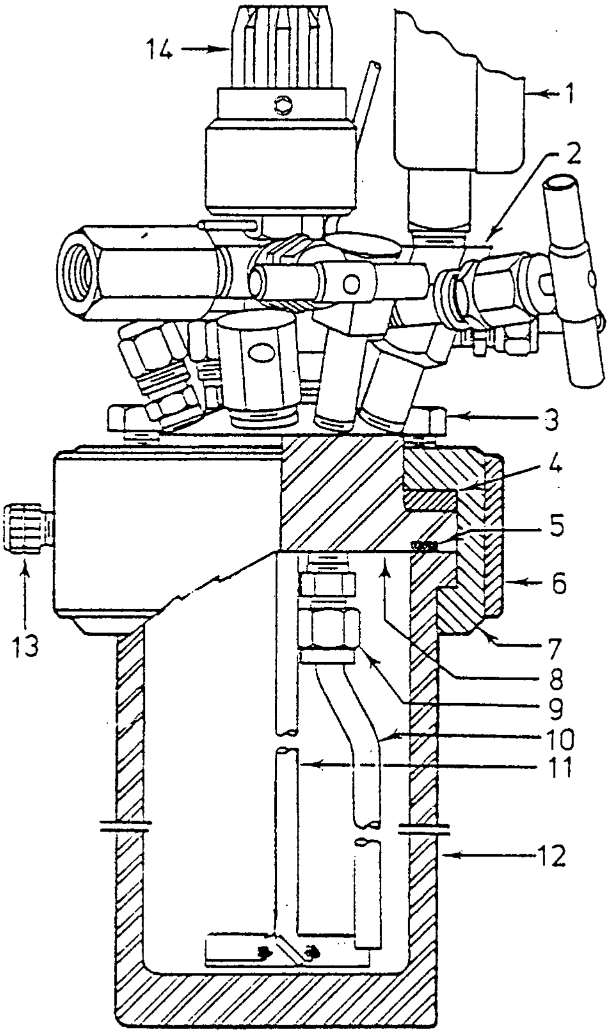

Key to Figure 2.2.

1	Pressure gauge
2	Gauge/outlet adaptor
3	Cap screw for reactor lid retaining ring
4	Compression ring
5	Head gasket (teflon)
6	Drop band with screw
7	Reactor lid retaining ring (split ring)
8	Bomb head
9	Connector
10	Dip tube
11	Stirrer shaft (hollow for gas entrainment)
12	Bomb cylinder (450ml)
13	Set screw for drop band
14	Spined coupling with screw: Inserts into connector from stirrer motor

Details of the reactor/bomb head assembly are given in Figures 2.3 and 2.4. Unless otherwise stated, all materials used were 316 stainless steel.

Figure 2.3 Top view of Parr reactor/bomb head assembly*

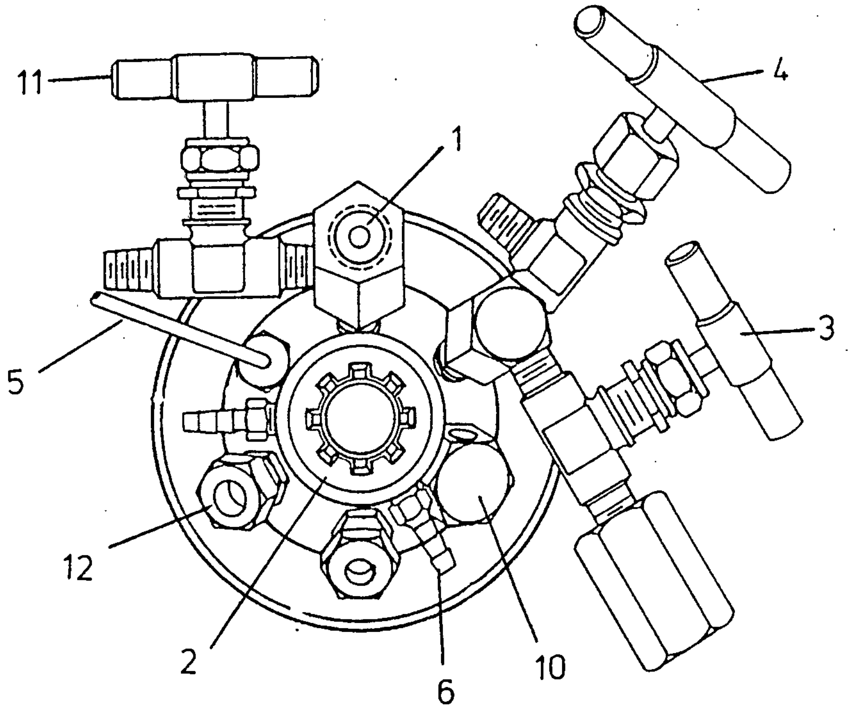

Key to Figures 2.3 and 2.4

1	Pressure gauge
2	Magnetic stirrer drive system
3	Gas inlet valve
4	Liquid sampling valve
5	Thermocouple
6	Water cooling channel (for magnetic stirrer)
7	Dip tube (for gas inlet and liquid sampling)
8	Stirrer guide
9	Gas entrainment impeller shaft (hollow)
10	Safety rupture disc
11	Gas release (outlet) valve
12	Reactor cooling coil inlet (optional) removed for this study

Figure 2.4 Side view of Parr reactor/bomb head assembly

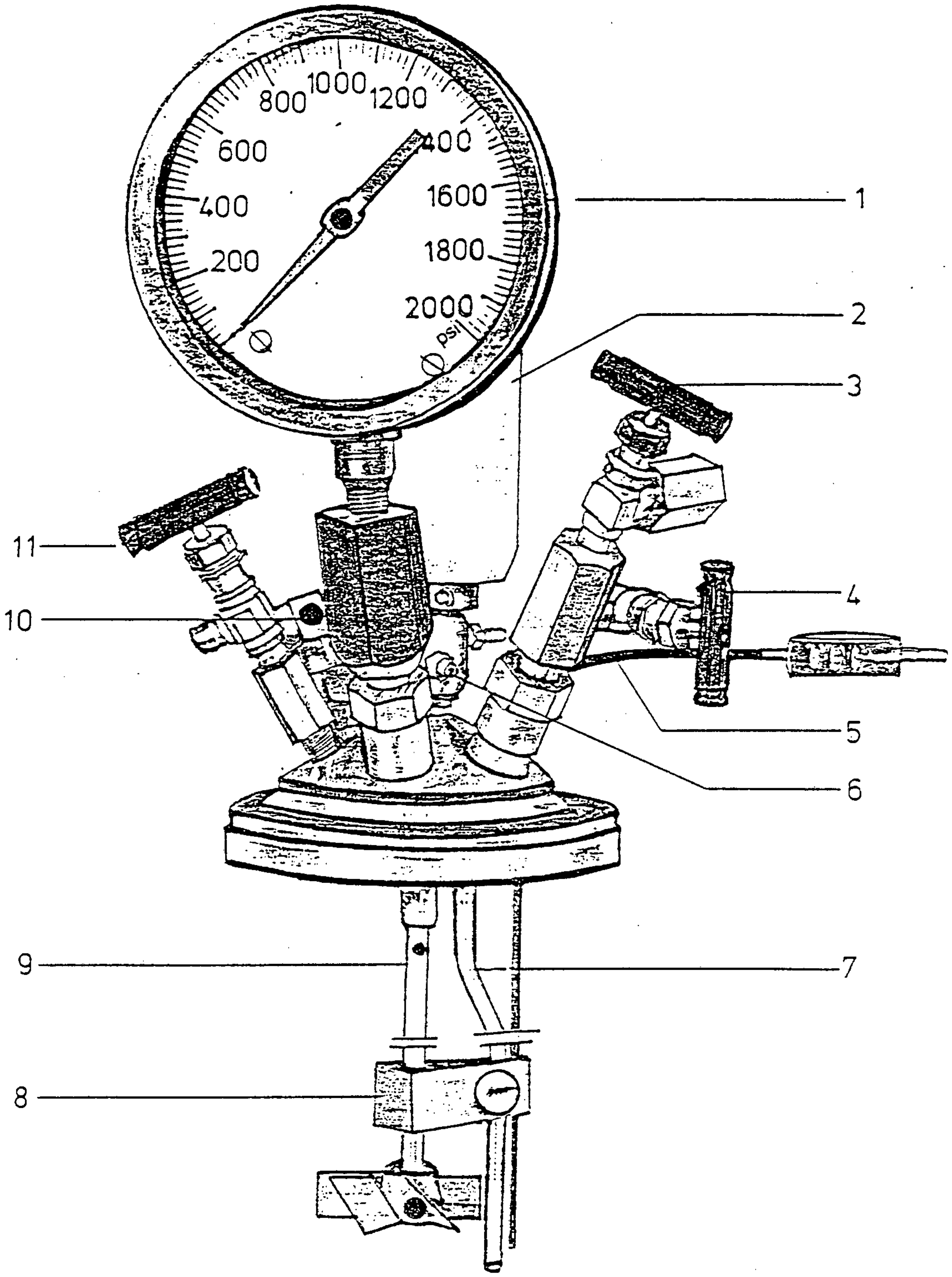

Figure 2.5 Gas handling system and instrumentation (Constant pressure reactions).

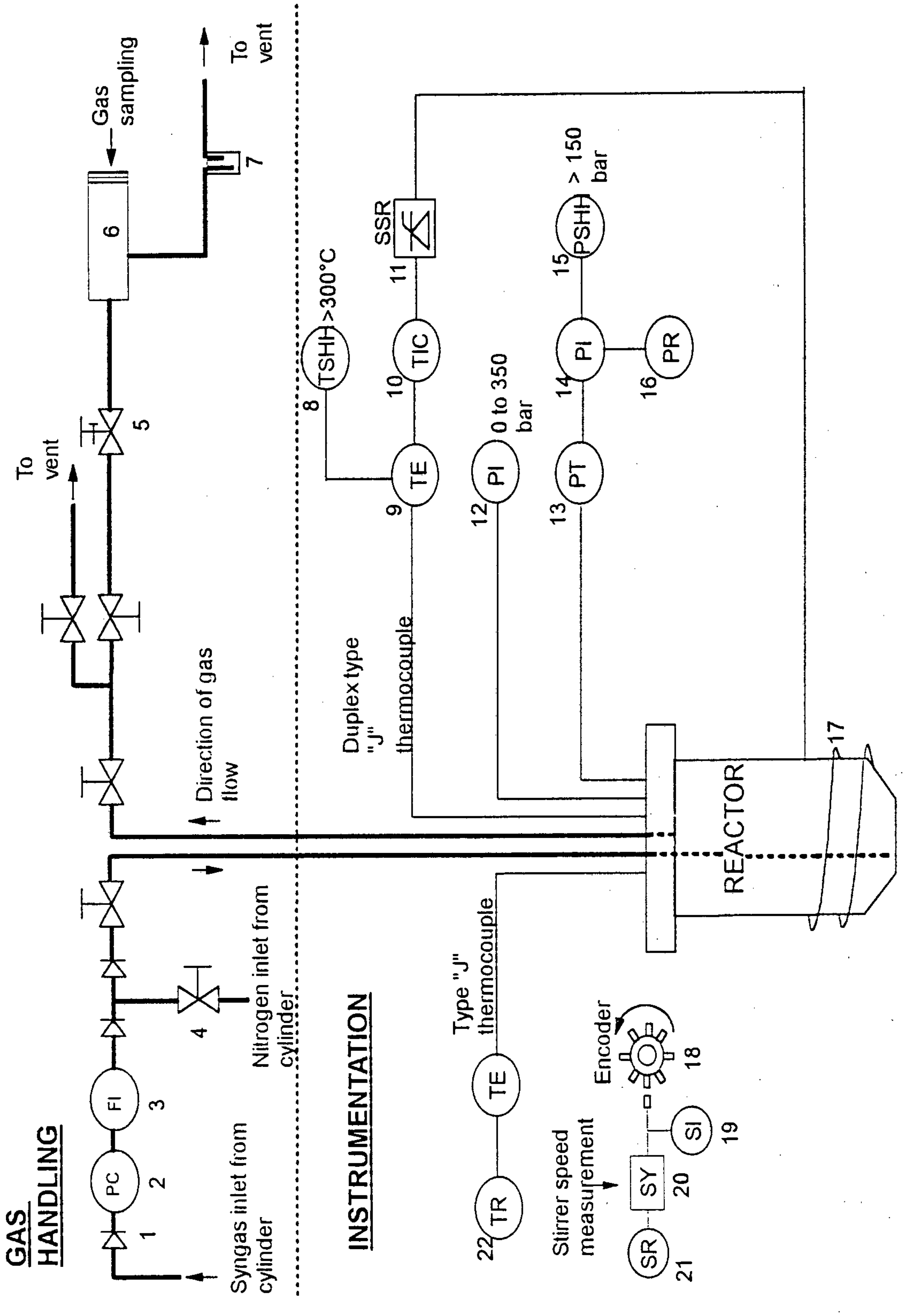

Key to Figure 2.5

Gas Handling system: ┃ (lines indicated in "bold").

1 Check (one-way) valve
2 Pressure controller
3 Flow indicator
4 Hand control valve (for connection to N_2 cylinder)
5 Metering valve
6 Gas ampule sampler (see Figure 2.6)
7 Bubbler on outlet of gas sampler

Instrumentation for reactor: │ (lines indicated as "normal").

8 Temperature switch high-high (designates a trip signal)
9 Temperature emitter (readout)
10 Temperature indicator + controller
11 Solid state relay
12 Pressure indicator (pressure gauge)
13 Pressure transducer
14 Pressure indicator
15 Pressure switch high-high (designates a trip signal)
16 Pressure recorder
17 Reactor heating (mantle)
18 Encoder for stirrer speed measurement
19 Speed indicator
20 Speed conditioner (thyristor drive)
21 Speed recorder
22 Temperature recorder

Figure 2.6 Details of gas ampule equipment:

Longitudinal Section of the Ampule Sampler

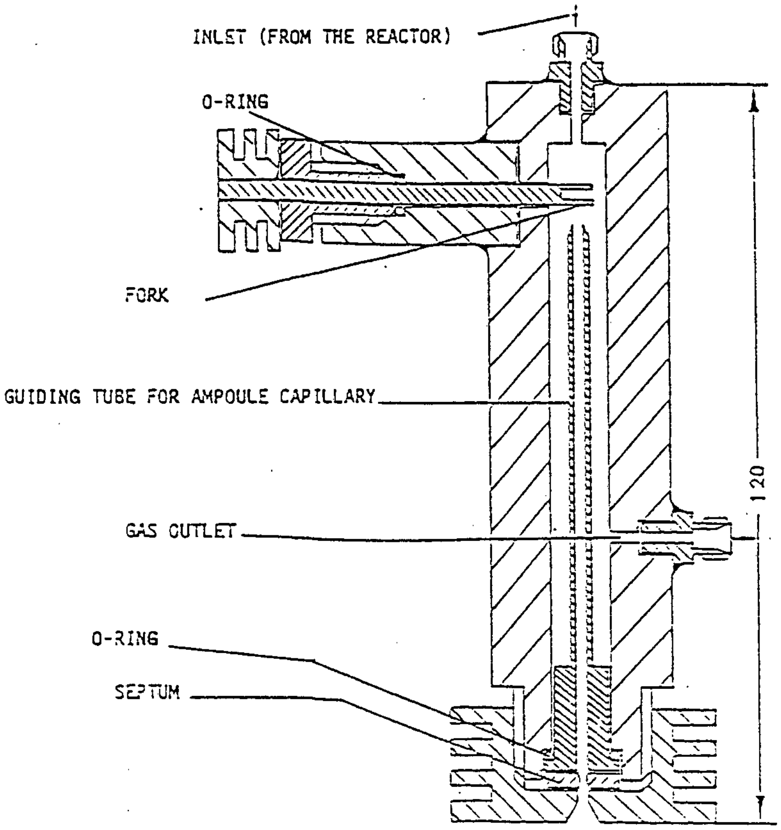

Dimensions of an Evacuated Gas Ampule

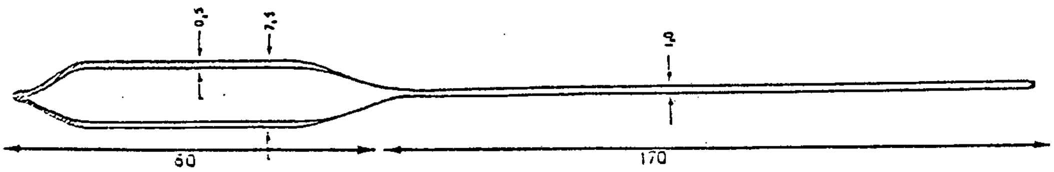

Dimensions = mm.

Drawings courtesy of P. van Berge

2.1.3 Continuous Reactor System for Process Demonstration (Work in Chapter 6)

The system was used to a) test whether Synthol feeds could be hydroformylated continuously, b) to demonstrate a method of continuous homogeneous catalyst recycle and c) test an applicable kinetic model generated from the smaller micro-reactor work.

The system is illustrated by means of a flow diagram in Figure 2.7, and a brief description of the operation follows. Various numbered items are referred to in the text describing the system so as to assist the reader.

A commercial F-T synthesis gas termed Arge Pure Gas (APG) was compressed from 25 bar(g) to 150 bar(g) by means of a Haskel compressor (45). This pressure was stepped down to 90 bar (g) by means of a Brooks thermal mass flow controller (47) which also regulated the gas flow to the reactor.

The reactor (B) consisted of a 9 litre vessel to which an air driven magnetic stirrer supplied by Autoclave Engineers was fitted. The liquid volume inside the reactor was determined by the distance that a dip tube (19) was inserted from the top of the reactor, and the remainder of the volume was occupied by synthesis gas. For more detail of the reactor see Figure 2.9.

The syngas, fresh-feed oil and recycle (which contained catalyst) streams entered through nozzles at the bottom of the reactor. The fresh feed was delivered to the reactor via a positive displacement pump from a 15 litre feed vessel (A), the contents of which were kept under Argon. The recycle stream was also re-introduced via a positive displacement pump as discussed below. The reactor off-gas and product stream was taken off via the dip tube. The contents of the outlet were cooled in a knock-out vessel (C) in which gas-liquid separation occurred.

The off-gases passed via an additional vessel - the level pot (D) - to a Grove back pressure regulator (37), which controlled the pressure in the reactor system. When the pressure in the reactor system exceeded the setting on the back pressure regulator, the diaphragm on the Grove opened. The excess gas was then released and passed through a cooling knock-out pot (G), and an additional knock out pot (H) to remove any traces of entrained liquid before being flared. Liquid from the reactor which was separated from the off-gas in the first knockout pot (C), was still at high pressure. This liquid flowed to the level pot (D). The liquid level in the level pot was controlled by communication between a level probe in the level pot and the fresh feed pump. Liquid - at high pressure - in the level pot passed through a control valve (34), the function of which was regulated by the level in a downstream vessel termed the Short Path Distillation (SPD) feed pot (E) which was at low pressure and in which additional outgassing occurred.

Non destructive recycle of the catalyst was achieved by SPD. (See Figure 2.8).

The reactor content, or product, was introduced into a UIC manufactured model KD4 SPD unit from the SPD feed pot via a gear pump. The liquid entering the SPD unit (which was under vacuum), was spread around the heated walls of the unit by means of rollers. As the liquid moved down along the walls of the unit, the more volatile components were flashed off and condensed onto a "cold finger" or condenser situated internally along the length in the middle of the cylindrical unit. This distillate was collected in a product collection flask. The heavier residue which continued down the SPD walls, and contained the catalyst, ligand, heavies and some remaining hydroformylation product, was pumped by means of an additional gear pump to a catalyst holding vessel termed the purge vessel (F).

The purge vessel was kept under an argon atmosphere to prevent oxidation of the catalyst and ligand. A small portion of the purge pot contents was purged at regular intervals to prevent buildup of "heavy" components in the system. The catalyst lost during the purging process was replaced by introduction of a quantitative amount of "fresh catalyst" into the purge pot vessel.

The liquid level in the purge pot was maintained by a level probe in the said vessel that communicated with a positive displacement pump which recycled the catalyst and heavy recycle liquids to the reactor (B).

In essence the plant was therefore controlled by the following "cascade" effect: The SPD feed pump speed which was set, determined the level in the SPD feed vessel (E). The SPD feed vessel level (probe) communicated with the upstream control valve. The control valve opened (to drain the upstream level pot (D)) and closed so that the level in the SPD feed vessel (E) was maintained at the appropriate set value. The level pot (probe) communicated with the fresh feed pump, and "asked" for more liquid feed from the feed pump when the level was low (*ie.* fresh feed volume was not a control variable). The amount of liquid in the level pot was also determined by the size of the liquid recycle stream being sent back to the reactor. The recycle stream was regulated by the level in the purge vessel (F). The size of the recycle stream was determined by the operating conditions in the SPD unit, as well as the size of the purge.

The system incorporated Process Logic Control (PLC) in which variables including levels, flows, temperatures, pressures, and pump speeds were monitored, and the data for mass balance purposes was automatically logged by computer.

Additional discussions and details pertaining to the continuous reactor system are undertaken in Chapter 6.

Figure 2.7 Flow diagram (vessels, piping and instrumentation) of the continuous reactor system.

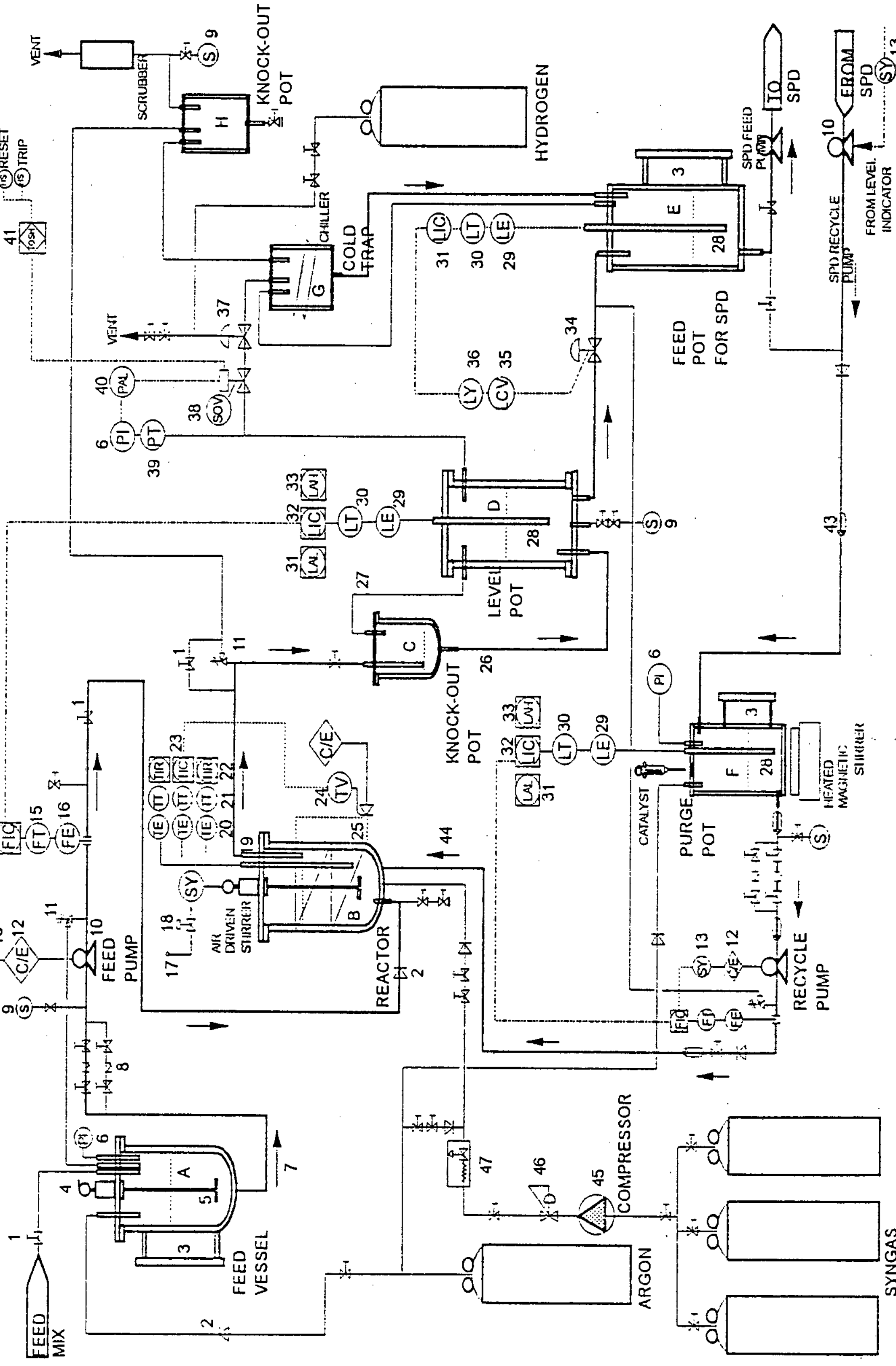

Key to Figure 2.7.

Vessels

A	Feed pot
B	Reactor
C	Knock-out pot
D	Level pot
E	SPD feed pot
F	Purge pot
G	Cold trap for entrained liquid condensation
H	Additional knock-out pot for remaining liquids in off gas

Piping and Instrumentation

1	Hand control valve	28	Level probe
2	Check (one way) valve	29	Level emitter
3	Sight glass (for visualization of liquid levels)	30	Level transmitter
4	Magnetic drive	31	Level alarm high
5	Stirrer paddles and shaft	32	Level indicator controller
6	Pressure indicator (gauge)	33	Level alarm low
7	Liquid line (direction of flow indicated)	34	Control valve (for taking liquids from high to low pressure)
8	In-line filters		
9	Sampling point	35	Level control valve (electrical)
10	liquid pump	36	Level thyristor
11	Safety release valve	37	Grove (back pressure regulator)
12	Designates "Control to Electrical"	38	Solenoid shut-off valve
13	Speed conditioner (thyristor drive)	39	Pressure transmitter
14	Flow indicator controller	40	Pressure alarm low
15	Flow transmitter	41	Electrical signal converter
16	Flow emitter	42	Trip / reset buttons
17	Air line for air driven stirrer motor	43	Heated catalyst recycle line
18	Air valve	44	Recycle line to the reactor
19	Dip tube (determines level of liquids in reactor)	45	Syngas compressor
20	Temperature emitter	46	In line pressure regulator
21	Temperature transmitter	47	Thermal mass flow controller
22	Temperature indicator recorder		
23	Control signal to temperature valve (= solid state relay)		
24	Temperature valve (= solid state relay)		
25	Reactor heating element		
26	Liquid flow line from knock out pot		
27	Gas flow line from knock out pot		

Figure 2.8 Flow diagram of the SPD unit and peripheral equipment

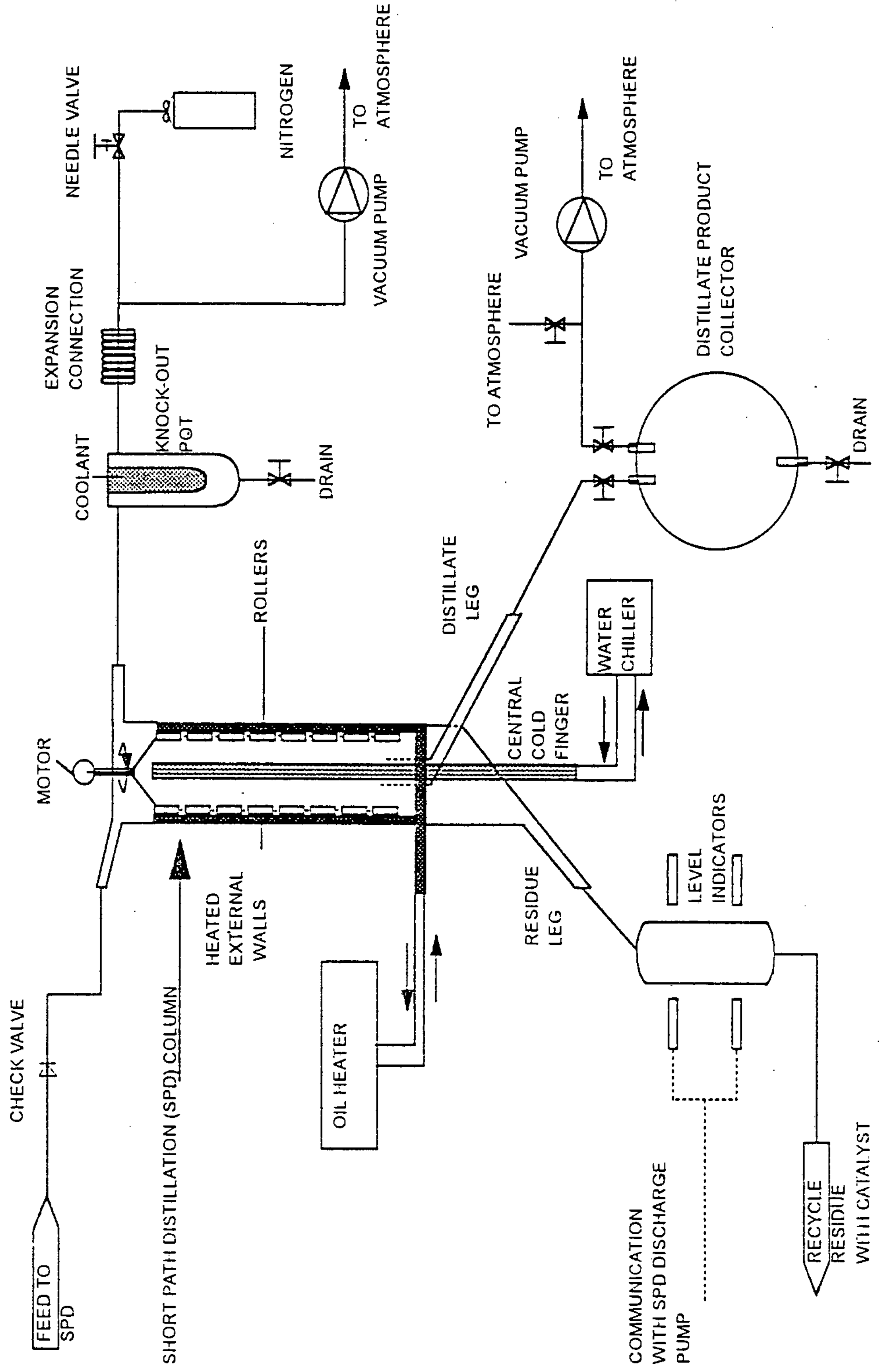

Figure 2.9 Schematic of the reactor used for continuous catalyst testing

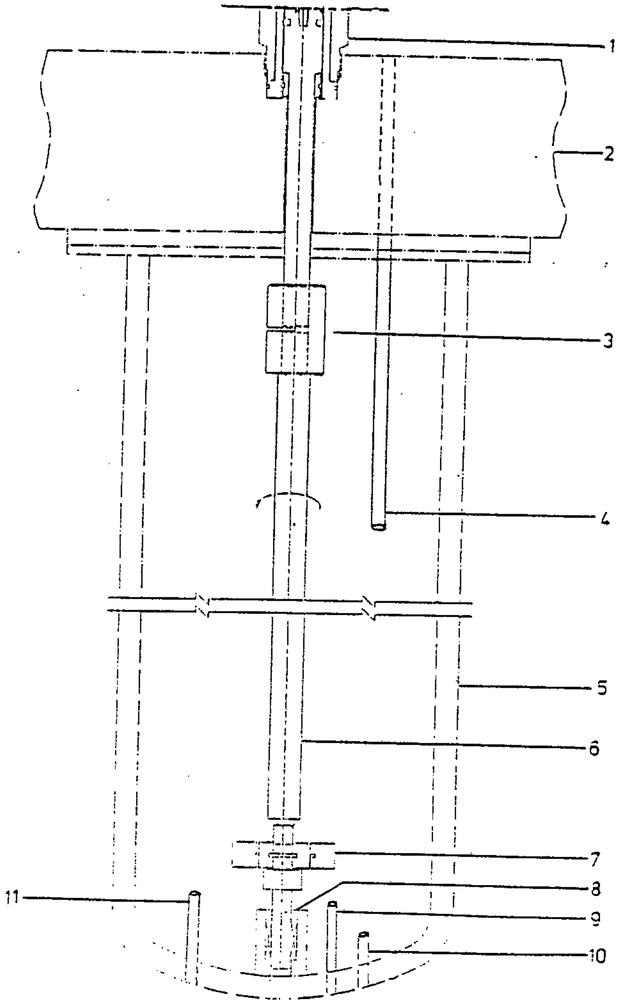

Key to Figure 2.9

1	Magnetic stirrer housing
2	Top flange cover
3	Shaft coupling
4	Dip tube (determines and maintains liquid level in the reactor)
5	Reactor vessel
6	Stirrer shaft
7	Impeller
8	Bottom housing for stirrer
9	Recycle (with catalyst) inlet line
9	Fresh feed inlet line
10	Gas inlet line
11	Feed inlet line

2.2 MATERIALS

2.2.1 Liquid Feeds

In this thesis, SLO is the general term referring to the petroleum and diesel fraction of the Synthol F-T product spectrum, and should not be confused with stabilized light oil terminology.

Feeds were prepared by distillation of HTF-T SLO reactor products to yield single and double carbon fractions. As an example, fractionation of the C_{10} portion of the HTF-T product spectrum yielded a "cut" of the type illustrated by way of a GC trace in Figure 2.10. The dark peaks are olefinic in character (identified by GC-MS). These correspond with Dry's model for predicting olefins and their distribution in HTF-T products in the C_{10} boiling range [Dry, 1993].

Figure 2.10 GC trace of C_{10} SLO fraction.

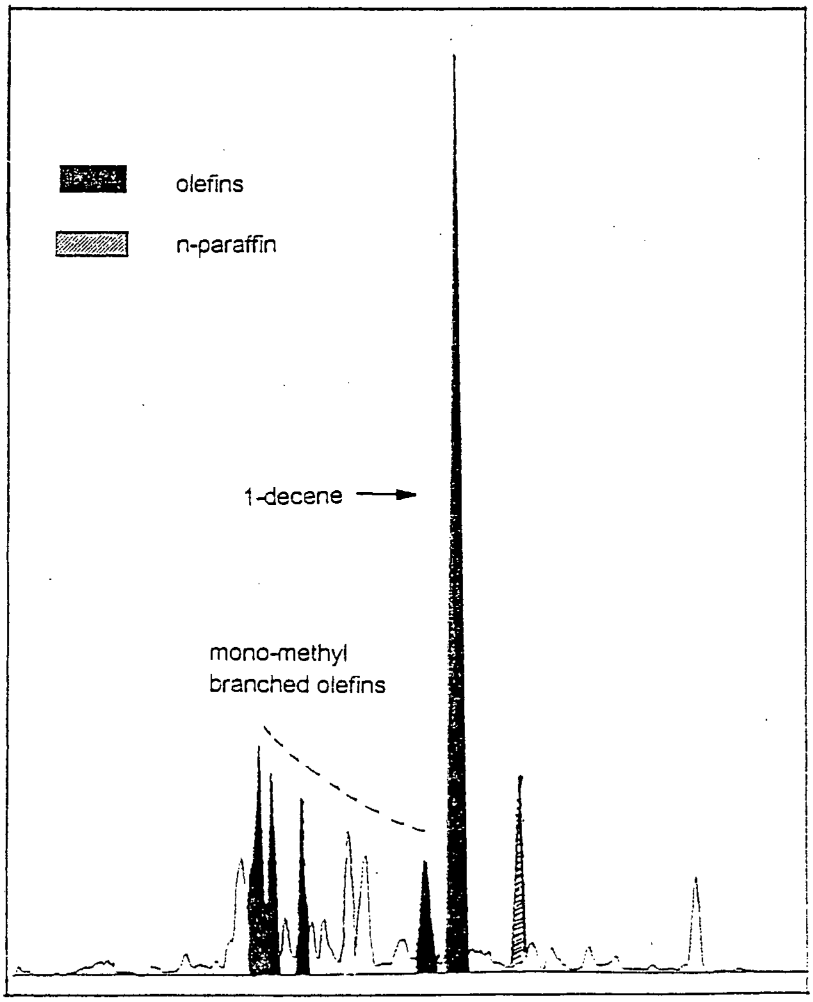

The model prediction of expected olefin distribution in a C_{10} SLO fraction is illustrated by way of a bar-chart in Figure 2.11.

Figure 2.11 Theoretical olefin distribution of the C_{10} portion of a HTF-T product spectrum: As predicted by modelling [Dry, 1993].

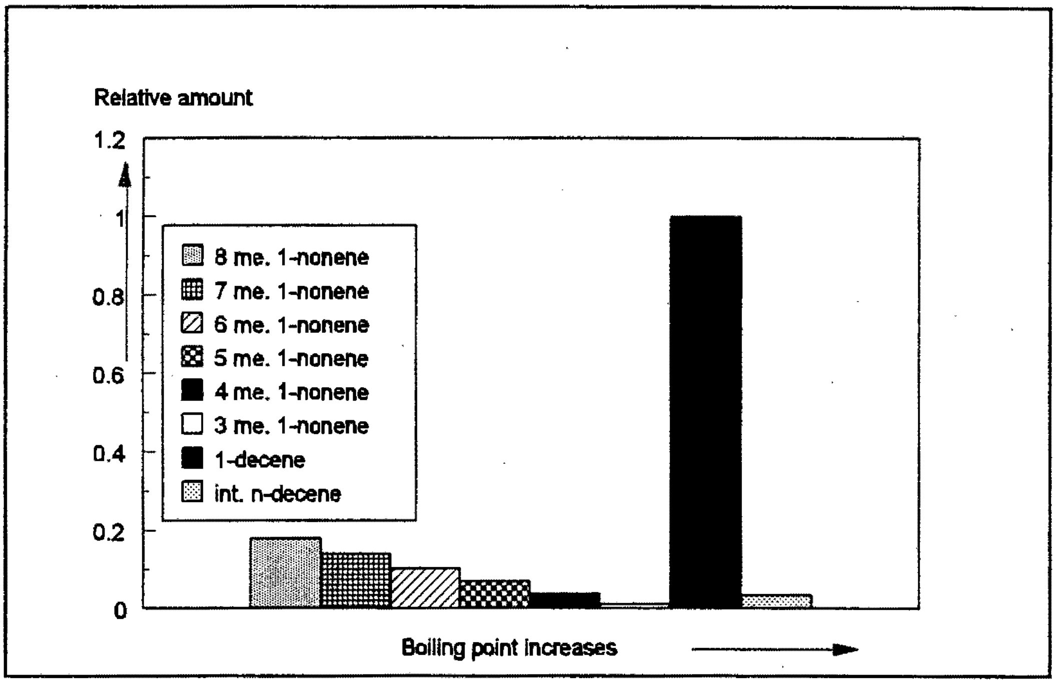

Hydroformylation results comparing 1-decene (> 94% pure from Aldrich and >96% pure from Merck) and SLO feeds were regularly undertaken during this study. n-Octane (99+% from Aldrich) was originally added to the pure olefin feeds in order to act as an inert internal standard and diluent, thereby acting as an additional "reference" for the SLO components. This was undertaken as all the SLO feeds contain non-olefinic components, which may or may not contain reactables, and the SLO fractions tested always contained diluted olefins. Possible "non-olefinic reactables" include aromatics and oxygenates with unsaturated alkyl chains. It was therefore reasoned that comparing pure with diluted feeds would not be as meaningful.

During the course of the work, n-octane was substituted by n-hexadecane (99+% pure from Aldrich) due to hexadecane's lower volatility compared with octane. This made analyses less prone to error due to lower losses caused by sample evaporation.

SLO $C_{8\text{-}9}$ broad, C_9 narrow, C_{10} broad, C_{10} narrow, and $C_{11\text{-}12}$ fractions were prepared by fractionation of SLO. Details on the feed compositions are outlined in the relevant chapters discussing testing of these feeds. The α-olefin content in the feeds could be increased by re-distillation of "broad" SLO fractions to isolate a desired portion of the F-T product spectrum into "narrow" fractions. (See Figure 3.1). It was demonstrated during the course of the work that carboxylic acids should be removed. This could easily be achieved by washing the feeds with equivolume quantities of 10% aqueous NaOH solution, followed by phase separation. In cases where emulsions formed, these were broken by means of CO_2 (solid dry ice) addition.

Until required, the SLO fractions were placed under refrigeration in sealed glass or stainless steel containers. It was demonstrated that allowing the feeds to stand for lengthy periods gave rise to peroxide formation [Kindermans, 1995] which had a significant impact on catalytic systems. The material was always used in as "fresh" a state as possible.

During the course of experiments various chemicals (all purchased from Aldrich) were added to the SLO feeds, for analysis confirmation purposes and on occasion for testing in the feeds. These included Indan (97%), propyl benzene (98%), cylopropyl benzene (97%), ethyltoluene (95%), butyl ether (99%), undecyclic aldehyde (or 1-undecanal) (97%), butyric acid (99+%), trans-5-decene (99+%) and n-decane (>95%).

Measured compositions of the various pure and SLO feeds are listed in the subsequent chapters (see Tables 3.1, 4.3 and 5.3) and in Appendices 1 to 3. It should be noted that as Synthol operating conditions can be changed over a wide spectrum (as indicated in Section 1.2.3), the SLO composition can vary significantly. Furthermore, because of the way in which the SLO fractions were "cut", the feeds used in this study was not necessarily typical of commercial Synthol product fractions.

2.2.2 Gases

Pure syngas mixtures consisting only of H_2 and CO were tested. The H_2:CO composition (%v:v) in these "pure" mixtures were typically 1:1, 1:2 and 2:1. These mixtures, bottled at approximately 130 bar(g), were supplied by the Fedgas company which claimed a syngas purity of 99.99%.

Gas simulating a commmercial syngas mixture was used and compared to the "pure" syngas in various experiments. The gas mixture tested had the following composition (volume %): H_2 = 56%; CO = 29%; CO_2 = 1%; CH_4 = 12%; N_2 (balance) = 2%.

2.2.3 Catalyst Precursors and Additives

The catalysts were mostly generated *in situ* under reaction conditions from the relevant metal precursors, ligands and synthesis gas. Additives were used in various experiments. Details of "heterogeneous" catalysts tested are in Table 3.5.1.

2.2.3.1 Metal precursors

The following metal salts and precursors were used (see Table 2.1):

Table 2.1 Metal precursors employed.

Metal Precursor	Chemical Formula	Supply Details
Rhodium (I) triacetylacetonate	$Rh(O_2C_5H_7)_3$	Strem Chemicals Inc. (99+%)
Hydrocarbonyl tris(triphenylphosphine) rhodium (I)	$HCORh(P(C_6H_5)_3)_3$	Strem Chemicals Inc. (99+%)
Rhodium (II) acetate dimer	$[Rh(O_2C_2H_3)_2]_2$	Strem Chemicals Inc. (99+%)
Tris (triphenylphosphine) rhodium (I) chloride	$((C_6H_5)_3P)_3RhCl$	Strem Chemicals Inc. (99+%)
Cobalt acetate	$Co(O_2C_2H_3)_2.4H_2O$	Saarchem; Merc; (99+%)
Cobalt octanoate	$Co(O_2C_8H_{15})_2$	Borchers: 10% Co containing solution : "Octasoligen"

2.2.3.2 Ligands

The following phosphine ligands were evaluated.

Table 2.2 Ligands evaluated.

Ligand tested	Abbreviation	Chemical formula	Supply details
Tri-PhenylPhosphine	TPP	$P(C_6H_5)_3$ MW = 262	From Aldrich; 99+% pure
Tri-n-ButylPhosphine	TBP	$P((CH_2)_3CH_3)_3$ MW = 202	From Fluka; 95% pure
Tri-n-OctylPhosphine	TOP	$P((CH_2)_7CH_3)_3$ MW = 371	From Fluka: 95% pure
bis-diPhenylPhosphinoButane	bis-PPB	$(C_6H_5)_2P(CH_2)_4P(C_6H_5)_2$ MW = 426	From Aldrich: 96% pure
Mixture of the following two isomers 9-Eicosyl-9-Phospha (3,3,1) bicylcononane 9-Eicosyl-9-Phospha (4,2,1) bicylcononane	EP	$(C_8H_{14})\ P(CH_2)_{19}CH_3$ MW = 442	From Hoechst 90% pure

MW denotes Molecular Weight.

Figure 2.12 Ligand Structures.

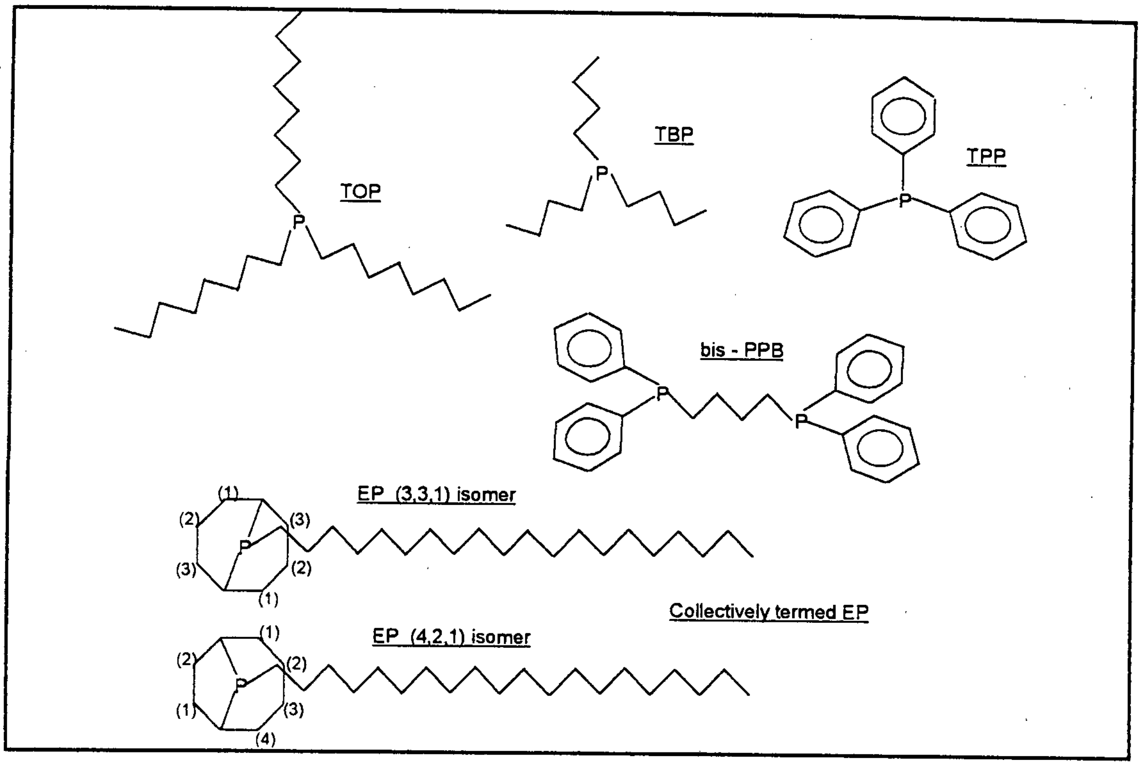

2.2.3.3 Additives

Potassium hydroxide (KOH; 90+% pure from CJ Chem.), and a linear alkylbenzene sulphonate (LAS) surfactant, dodecylbenzenesulphonic acid sodium salt, were used in various experiments.

2.3 CHARACTERIZATION AND QUANTIFICATION PROCEDURES

2.3.1 Liquids: By Gas Chromatography (GC)

Analysis of reactor liquids was undertaken on Perkin Elmer Model 8420 and Perkin Elmer Autosystem Gas Chromatographs using the conditions listed in Table 2.3.

Table 2.3 GC Conditions for analysis of liquids.

Column	Perkin Elmer; PONA capillary non-polar type; coated internally with 0.5µm methyl silicone stationary phase film; 50m long ; 0.25 mm ID;
Temperature program:	
Initial oven temperature	100°C
Time at initial temperature	20 minutes
Final Temperature	300°C
Time at final temperature	10 minutes
Temperature ramp	4°C / minute
Total analysis time	80 minutes
Carrier gas	He, purity >99.9%, 2 bar g head pressure
Detector	Flame Ionization Detector (FID): Air to H_2 flow ratio = 10:1.
Injector temperature	300°C
Detector temperature	300°C
Sample volume	0.2 µl (using a 0.5 µ SGE Syringe)
Sample splitter ratio	1 : 100

A typical gas chromatogram generated using the above conditions is illustrated in Figure 2.13. (Also see Appendixes 1, 2, and 3). The GC peak and peak area data in ASCII file format were transferred to Lotus spreadsheet files for further data handling. Identification of the peaks was facilitated by making use of Kovat's indices [Sadtler and Heyden, 1986], and GC-MS. In this regard, use was made of a Wiley 138 Mass Spectra Library on HPChem software. In addition, the appearance and disappearance of peaks was monitored, and known compounds were injected as an additional check. The peak areas were divided by known FID response or sensitivity factors [Dietz, 1967], and the sum of the corrected areas used to calculate the mass % of each component peak.

Figure 2.13 Typical GC Chromatogram of reactor liquids.

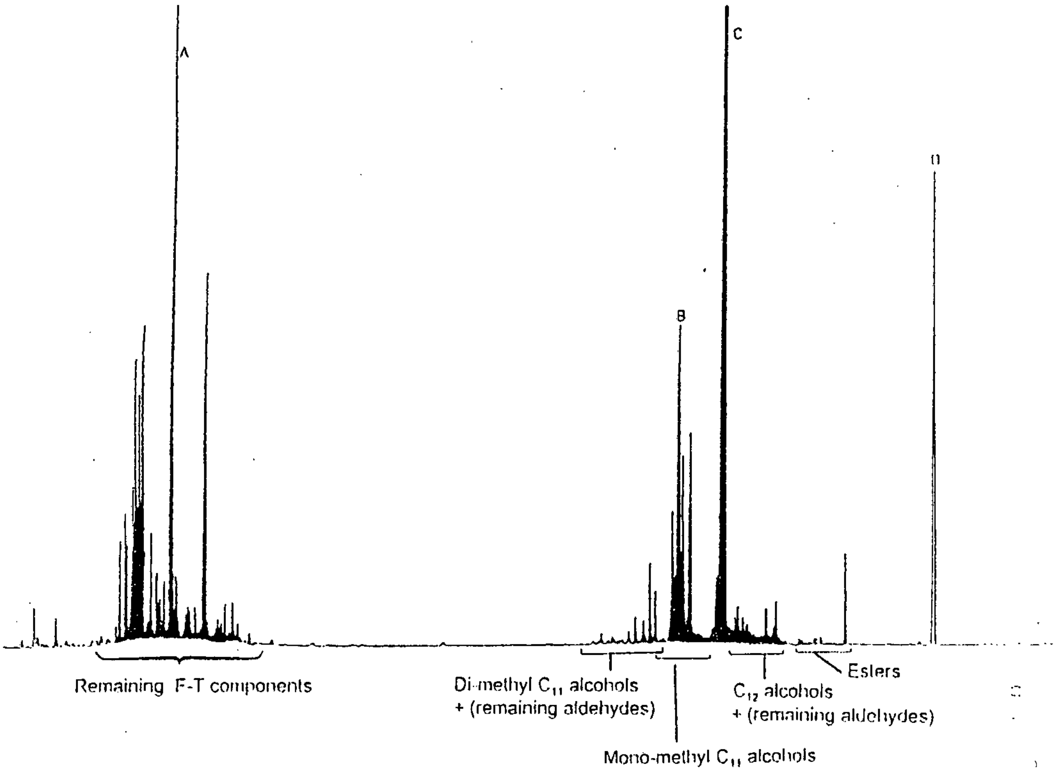

Key to main peaks in Figure 2.13.

A	n-paraffin (decane)
B	2-methyl decanol
C	1-undecanol
D	n-hexadecane (internal standard)

2.3.1.2 Quantification of Oxo Olefin Reactables in Synthol Products: A New Approach

Measuring the olefin content and distribution in Synthol products (especially the heavier fractions) represents a challenge. This is because of the large number of components present in the material, which often "mask" olefins in GC and GC-MS analysis. Hydrogenation of the F-T products in order to simplify the product spectrum has previously been used as an analytical tool by Pichler *et al.* [1967] and Beck [1967]. This entails hydrogenation of all the olefins and oxygenates without isomerization, thus improving the skeletal characterization of the F-T product spectrum. Although convenient for simplifying analyses, the hydrogenation technique still does not completely solve the problem of peak masking, and olefin quantification, especially not in the context of quantifying "oxo reactables."

Comparing samples before and after hydrogenation on a polar GC column which can separate olefins, paraffins and oxygenates may be useful in this regard. However, in higher olefin containing fractions, various unsaturated compounds such as cyclics with unsaturated side-chains exist which may be difficult to distinguish from other olefins. In addition, these compounds may or may not be hydroformylated due to stearic constraints.

Quantification of "oxo reactable" has largely been solved by the use of exhaustive hydroformylation reaction chemistry as a tool for measuring the aliphatic olefin content and distribution. This was achieved by making use of detailed analysis of the remaining SLO as well as reaction products. Reaction selectivities, mass balances and product data were then used to "back compute" the reactive olefin composition in the feed/s using the methodology discussed below.

Examples of GC traces with MS peak identifications and breakdowns of reactor contents measured using this approach are included in Appendices 1 to 3.

The following approach to <u>quantification</u> of the data obtained from GC and GC-MS was used:

The contributions of liquid components measured by GC were expressed as mass%. This necessitated making use of internal standards to correct for the mass increase/s of the system/s as a result of hydroformylation.

The internal standard may be added as an additional inert component. Alternatively, the mass increase in the system can be determined from GC analyses by theoretically calculating a "dilution factor" , *f*.

Dilution factors were calculated on the basis of the increase in mass of liquid initially in the reactor as a fraction of the mass of liquid at time *t* using the following equations:

$$f(t) = \frac{M_{\mathit{internal\ std.}\ t_t}}{M_{\mathit{internal\ std.}\ t_0}} \tag{2.1}$$

where t_0 = time zero.

Alternatively,

$$f(t) = \frac{1 - F(t)}{1 - F(0)} \tag{2.2}$$

where

$$F(t) = \sum_{j=1}^{n} \left(\frac{MW_j - MW_r}{MW_r} \right) M_j \tag{2.3}$$

where n is the number of liquid species present in the reactor, M_j and MW_j the mass fraction and the molecular weight of component "j" respectively which was produced from reactant olefin "r" with molecular weight MW_r

Internal standards were made use of in various runs whilst calculated dilution factors were used for the balance of the experiments. No significant differences in the calculated results were evident when using the "internal standard" or calculated "dilution factor" as a method to allow for an increase in mass of the reactor liquids. This is illustrated by means of a comparison in Appendix 4.

The following formulae were used for calculating olefin content (corrected for peak masking) from exhaustive hydroformylation reactions, as well as for calculating conversions and selectivities. The corrected olefin mass fraction $M_{r,t}$ in the reactor at time t was calculated as follows:

$$M_{r,t} - M_{r,t\,(measured)} - M_{r,t_{ex}} \frac{f_t}{f_{t_{ex}}} \qquad (2.4)$$

Where $M_{r,tex}$ was the contribution to the mass fraction of the peak which masked the olefin peak. This peak was exposed after exhaustive hydroformylation at time $t_{ex.}$, and was identified by GC-MS.

The percent olefin conversion at time t was calculated using the following formula:

$$100\left(1 - \left(\frac{M_{r,t}}{M_{r,t_0}}\,\frac{f_{t,0}}{f_t}\right)\right) \qquad (2.5)$$

The reaction selectivities to paraffins, aldehydes, alcohols and heavy oxygenates were calculated on the basis of moles of olefin converted. For example, the percent selectivity to component *x* at time *t* was calculated as follows:

$$100\left(\frac{M_{x,t}/f_t - M_{x,0}/f_0}{MW_x}\right)\left(\frac{MW_r}{M_{r,0}/f_0 - M_{r,t}/f_t}\right) \qquad (2.6)$$

The selectivity values for the various reactions were normalized to sum to 100%. Typically, errors of between 0% and 12% were encountered. The average error was approximately 3%. Data points / samples giving rise to relatively large errors were discarded. A "selectivity fingerprint" was used to ascertain the validity of the experimental data as well as the identification and quantification of components in the feeds and products.

Further confidence in the quantification and reliability of analyses is illustrated by way of examples in Appendices 5 and 6, which give results of a mass balance over a batch system, as well as the GC result of a "make-up" mixture of SLO and pure oxo alcohols derived from SLO olefins.

2.3.2 Gases : GC Analysis

Glass gas containing ampules (see Figure 2.6) were broken under vacuum by means of an ampule breaker designed specially for this purpose. The released gases passed into a sample loop system before being analyzed on a Chrompack, Model CP 900 Gas Chromatogram with peripheral adaptions for analysing gas from ampules. The GC was equipped with two Thermal Conductivity Detectors (TCD's) to enable simultaneous determination of H_2, Ar, N_2, CO, CH_4 and CO_2 gases. This is due to the fact that no commonly used carrier gas can facilitate simultaneous determination of these gases. H_2 was analyzed separately on one channel using Ar carrier gas after passing through a packed molsieve column. The balance of the above mentioned gases were analysed (CO was of interest in this study) on the other TCD channel after passing through a packed carboxen column and using He as a carrier gas. A sample valve switching system ensured that the same syngas pressure was achieved at the head of the two columns. This simplified the quantification of the GC results. Calibration gas samples (see Figure 2.14) were run regularly, and the results used to determine the correction factors required for quantification of the GC analyses.

The gas ampule techniques is very useful as it allows for more than one sample to be taken (*ie.* repeatability can be checked) and gas sample storage is facilitated.

Table 2.4 GC conditions for gas analysis.

Temperature Program:	
Initial oven temperature	10°C
Time at initial temperature	7 minutes
Final temperature	210°C
Time at final temperature	zero
Temperature ramp	30°C per minute
Total analysis time	16 minutes
Carrier gases	He, Ar
Detector	TCD
Injector temperature	250°C
Detector temperature	150°C

Figure 2.14 A typical gas chromatogram of the TCD analysis of an ampule containing a mixture of the permanent gases.

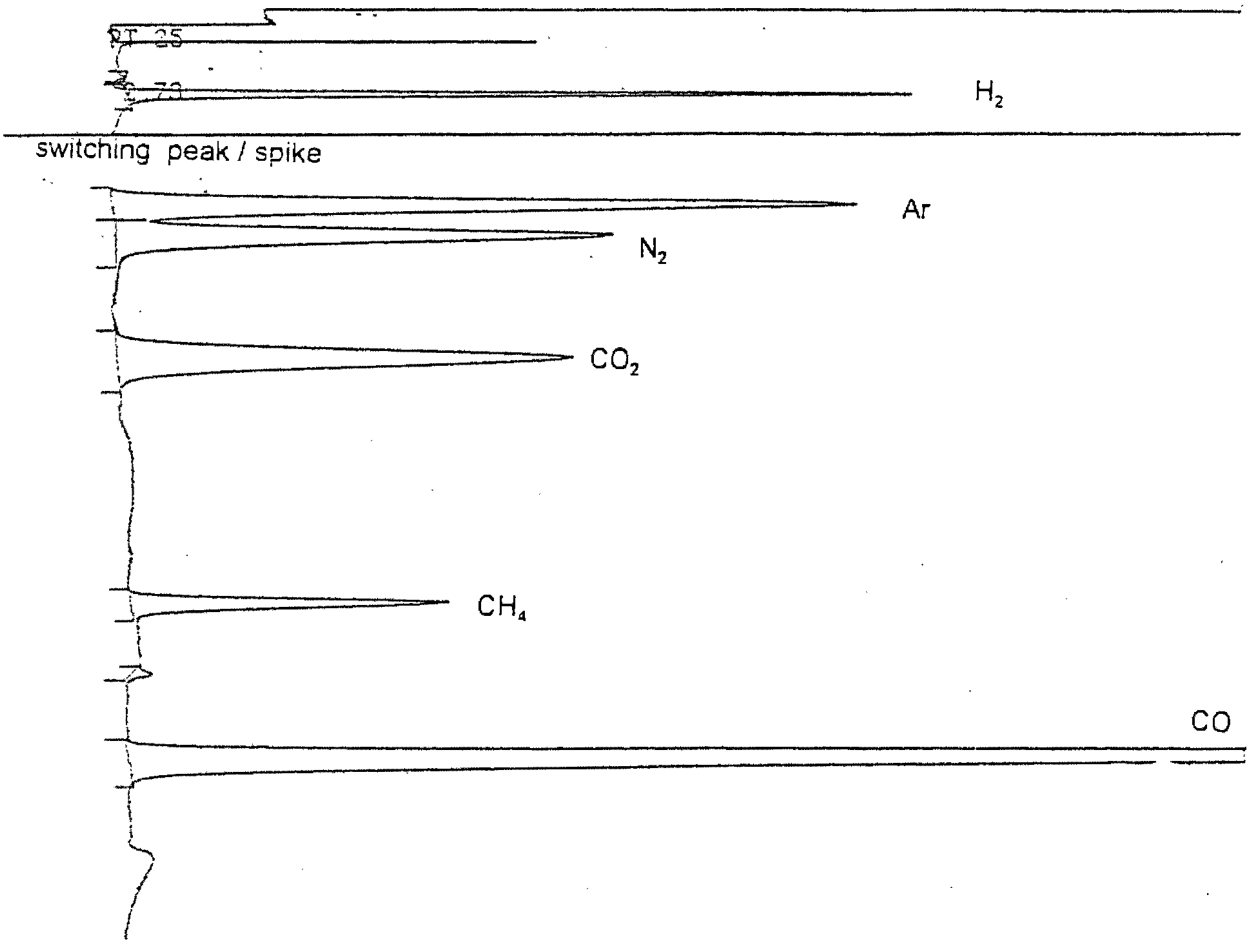

2.3.3 Catalyst Analyses

Not much emphasis was placed on this topic, since conversions, selectivities, product linearities and reaction kinetics were of primary importance. However, towards the end of the study it became evident that more detailed characterization of the actual catalyst complexes could have proven useful in explaining various observations. Various methods, as outlined below, were used from time to time for quantifying the catalyst metal and ligand components after hydroformylation. This however did not prove very useful, since removing the catalyst complexes from the reactor possibly resulted in their disintegration and/or oxidation.

2.3.3.1 Cobalt determinations

A UV-VIS colorimetric method was used to determine the concentration of cobalt in the reactor contents from time to time to check for cobalt deposition or plating. Cobalt was extracted from the relevant samples with HCl solution to form a blue $[CoCl_4]^{2-}$ complex using the following procedure:

- 2ml of cobalt containing sample was mixed with 20ml of fuming HCl containing 6g per litre of $SnCl_2$.
- Mixing took place in a separating funnel and was followed by separation of the organic and aqueous phases. This extraction procedure was repeated an additional three times.
- The blue acidic cobalt containing solution was made to 100ml in a volumetric flask.
- After filtering the contents, the absorbance of the solution was measured at 690nm on a UV-VIS spectrophotometer with a 1cm pathlength quartz cell.
- The [Co] was determined by making use of a calibration curve of absorbance vs Co concentrations for standard cobalt solutions.

Various Co determinations where also undertaken on "heterogeneous" catalyst particles. Soxhlet extraction was used to separate particles from the organic liquid. ICP, SEM/EDAX and wet chemical techniques were used to analyze and characterize the particles before and after hydroformylation. UV-VIS spectroscopy was used to measure for Co in solution as described above.

2.3.3.2 Ligand analyses

With the exception of EP and bis-PPB, the analysis of the TPP, TBP and TOP ligands and their corresponding oxides could be undertaken directly using the same GC conditions and column on which the product analyses were performed.

In hindsight again, insufficient care was probably taken during the sampling of reactor contents during this study, so that the degree of ligand oxidation - which was often observed with pure and SLO feeds - could not be ascribed to oxidation in or outside the reactor. This was not considered important at the time, since it was shown fairly early on in the study that similar results for pure and SLO feeds were obtained in this regard. In addition, it was previously demonstrated by others (see Section 4.4.9.2), that the kinetics and selectivities are relatively insensitive to the P:Co molar ratio if this ratio is maintained above a value of around one for alkylphosphine modified systems. However, on the continuous reactor system, these considerations were important, and the GC analyses were complimented by GC-Atomic Emission Detection (AED) analyses run in the phosphorous and oxygen modes.

The use of Infra-Red (IR) techniques to characterize hydroformylation catalyst complexes, and specifically *in-situ* IR measurements [Mirbach *et al.*, 1981] would prove useful in ascertaining the effect of reaction variables on the catalyst and ligand structures and possibly give insights into reaction mechanisms, and the effect of various additives. This is, on its own, is a subject for a detailed study.

CHAPTER 3

EVALUATION OF CATALYST SYSTEMS FOR HYDROFORMYLATION OF HTF-T PRODUCTS

3 EVALUATION OF CATALYST SYSTEMS FOR HYDROFORMYLATION OF HTF-T PRODUCTS

3.1 INTRODUCTION

3.1.1 Approaching the Problem: Selection of Catalyst Systems for Testing

A number of exploratory phosphine modified rhodium and cobalt catalyzed hydroformylation experiments were performed. The aim was to achieve high selectivities to linear aldehydes and/or alcohols from 1-decene and various Synthol Light Oil (SLO) fractions, in order to test their suitability as hydroformylation feeds.

Under consideration were; feed - catalyst compatibility; the hydroformylation product "fingerprint" (GC spectrum); as well as unwanted side reactions. For the exploratory experiments, C_8 (purified), C_9 and C_{10} portions of the HTF-T product spectrum were tested as feeds (see Section 3.1.2) for comparison with 1-decene.

Selection of reaction conditions

Initial reaction conditions for these systems were selected using the information listed in Table 1.6 (see Section 1.3.3) as a guideline. For the "pure" 1-decene runs, n-octane was added in quantities similar to those expected to constitute non-olefinic components in the SLO fractions. Apart from acting as a diluent, the n-octane also served as an internal standard (see Section 2.2.1).

Rh experiments

TPP was selected as the only ligand for testing as it finds widespread application in the hydroformylation of light olefins [Falbe,1980]. Numerous reports on the use of TPPite (tri-phenylphosphite) for use with Rh also appear in the literature, but use of this ligand can give rise to olefin isomerization [Jongsma *et al.*, 1991][Pruett and Smith, 1969]. Furthermore, it does not at present appear to be used in industrial processes. In addition, making use of large excess of TPP has been reported by Fell [1977] to facilitate virtually isomerization free hydroformylation. If one plots reaction rates against TPP concentration, the curves pass through a maximum and then remain constant at higher concentrations of TPP [Hjortkjaer, 1979][Brown and Wilkinson, 1970][Sanger, 1977/78]. Deshpande *et al.* [1993] confirmed this in a later study on the effects of various solvents in the Rh/TPP catalyzed hydroformylation of 1-octene. Oswald *et al.* [1982, 1992] have undertaken an extensive series of experiments on the Rh/TPP catalyzed hydroformylation of 1-butene in which the effects of excess ligand, temperature and P_{CO} were studied.

Co experiments

Cornils, in Falbe's review [1980], lists numerous ligands that have been reported suitable for use with Co. However, the use of phosphines is most widespread, and alkyl phosphines as patented by Shell [Slaugh and Mullineaux, 1966, 1968,1969] appear to be the only ligands used commercially with Co. Most of the literature concerning the use of phosphines with cobalt, refers to the use of linear alkyl phosphines, and specifically tri-n-butyl phosphine (TBP). It was therefore decided to undertake screening experiments with this ligand, and compare the results with TPP ligands (which may also be used with Co). These experiments were undertaken with a view to achieving high alcohol product linearities. The same approach was followed as with the Rh/TPP experiments discussed previously, namely, comparing the performance of the catalysts when using 1-decene and SLO, and using this as a measure of feed-catalyst compatibility.

3.1.2 SLO Feeds Evaluated

A breakdown of the "broad" and "narrow" F-T fractions used as feeds in this chapter are listed in Table 3.1. These analyses may be taken as representative of the C_8, C_9 and C_{10} feeds used in this chapter, but are not necessarily representative of actual Synthol product fractions. This is due to various components being concentrated up or down during distillative preparations of the fractions. Azeotropic distillation with methanol was made use of in preparing the C_8 fraction.

Table 3.1. Typical analyses of broad and narrow SLO fractions as used in this Chapter: GC FID results.*

	SLO Fractions Tested			
Composition (by mass%)	C_{10} broad	C_{10} narrow	C_9 narrow	C_8 narrow (excl. methanol contribution)
1-octene	-	-	-	81.0
C_8 paraffins	-	-	-	9.2
C_9 iso-olefins	-	-	5.1	-
1-nonene	2.9	-	61.0	-
C_9 paraffins	0.1	-	9.8	-
C_{10} iso-olefins	19.7	3.3	-	-
1-decene	37.3	70.0	-	-
C_{10} paraffins	11.6	3.3	-	-
Aromatics	11.9	10.3	1.3	-
Oxygenates	8.3	12.3	-	-
Balance of unidentified components. (Collectively termed SLO)	8.3	0.8	18.3	9.8
Approximate olefin linearity (%)	65%	95%	92%	>99%

* Possible peak masking/overlapping is not taken into account

The effect of refractionating C_{10} F-T material so as to concentrate the linear α-olefin (in order to improve hydroformylation product linearity) is illustrated in Figure 3.1. This can be taken to represent a "cleanup" of the feed, in that the linear α-olefin concentration is increased.

Figure 3.1 Effect of refractionating a "broad" C_{10} F-T fraction into a "narrow" fraction.

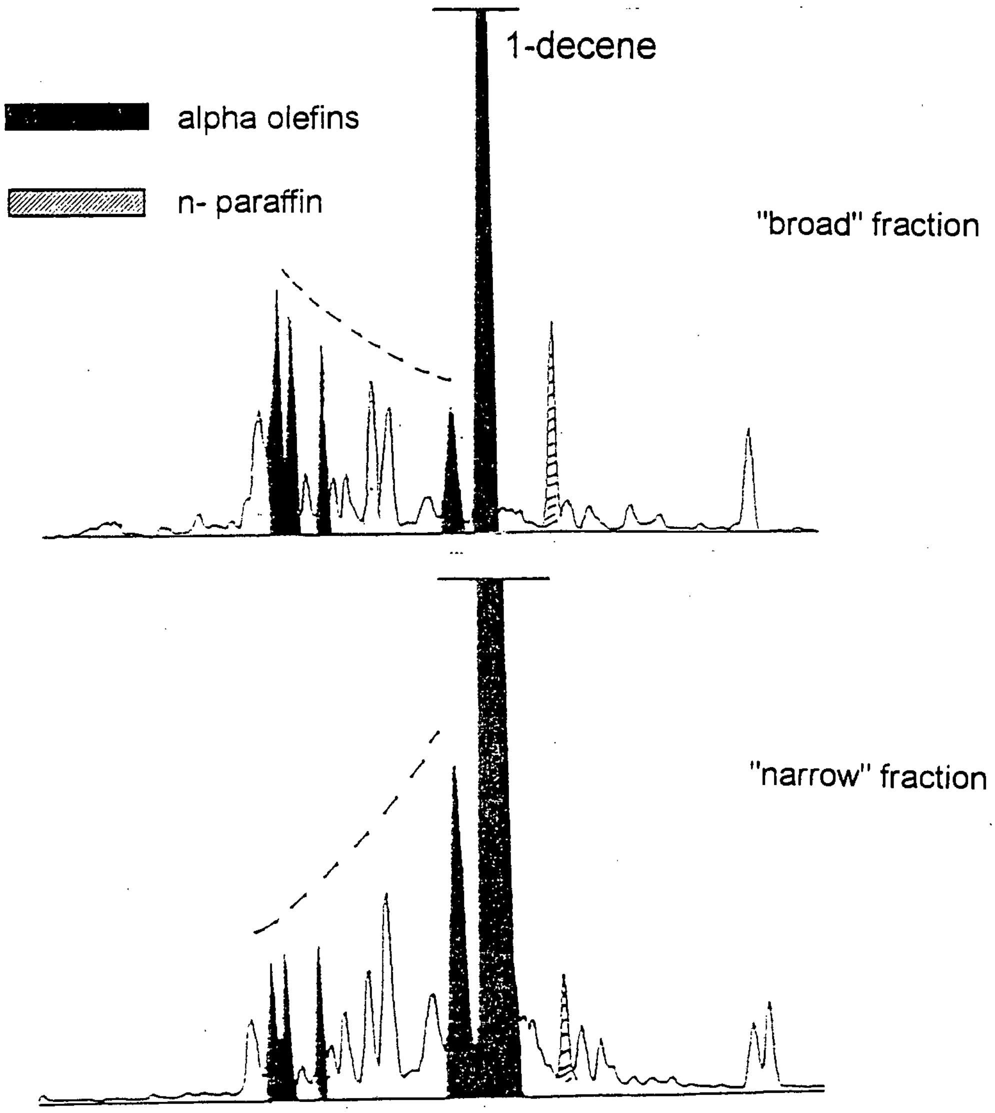

3.1.3 Theoretical Effect of Feed Refractionation on Product Linearities

The hydroformylation product linearity attainable with a linear feed is in the region of 90% for Rh/Phosphine and 85% for Co/Phosphine catalysts (see Table 1.6). Table 3.2 gives an <u>estimation</u> as to the extent of SLO cleanup (in terms of branched material removal) which would be required to produce products having various linearities. The table gives the theoretical values that may be obtained using phosphine modified Co and Rh (in brackets) catalysts. Parts of this table have been represented graphically in Figure 3.2.

In order to compile the table, the following assumptions were made:

(a) A "rough" or "broad" SLO cut typically contains 36% linear α-olefin; 22% branched α-olefins and 2% internal olefins.

(b) All the olefins become converted to hydroformylation products (*ie*; the olefins stand an equal probability of reacting).

(c) Branched olefins yield only branched products.

(d) Internal olefins yield only branched products with the phosphine modified Rh catalyst (as isomerization of the internal double bond is not common with these catalysts).

(e) Internal olefins yield linear products with the same selectivity as does the linear α-olefin when using a phosphine modified Co catalyst (isomerization of the olefin double bond to form the linear α-olefin which undergoes hydroformylation does occur with these catalysts)

From Table 3.2 and Figure 3.2 it is evident that theoretically, most of the branched material would have to be removed in order to yield a product with the desired linearity of ≥80%. This would make preparation of these feeds for producing linear hydroformylation products more costly. However, it may be possible to manipulate the reaction chemistry. Wender *et al.* [1956] have shown that in conventional Co systems, the respective reaction rates of 2-methyl 1-

pentene and 4-methyl 1-pentene are ± 88% and 3% slower than the rate for 1-hexene. If one considers Figure 3.1 (and compares it to Figure 2.11), it appears that the methyl branched α-olefins having branches closer to the olefin double bond and linear α-olefins are concentrated up at the expense of the other branched olefins. If 2 methyl α-olefins (and possibly 3- methyl α-olefins) are less reactive using an unmodified catalyst, these molecules should be even less reactive in a modified system due the electronic and steric factors already discussed. This possibility could be exploited in order to improve product linearities.

Figure 3.2 Theoretical product % linearities versus % of branched olefin removal from SLO at various selectivities to linear products (Phosphine modified Co catalysed).

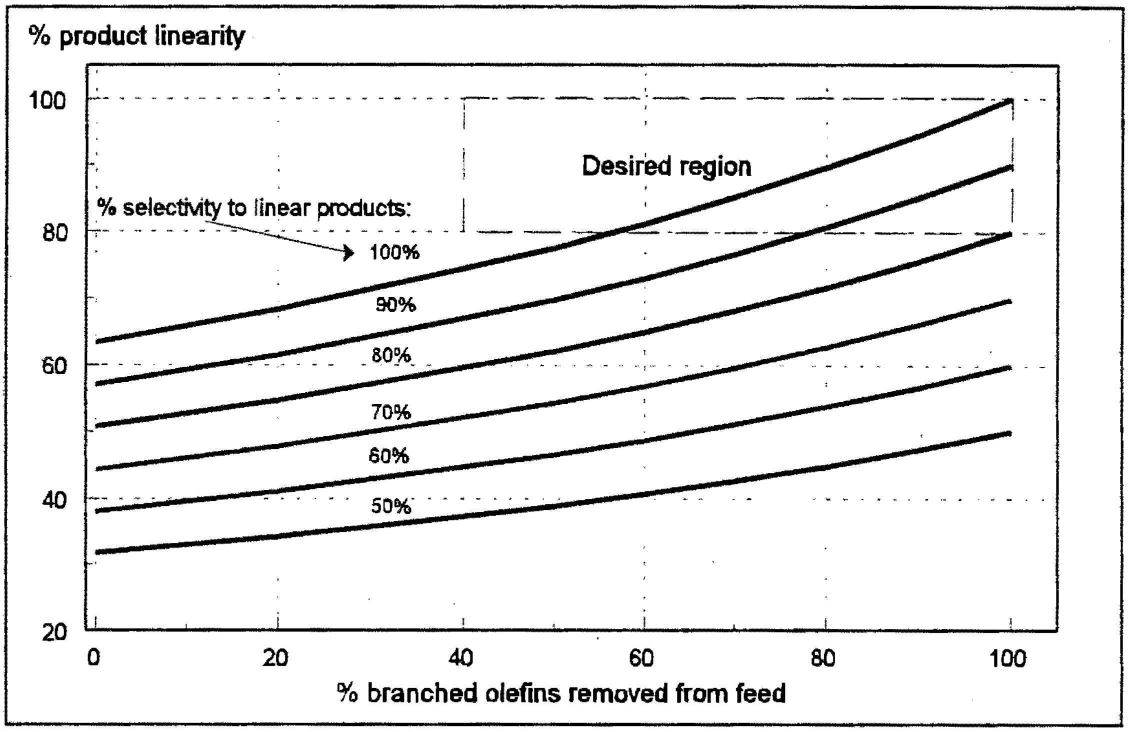

Table 3.2. Theoretical product linearities resulting from various degrees of branched olefin removal from SLO: Phosphine modified Co and (Rh) catalysts.

	Selectivity to linear products → → → → →	50%	60%	70%	80%	90%	100%
Degree of branched material removal ↓	SLO olefins distribution ↓	Overall hydroformylation product linearity					
0%	(1) 36 (2) 22 (3) 2	32 (30)	38 (36)	44 (42)	51 (48)	57 (54)	63 (60)
50%	(1) 36 (2) 11 (3) 2	39 (37)	47 (44)	54 (51)	62 (59)	70 (66)	78 (74)
60%	(1) 36 (2) 9 (3) 2	41 (39)	49 (46)	57 (54)	65 (62)	73 (69)	81 (77)
70%	(1) 36 (2) 7 (3) 2	43 (40)	51 (48)	60 (57)	68 (65)	77 (73)	85 (81)
80%	(1) 36 (2) 4 (3) 2	45 (43)	54 (51)	63 (59)	72 (68)	81 (76)	90 (85)
90%	(1) 36 (2) 2 (3) 2	47 (45)	57 (54)	66 (63)	76 (72)	85 (81)	95 (90)
100%	(1) 36 (2) 0 (3) 2	50 (47)	60 (57)	70 (66)	80 (76)	90 (85)	100 (95)

(1) Denotes % linear α-olefin

(2) Denotes % branched α-olefin

(3) Denotes % linear internal olefin

3.2 SCREENING EXPERIMENTS UNDERTAKEN (GENERAL)

Experiments were undertaken with phosphine modified Rh and Co catalysts as indicated in Tables 3.3.1 and 3.4.1. In addition, a number of "heterogenous" screening experiments were also undertaken as described in Table 3.5.1.

The general experimental procedures as explained in Chapter 2 were followed, whereby the runs were terminated (or re-pressurized and continued) once the pressure drop in the batch reactors ceased. *It should be emphasized that these were screening tests, a complication being that the pressure dropped during the course of the runs due to syngas consumption. This makes accurate comparisons between the runs difficult.* An additional complication is that sometimes more than one variable was changed in an attempt to arrive at a result (for example high conversion). Many of the results with pure feeds do not contribute anything "new" and merely confirm results already reported in the literature. However, these results are included in this study as they do shed some light on SLO versus 1-decene hydroformylation.

In order to present the experimental data and results in the least cumbersome manner, the following format has been chosen: For each catalyst system; tables of the experiments, will precede tables summarizing the results which will be followed by a short discussion. Mini-tables containing various information are included in the discussion to facilitate easier comparisons and assist the reader. A general conclusion comparing the various systems is included at the end of the chapter.

3.3 SCREENING EXPERIMENTS WITH Rh/TPP CATALYSTS.

3.3.1 Rh/TPP Experiments

Table 3.3.1 Screening experiments with Rh/TPP catalysts.

Run	Metal Precursor	[Rh] g/100 ml feed	Rh/olefin (mass%)	M:L * Molar ratio	Feed composition (volume/volume)	Temp °C	H_2:CO Molar ratio	Pi ** bar $_{(g)}$	Time (hours)	Reactor
1	$Rh(O_2C_5H_7)_3$	0.024	0.100	1/10	n-octane/1-decene = 3	100	1	$25_{init.}$	5.3	1 litre
2	$Rh(O_2C_5H_7)_3$	0.024	0.100	1/100	n-octane/1-decene = 3	100	1	$25_{init.}$	5.3	1 litre
3.1	$Rh(O_2C_5H_7)_3$	0.038	0.100	1/100	n-octane/1-decene = 2	100	2	$25_{init.}$	6.6	1 litre
3.2	Continuation of run 3.1 using 25 bar constant pressure of syngas					100	2	25_{const}	24	1 litre
4.1	$Rh(O_2C_5H_7)_3$	0.038	0.100	1/100	n-octane/1-decene = 1	100	2	$25_{init.}$	5.3	450 ml
4.2	Continuation of run 4.1 using 25 bar constant pressure of syngas					100	2	25_{const}	15	450 ml
5.1	$Rh(O_2C_5H_7)_3$	0.038	0.100	1/100	n-octane/1-decene = 2	100	2	$25_{init.}$	4	450 ml
5.2	Continuation of run 5.1; repressurizing to 25 bar					100	2	$25_{init.}$	4.5	450 ml
5.3	Continuation of run 5.2 using 25 bar constant pressure of syngas					100	2	25_{const}	15	450ml
6.1	$Rh(O_2C_5H_7)_3$	0.038	0.100	1/100	n-octane/1-decene = 2	100	2	$25_{init.}$	5	450 ml
6.2	Continuation of run 6.1 using 25 bar constant pressure of syngas					100	2	25_{const}	15	450 ml
7	$HCORh(P(C_6H_5)_3)_3$	0.017	0.025	1/200	n-octane/1-decene = 1	100	2	$25_{init.}$	1.5	1 litre
8	$[Rh(O_2C_2H_3)_2]_2$	0.035	0.050	1/100	n-octane/1-decene = 1	100	2	$25_{init.}$	1.5	1 litre
9	$Rh(O_2C_5H_7)_3$	0.07	0.100	1/100	n-octane/1-decene = 1	100	2	$25_{init.}$	12.3	1 litre
10	$((C_6H_5)_3P)_3RhCl$	0.07	0.100	1/100	n-octane/1-decene = 1	100	2	$25_{init.}$	15	1 litre
11	$Rh(O_2C_5H_7)_3$	0.056	0.156	1/10	SLO C_{10} fraction	100	1	$25_{init.}$	3.3	1 litre
12.1	$Rh(O_2C_5H_7)_3$	0.026	0.100	1/100	SLO C_{10} fraction	100	2	$25_{init.}$	7.7	450 ml
12.2	Continuation of run 12.1 using 25 bar constant pressure of syngas					100	2	25_{const}	7.7	450 ml
12.3	Continuation of run 12.2 using 120°C					120	2	25_{const}	6	450 ml
12.4	Continuation of run 12.3 using 35 bar constant pressure of syngas					120	2	35_{const}	15	450 ml
13	$HCORh(P(C_6H_5)_3)_3$	0.017	0.025	1/200	SLO C_{10} fraction	100	2	$25_{init.}$	1.5	450ml
14	$[Rh(O_2C_2H_3)_2]_2$	0.027	0.040	1/100	SLO C_9 narrow fraction (150ml) + 50ml octane	80	2	$25_{init.}$	4.1	1 litre
15	$[Rh(O_2C_2H_3)_2]_2$	0.015	0.080	1/100	100ml SLO C_8 narrow fraction (33%) + methanol (67%)	90	2	$25_{init.}$	5	1 litre
16	$[Rh(O_2C_2H_3)_2]_2$	0.027	0.040	1/100	150 ml C_{10} narrow fraction +50ml octane	90	2	$25_{init.}$	8	1 litre

* M:L denotes Metal:Ligand

** Pi denotes initial pressure

Note: Continuation of various runs was undertaken by repressurizing the reactor. This was done so as to increase the conversions, and in some cases to ascertain the effect of changing reaction conditions.

3.3.2 Results of Rh/TPP Screening Experiments

Table 3.3.2 Results of Rh/TPP catalyst screening experiments.

Run	%lin. α-ole conversion	%Sel. to int. olefin	%Sel. to paraffin	%Sel. to aldehyde	%Sel. to alcohol	%Sel. to HOF	%Product linearity. From lin α-ole.	%Overall product linearity. (aldehyde)
1	100	5.2	0.5	94	0 (tr)	0 (tr)	74.5	74.5
2	63.3	6.2	0.7	93	0 (tr)	0 (tr)	83.5	83.5
3.1	29.3	16.3	4.1	80	0 (tr)	0 (tr)	92.3	92.3
3.2	98.9	8.3	2.1	90	0 (tr)	0 (tr)	86.5	86.5
4.1	34.8	9.3	4.1	87	0 (tr)	0 (tr)	90.9	90.9
4.2	94.6	6.9	2.4	91	0 (tr)	0 (tr)	89.3	89.4
5.1	30	10.3	3	86	0 (tr)	0 (tr)	91.7	91.7
5.2	71.8	8.9	2.3	88	0 (tr)	0 (tr)	91.7	91.7
5.3	95.6	9	2.6	88	0 (tr)	0 (tr)	87.2	87.2
6.1	38.4	18.5	5.5	76	0 (tr)	0 (tr)	91.2	91.2
6.2	97.7	10.4	6.8	83	0 (tr)	0 (tr)	88.7	88.7
7	99.2	32.6	6.6	60	0 (tr)	0 (tr)	88.5	88.5
8	92.8	32.7	17.9	52	0 (tr)	0 (tr)	90.4	90.4
9	90.2	2.7	2	94	0 (tr)	0 (tr)	85	85
10	95.6	2.9	2.2	95	0 (tr)	0 (tr)	85	85
11	97.2	9.7	1.7	89	0 (tr)	0 (tr)	64.5	41.1
12.1	14.7	2.3	1.4	96	0 (tr)	0 (tr)	79.3	62.8
12.2	29.4	1.4	1.4	97	0 (tr)	0 (tr)	76.1	55.5
12.3	41.3	2.5	2.3	95	0 (tr)	0 (tr)	75	56.4
12.4	68.7	4.6	8.3	87	0 (tr)	0 (tr)	63.4	46.2
13	97.8	4.1	7.2	89	0 (tr.)	0 (tr.)	76.9	54.1
14	93.2	0 (tr.)	2.8	97	0 (tr.)	0 (tr.)	80.6	4.1
15	99.2	0 (tr.)	1.7	92	0 (tr)	3.8	87.6	84.4
16	97.6	17.5	14.5	66	0 (tr)	0 (tr)	88.9	83

3.3.3 Discussion of Results: Rh/TPP Screening

3.3.3.1 Rh/TPP Testing: 1-Decene Feeds

The Ligand to Metal Ratio

Table 3.3.3 Testing of 1-decene with Rh/TPP: Effect of TPP/Rh molar ratio.

Run	1	2
Feed (volume / volume)	50ml 1-Decene / 150ml n-octane	50ml 1-Decene / 150ml n-octane
Pressure (bar (g))	25 bar (initial)	25 bar (initial)
grams Rh/100ml of feed	0.0244	0.0244
TPP:Rh molar ratio	**10**	**100**
H_2:CO	1:1	1:1
%1-decene conversion	100	63.3
% Linearity of aldehyde products	74.5	83.5
% n-Decane selectivity	0.5	0.7
% Internal olefin selectivity	5.2	6.2
% Aldehyde selectivity	94	93
% Alcohol selectivity	- (tr.)	- (tr.)
% HOF selectivity	- (tr.)	- (tr.)

A comparison of runs 1 and 2 shows the effect of increasing the TPP:Rh ratio from 10 to 100 with the 1-decene feed. The 1-decene conversion decreased from 100% to 63% whilst the product linearity increased from 75% to 84%. Increasing the ligand/metal ratio therefore lowers the catalyst activity and increases the selectivity to linear aldehydes and this is consistent with reports in the literature [Oswald *et al.*, 1982, 1992].

The paraffin selectivities remained at less than 1%, thereby indicating that the hydrogenation activities of these systems is negligible, regardless of the ligand/metal ratios used. Small amounts of branched olefins in the 1-decene feed of around 1.5% by weight, were shown to be "inert" as their concentrations did not vary significantly, even at the high conversions attained in run 1. Apart from the expected two C_{11} aldehyde peaks, two additional peaks appeared in the C_{10} portion of the GC trace of the reactor contents after hydroformylation. Since these peaks (contributing approximately 4% by mass of the reactor contents) do not arise from the branched olefins in the feed and are not n-decane, they most probably result from 1-decene, and by default were assigned to linear internal decene isomers. The appearance of these two peaks was however a consistent observation for the subsequent 1-decene/octane experiments. The presence of no additional C_{11} aldehyde isomers in the product would appear to indicate that these decene isomers are unreactive for hydroformylation. Figure 3.3 shows a typical gas chromatogram of these systems. An examination of Table 3.3.3 indicates that this "isomerization activity" appears to be unaffected by the ligand/metal ratio. Reports in the literature on this "isomerization activity" are in evidence [Mieczyńska *et al.*, 1992][Trzeciak, *et al.*, 1988, 1990, 1993, 1995]. However, the work undertaken by Trzeciak *et al.* employed L:M ratios of ≤13, which are significantly lower than the ratios of around 100 used in this study. This isomerization of terminal olefins (the work was reported on 1-hexene feeds) is said to diminish hydroformylation reaction selectivity and is regarded as an undesirable side reaction. These "isomerization" reports contradict others [Falbe, 1980][Burnham-Tinker and Morris, 1977][Rogier, 1980] which state that little or no isomerization should occur. On consideration of subsequent Tables 3.3.4 - 3.3.6, it is evident from the high internal olefin selectivities (33% for runs 7 and 8), that isomerization did occur.

Figure 3.3 GC trace of Rh/TPP catalyzed hydroformylation of 1-decene: Reactor liquid composition.

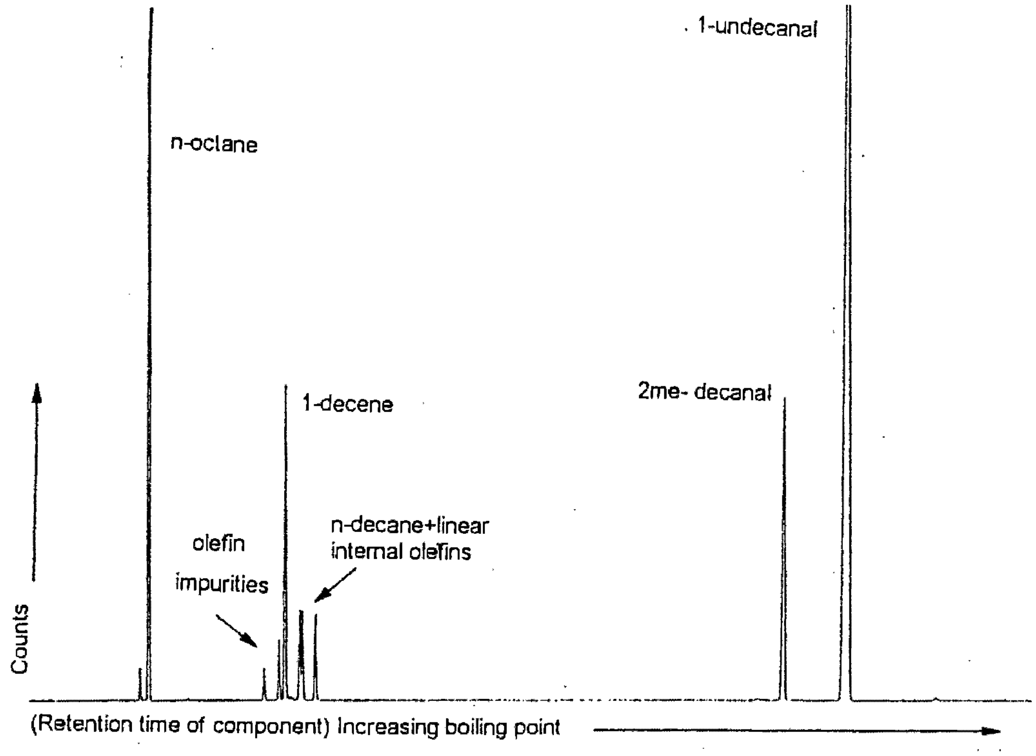

Reactor size

Runs 3 - 6 were undertaken under the same starting conditions.

Table 3.3.4a Results of runs undertaken under the same starting conditions: 1-decene Rh/TPP systems.

Run	3.1	4.1	5.1	6.1
Initial syngas H_2:CO	2:1	2:1	2:1	2:1
Reactor	1 litre	450ml	450ml	450ml
Reaction time (hours)	6.6	5.3	4.0	5.0
[Rh] g/100ml of feed	0.038	0.038	0.038	0.038
%1-Decene conversion	29.3	34.8	30.0	38.4
% Linearity of aldehyde products	92.3	90.9	91.7	91.2
% n-Decane selectivity	4.1	4.1	3.0	5.5
% Internal olefin selectivity	16.3	9.3	10.3	18.5
% Aldehyde selectivity	80	87	86	76
% Alcohol selectivity	- (tr.)	- (tr.)	- (tr.)	- (tr.)
% HOF selectivity	- (tr.)	- (tr.)	- (tr.)	- (tr.)

The results in Table 3.3.4a and Table 3.3.5 appear to indicate that the reactions in the smaller stirred micro-reactor were somewhat faster. A comparison of the final conversions, selectivities and linearities of runs 3.2 to 6.2 (in Table 3.3.5), indicates that the results are similar. This notwithstanding the fact that runs 3.1 and 3.2 were undertaken in the larger 1 litre reactor which makes use of a vertical plunger mixing mechanism compared with the gas entrainment impeller used for the other runs. A comparison of the results before applying constant pressure as means of checking reproducibility would not be meaningful due to the different reaction times used. However, selectivities for both reactors were similar at similar conversions.

Syngas composition

Table 3.3.4b Effect of syngas composition: 1-decene Rh/TPP systems.

Run	2	3.1
Initial syngas H_2:CO	1:1	2:1
Reactor	1 litre	1 litre
Reaction time (hours)	5.3	6.6
grams Rh /100ml of feed	0.024	0.038
%1-Decene conversion	63.3	29.3
% Linearity of aldehyde products	83.5	92.3
% n-Decane selectivity	0.7	4.1
% Internal olefin selectivity	6.2	16.3
% Aldehyde selectivity	93	80
% Alcohol selectivity	-(tr.)	- (tr.)
% HOF selectivity	- (tr.)	- (tr.)

On doubling the H_2:CO ratio from 1 to 2 (see Table 3.3.4b), an increase in the aldehyde linearity from 84% to 92% was observed. There was also a decrease in the 1-decene conversion from 63% to 29%. This was observed notwithstanding the higher catalyst concentration used in the 2:1 H_2:CO runs.

Doubling the H_2:CO ratio increased the hydrogenation activity. This is evidenced by the higher paraffin selectivities of 4.1% compared with 0.7% for run 2 in Table 3.3.4.b.

Isomerization to the internal olefins appeared to be enhanced by increasing the H_2:CO ratio.

Syngas Pressure

Table 3.3.5 Effect of overall syngas pressure on Rh/TPP catalyzed hydroformylation in batch reactors.

Run	3.1	3.2	4.1	4.2	6.1	6.2
Reactor	1 litre		450ml		450 ml	
Initial syngas H_2:CO ratio	2:1		2:1		2:1	
Pressure (bar):	25_{init} ("Low")	$25_{\text{const.}}$ ("High")	25_{init} ("Low")	$25_{\text{const.}}$ ("High")	25_{init} ("Low")	$25_{\text{const.}}$ ("High")
Cumulative reaction time (hours)	6.6	24	5.3	15	5.0	15
%1-Decene conversion	29.3	98.9	34.8	94.6	38.4	97.7
% Linearity of aldehyde products	92.3	86.5	90.9	89.3	91.2	88.8
% n-Decane selectivity	4.1	2.1	4.1	2.4	5.5	6.8
% Internal olefin selectivity	16.3	8.3	9.3	6.9	18.5	10.4
% Aldehyde selectivity	80	90	87	91	76	83
% Alcohol selectivity	- (tr.)	- (tr.)	- (tr.)	- (tr.)	- (tr.)	- (tr.)
% HOF selectivity	- (tr.)	- (tr.)	- (tr.)	- (tr.)	- (tr.)	- (tr.)

Bearing in mind that runs were considered "over" once the pressure drop ceased, it is tempting to claim that conversion was increased by running the reactors at a higher overall pressure of syngas notwithstanding the longer reaction times used. (See Table 3.3.5). The higher conversions resulted in lowering of the C_{11} aldehyde product linearity by around 4%. Overall high pressures therefore suppress the reaction selectivity to linear products, and increase olefin conversions, and this is in agreement with literature reports [Oswald *et al.*, 1982, 1992]. Better linearity and conversion could presumably be obtained by using lower pressures and longer reaction times.

Various data from runs 3 to 6 are plotted in Figure 3.4. Although runs 3.1 and 3.2 were performed on a different reactor, data for this experiment is included.

Figure 3.4 Plot of % conversion versus % product linearity: Rh/TPP with a 1-decene feed and H_2:CO = 2; (Runs 3 to 6).

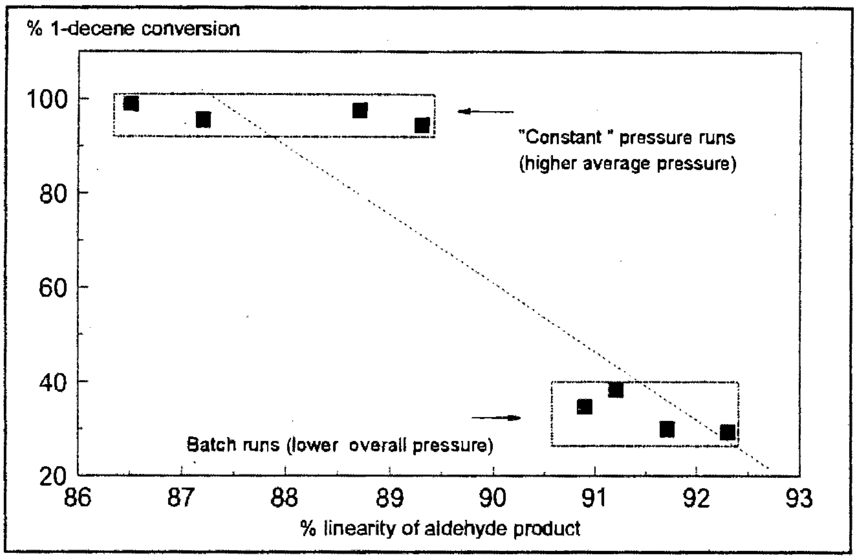

The "grouping" of data points in Figure 3.4 illustrates that higher olefin conversions correspond with lower product linearities. Because of the syngas pressure variations, there is too much scatter in the data points to ascertain if a linear relationship exists between linearity and conversion. This trend of lower linearities being associated with higher conversions (with the same catalyst) is consistent throughout this study.

Effect of Rh Precursor Salts on Hydroformylation of 1-decene

Runs 7 to 10 were undertaken to investigate the effect of the Rh precursor salt composition. The following alternative Rh precursors were tested using a pure 1-decene feed:

1. $HCORh(P(C_6H_5)_3)_3$
2. $[Rh(O_2C_2H_3)_2]_2$
3. $Rh(O_2C_5H_7)_2$
4. $((C_6H_5)_3P)_3RhCl$

Table 3.3.6 Testing of 1-decene with Rh/TPP: Effect of Rh precursor.

Run	7	8	9	10
Rh precursor	$HRhCO(P(C_6H_5)_3)_3$	$[Rh(O_2C_2H_3)_2]_2$	$Rh(O_2C_5H_7)_2$	$((C_6H_5)_3P)_3RhCl$
Salt number	1	2	3	4
Reactor	1 litre	1 litre	1 litre	1 litre
grams Rh per 100ml of feed	0.0174	0.0348	0.0696	0.0696
grams Rh per gram olefin (%)	0.025	0.050	0.100	0.100
TPP/Rh molar ratio	100	100	100	100
H_2:CO	2:1	2:1	2:1	2:1
Reaction time (hours)	1.5	1.5	12.3	15
%1-Decene conversion	99.2	92.8	90.2	95.6
% of aldehyde products linear	88.5	90.4	85.0	85.0
% n-Decane selectivity	6.6	17.9	2.0	2.2
% Internal olefin selectivity	32.6	32.7	2.7	2.9
% Aldehyde selectivity	60	52	94	95
% Alcohol selectivity	- (tr.)	- (tr.)	- (tr.)	- (tr.)
% HOF selectivity	- (tr.)	- (tr.)	- (tr.)	- (tr.)

The time taken for the reactor pressure to fall (and subsequently remain approximately constant) is markedly different for salts 1 and 2 compared with salts 3 and 4. Given the short reaction times and lower catalyst concentrations for salts 1 and 2 it appears that they are more active than salts 3 and 4. Hydrogenation and isomerization activities are higher for the "active" precursor systems which gave rise to higher α-olefin "losses". It would have been useful to continue the runs with salts 1 and 2 to monitor the behaviour of the internal olefins by using longer reaction times so as to ascertain if the aldehyde yields would have improved.

Although no specific precursor can be recommended given the above data, it may nevertheless be prudent to more systematically investigate the role of precursors if one was to undertake a detailed study of Rh/TPP catalyzed hydroformylation. This is subsequently confirmed in Table 3.3.8 of Section 3.3.3.2 where different acitivities are evident between the $Rh(O_2C_5H_7)_3$ and $HRhCO(P(C_6H_5)_3)_3$"precursors".

3.3.3.2 Rh/TPP Testing: "Broad" SLO C_{10} Fraction

Runs 11, 12 and 13 were undertaken with a C_{10} SLO fraction (described in Table 3.1) and demonstrate the effects of using different ligand:metal and H_2:CO ratios, temperature, pressure and Rh precursors. The effects of the additional components in the SLO on reaction selectivities and conversions are discussed.

Results with a Ligand:Metal molar ratio of 10

A SLO C_{10} fraction (run 11) was tested and the results compared to those obtained with a pure 1-decene feed (run 1).

The linear α-olefin product linearities or 1-decene product linearities were calculated using equation (3.1).

$$(\text{linear } \alpha\text{-olefin product linearity}) = \frac{(\text{mass \% linear aldehyde}) \times 100\,\%}{(\text{mass \% 2-methyl aldehyde}) + (\text{mass \% linear aldehyde})} \qquad (3.1)$$

Equation (3.1) gives an indication of the selectivity of the catalyst system for linear products. More specifically, it measures the extent to which pathway in Figure 1.15 is preferred.

Table 3.3.7 Testing of SLO C_{10} material and 1-decene with TPP:Rh molar ratio of 10.

Run	11	1
Feed	**SLO C_{10} fraction**	**50ml 1-decene / 150ml n-octane**
Pressure (bar (g))	25 bar (initial)	25 bar (initial)
grams Rh/100ml of liquid feed	0.0555	0.0244
TPP/Rh molar ratio	**10**	**10**
H_2:CO	1:1	1:1
Reaction time (hours)	3.3	5.3
%1-Decene conversion	97.2	100
1-Decene products % linear	64.5	74.5
Overall aldehydes % linear	41.5	74.5
% n-Decane selectivity	1.7	0.5
% Internal olefin selectivity	9.7	5.2
% Aldehyde selectivity	89	94
% Alcohol selectivity	- (tr.)	- (tr.)
% HOF selectivity	- (tr.)	- (tr.)

The aldehyde product linearities from 1-decene were measured as 65% and 75% for the SLO and 1-decene feeds respectively. The linearity results correspond to normal:iso (n:i) ratios of 1.9 and 3. These values are unsatisfactory and were presumably due to the relatively "low" TPP:Rh molar ratio of 10 that was employed. The lower n:i ratio of the 1-decene hydroformylation product obtained with SLO may possibly be attributed to the higher catalyst concentration that was used. However, comparing runs 4.1 and 12.1 in Table 3.3.8, indicates that SLO gave rise to a slower reaction rate, but still yielded a lower linearity. The lower linearity for run 11 may therefore be due to "SLO" and not only due to a faster reaction rate.

A GC trace of the SLO products as shown in Figure 3.5 indicates the presence of mono and corresponding di-methyl aldehydes, consistent with the expected olefin distribution in the feed. The α:β addition ratios (see Figure 1.15) of the different α-olefins are similar to the 1-decene n:i ratio, thereby indicating that the mono-methyl α-olefins had similar α:β addition preferences to the linear α-olefin.

Figure 3.5 GC trace of reaction products: Run 11, illustrating aldehyde product pairs.

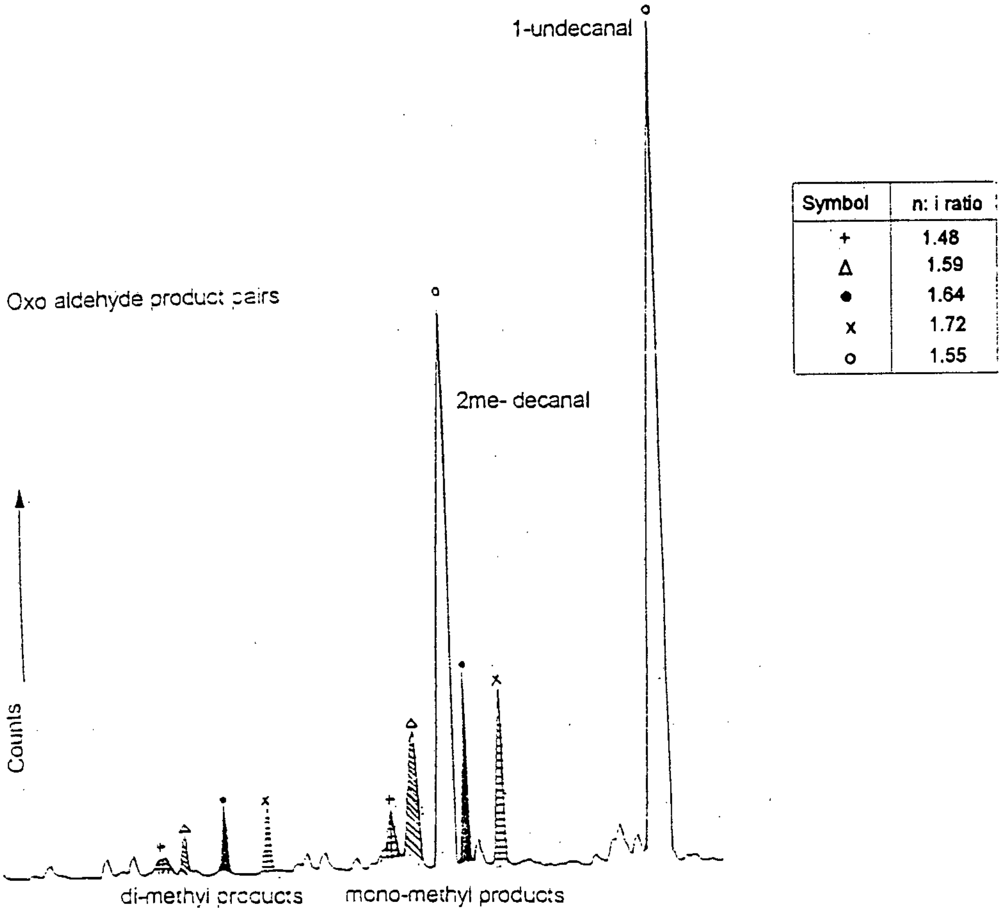

Symbol	n: i ratio
+	1.48
Δ	1.59
●	1.64
x	1.72
o	1.55

Testing of the C_{10} SLO Fraction Under Conditions giving High Linearities with a 1-Decene Feed

Run 12.1 was undertaken using similar conditions that gave rise to product linearities in the region of 90% with 1-decene feeds (for example run 4.1 in Table 3.3.8). Notwithstanding a 30% lower catalyst concentration in run 12.1, the SLO yielded a lower selectivity to linear products (79% against 90% for the 1-decene), with the 1-decene conversion approximately halved to 15%. It hence appears that components in the SLO possibly appeared to exert a negative influence on performance of the system under investigation.

Table 3.3.8 Testing of the C_{10} SLO fraction under conditions giving high linearities with a 1-decene feed.

Run	4.1	12.1	7	13
Feed	1-decene/ octane	SLO C_{10} fraction	1-decene/ octane	SLO C_{10} fraction
Rh precursor	$Rh(O_2C_5H_7)_3$	$Rh(O_2C_5H_7)_3$	$HRhCO(P(C_6H_5)_3)_3$	$HRhCO(P(C_6H_5)_3)_3$
Initial Pressure (bar (g))	25	25	25	25
Temperature (°C)	100	100	100	100
grams Rh/100ml of feed	0.0382	0.0259	0.0174	0.0174
g Rh / g olefin (mass%)	0.100	0.100	0.025	0.025
TPP:Rh molar ratio	100	100	100	100
Initial H_2:CO ratio	2:1	2:1	2:1	2:1
Reaction Time (hours)	5.3	7.7	1.5	1.5
% Total decene conversion	34.8	14.7	99.2	97.8
1-Decene products % linear	90.9	79.3	88.5	76.9
Overall aldehydes % linear	90.9	62.8	88.5	54.1
% n-Decane selectivity	4.1	1.4	6.6	7.2
% Internal olefin selectivity	9.3	2.3	32.6	4.1
% Aldehyde selectivity	87	96	60	89
% Alcohol selectivity	- (tr.)	- (tr.)	- (tr.)	- (tr.)
% HOF selectivity	- (tr.)	- (tr.)	- (tr.)	- (tr.)
% Decene converted to aldehydes	30.3	14.1	59.5	87.0

On comparing runs 12.1 and 13 (see Table 3.3.8) the effect of the catalyst precursor is evident. Despite a lower Rh concentration, a higher hydroformylation activity was obtained with the $HRhCO(P(C_6H_5)_3)_3$ "precursor" compared to $Rh(O_2C_5H_7)_2$ in SLO. A comparison of runs 7 and 13 indicate that the SLO medium does not adversely effect the catalyst activity when the $HRhCO(P(C_6H_5)_3)_3$ complex is used as the catalyst. In run 13, the hydroformylation activity was higher than that obtained using a "pure" 1-decene feed as in reaction 7. However, the 1-decene product linearity for SLO of 77% is considerably lower than the 89% measured for run 7.

Table 3.3.9 Runs undertaken with C_{10} SLO in which conditions were changed to increase conversions: Rh/TPP catalysts.

Run	12.1	12.2	12.3	12.4
Precursor	$Rh(O_2C_5H_7)_3$			
Notes:	Runs are continuation of each other: *ie*, 12.2 is a continuation of 12.1 *etc.*			
Pressure (bar (g))	25 initial	25 constant	25 constant	35 constant
Temperature (°C)	100	100	120	120
Reaction time (hours)	7.7	7.7	6.0	15
%1-Decene conversion	14.7	29.4	41.3	68.7
1-Decene products % linear	79.3	76.1	75	63.4
Overall aldehydes % linear	62.8	55.5	56.4	46.2
% n-Decane selectivity	1.4	1.4	2.3	8.3
% Internal olefin selectivity	2.3	1.4	2.5	4.6
% Aldehyde selectivity	88	96	97	95
% Alcohol selectivity	- (tr.)	- (tr.)	- (tr.)	- (tr.)
% HOF selectivity	- (tr.)	- (tr.)	- (tr.)	- (tr.)

In an attempt to increase the olefin conversion, and also to check if the catalyst had deactivated, run 12.1 was extended (see Table 3.3.9). Run 12.2 was performed at a constant pressure of 25 bar, which resulted in an increase in the

1-decene conversion from 15% to 29% and decreasing the 1-decene product linearity from 79% to 76%. These trends are similar to those observed with the 1-decene feed. Namely, that higher conversions correspond with lower product linearities.

In order to further increase the conversion, the reaction temperature was increased from 100°C to 120°C in run 12.3 and the pressure increased further to 35 bar in run 12.4. Even under these conditions, the respective linear α-olefin conversion and product linearity was 69% and 63%, indicating an inactive catalyst.

Given the consistently low amounts of unwanted by-products obtained with the SLO experiments as demonstrated in Tables 3.3.8 and 3.3.9 (only traces of a Heavy Oxo Fraction - (HOF)), and the promising result obtained with run 13 (high hydroformylation activity in SLO with the $HRhCO(P(C_6H_5)_3)_3$ "precursor"), the possibility of excluding or avoiding processes for the removal of oxygenates and aromatics in order to prepare a suitable hydroformylation feedstock appeared to be a real one. This could be achieved by distillation and refractionation procedures only. As a follow-up, narrow SLO fractions were tested as feeds.

3.3.3.3 Rh/TPP Testing: "Narrow" SLO Fractions

Runs 14, 15 and 16 were undertaken with C_8, C_9 and C_{10} narrow SLO fractions respectively.

A purified C_8 fraction was tested in a methanol solvent (65% by mass). The 1-octene in the SLO portion was 81% by mass. The C_9 and C_{10} cuts were prepared by refractionation to yield linear α-olefin concentrations of 61% and 70% respectively (see Table 3.1).

Table 3.3.10 Summary of SLO narrow fraction results: Rh/TPP catalysts.

Run	14	15	16
C_{number} of "narrow" SLO fraction	C_8	C_9	C_{10}
Reactor	1 litre	1 litre	1 litre
Pressure (bar (g))	25_{initial}	25_{initial}	25_{initial}
Temperature (°C)	80	90	90
grams Rh/100ml of feed	0.027	0.015	0.027
grams Rh/ grams olefin (mass%)	0.040	0.080	0.040
Rh precursor	$[Rh(O_2C_2H_3)_2]_2$	$[Rh(O_2C_2H_3)_2]_2$	$[Rh(O_2C_2H_3)_2]_2$
TPP:Rh molar ratio	100:1	100:1	100:1
Reaction time (hours)	4.1	5.0	8.0
%1-Olefin conversion	93.2	99.2	97.6
1-Olefin products % linear	80.6	87.6	88.9
Overall aldehydes % linear	80.6	84.4	83.0
% n-Paraffin selectivity	2.8	1.7	14.5
% Internal olefin selectivity	0 (tr.)	0 (tr.)	17.5
% Aldehyde selectivity	97	92	66
% Alcohol selectivity	0 (tr.)	0 (tr.)	0 (tr.)
% HOF selectivity	0 (tr.)	0 (tr.)	0 (tr.)

For each of the reactions (in Table 3.3.10), only two main hydroformylation products were observed. These were the 2-methyl and linear aldehydes which are derived from the linear α-olefin in the feed. Small amounts of branched aldehyde products (from iso-olefins) were also present, but their combined concentration (of the hydroformylation products) was between 3% and 6%. The appearance of the two main product peaks (2 methyl decanal and 1-undecanal) for the narrow fractions tested is demonstrated in Figure 3.6. The result implies that the refractionation procedure removed most of the reactive branched olefins.

Figure 3.6 GC trace of reaction products: C_{10} SLO narrow fraction illustrating two main products (from 1-decene).

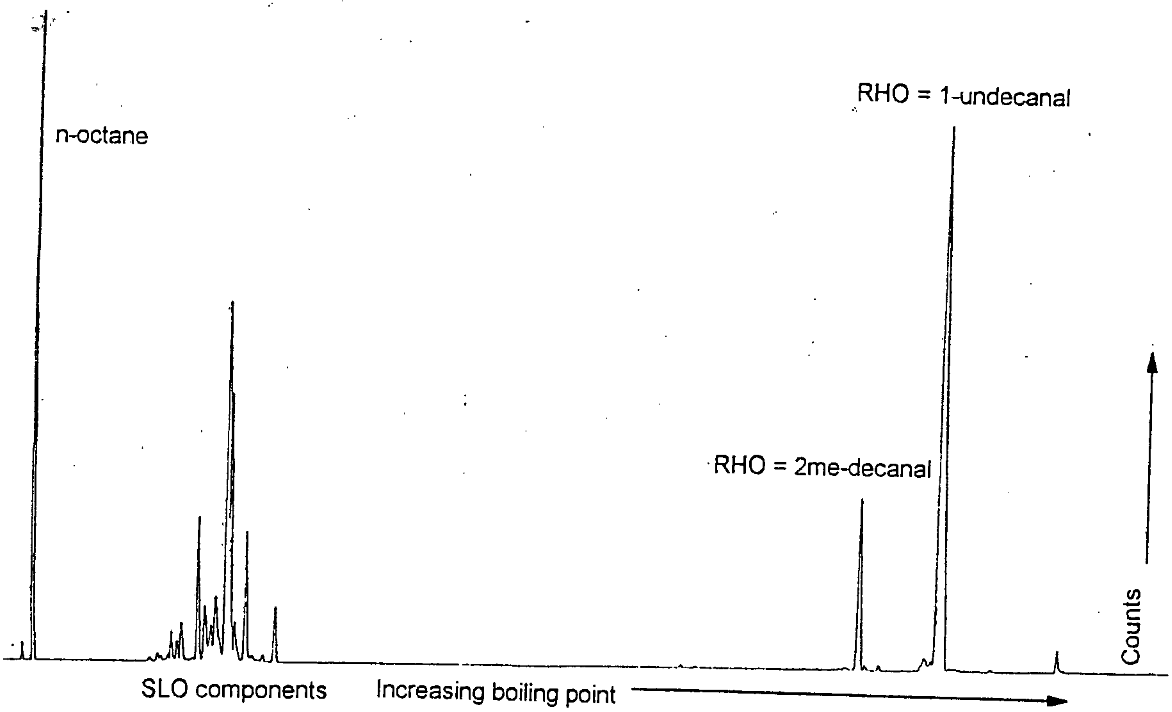

The reasons for the higher paraffin and internal olefin selectivities and resultant lower aldehyde selectivity observed with the C_{10} fraction were unclear.

<u>Overall</u> product linearities of >80% were achieved with all three SLO narrow fractions. This result was viewed as being encouraging since it indicated that preparation of narrow SLO cuts by refractionation alone can give rise to feedstocks which yield hydroformylation products which are ≥ 80% linear. For synthetic higher alcohols these values are considered to be highly acceptable.

3.4 SCREENING EXPERIMENTS WITH Co/PHOSPHINE CATALYSTS

3.4.1 Co/Phosphine Experiments

Table 3.4.1 Screening experiments undertaken with Co; TPP and TBP ligands.

Run	Ligand	[Co] g/100ml	Co/Ole. % by mass	L:M Molar ratio	Feed composition (volume/volume)	Temp °C	H_2:CO Molar ratio	Pi bar	Time Hours	Reactor
17	TPP	0.0852	0.32	5	1/1 n-octane/1-decene	200	1	$100_{init.}$	3.4	1 litre
18	TPP	0.1326	0.50	5	1/1 n-octane/1-decene	200	1	$100_{init.}$	2.6	1 litre
19	TPP	0.0852	0.50	10	1/1/1 (n-octane)/(butyl ether)/(1-decene)	200	1	$100_{init.}$	8	1 litre
20	TPP	0.1739	0.50	10	1/1 n-octane/1-decene	200	1	$100_{init.}$	6.5	450ml
21.1	TPP	0.1739	0.50	10	1/1 n-octane/1-decene	200	2	$100_{init.}$	2	450ml
21.2	Continuation of run 21.1; repressurized to 100 bar after 2 hours							$100_{init.}$	8.8	450ml
22.1	TPP	0.1739	0.50	10	1/1 n-octane/1-decene	150	2	$50_{init.}$	3	450ml
22.2	Continuation of run 22.1; repressurized to 50 bar and kept constant							50_{const}	4.5	450ml
22.3	Continuation of run 22.2: Temp. increased to 175°C, and depressurized to 30 bar					175	2	$30_{init.}$	15	450ml
22.4	Continuation of run 22.3; repressurized to 65 bar and kept constant					175	2	65_{const}	6	450ml
22.5	Continuation of run 22.4: Temp. increased to 200°C, and pressurized to 100 bar					200	2	$100_{init.}$	3	450ml
23	TBP	0.1739	0.50	5	1/1 n-octane/1-decene	200	2	$98_{init.}$	3.7	450ml
24	TBP	0.1258	0.50	5	SLO C_{10} fraction	200	2	$99_{init.}$	3.7	450ml
25.1	TBP	0.1258	0.50	5	SLO C_{10} fraction	150	2	$70_{init.}$	10.8	450ml
25.2	Continuation of run 25.1; repressurized to 70 bar and kept constant					150	2	$70_{init.}$	3	450ml
26.1	TBP	0.1665	0.50	5	3/1 (SLO C_9 narrow fraction)/(n-octane)	200	2	$100_{init.}$	5	450ml
26.2	Continuation of run 26.1; depressurized to 70 bar and kept constant, temperature decreased to 150°C					150	2	70_{const}	5	450ml
27.1	TBP	0.1665	0.50	5	3/1 (SLO C_9 narrow fraction)/(n-octane)	150	2	$70_{init.}$	5	450ml
27.2	Continuation of run 27.1; repressurized to 70 bar and kept constant							70_{const}	3	450ml

Metal precursor: $Co(OOCCH_3)_2.4H_2O$

The results are summarized in Table 3.4.2.

3.4.2 Results of Co/Phosphine Screening Experiments

Table 3.4.2 Results of Co/P screening experiments.

Run	% Total olefin conv.	%lin. α-olefin conv.	%Sel. to int. ole	%Sel. to par.	%Sel. to ald.	%Sel. to alcohol	%Sel. to HOF	%Prod. linearity. From lin α-ole. (ald.+alc.)	%Overall product linearity. (ald.+alc.)
17	100	100	0	7	6	84	3	72	47
18	100	100	0	10	0	87	3	63	41
19	100	100	0	11	6	80	3	74	41
20	100	100	0	21	5	70	4	70	57
21.1	51	76	33	16	3	43	5	72	57
21.2	99	99	0	25	5	65	5	73	61
22.1	9	15	42	9	19	25	5	73	31
22.2	15	21	28	5	27	34	6	73	21
22.3	54	78	31	11	4	49	6	72	60
22.4	66	84	21	14	10	49	5	72	56
22.5	86	99	13	13	6	62	6	76	65
23	100	100	0	21	3	71	5	86	79
24	89	93	4	8	5	78	5	79	50
25.1	54	92	41	4	14	36	7	83	51
25.2	83	95	13	5	5	71	7	83	65
26.1	81	85	5	34	1	53	7	79	66
26.2	81	94	14	28	2	46	10	80	67
27.1	51	62	18	9	2	64	6	90	84
27.2	54	68	20	11	8	53	8	89	89

All selectivities in Table 3.4.2 are based on α-olefins converted.
Selectivities normalized to sum to 100%; average error around 5%.

3.4.3 Discussion of Results: Co/Phosphine Screening Experiments

In addition to TPP and TBP, TBPite was also tested as a ligand but for the latter only isomerization and a small amount of hydrogenation activity was measured. No hydroformylation activity was obtained with the SLO feed using this ligand.

3.4.3.1 Co/TPP Testing: 1-Decene Feed

Runs 17-22 were performed to ascertain the suitability of TPP as a possible ligand for use with Co to produce linear products.

Initial runs: See Table 3.4.3.

Runs 17 and 18 confirmed that selectivities obtained using a 1-decene feed were consistent with those in the literature [Falbe, 1980] for Co/P systems. This was evidenced by the formation of 2-methyl decanal, 1-undecanal, 2-methyl decanol and 1-undecanol, and additional branched hydroformylation products, as well as small amounts of heavy oxygenates (HOF), and paraffins. This is consistent with reports that isomerization of olefins occurs with these catalysts. The "additional" products implied that hydroformylation of the internal olefins also occurred. This is evident when one compares the percent product linearities from the linear α-olefin (72%) with the overall product linearity (47%) in Table 3.4.3 (run 17).

Comparison of runs 17 and 18 gives an indication as to the effect of catalyst concentration. The cobalt concentrations in runs 17 and 18 were 0.0852 and 0.1326 g/100ml respectively. Run 18 appeared to have proceeded faster as evidenced by the shorter reaction time (2.6 hours versus 3.4), and this can explain the lower product linearity. Increasing the cobalt concentration appeared to also result in a higher hydrogenation activity in run 18 as evidenced by the lower aldehyde and slightly higher paraffin selectivities . Apart from the linearities, the results appeared to be satisfactory.

Table 3.4.3 Initial runs undertaken with Co/TPP: Hydroformylation of 1-decene.

Run	17	18	19	20
Feed composition (vol. / vol.) (n-octane / 1-decene /butyl ether)	1 / 1 / -	1 / 1 / -	1 / 1 / 1	1 / 1 / -
Grams Co per 100ml of feed	0.0852	0.1326	0.0852	0.1739
Grams Co per grams olefin (%)	0.32	0.50	0.50	0.50
Reactor	1 litre	1 litre	1 litre	450 ml
TPP:Co molar ratio	5:1	5.1	10:1	10:1
H_2:CO	1:1	1:1	1:1	1:1
Temperature (°C)	200	200	200	200
Initial pressure (Bar (g))	100	100	100	100
Reaction time (hours)	3.4	2.6	8	6.5
% Overall Olefin Conversion	100	100	100	100
1-Decene (alc. + ald.) products % linear	72	63	74	70
Overall (alc.+ald.) products % linear	47	41	41	57
% n-Decane selectivity	7	10	11	21
% Internal olefin selectivity	0	0	0	0
% Aldehyde selectivity	6	0	6	5
% Alcohol selectivity	84	87	80	70
% HOF selectivity	3	3	3	4

Reactor configuration; Ligand:Metal Ratio and the Effect of di-Butyl Ether

See Table 3.4.3

Runs 19 and 20 were undertaken using a higher TPP:Co ratio of 10 compared with a ratio of 5 for runs 17 and 18. In order to investigate the effect of an oxygenate, run 19 was undertaken with octane and di-butyl ether. On comparing runs 19 and 20, the results appear to indicate a higher hydrogenation activity (higher paraffin selectivity) and higher product linearity for run 20. The rate (as estimated from the time taken for the pressure to drop) did decrease, and this may be ascribed to the higher catalyst concentration used in run 20. Comparing runs 18 and 20 shows that the higher TPP:Co ratio resulted in an increase in the overall product linearity from 41% to 57%. Increasing the L:M ratio therefore appears to suppress the hydroformylation of internal olefins. The decane selectivity increased from 10% to 21% on doubling the L:M ratio. When comparing these results, the two reactor sizes for runs 18 and 20 of 1 litre and 450ml respectively, should be borne in mind. The smaller volume of the 450ml Parr reactor resulted in a larger pressure drop over the course of the experiment, thereby resulting in a lower average pressure for run 20 compared with run 18. The fact that the H_2:CO usage ratio in these systems was approximately 2:1 implies that the P_{CO} increased relative to the P_{H2} as gas in the system was consumed, bearing in mind that the initial H_2:CO composition was 1:1. The higher TPP:Co ratio in run 20 may have masked the effect of the higher P_{CO}, since phosphine ligands do result in a higher hydrogenation activity (see Table 1.6).

H_2:CO Ratio in Syngas: See Table 3.4.4.

Runs 21.1 and 21.2 were undertaken in an attempt to further improve the product linearities and to determine the effect of changing the H_2:CO ratio in the syngas from 1 to 2. A sample was taken at low conversions (run 21.1) with the reactor subsequently re-pressurized and the reaction continued to completion (21.2). The results are summarized and compared to run 20 in Table 3.4.4.

Table 3.4.4 Effect of H_2:CO ratio in the syngas: Co/TPP catalyzed hydroformylation of 1-decene.

Run	20	21.1		21.2
Grams Co per 100ml of feed	0.1739	0.1739		Continuation of 21.1, repressurized the system to 100 bar after 2 hours
Grams Co per grams olefin (%)	0.50	0.50		
Reactor	450 ml	450 ml		
TPP:Co molar ratio	10:1	10:1		
H_2:CO (initial)	**1:1**	**2:1**		
Temperature (°C)	200	200		
Initial pressure (Bar (g))	100	100		
Reaction time (hours)	6.5	2.0		8.8
% Overall[1] Olefin Conversion	100	51		99
1-Decene products %linear	70	72		73
Overall alcohols % linear	57	57		61
			Note [2]	
% n-Decane selectivity	21	16	24	25
% Internal olefin selectivity	0	33	0	0
% Aldehyde selectivity	5	3	4	5
% Alcohol selectivity	70	43	64	65
% HOF selectivity	4	5	7	5

[1] Includes internal olefin conversion.

[2] Normalized selectivities (ignoring internal olefins), indicate that the 3 runs give fairly similar selectivities.

There was direct evidence for the presence of a large amount of internal decenes as a consequence of isomerization observed at lower conversion in run 21.1. The fact that the overall product linearity of 57% for run 21.1 was similar to the 61% for run 21.2 indicates that most of the internal olefins "re-isomerized" to the α-olefin before being hydroformylated. Changing the H_2:CO ratio from 1 to 2 appears to be slightly disadvantageous as evidenced by the longer reaction time required to achieve complete conversion. Similar linearities were obtained with H_2:CO ratios of 1 and 2. From the selectivity comparisons in Table 3.4.4, it appears that overall, the hydrogenation activity of the Co/TPP system is not very dependent of the H_2:CO ratio of the syngas.

Combined Effects of Time, Temperature and Pressure: See Table 3.4.5.

Runs 22.1 to 22.5 were undertaken to ascertain the effect of changing the temperature and pressure during a run in a Co/TPP system with a 1-decene feed. Samples were taken at certain times, after which the reaction was allowed to proceed under different conditions. Conditions were selected such that the reaction was initiated under "mild conditions" which were altered to become "harsher" as the run progressed. This was undertaken primarily in an attempt to roughly screen if any of the treatments / conditions would give rise to a poor result. A complication with this approach is that a time effect is superimposed which makes it difficult to draw firm conclusions. The results have however been included since the "harsher" treatments of higher temperature and pressure did not result in a decrease in the product linearity. Furthermore, the results of the consecutive treatments (using the same starting feed) confirm the previous observations on isomerization and re-isomerization of the olefins.

On consideration of Table 3.4.5, it should be borne in mind that during the course of a "normal run" (*ie.* constant pressure and temperature), the batch reactor composition changes with time as indicated in Figure 4.2. These changes are that internal olefins appear and then disappear; similarly, the aldehydes appear and are hydrogenated with time to alcohols; in addition, paraffins and the HOF increase during the course of the reaction. With the exception of the paraffin selectivity for run 22.2 and the aldehyde selectivity for run 22.3, the normalized selectivities (ignoring the internal olefins) follow this approximate profile.

The following additional observations are made:

Under conditions of low conversion at 150°C and 50 bar (g), giving rise to low conversions and high internal olefin selectivities, the internal olefins were hydroformylated. This is witnessed by the low overall alcohol and aldehyde product linearities (31% and 21% for reactions 22.1 and 22.2).

Increasing the reaction temperature from 150°C to 175°C and decreasing the initial pressure from 50 to 30 bar (g) in reaction 22.3 had the following effects: Large increases in the 1-decene conversion and in the overall hydroformylation product linearity, coupled with a significant decrease in the aldehyde selectivity. It would appear that the higher 1-decene conversion linked to the higher overall product linearity implies that "re-isomerization" of the internal olefins to the α-olefin and subsequent hydroformylation was more easily achieved at higher temperatures. One would presume this effect to be less dependent on the reaction pressure since, in general, temperature effects are exponential whilst time and pressure effects are more linear. The lower aldehyde selectivity, coupled with the higher paraffin and alcohol selectivities point to higher hydrogenation activity at higher temperature.

Table 3.4.5 Temperature and pressure effects: Co/TPP catalyzed hydroformylation of 1-decene.

Run	22.1	22.2	22.3	22.4	22.5
Notes:	Run 22.2 is an extension of run 22.1 *etc.* The reactor was <u>not</u> recharged with 1-decene between successive runs.				
Grams Co per 100ml of feed	0.1739				
Grams Co per grams olefin (%)	0.50				
Reactor	450 ml				
TPP:Co molar ratio	10:1				
H_2:CO (initial)	2:1				
Temperature (°C)	150	150	175	175	200
Pressure (Bar (g))	50_{initial}	50_{constant}	30_{initial}	65_{constant}	100_{initial}
Reaction time (hours)	3	4.5	15	6	3
$\sum$ time (hours)	3	7.5	22.5	28.5	31.5
% Overall Olefin Conversion	9	15	54	66	86
1-Decene products %linear	73	73	72	72	76
Overall alcohols + aldehydes% linear	31	21	60	56	65
% n-Decane selectivity	9	5	11	14	13
% Internal olefin selectivity	42	28	31	21	13
% Aldehyde selectivity	19	27	4	10	6
% Alcohol selectivity	25	34	49	49	62
% HOF selectivity	5	6	6	5	6
Normalized selectivities (ignoring contribution of the internal olefins)					
% n-Decane selectivity	16	7	16	18	15
% Aldehyde selectivity	33	37	6	13	7
% Alcohol selectivity	43	47	70	62	71
% HOF selectivity	9	8	8	6	7

Increasing the reaction pressure to a constant 65 bar in reaction 22.4 did not result in marked changes in the 1-decene conversion, product linearity or reaction selectivity. The internal olefin selectivity did however drop from 31% to 21% and the 1-decene conversion and aldehyde selectivity both rose by approximately 6 percentage points. Given the additional reaction time of 6 hours under these conditions, the relatively low additional conversion was surprising. Further increasing the reaction temperature and pressure in reaction 22.5 for an additional 3 hours resulted in 86% conversion of the total decene and increased product linearity and alcohol selectivity. The internal olefin selectivity was still 13% which may indicate that one of the treatments had caused the catalyst to deactivate.

3.4.3.2 Co/TBP Testing: 1-Decene and SLO Feeds

See Table 3.4.6.

Run 23 shows the result obtained when using a TBP ligand with a 1-decene feed and can be compared with run 21.2 which used a TPP ligand (see Table 3.4.6). Better results were obtained with the TBP ligand compared to TPP, especially with regards to the product linearity despite a lower ligand to metal ratio. It was therefore decided to test SLO fractions with this catalyst under the same conditions (run 24) as shown in Table 3.4.6. The SLO result was viewed as being very encouraging as lower paraffin and higher alcohol selectivities were obtained compared to the 1-decene feed. The selectivity of the catalyst to linear products was however lower as evidenced by the lower 1-decene product linearity. This may be explained by higher hydroformylation activity of the catalyst in C_{10} SLO. This higher activity is assumed, since the cobalt concentration was considerably lower in the SLO run and the time taken for the pressure drop was approximately the same. The lower olefin conversions with the SLO feed appear to contradict this argument. Alternatively, there may have been unreactive olefins or an over determination of the olefins in the SLO.

Table 3.4.6 Comparison of TPP and TBP ligands used with Co to hydroformylate 1-decene (and SLO)[1].

Run	21.2	23	24
Ligand	**TPP**	**TBP**	**TBP**
Ligand:Metal (molar ratio)	10	5	5
Feed	**1-Decene**	**1-Decene**	**SLO C_{10}**
Grams Co per 100 ml feed	0.1739	0.1739	0.1258
Time (hours)	8.8	3.7	3.7
%1-Decene conversion	99	100	93
% Overall decene conversion	99	100	89
1-Decene products %linear	73	86	79
Overall products % linear	61	79	50
% n-Decane selectivity[2]	25	21	8
% Internal olefin selectivity	0	0	4
% Aldehyde selectivity	5	3	5
% Alcohol selectivity	65	71	78
% HOF selectivity	5	5	5

[1]Common reaction conditions: 100 bar (g) 2:1 H_2:CO syngas; 200°C.

[2]Selectivities are based on 1-decene converted.

The syngas pressure was subsequently reduced from 100 bar to 70 bar and the reaction temperature reduced from 200°C to 150°C with the C_{10} SLO feed in runs 25.1 and 25.2, specifically in an attempt to improve the product linearity. The results are given in Table 3.4.7.

Table 3.4.7 Effect of temperature and pressure on Co/TBP catalyzed hydroformylation of C_{10} SLO. (Ligand to metal molar ratio = 5).

Run	24	25.1	25.2
Temperature (°C)	200	150	150
Pressure (bar (g))	99 $_{\text{initial}}$	70 $_{\text{initial}}$	70 $_{\text{const.}}$
Time (hours)	3.7	10.8	3.0
%1-Decene conversion	100	92	95
% Total decene converted	89	54	83
1-Decene products %linear	79	83	83
Overall hydroformylation products % linear	50	51	65
% n-Decane selectivity	8	4	5
% Internal olefin selectivity	4	41	13
% Aldehyde selectivity	5	14	5
% Alcohol selectivity	78	36	71
% HOF selectivity	5	7	7

An improvement in the overall product linearity on continuation of run 25.1 to 25.2 was evident. It would appear as if the internal olefins (high internal olefin selectivity for run 25.1) were relatively inert to direct hydroformylation. The branched alcohols were therefore derived mainly from branched olefins in SLO. The branched α-olefins therefore initially reacted away faster than the linear α-olefins. This is subsequently explained by differences in the "reactivities" of olefins in SLO.

Figures 3.7 and 3.8 respectively show GC traces of hydroformylation products derived from pure (run 23) and SLO (run 24) feeds. A comparison of the peak <u>positions</u> in Figures 3.7 and 3.8 indicates which components are derived from hydroformylation of internal olefins and methyl branched α-olefins.

Figure 3.7 Gas Chromatogram of hydroformylation products for a Co/TBP catalyzed reaction of a "pure" 1-decene feed.

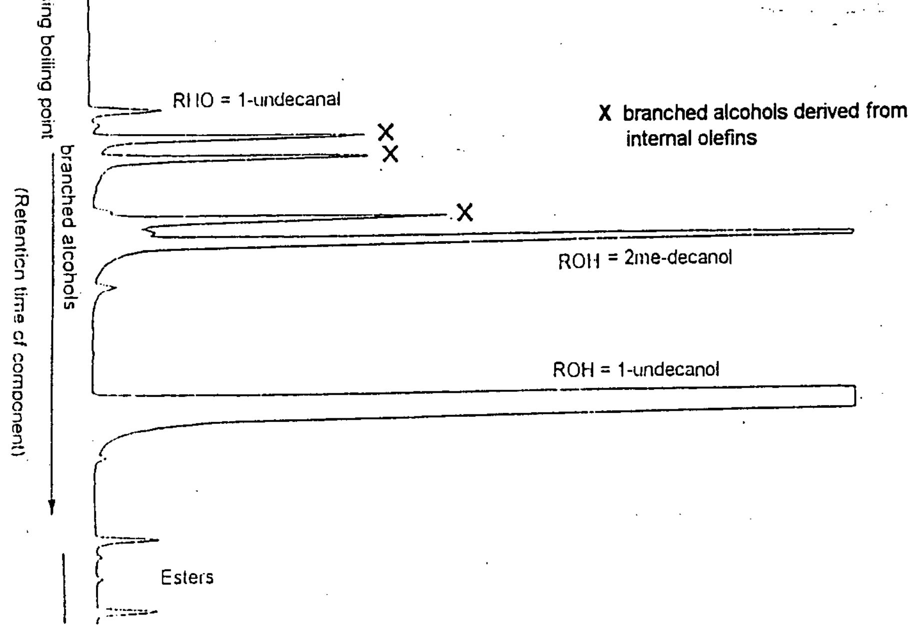

Figure 3.8 Gas Chromatogram of hydroformylation products for a Co/TBP catalyzed reaction of a "broad" SLO C_{10} fraction.

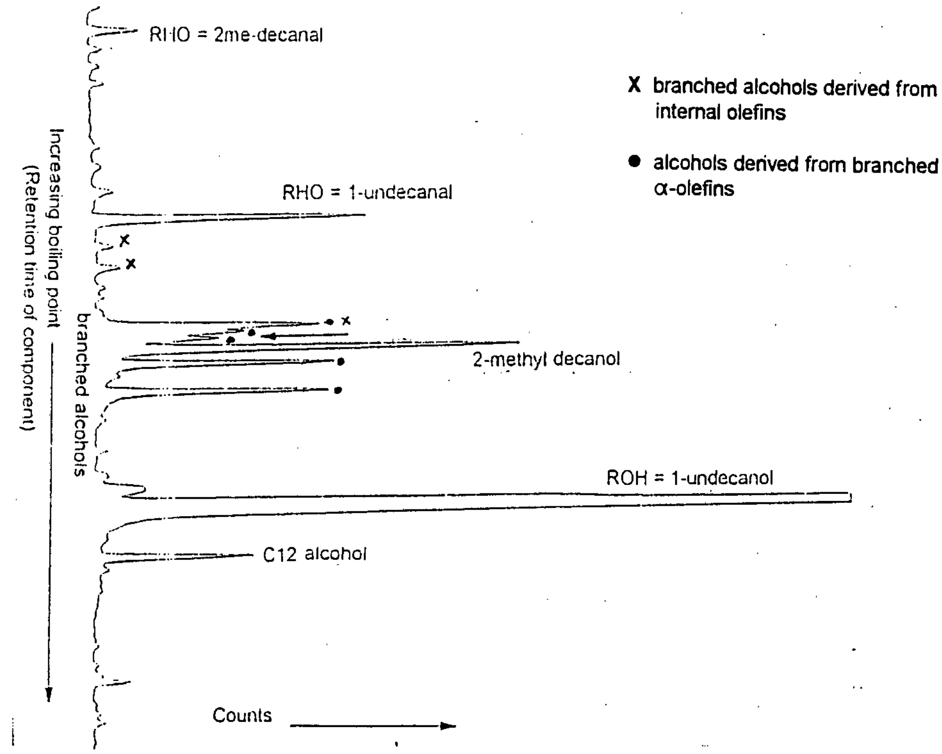

The presence of 4 branched alcohols from 1-decene in Figure 3.7, is consistent with the theory that only four can form as a result of hydroformylation of the possible internal olefin isomers. This argument is represented schematically by way of Figure 3.9 . If the same argument holds for a SLO feed, one could expect 4 isomers from each of the linear olefins, and <u>at least</u> 4 isomers from each of the mono-methyl α-olefins in such a feed.

Figure 3.9 Hydroformylation reaction possibilities with a 1-decene feed, given that olefin isomerization occurs.

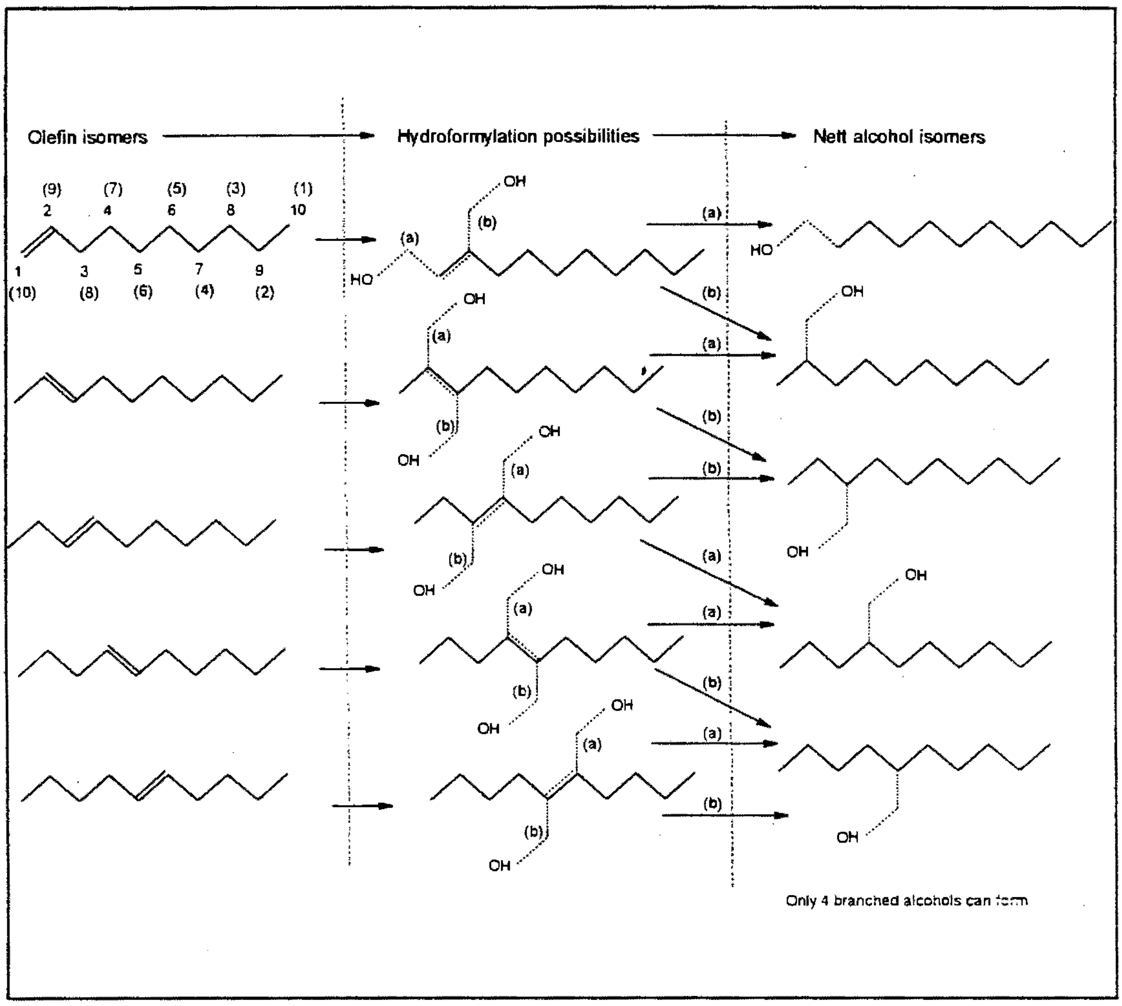

If one compares the "alcohol fingerprints" of the GC spectra of Figures 3.7 and 3.8, it appears as if internal olefins (which do form) in SLO were relatively inert to hydroformylation. The branched alcohols from the SLO feed were therefore derived mainly from the mono-methyl α-olefins. There exists a possibility of 8 mono-methyl α-olefins being present in a C_{10} SLO feed. Since the main hydroformylation reaction is via α addition, the possibility exists for the presence of 8 mono-methyl branched primary alcohols. There are enough peaks as indicated in Figure 3.8 to account for this possibility. In Figure 3.8, the main branched alcohols derived from mono-methyl olefins, in addition to the 2-methyl alcohol, are consistent with the main branched olefins in the C_{10} broad fraction. (see Figure 3.1).

Components (or the olefins themselves) in the SLO may therefore have an effect on the reactivity of internal olefins to hydroformylation with the Co/TBP catalysts. The structure of the mono-methyl branched olefins may explain their lack of "isomerization activity", and their apparent reluctance to form the di-branched alcohols by reaction of the internal olefin isomer. Internal mono-methyl isomers of the type

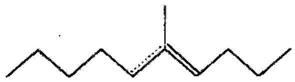

would be the most thermodynamically stable. However, the steric effects exerted by the ligand may discourage their formation. Once formed, they may be relatively inert to hydroformylation as a result of the steric influence of the proximity of the double bond to the methyl branch. These factors could result in a changing internal olefin distribution with reaction time using SLO feeds. This may explain the observed increase in product linearity in runs 25.1 and 25.2 due to the relatively larger amounts of methyl branched olefins present during the initial stages of the reaction. The argument is represented schematically in Figure 3.10.

Figure 3.10 Postulated effect of olefin structure on isomerization and hydroformylation reactivity in phosphine modified Co catalyst systems.

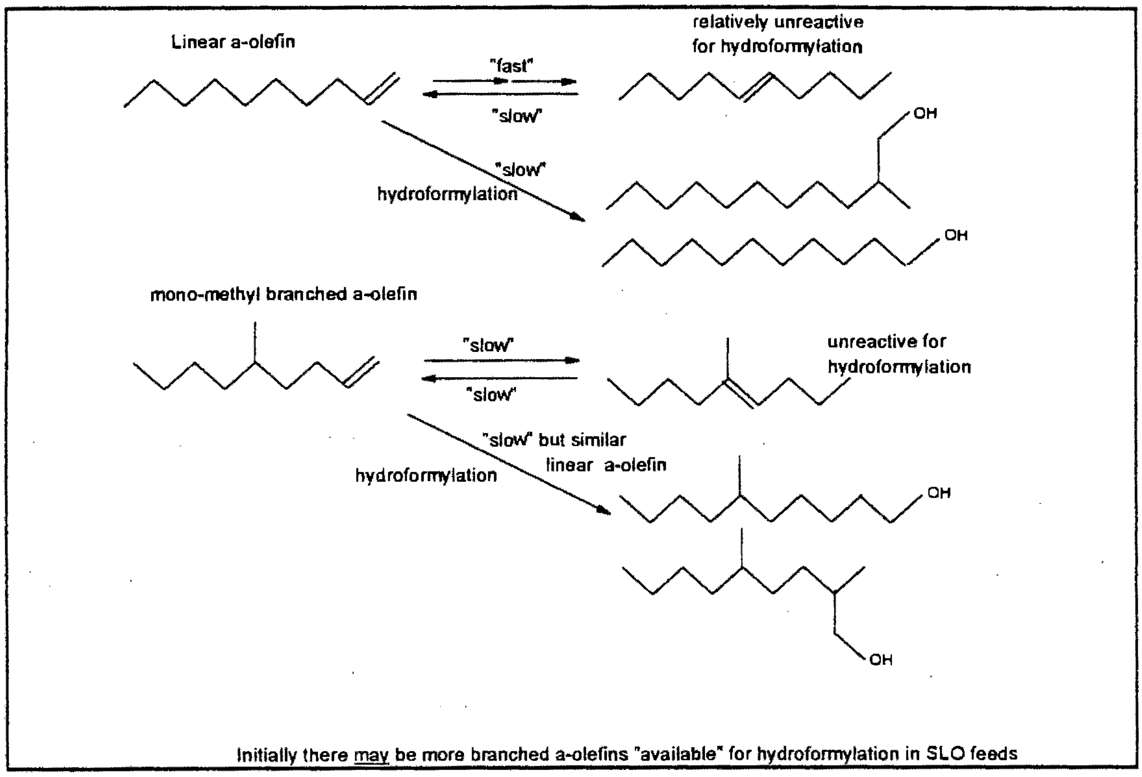

3.4.3.3 Co/TBP Testing: "Narrow" SLO Fraction

As demonstrated with the Rh/TPP catalyst, it is possible to obtain better selectivities to linear products with SLO feeds if the mono-methyl α-olefins could be removed (or partially removed). This may be achieved to a degree by refractionating SLO to increase the linear α-olefin concentration, as is done in manufacturing "narrow" cuts.

Runs 26 and 27 were performed on the same C_9 narrow SLO cut used in the Rh/TPP runs described in Section 3.3.3.3.

Table 3.4.8 Hydroformylation of a C_9 SLO "narrow" fraction (H_2:CO ratio = 2).

Run	26.1	27.1	14
Ligand	TBP	TBP	TPP
Metal	Co	Co	Rh
Temperature (°C)	200	150	80
Pressure (bar (g))	100 $_{\text{initial}}$	70 $_{\text{initial}}$	25 $_{\text{initial}}$
Time (hours)	5	5	4.1
%1-Nonene conversion	85	62	93
% Total nonene converted	81	51	93
1-Nonene products %linear	79	90	81
Overall products % linear	66	84	81
% n-Nonane selectivity	34	9	3
% Internal olefin selectivity	5	18	0 (tr.)
% Aldehyde selectivity	1	2	97
% Alcohol selectivity	53	64	0 (tr.)
% HOF selectivity	7	6	0 (tr.)

Promising results were obtained with this feed. On comparing the results of reactions 26 and 27, the following is evident:

Lowering the reaction temperature and pressure from 200°C to 150°C and 100 bar to 70 bar respectively gave rise to high 1-nonene (90%) and overall product linearities (84%) in reaction 27.1. The n-paraffin selectivity was lowered from 34% to 9%. The improved selectivities are at the expense of total olefin conversion.

The high internal olefin selectivities for run 27 may again be associated with lower total olefin conversions. This relationship between internal olefin selectivity and overall conversion implies that at high conversions the internal olefins are hydroformylated via the α-olefin. This is represented schematically in Figure 3.11.

Figure 3.11 Possible relationship between internal and α-olefins in Co/phosphine catalyzed hydroformylation systems.

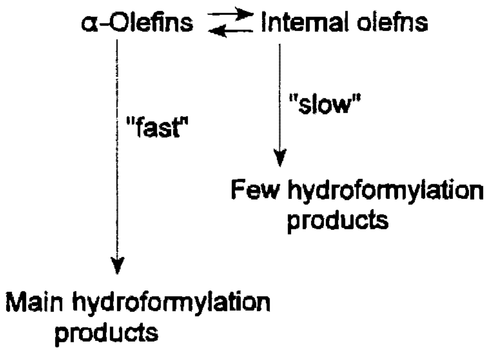

Allowing the reactions to proceed for longer would presumably have allowed the internal olefins to "re-isomerize" and subsequently undergo hydroformylation with a resultant improvement in the aldehyde and alcohol selectivities. Similar overall product linearities were obtained with the Co/TBP system in run 27.1 compared with the Rh/TPP system (Run 14 discussed previously) using the same SLO C_9 narrow fraction.

From the theoretical calculation of the extent of SLO "cleanup" (branched material removal) listed in Table 3.2, it is postulated that >90% of the branched olefins would have had to be removed from the C_9 cut in order to achieve the overall product linearity of 84% assuming the catalyst selectivity was similar to that expected when using a pure linear α-olefin feed. This is in agreement with the C_9 cut analysis in Table 3.1 which shows an olefin linearity of approximately 92%.

Figure 3.12, which is a GC product trace from run 27.1, can be compared with Figures 3.7 and 3.8. Apart from the linear and 2-methyl alcohol product peaks, there are 3 alcohol peaks derived from hydroformylation of internal olefins (marked as "x") and 3-4 peaks derived from methyl branched α-olefins (marked as "•"). It is interesting that the "internal olefin alcohols" are in somewhat higher concentration relative to the alcohols derived from branched α-olefins (including the 2-methyl alcohol), whereas the situation is reversed in the case of the SLO C_{10}broad fraction in Figure 3.8. It is therefore tentatively proposed that for Co/TBP catalysed hydroformylation of SLO; more linear feeds will give rise to more "internal olefin alcohols" in the product.

Figure 3.12 Gas Chromatogram of hydroformylation products for a Co/TBP catalyzed reaction of a C_9 SLO "narrow" fraction.

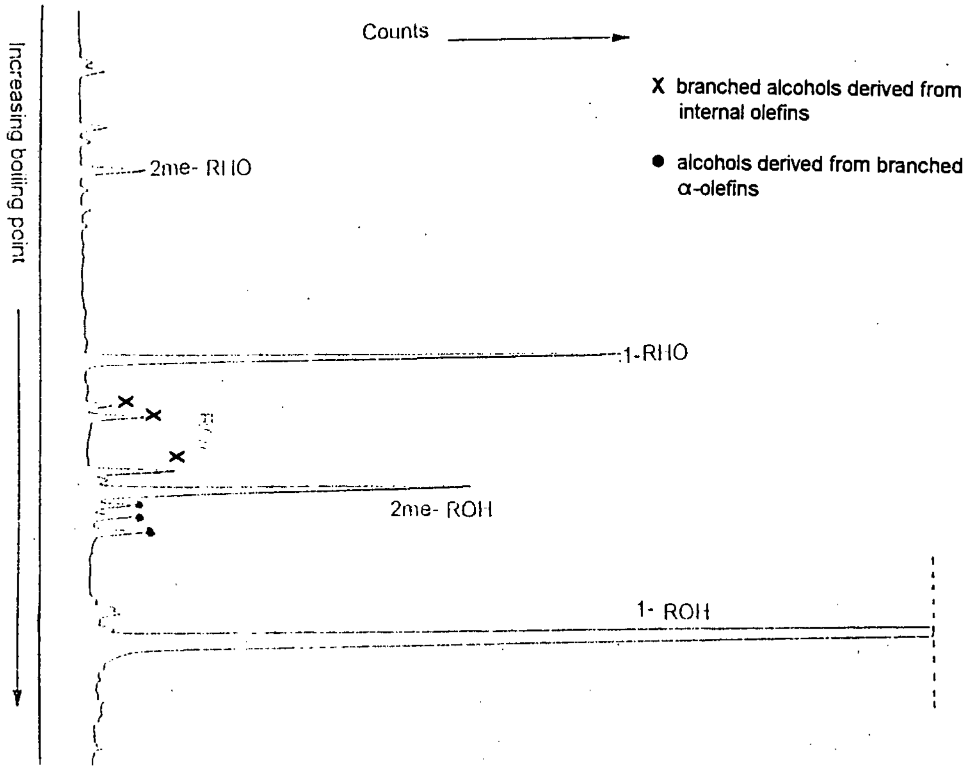

General note on the TBP ligand

The GC peak of TBP overlaps the 1-undecanol product peak. This implies that separation of TBP from C_{11} oxygenates using fractionation would not be feasible. Indeed, the relatively high volatility coupled with toxicity and instability of this ligand would probably make it unsuitable for commercial use. Similar alkyl-phosphine ligands, but with a higher molecular mass, would probably be more suitable.

3.5 TESTING OF "HETEROGENEOUS" CATALYST POSSIBILITIES

Given the interesting results obtained with the Co/P modified catalysts, it was decided to perform "orientating" tests on a few phosphine modified Co-based "heterogeneous" catalysts. Furthermore, reports on these types of catalyst are not readily evident in the literature.

3.5.1 "Heterogeneous" Reactions

See Table 3.5.1 for reactions undertaken and for a summary of the results.

3.5.2 Discussion of Heterogeneous Results

3.5.2.1 "Polymer-Bound Co/TPP" Hydroformylation Catalyst (Run 28):

A batch run was undertaken to ascertain if the phosphine would anchor the cobalt. Cobalt was added *in situ*, such that the TPP:Co molar ratio was 2:1. Approximately 20% of the cobalt added was not anchored (see Section 2.3.3.1). Similar results in terms of reaction selectivity and product linearity, were obtained compared with the homogeneous Co/TPP systems. The poor linearity of 40%, once again confirmed that tri-aryl phosphines are unsuitable for use with Co if high linearities are required.

Table 3.5.1 Testing of "anchored" P modified Co catalysts: **Runs Undertaken and Results.**

Run	System Tested	[Co] g/100ml	Feed composition (volume/volume)
28	$Co(OOCCH_3)_2.4H_20$ added *in situ* to: Polymer bound TPP on styrene divinyl benzene polymer (20% cross-linked) (purchased from Strem).	0.108	(30ml n-octane)/ (70ml 1-decene)
29	Co impregnated onto spray dried SiO_2 (±20% Co on SiO_2): Pre-reduced with H_2 at 285°C for 4 hours. TBP ligand added *in situ*.	0.481	C_{10} SLO narrow fraction 100ml
30.1-30.5 [1]	Co impregnated onto spray dried SiO_2 (±30% Co on SiO_2): Pre-reduced with H_2 at 290°C for 16 hours.TBP ligand added *in situ*.	0.481	C_{10} SLO narrow fraction 100ml
31	Co impregnated onto spray dried SiO_2: (±20% Co on SiO_2): No pre-reduction. TBP ligand added *in situ*.	0.481	C_{10} SLO narrow fraction 100ml
32	Ion exchanged Co on amorphous 1:1 SiO_2/Al_2O_3: (±2.5% Co on SiO_2/Al_2O_3): No pre-reduction. TOP ligand added *in situ*.	0.259	(70ml 1-decene)/ (25ml n-octane)/ (5ml C_{16} int. std.)

Run	Run time(hrs)	ΔP (bars)	% α-olefin conversion	% Paraffin selectivity	% Aldehyde selectivity	% Alcohol selectivity	% HOF selectivity	% Oxo product linearity	% of Co_m leached into solution.
28	15.5	-*	97.9	0 (tr.)	20.21	74.17	0 (tr.)	40.12	20
29	23	70	88.7	11.6	1.1	74.9	7.8	79.1	12
30.1	4.8	32	76.9	11.0	5.4	43.8	3.3	85.4	10
30.2	5.1	19	63.0	18.5	7.4	47.1	11.6	84.1	(10) + 6 = 16
30.3	4.4	16	67.2	17.7	9.4	64.2	3.0	84.7	(16) + 7 = 21
30.4	7.6	24	62.3	7.0	0.2	77.3	4.9	84.4	(21) + 4 = 25
30.5	4.8	22	48.6	24.2	14.0	56.9	4.9	84.3	(25) + 4 = 29
31	5	-	53.2	9.4	8.4	63.4	1.3	73.9	86
32	8	-	37.4	31.3	4.9	12.5	9.4	83.4	≤1

[1] Runs 30.1 - 30.5 :

A semi-batch mode of operation was employed. The reactions were stopped once the pressure drop had ceased for each run. 50 ml of liquid was extracted and replaced with 50ml of fresh SLO feed before resuming the reaction at the original starting pressure of 50 bar (g).

The following common reaction conditions apply to Table 3.5.1:
Ligand: Co molar ratio : 2:1.
Reaction temperature (°C) : 170.
H_2:CO ratio : 2:1.
Initial pressure (bar (g)) : 75. Unless indicated, the reactor pressure was kept constant.
Reactor used : 450ml Parr.

Selectivities are based on the amount of α-olefin converted; where selectivities do not total to 100%, the balance of the α-olefins have been converted to internal olefins.

3.5.2.2 "Supported Co/TBP on SiO_2 " Hydroformylation Catalysts

Use was made of a SiO_2 support in the hope that it would anchor Co. The Co was added to the support by means of impregnation for runs 29,30 and 31 and by means of ion exchange in run 32. Reduction temperatures (where applicable) were chosen from results of temperature programmed reduction profiles of the precursors. The supported Co was reduced in a separate vessel and introduced along with the liquid feed and TBP ligand into the micro-reactor. Hydroformylation batch experiments were undertaken to ascertain if the material would function as catalyst without substantial Co leaching.

Reduced Co/SiO_2 Precursor (Runs 29 and 30):

Reactions 30.1 to 30.4 showed a successive decline in activity. Selectivities varied, but the product linearities were similar for all the reactions. The phosphine ligand became diluted (see footnote [1] of Table 3.5.1) with successive runs indicating that the ligand did not adsorb strongly to the supported cobalt. Alternatively, cobalt was leached from the support, and then associated with the ligand. On introducing "make-up" phosphine ligand (run 30.5), an increase in activity was not observed, thereby indicating that the remaining Co was relatively "inactive".

The SEM, EDAX and ICP analyses on the used and "fresh" particles correlate well with the wet chemical and cobalt in solution determinations. It appears as if Co "leached" out of the Co/SiO_2 particles, and that the "working" catalyst was comprised of a homogeneous organometallic complex. This was observed for runs 29 and 30.

The SEM showed that the fresh and used samples did not all have the same properties in terms of Co crystallite size and distribution, cobalt content, shape *etc.* EDAX analyses of two random particles showed similar Co:Si ratios for the spheres used in runs 29 and 30, although the average mass % of Co leached from the samples was markedly different as indicated in Table 3.5.1. Although the EDAX result is unrepresentative, it may indicate that certain crystallites behave differently under hydroformylation conditions.

Unreduced Co/SiO$_2$ Precursors (Runs 31 and 32):

Comparing the results of reactions 29 and 31 in Table 3.5.1 demonstrates the effect of reduction of the Co/SiO$_2$ precursor. Pre-reduction appears to hold advantages in terms of yielding a lower % Co leaching and better selectivity to alcohol, as well as higher conversions. Indeed with the exception of the higher HOF selectivity, all the other selectivities are more favourable with the pre-reduced Co/SiO$_2$.

Although promising in terms of the low Co leaching achieved with the ion exchanged Co on SiO$_2$ catalyst, a low conversion and alcohol selectivity was obtained. In addition, the ion exchanged material contained a relatively low cobalt loading which necessitated a large amount of solid in the batch reactor in order to achieve the desired cobalt concentration. This would be unpractical for scale-up. For these reasons it was decided not to test this precursor in the pre-reduced form.

Comment:

In order to achieve success with heterogeneous hydroformylation catalysts, metal carbonyls would have to be stable on the surface of the catalyst. This could have a negative impact on the reaction rates, which could be under diffusion control and hence be slower. The larger amounts of solids in reactors, and the localization of active centres/sites on or inside these solids could lead to process difficulties. It is thus conceivable that attempts to heterogenize homogeneous systems by anchoring the catalyst on or inside a solid support in order to combine the advantages of both heterogeneous and homogeneous catalysts may have the opposite effect, resulting in a combination of the disadvantages instead.

3.6. CONCLUSIONS

The results of the foregoing experiments indicate that phosphine modified Rh and Co homogeneous catalysts are suitable for the hydroformylation of HTF-T diesel or gasoline product streams. No gross poisons were evident in the feedstocks that were evaluated.

Experimental conditions giving rise to high product linearities with SLO feeds were achieved. Total product linearities of >80% were achieved with SLO "narrow" fractions. This indicates that preparation of the feeds by refractionation of SLO in order to increase the concentration of the linear α-olefin gives rise to predominantly linear hydroformylation products.

For the Rh/TPP experiments, the chemical form of the metal precursor and the nature of the SLO fraction had an effect on the catalyst activity. The preferred "precursors" for SLO fractions were $HRhCO(P(C_6H_5)_3)_3$ and $[Rh(O_2C_2H_3)_2]_2$. Lower catalyst activities and corresponding higher linearities were evident at higher H_2:CO and TPP:Rh ratios. Overall product linearities of >80% and conversions of > 90% were achieved with C_8, C_9 and C_{10} SLO "narrow" fractions using the Rh/TPP catalysts.

For the phosphine modified Co experiments, alkyl phosphine (TBP) ligand was shown to be superior to the aryl phosphine (TPP) in terms of product linearity. Similar selectivities were evident with H_2:CO ratios of 1 and 2. A product linearity of >80% was also demonstrated with the C_9 narrow fraction.

Differences in the reactivity of internal olefins in SLO were observed with the phosphine modified Co catalysts. There is evidence indicating that branched internal olefins are less easily hydroformylated in SLO feeds and this appears to be a function of the branched α-olefin structures. With the exception of the 2 methyl alcohol, branched alcohols in products from SLO streams form mainly from mono-methyl α-olefins. In the case of pure linear feeds, the branched products (with the exception of the 2 methyl product) form as a result of internal olefin hydroformylation/s. If fewer mono-methyl α-olefins are present, as is the case with narrow SLO cuts, then more of the internal olefins undergo hydroformylation directly.

The very limited attempts to "heterogenize" the phosphine modified Co catalysts by anchoring on solid supports were unsuccessful. It was decided not to investigate this topic in detail, partly due to the limited success achieved by others in this field using pure feeds. For this reason, "heterogenous" Rh systems were also not considered. Although bimetallic or multimetallic catalyst systems have been shown by others [Bruanstein and Rose, 1988][Roberts and Geoffrey, 1982][Ishii *et al.*, 1988] to exhibit unique catalytic activities and selectivities which cannot be achieved by a single metal catalyst, these were not evaluated. These catalysts, such as Co-Ru systems [Hidai and Matsuzaka, 1988][Matsuzaka *et al.*, 1988] and Co-Rh systems [Garlasschelli *et al.*, 1991][Hunter *et al.*, 1985] were not considered due to the fact that they are also not applied commercially, probably due to limitations involving recycle and recovery.

Although the results were promising with Rh/TPP systems, it was decided to concentrate further work on Co/Phosphine catalysts with SLO feeds. One of the reasons being that Rh/TPP systems are not applied commercially for hydroformylation of detergent range olefins. This is presumably due to process difficulties or risks in the recycle and recovery of these catalysts (see Section 1.3.5.2). Bearing in mind that one of the original objectives of the work was to determine the kinetics of SLO hydroformylation and to test a resultant model on a continuous unit; Co/phosphine catalysts appeared to be a more interesting option. Reasons included the differences in olefin reactivities obtained using pure and SLO feeds with Co/TBP catalysts and the scarcity of detailed reports in the literature dealing with these catalyst systems. This is especially true for alkylphosphine ligand variants.

It was therefore decided that Co/Phosphine systems were the most suitable for further study.

CHAPTER 4

TRI-N-OCTYLPHOSPHINE MODIFIED Co SYSTEMS

4 TRI-n-OCTYLPHOSPHINE (TOP) MODIFIED Co SYSTEMS

4.1 CONSTANT PRESSURE REACTION STUDIES: GENERAL INTRODUCTION

Due to the results obtained with alkyl phosphine modified Co catalysts in Chapter 3, it was decided to concentrate on these systems. This class of hydroformylation catalyst appears to have been less frequently reported on than others. TOP was selected as the n-alkylphosphine ligand for further evaluation since the TBP GC peak interfered with C_{11} alcohol analyses (see Footnote on page 132).

In the constant pressure experiments listed in Table 4.1, the following aspects were investigated:

1) Repeatability, 2) Initial kinetic considerations, 3) Broad versus narrow SLO fractions, 4) SLO versus pure feeds, 5) Syngas composition and pressure, 6) KOH additive, 7) Effect of carboxylic acids, 8) Effect of water and, 9) Ligand structure.

4.1.1 Experimental Approach

The following methodology was employed:
"Semi-batch" experiments were undertaken, wherein the syngas that was consumed during reactions was replaced by maintaining the reactor at a constant pressure. When using a constant H_2:CO molar ratio = 2, the syngas composition did not change significantly during the course of the reaction. If one determines the moles of H_2 and CO consumed from reaction selectivities, and assumes that total moles of CO and H_2 consumed are replaced by 2:1 H_2:CO syngas in order to keep the pressure constant, then the theoretical P_{H2} and P_{CO}

in reactor can be determined. This is demonstrated for an experiment in Figure 4.1, which shows that the H_2:CO ratio within the reactor remained approximately constant.

Figure 4.1 Syngas composition: Co/TOP (run 33). Batch reactor under constant pressure of pure 2:1 H_2:CO syngas. (Sealed outlet).

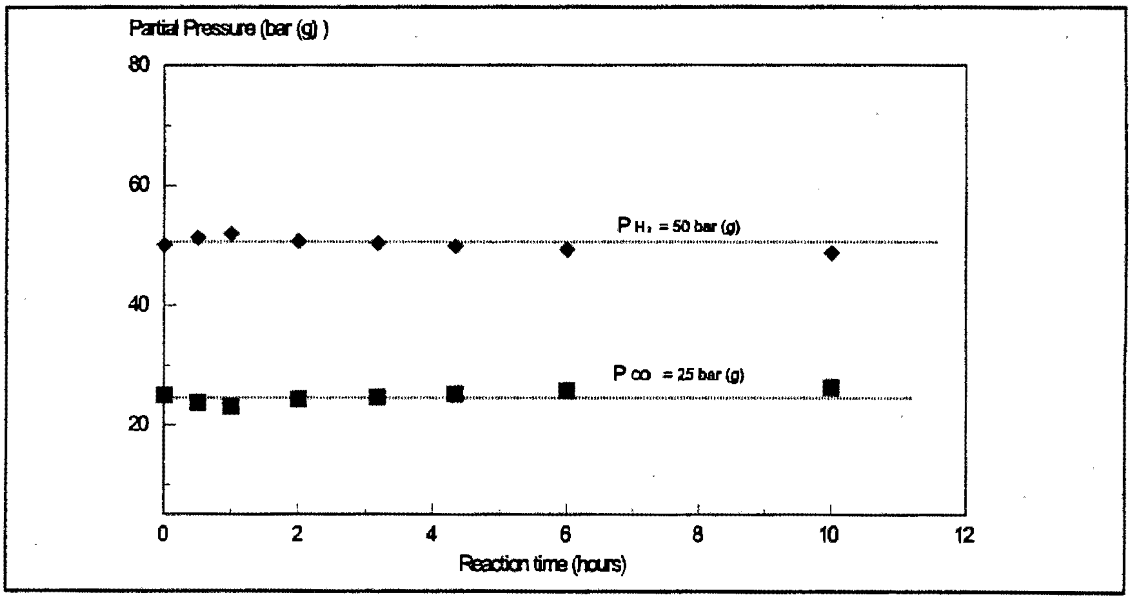

The agreement between the calculated and measured syngas compositions is demonstrated in Table 4.2.

Various experiments were also undertaken in which syngas was passed continuously through the system. In these experiments, the gas flow rate was in the order of 100 normal ml per minute which was slow enough to prevent liquid losses by carry over with the syngas.

4.1.2 Exhaustive Hydroformylation

This method was developed in order to characterize the complex olefin distributions in SLO, and especially in Co/P catalyzed systems where isomerization of olefins occurs. The additional, non-olefinic components, present in SLO often mask olefin peaks which makes quantification of the olefins difficult. It was found that the best method to quantify the olefins was to exhaustively hydroformylate the material in order to expose and quantify the non-olefinic components masking or present "under" the olefinic component peaks in the GC traces. These non-olefinic components were identified by GC-MS techniques. Their contribution to the olefinic material were then "subtracted", as discussed more fully in Section 2.3.1.2.

4.1.3 Reactor Profiles

By sampling the reactor liquid contents at various times during the course of an experiment, changes to the profile of reactants and products could be monitored against reaction time. Although various factors affected the reaction rate and selectivities as will be demonstrated, the following typical profile was observed for experiments undertaken at constant pressure (see Figure 4.2). The profile indicates that extensive isomerization of α-olefins to internal olefins occurs initially. The internal olefins re-isomerize to α-olefins prior to hydroformylation as evidenced by the high product linearities. Hydroformylation initially results in a relatively large quantity of aldehydes, most of which are subsequently hydrogenated to alcohols. A portion of the olefinic feed is hydrogenated to paraffin, and a Heavy Oxo Fraction (HOF) forms as a result of unwanted side reactions.

It therefore follows that the selectivity profiles would be similar. This is illustrated in Figure 4.3 which is based on the total olefins (α and internal olefins) converted.

Similar profiles for all the reactions listed in Chapters 4 and 5 and in Tables 4.1 and 5.1 were determined. The profiles all showed the same trends as illustrated in Figures 4.2 and 4.3. The results are summarized in Tables 4.2 to 4.4.2 in this chapter, and for Chapter 5 in Tables 5.2 to 5.4.2. Mini-tables are reproduced in the discussion to facilitate easier comparisons and assist the reader.

Figure 4.2 Profile of reactor contents with TOS: Run 29 SLO broad fraction.

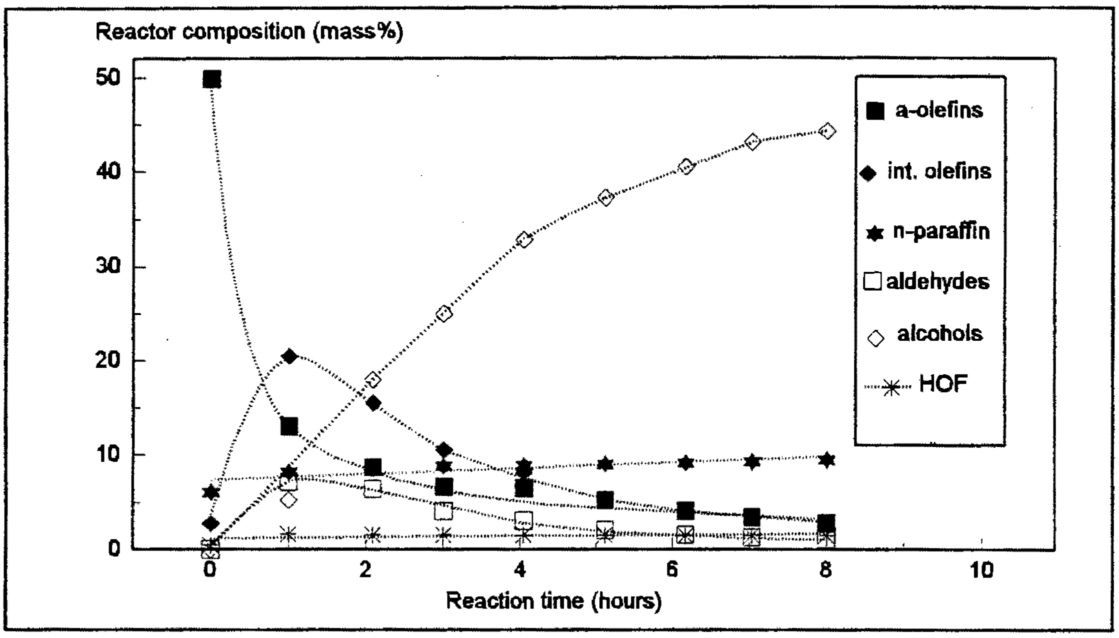

Figure 4.3 Selectivity and linearity profile for Run 29 (SLO broad fraction).

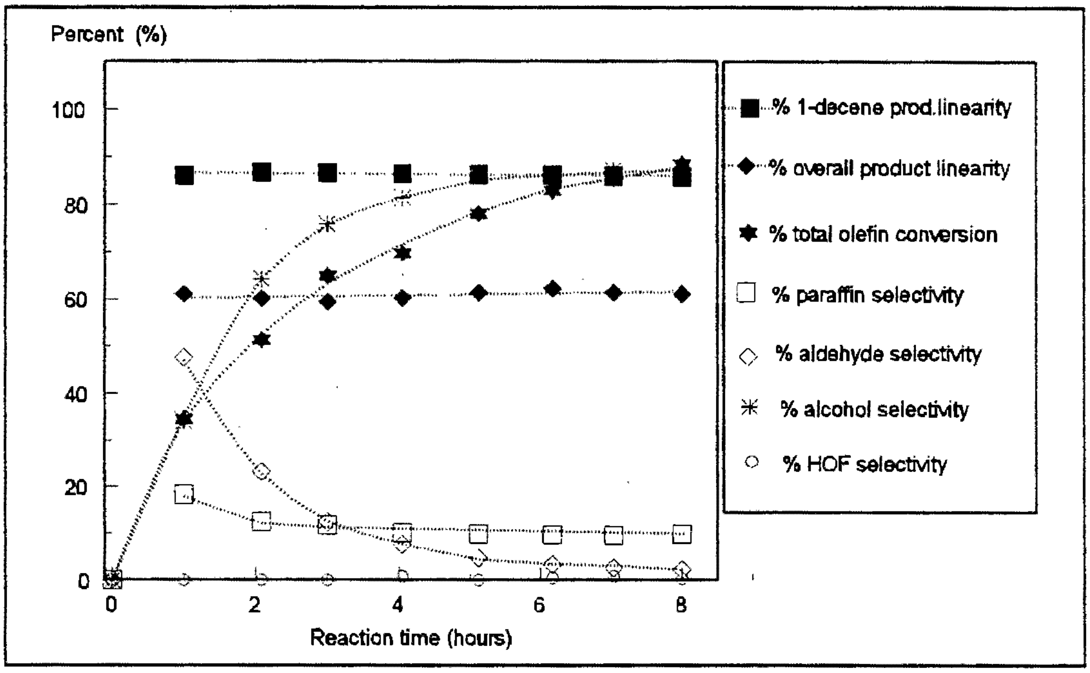

4.2 Co/P SYSTEMS: CONSTANT PRESSURE RUNS UNDERTAKEN

Table 4.1 Reaction studies: Co/P-modified systems.

Run	Ligand	[Co] g/100ml	L/M Molar ratio	Feed composition (volume/volume)	Feed pretreatment (for acid removal)	H_2:CO Molar ratio	Pi bar	Additives: KOH/LAS**/Co molar ratios
29a	TOP	0.22	2.0	SLO C_{10} broad fraction (B)	washed	2	75	- / - /1
29b	TOP	0.22	2.0	SLO C_{10} broad fraction (B)	washed	2	75	- / - /1
29c	TOP	0.22	2.0	SLO C_{10} broad fraction (B)	washed	2	75	- / - /1
29d	TOP	0.22	2.0	SLO C_{10} broad fraction (B)	washed	2	75	- / - /1
30	TOP	0.31	2.0	SLO C_{10} narrow fraction (B)	unwashed	2	75	- / - /1
31	TOP	0.26	2.0	SLO C_{10} broad fraction (A)	unwashed	2	75	- / - /1
32	TOP	0.32	2.0	SLO C_{10} narrow fraction (A)	unwashed	2	75	0.75/ - /1
33	TOP	0.25	2.0	3/1 (1-decene)/(n-octane)	-	2	75	0.75/ - /1
34	TOP	0.32	2.0	SLO C_{10} narrow fraction (A)	unwashed	*Comm Syngas	90	- / - /1
35	TOP	0.25	2.0	SLO C_{10} narrow fraction (A)	unwashed	2	75	- / - /1
36	TOP	0.25	2.0	3/1 (1-decene)/(n-octane)	-	2	75	- / - /1
37	TOP	0.25	2.0	3/1 (1-decene)/(n-octane)	-	Comm. Syngas	90	0.75/ - /1
38	TOP	0.26	2.0	3/1 (1-decene)/(n-octane)	-	Comm. Syngas	90	- / - /1
39	TOP	0.29	2.0	SLO C_{10} narrow fraction (B)	5ml butyric acid spiked	2	75	- / - /1 (+5% v/v C_4 acid)
40	TOP	0.23	2.0	SLO C_{8+9} broad fraction	unwashed	2	75	0.75/0.1/1
41	TOP	0.25	2.0	SLO C_{8+9} broad fraction	unwashed	2	75	0.75/0.1/1 (+10% v/v H_2O)
42	TBP	0.32	2.0	SLO C_{10} narrow fraction (A)	unwashed	2	70	0.75/ - /1
43	bis-PPB	0.24	2.0	SLO C_{10} narrow fraction (B)	unwashed	2	75	- / - /1
44	EP	0.26	2.0	SLO C_{10} broad fraction (A)	unwashed	2	75	0.75/ - /1

$Co(O_2C_2H_3)_2.4H_2O$ precursor was used for all the runs

*Comm. Syngas is typical of a commercial synthesis gas (see Section 2.2.2)

**LAS is a Linear Alkylbenzene Sulphonate (C_{12} alkyl) surfactant additive (see Section 4.4.6).

Stirring speed for all the runs: 500rpm

Temperature for all runs: 170°C

4.3 Co/P SYSTEMS: RESULTS OF CONSTANT PRESSURE RUNS

The results are summarized by way of Tables 4.2, 4.3 4.4.1 and 4.4.2 below:

Table 4.2 Gas breakdown of runs undertaken in Table 4.1.

Run	Gas composition (As supplied/ specified by manufacturer)	P(CO) initial bar. (g)	P(CO) final bar (g)	P(H_2) initial bar (g)	P(H_2) final bar (g)	P(total) bar (g)
29a	±33% CO; ±66% H_2	25		50		75
29b	±33% CO; ±66% H_2	25		50		75
29c	±33% CO; ±66% H_2	25		50		75
29d	±33% CO; ±66% H_2	25		50		75
30	±33% CO; ±66% H_2	25	°26.2 *27.8	50	°48.8 *47.2	75
31	±33% CO; ±66% H_2	25	°25.5 *27.6	50	°49.5 *47.5	75
32	±33% CO; ±66% H_2	25	°26.8	50	°48.2	75
33	±33% CO; ±66% H_2	25	°26.3	50	°48.7	75
34	Commercial syngas	26	°23.3	49.3	°36.8	90
35	±33% CO; ±66% H_2	25	°26.2 *27.5	50	°48.8 *47.5	75
36	±33% CO; ±66% H_2	25	°26.0 *26.9	50	°49.0 *48.2	75
37	±33% CO; ±66% H_2	25	°25.8	50	°49.2	75
38	Commercial syngas	26	°23.0	49.3	°36.3	90
39	±33% CO; ±66% H_2	25	°26.1 *27.7	50	°49.8 *47.3	75
40	±33% CO; ±66% H_2	25	°26.6	50	°48.4	75
41	±33% CO; ±66% H_2	25	°25.1	50	°49.9	75
42	±33% CO; ±66% H_2	23.3		46.7		70
43	±33% CO; ±66% H_2	25	°25.2	50	°49.8	75
44	±33% CO; ±66% H_2	25	*27.8	50	*47.2	75

°Calculated on the basis of reaction selectivities and moles of olefin converted.

*Measured (from gas ampule samples).

□ Empty blocks in the table assume that final values are approximately equal to initial values. Gas was passed continuously through the system.

Table 4.3 Breakdown of olefins measured in Feed: Runs described in Table 4.1. Measured Rate constants (*k*) from plots of ln(1-C) versus time where C = total fractional olefin conversion.

Run	Mass % in Feed								Total olefin % linear	Co/ olefin mass %	*k*	*k*'
	Total olefin	Total α-olefin	linear α-olefin	br. α-olefin	Total int. olefin	linear int. olefin	br. int. olefin	Inerts				
29a	52.7	49.9	36.0	13.9	2.8	2.8	0.00	47.3	73.7	0.32	0.30	1.33
29b	52.0	49.3	34.9	14.5	3.1	2.7	0.40	48.0	71.7	0.31	0.26	1.15
29c	52.0	49.5	35.7	13.9	2.4	1.8	0.63	48.0	72.5	0.31	0.29	1.29
29d	51.5	49.1	35.2	14.3	2.0	2.0	0.00	48.9	72.7	0.31	0.30	1.33
30	67.9	67.8	52.5	15.3	0.0	0.0	0.00	32.2	83.3	0.34	0.44	1.45
31	50.4	49.1	29.2	19.9	1.3	1.3	0.00	49.6	60.6	0.38	0.44	1.69
32	71.8	68.2	63.5	4.7	3.6	3.6	0.00	28.2	93.5	0.33	0.47	1.45
33	77.4	75.9	75.9	0.0	1.5	1.5	0.00	22.6	100	0.24	0.23	0.90
34	70.8	67.2	62.7	4.5	3.5	3.5	0.00	29.3	93.7	0.34	0.38	1.22
35	66.5	63.1	57.8	5.3	3.5	3.5	0.00	33.5	92.0	0.28	0.35	1.42
36	74.1	73.4	72.7	0.7	0.7	0.7	0.00	25.9	99.1	0.26	0.24	0.98
37	76.6	74.5	74.5	0.0	2.1	2.1	0.00	23.4	100	0.24	0.25	0.99
38	72.1	70.2	70.2	0.0	1.9	1.9	0.00	27.9	100	0.27	0.29	1.13
39	64.1	64.1	54.2	9.9	0.0	0.0	0.00	36.6	85.5	0.34	0.55	1.88
40:C8	49.0	49.0	39.00	4.5	5.6	5.6	0.00	38.0	90.9	0.34	0.54	2.38
40:C9	12.9	12.9	0.00	12.9	0.0	0.0	0.00		0.00	1.29	0.49	2.16
41:C8	51.0	44.3	39.7	4.6	6.7	6.7	0.00	35.6	91.0	0.36	0.62	2.52
41:C9	13.5	12.8	0.00	12.8	0.6	0.0	0.63		0.0	1.36	0.55	2.23
42	71.2	67.5	63.2	4.3	3.8	3.8	0.00	28.8	94.0	0.34	0.39	1.20
43	73.2	73.2	58.6	14.5	0.0	0.0	0.00	26.8	80.1	0.24	0.49	2.04
44	48.6	46.9	29.9	16.9	1.7	1.7	0.00	51.4	60.6	0.35	0.88	3.53

k' = k/[cat] where:

k = first order rate constant describing olefin disappearance

[cat] = grams of Co per 100 ml of feed.

Olefin breakdowns were determined for each run using "exhaustive hydroformylation" (see Section 2.3.1.2).

Table 4.4.1 Conversions and selectivities based on the total olefins converted at time 1 (as indicated below).

Run	Time (hours)	Total olefin converted (%)	Overall product linearity (%)	Linear α-olefin product linearity* (%)	Paraffin selectivity (%)	Aldehyde selectivity (%)	Alcohol selectivity (%)	HOF selectivity (%)
29a	2.08	46.2	60.1	86.8	12.5	23.2	64.3	- (tr.)
29b	2.13	52.3	62.9	87.0	13.4	18.2	68.4	- (tr.)
29c	2.00	49.9	60.2	89.0	13.3	23.8	62.9	- (tr.)
29d	2.00	49.8	61.3	86.8	12.9	23.1	64.0	- (tr.)
30	2.00	65.1	74.7	95.4	12.0	13.2	74.4	0.5
31	2.00	59.1	56.2	85.2	9.2	18.2	69.9	2.7
32	2.00	66.4	82.8	88.4	16.9	6.1	73.1	3.9
33	2.00	39.9	87.3	89.7	16.2	27.6	54.7	1.5
34	2.00	50.0	86.0	93.0	22.2	21.6	53.3	2.7
35	2.00	54.3	84.2	90.7	15.6	10.0	69.8	4.6
36	2.00	45.8	87.8	92.8	12.9	20.1	61.3	5.8
37	1.17	38.1	75.0	87.4	4.7	21.5	67.9	5.9
38	2.00	51.4	73.8	92.2	13.3	14.1	71.4	1.2
39	2.00	66.4	74.4	87.9	12.3	8.8	72.3	6.6
40:C8	2.00	67.5	74.5	91.2	15.3	15.3	68.7	0.7
40:C9	2.00	72.8	-	-	20.5	-	78.7	0.9
41:C8	2.00	73.1	75.3	88.9	16.8	6.4	76.5	0.4
41:C9	2.00	74.5	-	-	8.1	-	90.3	1.6
42	2.00	62.5	82.9	90.4	13.0	8.9	74.3	4
43	2.00	69.8	63.6	81.5	6.8	21.7	69.9	1.6
44	2.00	88.0	59.3	86.1	4.6	7.6	86.3	1.5

* Denotes the linearity of hydroformylation products derived from the linear α-olefin, *ie.* {linear alcohol}/{linear + 2 methyl alcohol} expressed as %.

Table 4.4.2 Conversions and selectivities based on the total olefins converted at time 2 (as indicated below).

Run	Time (hours)	Total olefin converted (%)	Overall product linearity (%)	Linear α-olefin product linearity* (%)	Paraffin selectivity (%)	Aldehyde selectivity (%)	Alcohol selectivity (%)	HOF selectivity (%)
29a	8.0	87.5	61	85.7	9.8	2.2	87.3	0.8
29b	8.0	88.2	62	85.8	10.0	2.2	87.0	0.8
29c	8.0	90.2	61.2	85.7	10.4	2.5	86.5	0.6
29d	8.0	89.2	60.9	85.7	10.3	2.2	86.8	0.8
30	8.0	100	71.8	87.2	11.1	0.5	87	1.5
31	8.0	100	55.9	83.8	10.0	1.4	85.9	2.9
32	6.5	95.3	79.3	88.3	10.4	2.1	81.8	5.7
33	6.5	76	86.4	90.6	12.1	4.8	82.1	1.0
34	6.0	94.3	79.2	88.0	17.0	1.4	75.7	5.8
35	8.0	93.3	78.5	87.9	13.1	1.2	78.3	7.4
36	8.0	83.8	83.2	90.5	13.4	3.2	82.3	1.0
37	6.0	81.3	85.3	92.1	8.5	3.8	82.8	4.9
38	8.0	88.4	83.3	90.5	12.0	1.3	83.6	3.2
39	8.0	100	71.4	86.9	11.7	1.6	74	12.7
40:C8	8.0	100	75.5	90.0	14.2	1.4	83.7	0.9
40:C9	8.0	100	-	-	13.4	-	85.2	1.5
41:C8	8.0	100	78.4	90.1	5.3	0.6	91.3	2.8
41:C9	8.0	100	-	-	3.9	-	91.8	4.3
42	6.5	91	79.4	87.0	11.5	1.9	81.9	6.1
43	8.0	100	60.8	79.6	5.9	4.2	88.7	1.2
44	8.0	99.9	52.9	84.6	3.0	3.7	90.6	2.8

* Denotes the linearity of hydroformylation products derived from the linear α-olefin, *ie* {linear alcohol}/{linear + 2 methyl alcohol} expressed as %.

4.4 DISCUSSION OF RESULTS: Co/P CONSTANT PRESSURE RUNS

4.4.1 Repeatability of Results

This was demonstrated in runs 29a-d as shown in Table 4.5 and in Figure 4.4 in Section 4.4.2. These data indicate repeatability of feed analyses and experimental results.

Table 4.5 Data and results for runs undertaken at the same conditions demonstrating repeatability.

Run	29a	29b	29c	29d
Measured olefin composition (mass% in feed)[1]				
Linear α-olefin	36.0	34.9	35.7	35.2
Branched α-olefin	13.9	14.5	13.9	14.3
Internal olefin (linear)	2.8	2.7	2.4	2.0
Total olefin	52.7	52.0	52.0	51.5
Linearities, conversions, selectivities[2]: At 8 hours TOS[3]				
%Total olefin converted	89.8	88.2	90.2	89.2
%Overall product linearity	61.0	62.0	61.2	60.9
%Linearity of 1-decene hydroformylation products	85.7	85.8	85.7	85.7
%Paraffin selectivity	9.8	10.0	10.4	10.3
%Aldehyde selectivity	2.2	2.2	2.5	2.2
%Alcohol selectivity	87.3	87.0	86.5	86.8
%HOF selectivity	0.8	0.8	0.6	0.8

[1] Olefin breakdowns determined using exhaustive hydroformylation

[2] Selectivities are based on the total olefins converted.

[3] TOS denotes Time On Stream

The common reaction conditions are listed in Table 4.1.

The way in which data (specifically GC data) for the constant pressure experiments were compiled and analyzed for in SLO fractions making use of spreadsheet calculations is demonstrated in Appendix 2. Included in the Appendix is a breakdown of data from run 29a in the form of a spreadsheet. The same methodology was followed for "pure" feeds. The calculations used to determine various parameters such as conversions, selectivities, linearities *etc.*, are fully described in Section 2.3.1.2.

4.4.2 Preliminary Kinetics

In order to simplify subsequent comparisons, the kinetics of olefin disappearance are considered first.

The kinetics of the hydroformylation reaction for <u>conventional</u> catalysts is generally accepted as being described by Natta *et al.*'s [1952,1954,1955] relationship,

$$\frac{d\ (\text{aldehyde})}{dt} = \text{constant}[\text{olefin}]^{w}[\text{Metal}]^{x}\frac{(P_{H_2})^{y}}{(P_{CO})^{z}} \tag{4.1}$$

In Natta *et al.'s* original equation the reaction orders with respect to olefin and metal concentration, as well as P_{H2} and P_{co} are "first order" *ie.*, w, x, y and z are all equal to 1. However, under certain conditions, x may also = 0.5. According to Natta *et al.*, due to the opposing effects of CO and H_2, the reaction rate is independent of the total pressure when the H_2:CO ratio is 1. Depending on the reaction conditions, variations of the rate equation as reviewed by Falbe [1980] exist, and these are summarised in Table 4.6.

Table 4.6 Hydroformylation reaction orders for unmodified (no ligand) systems. [Falbe, 1980].

	Hydroformylation Catalyst	
Reaction "order" of:	$HCo(CO)_{3-4}$	$HRh(CO)_4$
Olefin concentration (w)	1	0 or 1
Metal concentration (x)	1* or 0.5**	1 to 0.16
H_2 partial pressure (y)	1	1
C0 partial pressure (z)	1 to -1 ***	1 to -1

* $x = 1$ at $P_{co} = \pm 100$ bar

** according to Natta *et al.*

*** $z = 1$ at $P_{CO} < 10$ bar; $z = -1$ at $P_{CO} > 10$ bar.

For the reactions undertaken in this chapter, the H_2:CO ratios in the syngas were kept approximately constant. This implies that for the runs undertaken, equation (4.1) may be simplified to

$$\text{Rate} - k[\text{olefin}]^{w}[\text{Metal}]^{x} \qquad (4.2)$$

where

$$k - (\text{constant term of equation (4.1)}) \frac{P_{H_2}}{P_{CO}} \qquad (4.3)$$

Although the kinetics of the hydroformylation reaction using unmodified catalysts have been widely reported in the literature - Falbe [1980] gives 37 references - results of kinetics using phosphine modified Co systems appear to be far less widely publicized. Notable exceptions are Tucci [1970], Helfferich [1989] as well as Chern and Helfferich [1990], who agreed that the hydroformylation reaction is first order with respect to olefin concentration.

Wender *et al.* [1956] showed that for conventional Co catalysts, similar rates for linear and 4-methyl branched α-olefins occur. However, the 2-methyl α-olefin reacted at a 88% slower rate in Wender *et al.*'s study. No information in the literature on reaction rates of different olefin structures using Co/P systems was sourced.

It was found that for SLO fractions, the rate of reaction of all the olefin types for a given carbon number fraction were similar and approximately first order. It was further demonstrated that the olefins in SLO and pure feeds may be grouped together to give an approximately first order expression which describes their collective disappearance. Since low amounts of the 2-methyl α-olefins are encountered in SLO (see Section 2.2.1), their contribution to a possible deviation from overall first order behaviour has been ignored. However, if their concentration is enhanced significantly by feed preparative techniques, then distinction would have to be made between the 2-methyl and the balance of the olefins.

Demonstration of the ability to combine mono-methyl branched α-olefins with the linear olefins in terms of their reactivity is demonstrated for runs 29a-d. Repeated kinetic results obtained using a SLO C_{10} fraction having an olefin linearity of around 73%, are illustrated in Figure 4.4.

The lines in Figure 4.4 were generated from the equation:

$$-\ln(1-C) - kt \tag{4.5}$$

where C = total fractional olefin conversion.
t = reaction time (in hours).
k = first order rate constant describing olefin consumption.

Figure 4.4 First order rate plots demonstrating similar (first order) olefin reactivity for the sum of all olefins in a SLO C_{10} broad fraction: Runs 29a-d.

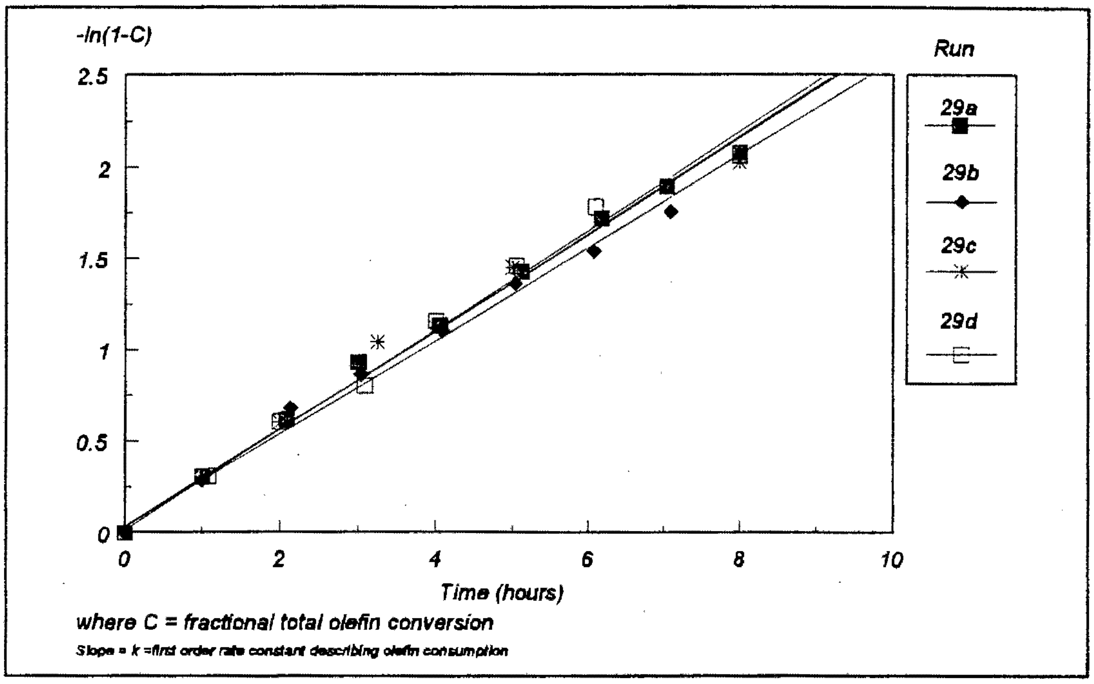

where C = fractional total olefin conversion

Slope = k =first order rate constant describing olefin consumption

The fact that the lines in Figure 4.4 pass through (or fractionally above) the origin, implies that the rate of *in situ* catalyst formation from the $Co(OOCCH_3)_2.4H_2O$ precursor was considerably faster than the hydroformylation reaction rate and did not impact on the kinetics.

As in Table 4.5, Figure 4.4 confirms the reproducibility of the results.

4.4.3 Broad versus Narrow SLO Feeds

The results in Figure 4.4 however do not imply that it is always possible to group linear and methyl α-olefins. The slope of the lines in Figure 4.4 (*ie. k* values) may change on varying the ratio of linear: methyl olefins in the feed. This is especially so if the 2-methyl and 3-methyl α-olefins are concentrated up in going from a broad fraction to a narrow one. First order olefin consumption kinetics was however still observed in broad and narrow SLO fractions (see Figure 4.5). The slopes of the two plots are similar indicating similar rate constants. Table 4.6 gives a breakdown of the reaction conditions and various results.

Figure 4.5 First order rate plots: Overall reactivity of olefins in SLO C_{10} broad and narrow fractions.

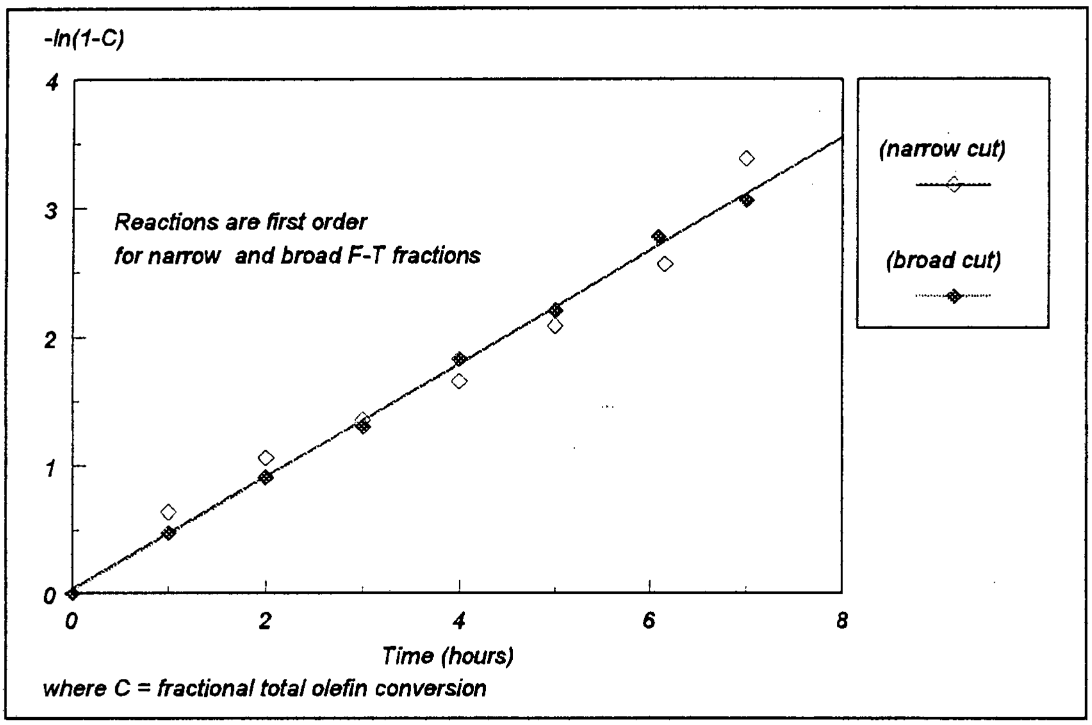

Given the differences in catalyst concentration (around 17%), the overall rate of olefin consumption in the broad fraction was faster (see Table 4.6). The difference may be ascribed to a higher concentration of methyl branched α-olefins with branching closer to the α-olefin double bond in the narrow fraction (see Figures 2.11 and 3.1). Except for the expected difference in the overall product linearity, the reaction selectivities were unaffected in going from a broad to a narrow fraction (see Table 4.6).

Table 4.6 Results obtained with "broad" and "narrow" HTF-T fractions.

Run	30	31
Feed (SLO fraction)	C_{10} "narrow"	C_{10} "broad"
Grams Co per 100grams of feed	0.31	0.26
Olefin content in Feed (Mass %)		
Linear α-olefin	52.5	29.2
Branched α-olefin	15.3	19.9
Internal olefins	0.0	1.3
Total olefins	67.9	50.4
Rate constant *k*	0.43	0.44
*Rate constant *k'*	1.45	1.69
Conversion, Product Linearities and Selectivties after 8 hours TOS		
%Total olefin converted	100	100
%1-Decene product linearity	87	84
%Overall product linearity	72	55
%Paraffin selectivity	11	10
%Aldehyde selectivity	0.5	1.4
%Alcohol selectivity	86	82
%HOF selectivity	1.5	2.9

* Rate constant *k'* values are corrected for differences in the catalyst concentration.

4.4.4 SLO Feeds Versus Pure Feeds

Figure 4.6 and Table 4.7 compare the relevant results.

Figure 4.6 gives an indication as to differences in the kinetics of "pure" and SLO feeds. Faster rates were evident in the SLO. This observation was consistent for the runs undertaken with Co/TOP - *ie*. faster rates with SLO feeds. The lower 1-decene product linearities obtained with the SLO feeds are presumably a result of the higher reaction rates. The reaction selectivities for the SLO and pure feeds appear similar, but a higher HOF resulted with the SLO, probably due to side reactions (see Figure 1.16).

Figure 4.6 First order rate plots: 1-Decene and SLO C_{10} narrow fraction: Runs 32 and 33.

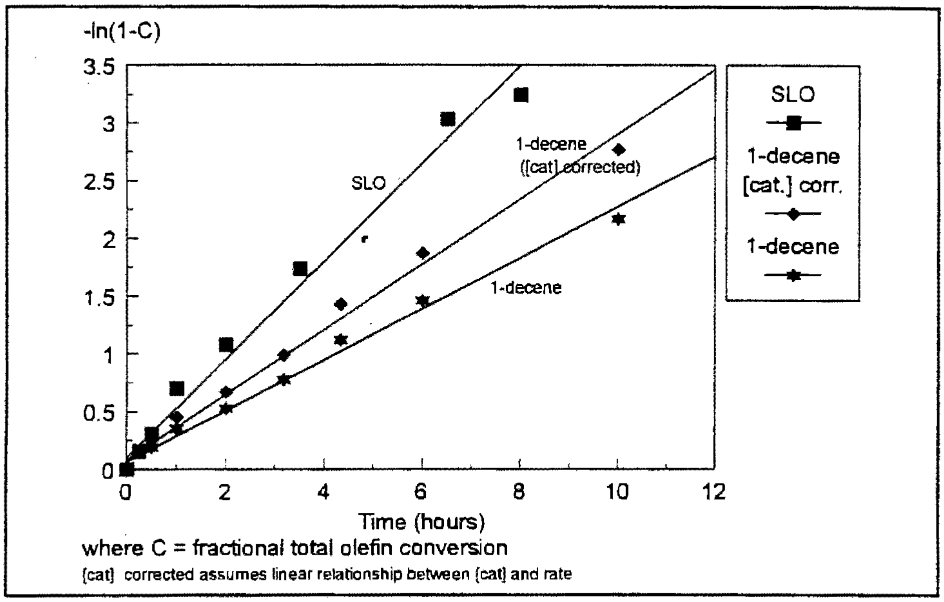

where C = fractional total olefin conversion

[cat] corrected assumes linear relationship between [cat] and rate

Table 4.7 Results obtained with 1-decene and a SLO C_{10} narrow fraction.

Run	32	33
Feed	SLO C_{10} "narrow"	3/1 1-decene/octane
Grams Co per 100grams of feed	0.32	0.25
Olefin content in Feed (Mass %)		
Linear α-olefin	63.5	75.9
Branched α-olefin	4.7	-
Internal olefins	3.6	1.5
Total olefins	71.8	77.4
Rate constant *k*	0.47	0.23
*Rate constant *k'*	1.45	0.90
Conversion, Product Linearities and Selectivties after 6.5 hours TOS		
% Total olefin converted	95.3	76.0
% 1-Decene product linearity	88.3	90.6
% Overall product linearity	79.3	86.4
% Paraffin selectivity	10.4	12.1
% Aldehyde selectivity	2.1	4.8
% Alcohol selectivity	81.2	82.1
% HOF selectivity	5.1	1.0

* Rate constant *k'* values are corrected for differences in the catalyst concentration.

4.4.5 Synthesis Gas Composition

If in a F-T complex, the F-T products are used as hydroformylation feeds, one would also like to utilise the F-T syngas for hydroformylation. Apart from H_2 and CO, commercial syngas contains quantities of CO_2, CH_4 and N_2. The CH_4 and N_2 are inert, but CO_2 could possibly exert an influence. Reports in the literature on the effect of CO_2 in phosphine modified Co hydroformylation systems are however unclear.

A patent by Massie and Vesely [1974] claims that the presence of CO_2 in the feed gas reduces the formation of by-product alkanes in these systems. Examples cited in this regard relate to the hydroformylation of C_5, C_7, C_{10}, C_{11}, C_{12}, C_{13} and C_{14} olefins using various alkyl phosphine ligands. According to Massie and Vesely, introducing CO_2 such that the P_{CO2} was typically $\geq$20atm. had the effect of "markedly decreasing the selectivity to paraffins" in the examples cited. A specific example related to hydroformylation of 5-decene undertaken using 20 atm. CO and 80 atm. H_2, at 195°C for 1 hour using a TBP ligand. Repeating the experiment with the addition of 20 atm. CO_2, resulted in a lowering of the total decene conversion from 100% to around 85%, and conversion to decane from 32% to 18% respectively. Seen in this context, CO_2 may be also described as a selectivity "modifier" or "promoter".

However, an earlier patent by Kummer *et al.* [1972], specified that low concentrations of CO_2 (<20ppm) are necessary to prevent metal precipitation in these systems, albeit that they were "modified" with alkali hydroxide (see Section 4.4.6). Kummer *et al.*'s report may be taken to imply that CO_2 facilitates catalyst degradation, and may therefore be a poison.

Commercial syngas having the following composition (volume %) was tested with a C_{10} narrow SLO feed: H_2 = 56%; CO = 29%; CO_2 = 1%; CH_4 = 12%, N_2

balance = 2%.

Undertaking the reactions at a constant inlet pressure with the outlet sealed, resulted in a build up of CO_2 and CH_4 due to a decrease in the P_{H2} and P_{CO}. This is demonstrated by way of Figure 4.7.

Figure 4.7 Gas profile with TOS: Batch run with commercial syngas, Co/TOP and C_{10} SLO: Run 34.

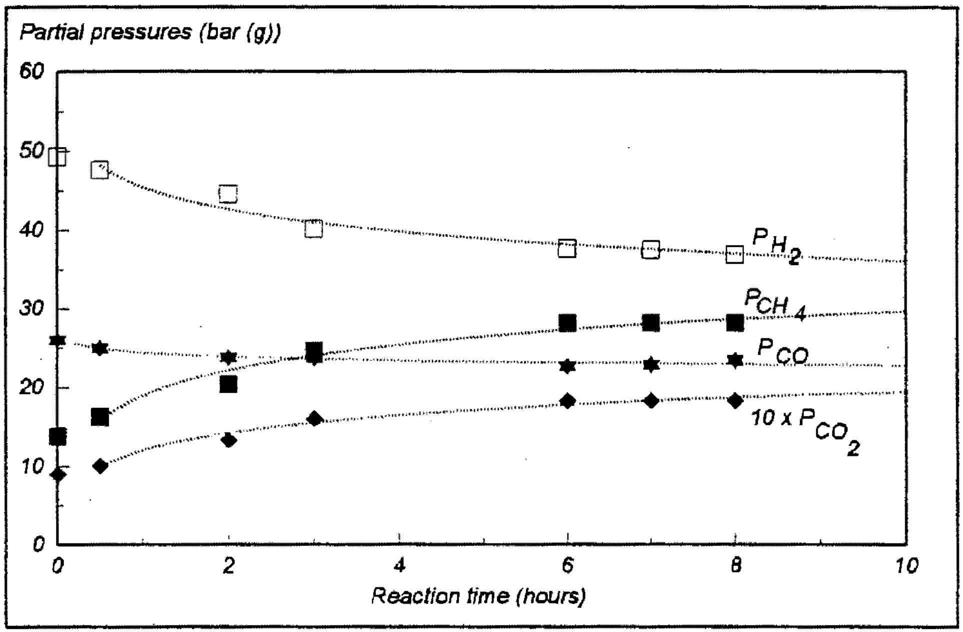

It is apparent that at a fixed total pressure the batch runs undertaken with commercial syngas employed lower overall pressures of CO and H_2 compared with pure 2:1 H_2:CO syngas. The effect (or lack of effect) is evident in the subsequent comparisons.

Activity comparisons may be undertaken by considering Figure 4.8 in which the slopes of the plots represent the rate constants of the olefin consumption reaction. Notwithstanding the lower overall syngas pressures and slightly rich CO gas (compared with pure 2:1 H_2:CO), the commercial syngas run kinetics were approximately first order, and appeared to be similar to runs undertaken with pure syngas. There was however some indication that syngas composition and/or pressure may play a role in influencing the kinetics. Correcting for differences in catalyst concentration, the commercial syngas run was approximately 14% slower than the pure syngas experiment. The observations are in line with Natta *et al.*'s reports that the rate (in unmodified systems) is independent of the total pressure over a specified range, as long as the ratio of H_2 and CO remain constant during the course of the experiment.

Figure 4.8 Comparison of kinetics obtained with 2:1 H_2:CO pure syngas and commercial syngas; Co/TOP catalyst with a narrow C_{10} fraction (A) feed: Runs 34 and 35.

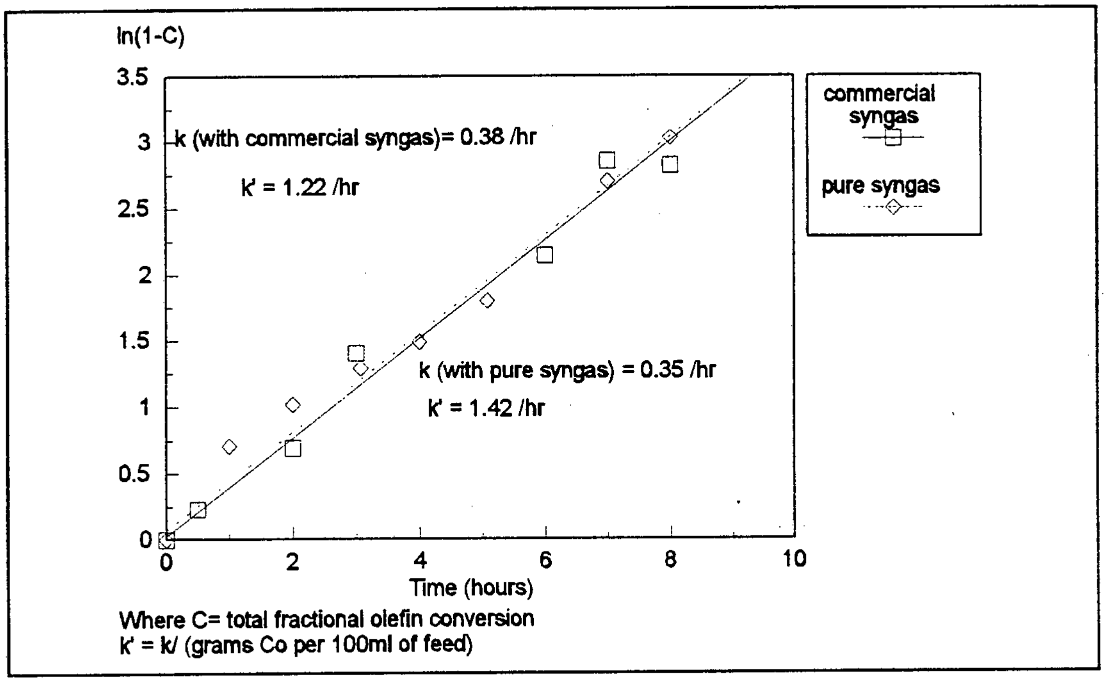

Similar product linearities as well as aldehyde and alcohol selectivities were observed for the two gaseous feeds, as demonstrated in Table 4.8.

Table 4.8 Effect of commercial syngas on reaction selectivities at 6 hours TOS; C_{10} SLO narrow fraction.

Run	34	35
Gas	Commercial syngas 1.93:1 H_2:CO ratio	Pure syngas 2:1 H_2:CO ratio
% 1-Decene product linearity	88.0	88.4
% Overall product linearity	79.2	80.2
% Paraffin selectivity	17.0	12.8
% Aldehyde selectivity	1.4	2.0
% Alcohol selectivity	75.7	77.5
% HOF selectivity	5.8	7.1

4.4.6 Alkali (KOH) "Modifier"

As with CO_2, reports on the effect of alkali modifiers on phosphine modified Co hydroformylation systems are unclear.

The patent by Kummer *et al*, [1972] serves as a reference describing the effects of alkali-modifiers in Co-phosphine catalyzed hydroformylation systems. The patent states that phosphines used to modify carbonyl complexes are partially converted to phosphine oxides which have to be removed after hydroformylation and are not re-useable. Kummer *et al.* found that treatment of the hot reaction mixture with alkali hydroxide (NaOH or KOH) during or after the hydroformylation reaction suppressed the formation of catalyst metal precipitates. Especially favourable results were reported when the CO_2 content in the H_2:CO syngas feed was kept below 20 ppm. The catalyst systems used to illustrate these observations were as follows: Cobalt hydrocarbonyls modified with tri-alkyl phosphines; atomic ratios of P: Co of between 1:1 and 1:4.; Co/ olefin = 0.2 to 1 mass% based on starting olefin; the catalyst was formed *in situ* from a cobalt salt, for example cobalt 2-ethyl hexanoate, tri-alkyl phosphine and syngas. The reaction mixtures were treated with aqueous alkali hydroxide such that the molar ratio of Co:alkali hydroxide was between 1:0.1 and 1:2. The alkali hydroxide content in the water was between 0.1 and 2% by mass. Reactor product containing the homogeneous catalyst complex was subjected to repeated vacuum distillation, and re-use. Phosphine and Co losses were shown to be lowered by the addition of alkali hydroxide. Specific examples given compared recycled catalyst that was concentrated up by distillation, with the catalyst containing residue subjected to the same recycling procedures, namely a purge of 10%. According to Kummer *et al.*, performing the hydroformylation experiment in the presence of aqueous NaOH, using a Co:NaOH ratio of 1:0.2 resulted in no Co losses after 15 cycles. However, in the absence of alkali hydroxide the Co content decreased from 0.15% (which was the expected value) to 0.12% by mass after 16 cycles. Repeating the alkali hydroxide experiment using a syngas containing <20 ppm of CO_2 resulted in no Co losses after 22 cycles.

However, alkali is also reported to catalyze aldol condensation reactions between aldehyde products in Co/phosphine systems [Chern and Helfferich, 1990][Falbe, 1980]. Such reactions would lead to an unwanted build up of the HOF.

Because of the foregoing reports, it was therefore decided to briefly investigate the effect of KOH on Co/TOP catalyzed hydroformylation systems.

Table 4.9 shows the results obtained with KOH in Co/TOP catalysed hydroformylation of a SLO C_{10} narrow fraction and of 1-decene.

Table 4.9 Effect of KOH on Co/TOP systems: "Narrow" SLO C_{10} and pure feeds.

Run	32	35	33	36	37	38
Feed composition (liquids)	SLO C_{10} narrow		3:1 (1-decene:octane)			
Gas composition (initial)	Pure 2:1 H_2:CO				Commercial syngas	
[1]KOH : Co molar ratio	0.75 : 1	0 : 1	0.75 : 1	0 : 1	0.75 : 1	0 : 1
Grams Co per 100ml of feed	0.32	0.25	0.25	0.30	0.26	0.25
k (first order rate constant)	0.47	0.35	0.23	0.23	0.25	0.29
[2]*k'* (first order rate constant corrected)	1.46	1.42	0.90	0.98	0.99	1.13
Product linearities and selectivities at 6 hours TOS						
% 1-Decene product linearity (%)	88.3	88.4	90.6	90.9	92.1	90.7
% Overall product linearity (%)	79.3	80.2	86.4	86.1	85.3	82.0
% Paraffin selectivity	10.4	12.8	12.1	12.8	8.5	10.6
% Aldehyde selectivity	2.1	2.0	4.8	2.8	3.8	2.9
% Alcohol selectivity	81.8	77.5	82.1	81.5	82.8	83.6
% HOF selectivity	5.7	7.1	1.0	2.8	4.9	2.9

[1] KOH was added as a solid powder to the reactor.

[2] Rate constant *k'* values are corrected for differences in the catalyst concentration: k'=k/(grams Co/100ml).

From Table 4.9, it is evident that KOH did not markedly effect the reaction kinetics and selectivities in SLO and pure feeds with the Co/TOP catalyst. The absence of the effect of KOH on reaction rates in these systems was also demonstrated with commercial syngas (runs 37 and 38).

No clear trend linking an increased HOF and the presence of KOH could be ascertained. The HOF did increase in the presence of KOH for the commercial syngas runs (*ie.* overall lower partial pressures of H_2 and CO and "high" partial pressures of CH_4 and CO_2). However, the reverse was evident for the pure syngas cases.

These results, in conjunction with the findings of Kummer *et al.* which state that alkali is effective in preventing catalyst decomposition, imply that KOH may be a suitable additive in phosphine modified Co catalyst systems.

Note on surfactant additives:

Another additive mentioned in the literature is alkylbenzene sulphonate/s (LAS). Addition of alkylbenzene sulphonates was proposed by Wilkes [1975] for the stabilization of previously formed carbonyls to prevent destructive dissociation which leads to deposition of metallic cobalt and loss of activity. The fact that these alkylbenzene sulphonates are surfactants, may play a role in facilitating better mass transfer by improving gas solubility (smaller bubbles). Mass transfer, or "starving" the catalyst complex of CO, causes catalyst decomposition with resultant loss of activity [Falbe, 1980]. As the experiments in this chapter were carried out in a well stirred micro-reactor, the effect of alkylbenzene sulphonates would be difficult to measure. This was confirmed by various experiments in this Chapter as well as in Chapter 5 which were undertaken in the presence and absence of a C_{12} LAS - see Tables 4.1 and 5.1.

4.4.7 Effect of Carboxylic Acids on Heavy Oxygenates (HOF)

Reports on the effect of carboxylic acids in hydroformylation systems appear to be contradictory. The presence of carboxylic acids in HTF-T products therefore necessitated that their effect on hydroformylation be re-investigated.

A patent by Greene and Meeker [1966] claims the use of carboxylic acids, and preferably long-chain carboxylic acids, as stabilizers in P-modified systems to prolong the catalyst lifetime by the formation of Co-salts. Their methodology made use of performing repeated batch experiments in the presence and absence of carboxylic acids, and monitoring the number of times that the catalyst, originally derived from the precursor $Co_2(CO)_6.2(n\text{-butyl})_3$, (*ie.* using TBP as a ligand) could be re-used without deactivation. In this regard, relatively small quantities of carboxylic acid were patented by Greene and Meeker, in that the mole ratio of octanoic acid to catalyst precursor was claimed as being suitable in the range of 1 to 3. Their results may be taken to imply a "downstream" effect in that acid recomplexes precipitated Co and so keeps the catalyst in solution. Alternatively, the effect of the carboxylic acid may also be to keep the Co in solution during the reaction.

Carboxylic acids have however been reported to cause deactivation of unmodified Co catalysts [Macho, 1971], and phosphine modified Rh catalysts [Deshpande *et al.*, 1991][Mieczyńska *et al.*, 1993].

During the course of experiments it became evident that there was a relationship between the carboxylic acid content in the feed and the HOF, whereby higher carboxylic acid concentrations were linked to a higher HOF selectivity. This resulted in lower alcohol and aldehyde selectivities as demonstrated in Figure 4.9.

Spiking a low carboxylic acid content SLO feed with butyric acid had a marked effect on the alcohol and HOF selectivities as demonstrated in Figure 4.9 and Table 4.10. On comparing runs 30 and 39, the reaction rate appeared to increase with addition of acid. This result is however unsubstantiated if one compares runs 35 and 30.

Figure 4.9 Bar chart: % Acid in feed; % HOF selectivity; % hydroformylation product selectivity. Various runs.

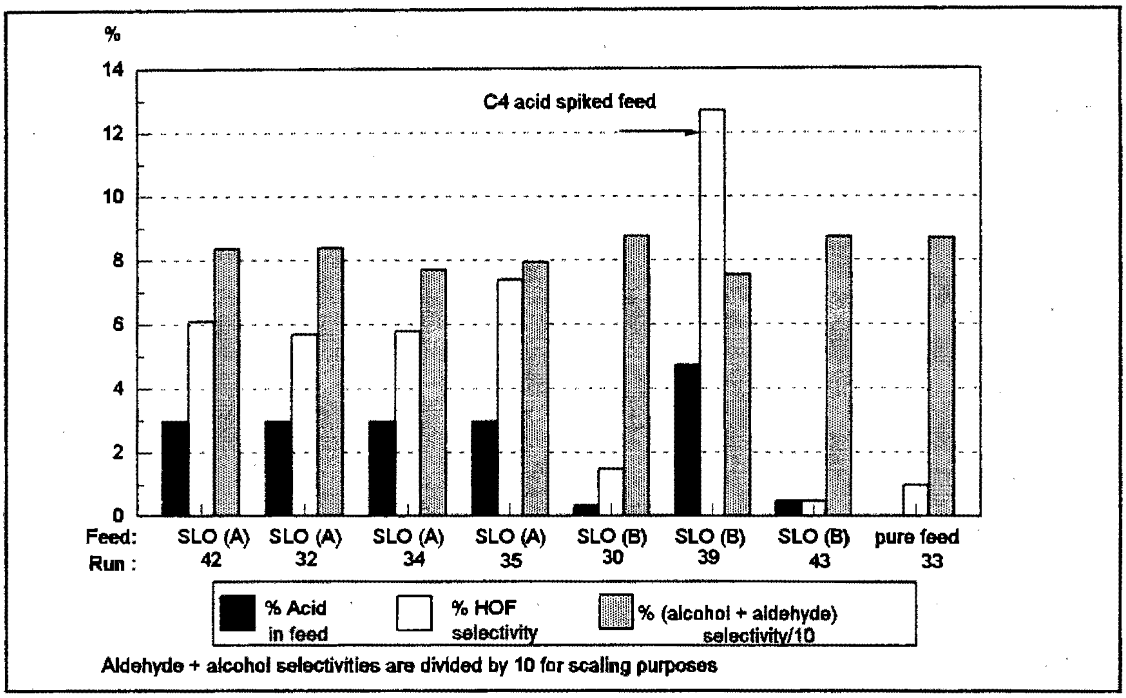

Table 4.10 Effect of acid content on C_{10} SLO hydroformylation: Co/TOP catalyzed.

Run	30	35	39
SLO fraction*	C_{10} narrow (B)	C_{10} narrow (A)	C_{10} narrow (B)
% acid in feed	0.40 ("low acid")	2.99 ("high acid")	4.75 (butyric acid spiked feed)
**Rate constant *k'*	1.45	1.42	1.88
Linearities and selectivities at 8 hours TOS			
% Overall product linearity	71.8	78.5	71.4
% 1-Decene product linearity	86.7	87.5	86.5
% Paraffin selectivity	11.1	13.1	11.7
% Aldehyde selectivity	0.5	1.2	1.6
% Alcohol selectivity	87.0	78.3	74.0
% HOF selectivity	1.5	7.4	12.7

* For breakdown of olefin content and distribution of SLO fractions - see Table 4.3

** Rate constant *k'* values are corrected for differences in the catalyst concentration.

Since the contribution of the HOF plays a crucial role in a continuous process

Since the contribution of the HOF plays a crucial role in a continuous process and represents unwanted products, it is important that this fraction be correctly characterized. The HOF fraction (for runs 30 and 39) was analyzed in more detail using GC-MS to identify the heavy oxygenate components. Virtually all the heavy oxygenates identified were esters, the main groups being, C_4 and C_2 acid esters and a smaller amounts of formic acid ester (formate). The C_4 acid esters can be quantified in terms of the amount of butyric acid introduced. In order to more accurately calculate selectivities based on olefins converted as well as model the system (as subsequently undertaken in Chapter 6), it is necessary to distinguish the HOF originating from the Co acetate catalyst precursor, and the balance of the HOF.

Carboxylic acids can react with alcohols to form esters [Streitwieser and Heathcock, 1981], and this reaction was apparent in these hydroformylation systems. The C_2 and C_4 acid-ester GC traces have similar patterns to the alcohols. This is demonstrated in Figures 4.10 and 4.11 which show the region of interest in a GC product trace after 8 hours TOS without and with spiking the feed with the C_4 carboxylic acid.

Because of these results, the use of the $Co(OOCCH_3)_2.4H_2O$ precursor was corrected for, since acetic acid formation by implication results in the C_2 acid esters which were measured in the HOF. These C_2 acid esters can be quantified in terms of the amount of $Co(OOCCH_3)_2.4H_2O$ precursor used. The following approach (see page 169) was used to correct for this in all the subsequent and preceding constant pressure experiments, *ie*. The effect of this has been taken into account for all the data presented in Chapters 4 - 6.

Figure 4.10 GC trace of alcohol and ester products resulting from hydroformylation of a SLO C_{10} (B) fraction: Low acid (Run 30).

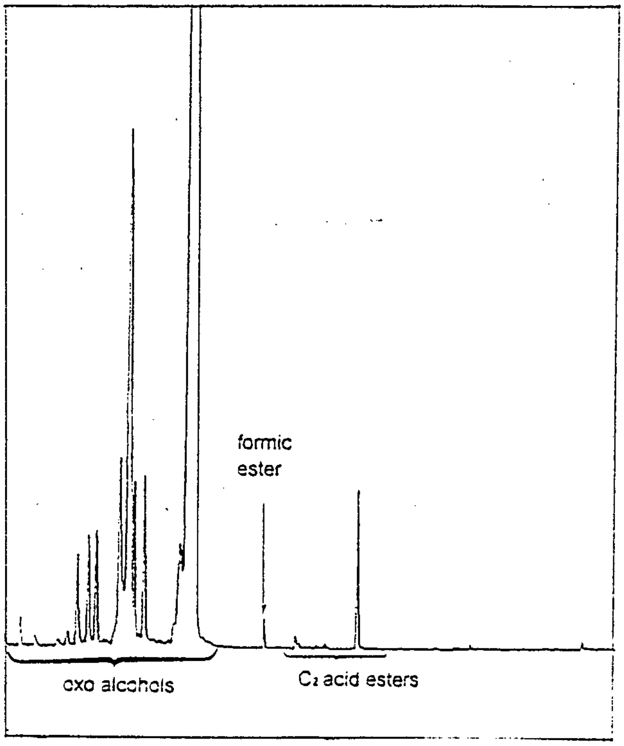

Figure 4.11 GC trace of alcohol and ester products resulting from hydroformylation of a SLO C_{10} (B) fraction: Spiked with C_4 acid (Run 39).

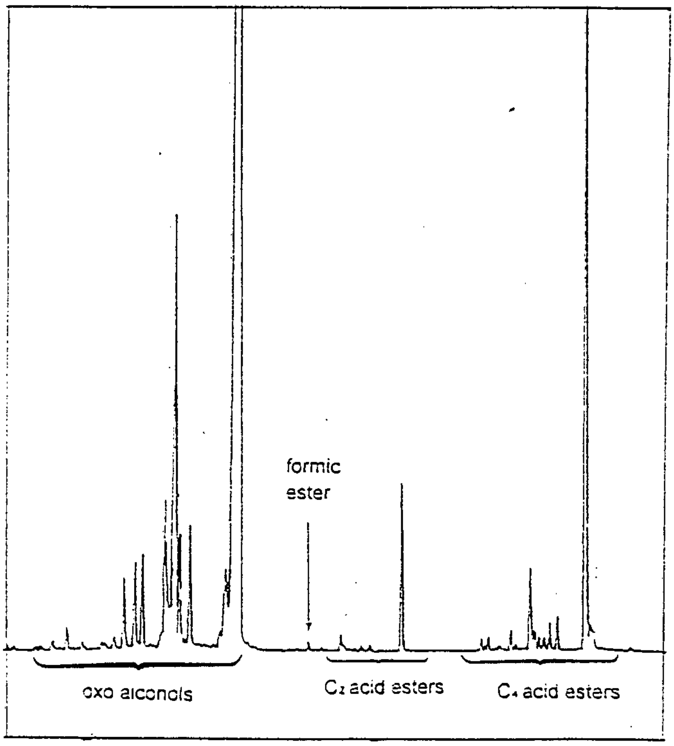

At time = zero, the mass contribution of the acetate ion $^{-}OOCCH_3$ is:

$$\frac{\text{mass of } Co(OOCCH_3).4H_2O \text{ weighed}}{\text{MW of } Co(OOCCH_3)_2.4H_2O} \times 2 \times (\text{MW of } -OOCCH_3) \qquad (4.5)$$

Acetic acid, or the acetate ion, was not observed on the GC traces of the feed or reactor products. It is therefore assumed to be complexed either to the Co and/or an alcohol. Since the catalyst complex forms at a considerably higher rate than the hydroformylation reaction rate on introduction of syngas (see Section 4.4.2), it is assumed that the acetate complexes with alcohols as they form. This partly explains the poor selectivity balances (total selectivities sum to well below 100%) originally calculated for samples taken at the beginning of various runs at low olefin conversions, when the acetate contribution was not corrected for.

The mass contribution in the HOF attributable to C_2 acid esters was calculated as follows:

$$\frac{\text{mass of } -OOCCH_3}{\text{MW of } -OOCCH_3} \times (\text{MW of } C_2 \text{ acid ester formed}) \qquad (4.6)$$

This calculated heavy component was subtracted from the balance of the HOF, and the alcohol component which reacted with the acetate was added to the alcohol component for each time period. The reports in the literature using organic Co salt precursors (which on dissociation may give rise to carboxylic acids and so influence the HOF analysis) have not employed this type of methodology.

Since C_2 acid ester formation involves a secondary reaction of the hydroformylation product which is continually corrected for, it is not necessary to model this reaction. The procedure of calculating the amount of C_2 acid esters formed, as above, subtracting this value from the total HOF, and adding the alcohol component to the total alcohols, thereby allowing the remaining HOF and corrected alcohols to be modelled, should suffice.

The identification of formates in these systems is in line with a report by Wood and Garrou [1984]. They studied the effect of tertiary phosphine ligands on formate selectivity during hydroformylation. Formate yields of <5% said to be observed during most hydroformylation reactions were rationalized from observation and isolation of catalytic intermediates by other workers [Heck, 1964][Milstein and Huckoby, 1982] as being due to CO insertion into the $RCH_2O\text{-}Co(CO)_3PR_3$ intermediate and subsequent hydrogenolysis. Wood and Garrou observed significant quantities of formates in their reactor products, and showed that there exists a dependence of formate selectivity on the steric nature of the organophosphine ligand (cone angle) and the reaction pressure. The formate yield decreased with decreasing cone angle and decreasing reaction pressure. As proof of this, a heptyl formate selectivity (based on the moles of 1-hexene converted) of 37% using $P(C_2H_5)_3$ as ligand compared with 4% when using a cyclic phosphine under the same reaction conditions, was reported. The results by Wood and Garrou and others [Aldrich and Jonassen, 1963][Polievka and Mistrik, 1972] including Markó and Szabo [1961](who showed that a 35% selectivity to formates could be achieved with conventional Co catalysts) indicate that formates may be expected in the P modified Co systems.

4.4.8 Effect of Water on $C_{8\text{-}9}$ SLO Hydroformylation

Because undesired esters result from the presence of carboxylic acids in feeds, such acids should be removed. The most common and practical way of removing carboxylic acids is by way of an aqueous caustic treatment which may result in small quantities of water being present in the feed after subsequent phase separation. In order to ascertain the extent of feed drying required, the effect of a significant quantity of water in the feed was tested using a $C_{8\text{-}9}$ SLO fraction, <u>without</u> previous caustic treatment to remove the acids.

The relevant experiments undertaken and various results are summarized in Table 4.11. Due to the feed having a double carbon number, the analysis the C_8 olefins and their products were grouped and treated separately from the C_9 olefins and their products.

From the results presented in Table 4.11, it appears as if a large quantity of H_2O, if anything, gives rise to beneficial results in terms of kinetics (faster rates). Lower paraffin "losses" and better alcohol selectivities appear to be definite advantages (see also Figures 4.12 and 4.13). However, the HOF increased in the presence of H_2O. For both runs, the C_8 olefins collectively reacted faster than the C_9's even though the C_9 fraction contained only branched olefins.

Table 4.11 Effect of H_2O on Co/TOP catalyzed hydroformylation of $C_{8\text{-}9}$ SLO.

Run	40		41	
Feed details	$C_{8\text{-}9}$ SLO "broad fraction"		$C_{8\text{-}9}$ SLO "broad fraction" + 10% by volume H_2O*	
Carbon number	C_8	C_9	C_8	C_9
Rate constant k' (hr^{-1}) (corrected for catalyst concentration)	2.38	2.16	2.52	2.23
Linearities and selectivities of products at 8 hours TOS				
% Overall product linearity	75.5	-**	78.4	-
% 1-decene product linearity	90.0	-	90.1	-
% Paraffin selectivity	14.2	13.4	5.3	3.9
% Aldehyde selectivity	1.4	0 (tr.)	0.6	0 (tr.)
% Alcohol selectivity	83.7	85.2	91.3	91.8
% HOF selectivity	0.9	1.5	2.8	4.3

* Co acetate precursor was pre-dissolved in the H_2O

** The C_9 fraction was distilled so as to remove all the linear nonene.

The results are interesting if one considers reports on the effect of water described in the literature:

The effect of water on phosphine modified cobalt hydrocarbonyl systems was studied more recently by other workers. A patent by Kohl *et al.* [1984] reports that addition of water accelerates the formation of $C_{16\text{-}19}$ alcohols in $P((CH_2)_{11}CH_3)_3$ modified cobalt hydrocarbonyl hydroformylation systems. Bartik *et al.* [1993] subsequently confirmed this observation when studying the effect of H_2O on $P((CH_2)_3CH_3)_3$ (or TBP) modified cobalt hydrocarbonyl catalysed hydroformylation of 1-octene in a batch reactor. It was claimed that water has a dramatic effect on the alcohol / aldehyde distribution, and that the rate of alcohol synthesis is greater in the presence of water. The rates of the various reactions in Bartik *et al.*'s report were compared by comparing the reactor contents at various reaction times. These differences were reported to be first noticeable at 5% by volume of water. At high conversions the effect was still observed, but it was not as noticeable. This report is in agreement with the data presented in Table 4.11 and Figures 4.12 and 4.13. In addition, water was also shown to deactivate unmodified Co carbonyl catalysts by Bartik *et al.*

Figure 4.12 Effect of 10% water in the feed on alcohol selectivities with TOS; Co/TOP catalyzed hydroformylation of a $C_{8\text{-}9}$ SLO fraction.

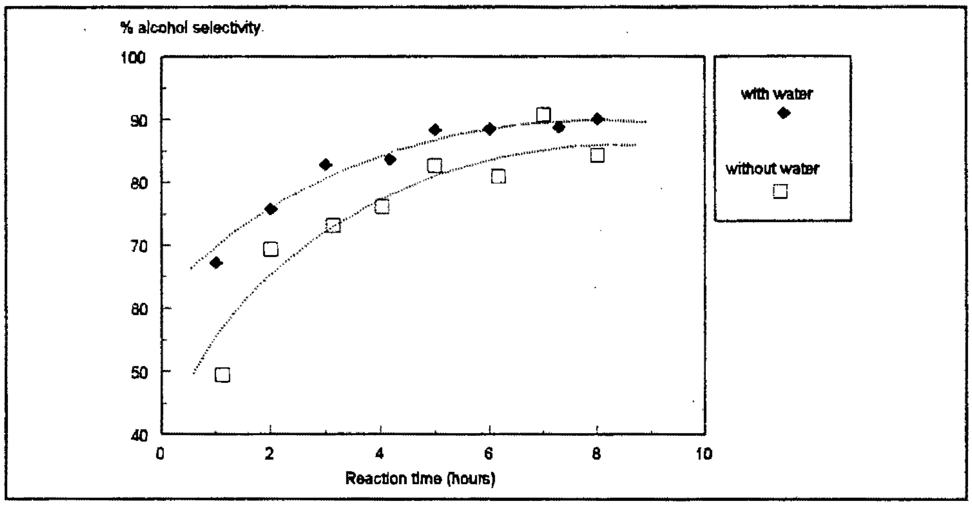

Figure 4.13 Effect of 10% H_2O in the feed on aldehyde selectivities with TOS; Co/TOP catalyzed hydroformylation of a $C_{8\text{-}9}$ SLO fraction.

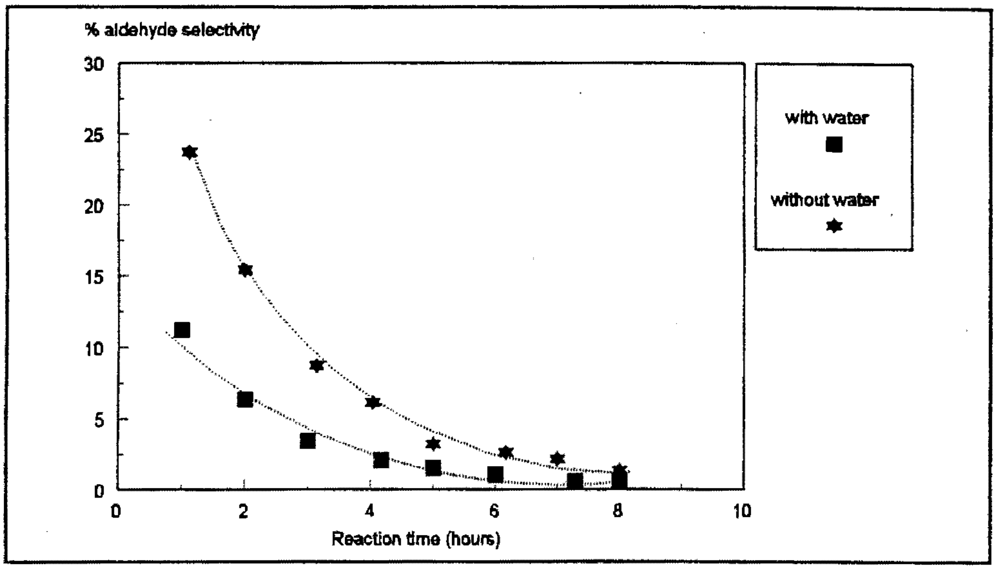

It is is tempting to explain the observed effects of water on hydroformylation in terms of the work undertaken by Karandikar *et al.* [1987] who studied the effect of water on the solubilities and mass transfer coefficients of CO, H_2, CH_4 and CO_2 in a heavy fraction of F-T products. It was proven by these workers that water promoted improved solubility of these gases at elevated temperatures and pressures.

Given the results obtained with significant quantities of water in the SLO feed that was tested in run 41, it appears that caustic washing of the feeds for acid removal in aqueous media can be recommended. Subsequent aqueous-organic phase separation need not be so precise as to remove traces of H_2O or caustic. Indeed some H_2O in the feed appears to be beneficial.

4.4.9 Ligand Comparisons (with TOP)

The effect of increasing the alkyl chainlength was tested by comparing TOP with TBP. In addition, the "bulkier" ligands; bis-PPB (bis-(diphenyl phosphinobutane); and EP (which is a mixture of 9 eicosyl-9-phospha (3.3.1) bicyclononane and 9 eicosyl-9-phospha (4.2.1) bicyclononane isomers) were tested. The relevant structures are represented in Figure 2.12.

Since the bis-PPB ligand has alkyl and phenyl groups attached to the phosphorous atom, it was considered to check the possibility of combining the benefits of TPP (faster reaction rates) [Tucci, 1970] and TBP/TOP (better product linearity with alkyl phosphines).

EP ligand was tested due to the patent reports by Mason and van Winkle [1970] which indicated suitability for use in modified Co hydroformylation systems. The heavier as well bulky structure which has a combination of cyclic and alkyl characteristics, made it an interesting ligand for testing. Given the favourable, though limited, patent results of Mason and van Winkle, it is surprising that follow up work in the open literature using the same or similar "cyclic" phosphines was not encountered. It can be speculated that patenting this ligand around 1970, some time after the original alkyl phosphine patents by Slaugh and Mullineaux in 1966, could be taken to imply an improvement.

4.4.9.1 TOP versus TBP

A constant pressure run with TBP ligand and a SLO C_{10} narrow fraction (for purposes of reference termed "A") feed was undertaken for comparison with TOP. Relevant results are shown in Table 4.12.

Table 4.12 Comparison of TOP and TBP ligands with Co: Constant pressure runs.

Run	32	42
Ligand	TOP	TBP
Feed (unwashed)	SLO C_{10} narrow fraction (A) (high [acid])	
KOH:Co molar ratio	0.75 : 1	0.75 : 1
Rate constant k' (hr^{-1}) (corrected for catalyst concentration)	1.45	1.20
Linearities and selectivities of products at 6.5 hours TOS		
% Overall product linearity	79.0	79.4
% 1-decene product linearity	88.3	87.0
% Paraffin selectivity	10.4	11.5
% Aldehyde selectivity	2.1	1.9
% Alcohol selectivity	81.8	81.9
% HOF selectivity	5.7	6.1

From Table 4.12, it is evident that decreasing the linear alkyl chainlength of the phosphine ligand by four methylene groups did not appear to have a marked effect on the hydroformylation performance of the system, especially with respect to the product selectivities. A possibility exists that an improvement in the reaction kinetics occurred with the TOP ligand. This is surprising, since one would expect longer alkyl groups to impose a larger steric constraint. The faster reaction with TOP is however not borne out by correspondingly lower product linearities. This is may be an effect of the larger ligand size of TOP.

4.4.9.2 TOP Versus bis-PPB

A constant pressure run with bis-PPB ligand and a SLO C_{10} narrow fraction (B) feed was undertaken for comparison with TOP. Relevant results are shown in Table 4.13 and Figure 4.14.

Table 4.13 Comparison of TOP and bis-PPB ligands with Co: Constant pressure run (no KOH added).

Run	30	43
Ligand	TOP	bis-PPB
Feed (low acid content)	SLO C_{10} narrow fraction (B)	
Rate constant k' (hr^{-1}) (corrected for catalyst concentration)	1.45	2.04
Linearities and selectivities of products at 8 hours TOS (complete reaction)		
% Overall product linearity	71.8	60.8
% 1-decene product linearity	87.2	79.6
% Paraffin selectivity	11.1	5.9
% Aldehyde selectivity	0.5	4.2
% Alcohol selectivity	87.0	88.7
% HOF selectivity	1.5	1.2

Figure 4.14 First order rate plots with bis-PPB and TOP: SLO C_{10} narrow fraction: Runs 30 and 43.

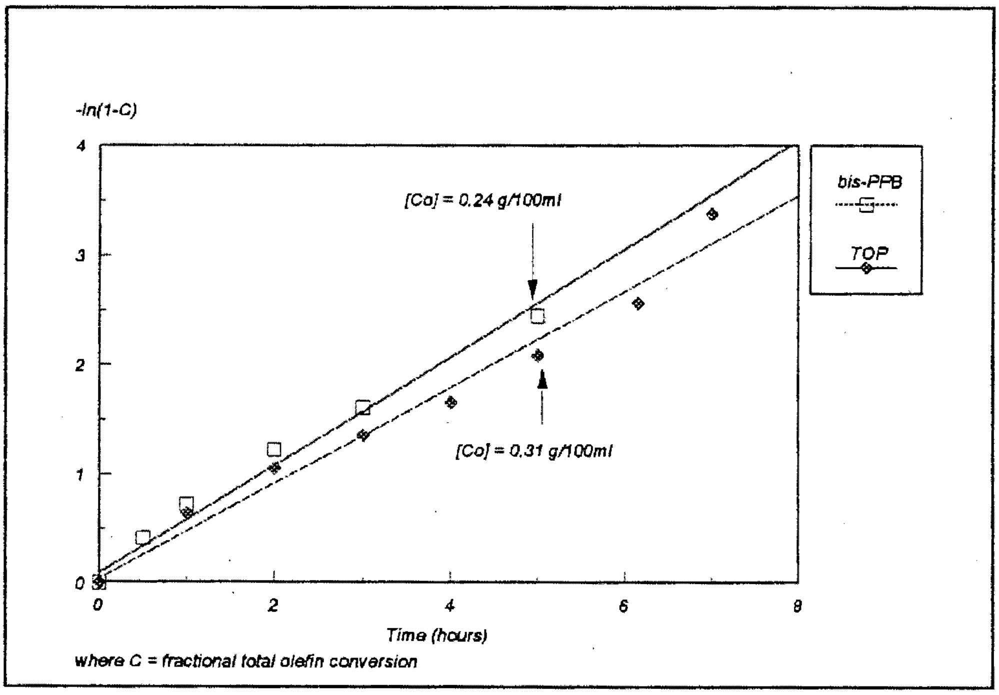

where C = fractional total olefin conversion

Faster (41%) first order reaction rates were obtained with the bis-PPB ligand compared with TOP. The improved reaction rates with bis-PPB were at the expense of product linearity which after 8 hours was 61% compared with 72% with TOP. Reaction selectivities were also effected on changing from TOP to bis-PPB. The lower hydrogenation activity and faster reaction rates measured with bis-PPB, are consistent with ligand "basicity" theory. Namely, that phenyl groups attached to the phosphorous atom should result in the catalyst complex being less stable and more reactive compared with linear alkyl phosphines. Increased electron density on the Co atom results in the CO groups being more strongly bonded [Falbe, 1970]. When CO groups are strongly attached to the Co centre, the hydridic character of the complex increases, which consequently results in higher hydrogenation activity [Falbe, 1970]. This was observed with tri-alkyl phosphine ligands. The reverse holds when the carbonyls are less stable. These results are in line with Tucci's report [1970] on the effect of ligand structure on the hydroformylation of 1-hexene in which it was shown that ligands of low basic character, for example TPP, favour faster reaction rates. Tucci attributed rate differences to δ-donor effects rather than steric effects for the following ligand series: PPh_3 (=TPP); PPh_2Et; $PPhEt_2$; PBu_3 (=TBP). If one considers the results of Tucci's study, it is evident that an approximately linear relationship between product linearity and ligand basicity occurs when using a P:Co molar ratio of 1 as demonstrated in Figure 4.15. According to Tucci, there is an approximately linear, but inverse relationship between ligand basicity and reaction rate.

Tucci also found relationships between the ligand basicity, reaction rate and Ligand :Co molar ratio as demonstrated in Figure 4.16. He showed that the relationship between reaction rate and ligand basicity was approximately linear. This implies that an approximately linear relationship between rate and product linearity is to be expected. Given Tucci's results in Figure 4.16 it is interesting that the rates with the bis-PPB ligand were so much higher than with TOP, since the P:Co ratio used with the bis-PPB was 4. This can be taken as indirect evidence that with the bis-PPB ligand, both P's were not linked to the same Co atom.

Figure 4.15 Relationship between product linearity and phosphine basicity [Tucci,1970]: Ligand:Co ratio = 1.

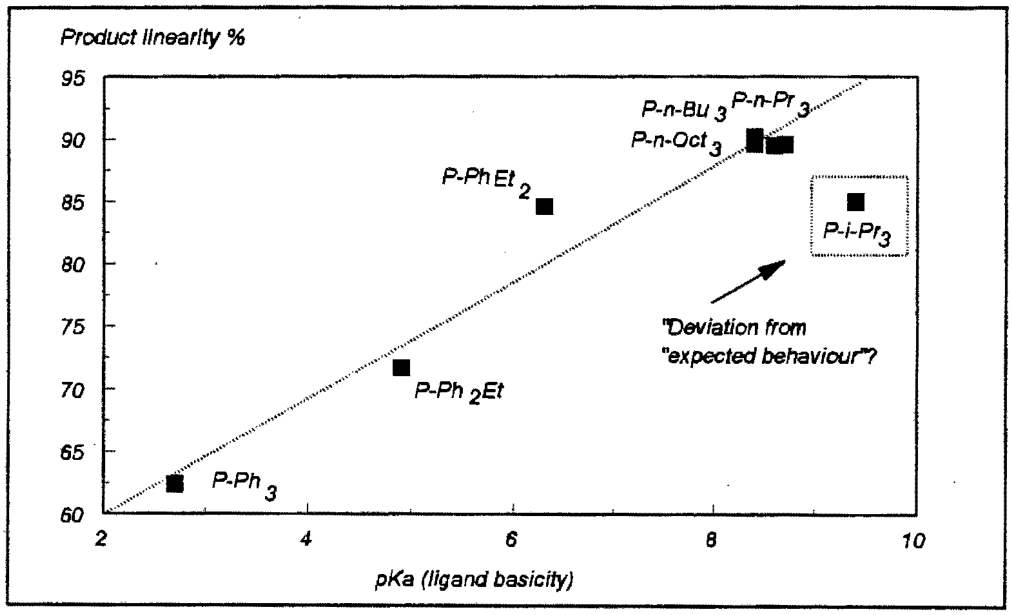

Figure 4.16 Relationship between ligand structure, P:Co ratio, and rate according to Tucci [1970].

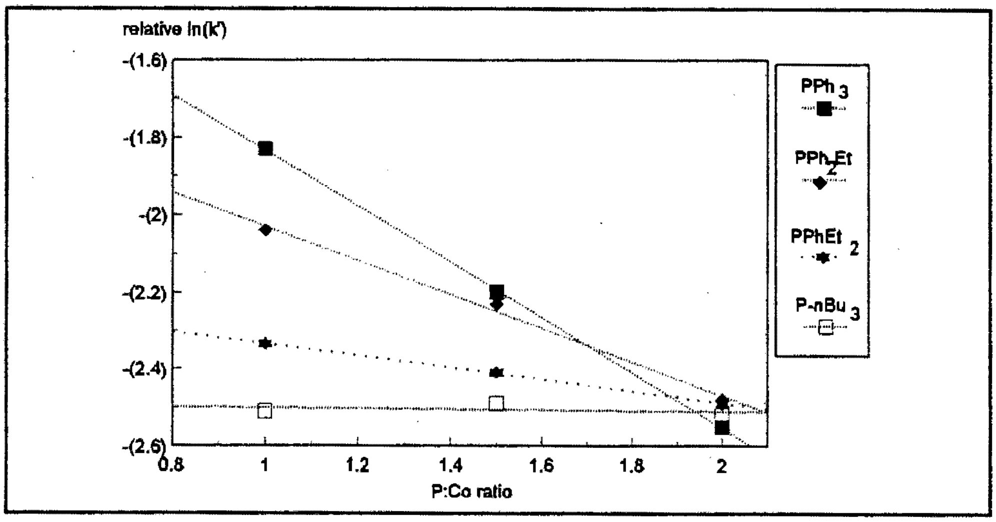

4.4.9.3 TOP Versus EP

4.4.9.3.1 Hydroformylation Performance

The EP ligand was tested with a SLO C_{10} broad fraction (A) in run 44 for comparison with run 31 using TOP. Various results are summarized in Table 4.14, and illustrated by way of Figures 4.17 to 4.20.

Table 4.14 Comparison of TOP and EP ligands with Co: Constant pressure runs.

Run	31	44
Ligand	TOP	EP
Feed ("unwashed")	SLO C_{10} broad fraction (A)	
KOH:Co molar ratio	0: 1	0.75 : 1
Rate constant k' (hr^{-1}) (corrected for catalyst concentration)	1.69	3.53
Linearities and selectivities of products at 8 hours TOS		
% Overall product linearity	55.9	52.9
% 1-decene product linearity	83.8	84.6
% Paraffin selectivity	10.0	3.0
% Aldehyde selectivity	1.4	3.7
% Alcohol selectivity	85.9	90.6
% HOF selectivity	2.9	2.8

A marked improvement in the reaction rates and selectivities (without compromising linearity) was achieved with EP implying that the relationship between linearity and activity (*ie.* basicity) is absent. The improved reaction selectivity is particularly relevant to the paraffin selectivity differences (see Figure 4.18).

Figure 4.17 Comparison of first order rate plots obtained with TOP and EP ligands: Using a SLO C_{10} broad fraction as feed.

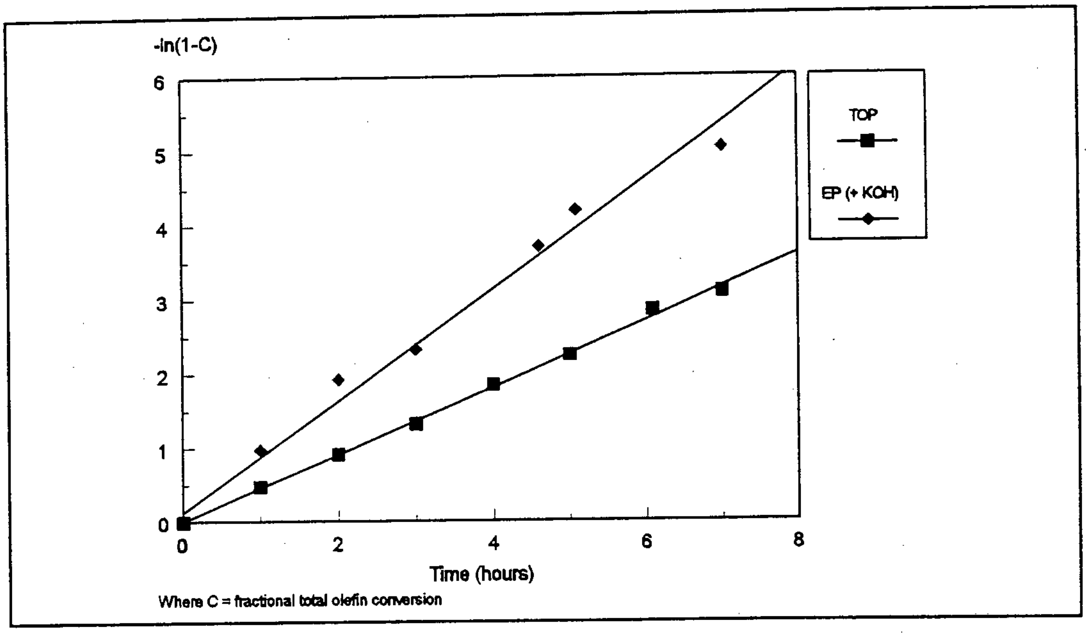

Where C = fractional total olefin conversion

Figure 4.18 Comparison of aldehyde, paraffin and HOF selectivities with TOS obtained with TOP and EP ligands: SLO C_{10} broad fraction as feed.

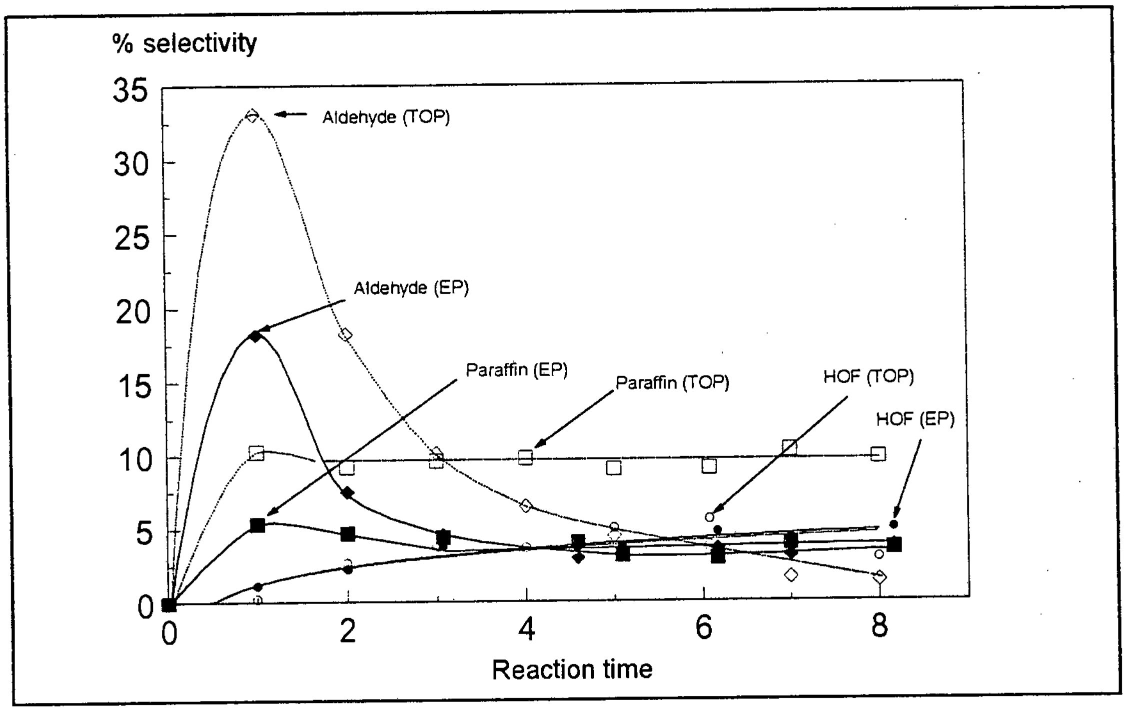

Figure 4.19 Comparison of alcohol selectivities with TOS obtained with TOP and EP ligands: SLO C_{10} broad fraction as feed.

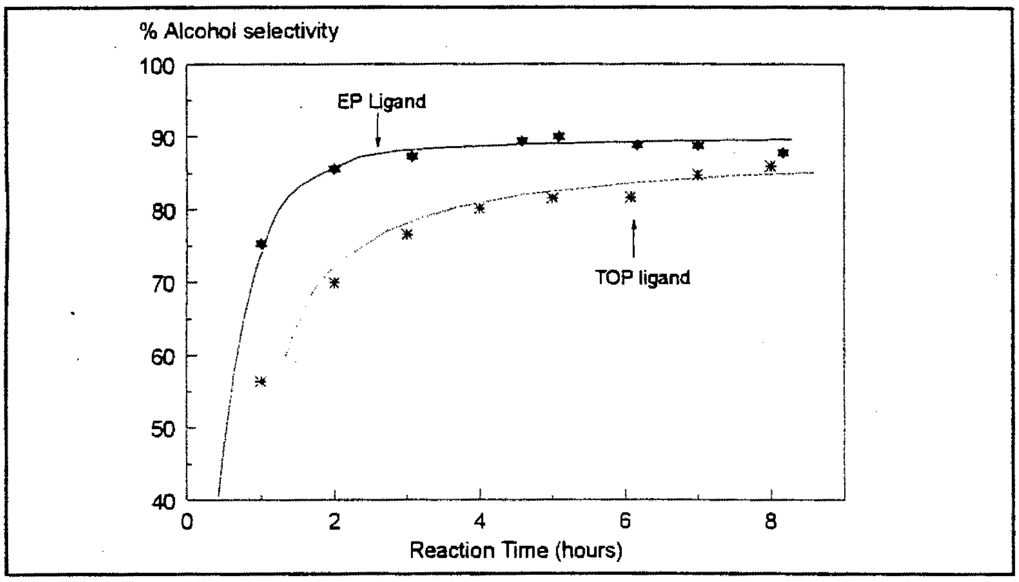

Figure 4.20 Comparison of product linearity with TOS obtained with TOP and EP ligands: SLO C_{10} broad fraction as feed.

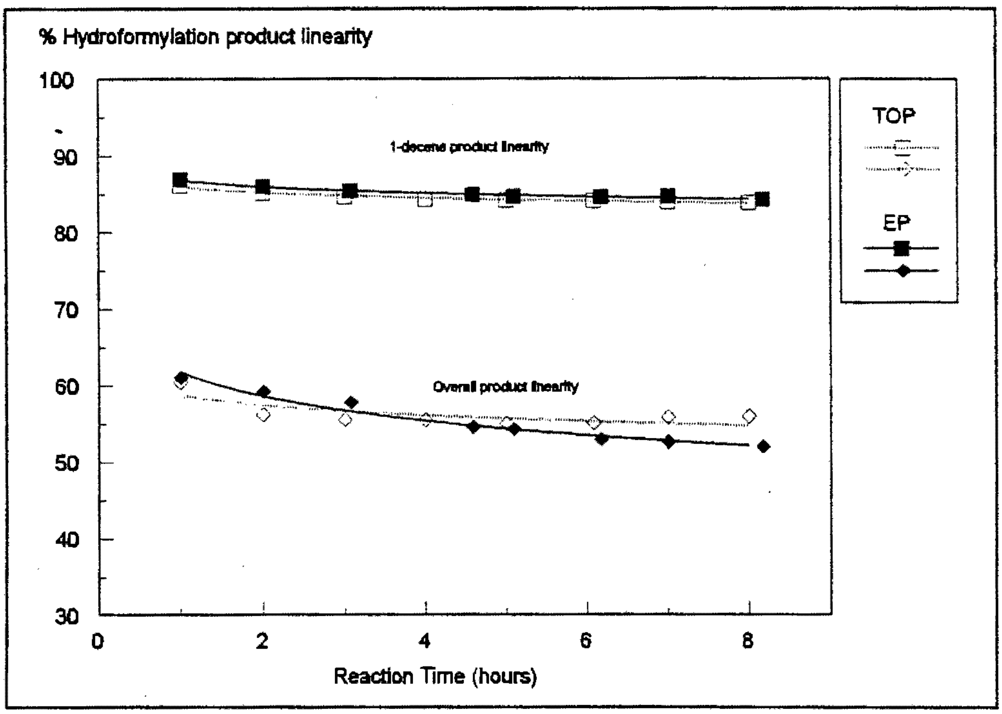

Figures 4.17 to 4.20 demonstrate the superiority of the EP ligand. If one considers the linearity profiles, it does appear as if linearity drops off with time for both ligands. This indicates the presence of less reactive olefins (possibly branched and/or internal olefins) which may react more slowly and give rise to branched alcohols. This would presumably affect the first order rate constant for olefin consumption. This effect is however small as evidenced by the linear nature of the plots of -ln(1-C) against time and the relatively flat nature of the curves in Figure 4.17.

Reports dealing with EP, or similar ligands are limited to patents by Mason and van Winkle *et al.*, [1968, 1970] and van Winkle *et al.*, [1969, 1971], which mainly deal with structural and synthesis aspects of these "ditertiary" phosphines. Furthermore, the examples cited in the relevant patents contain few comparative hydroformylation examples. Given this background, testing the EP ligand with cobalt could make an interesting subject for further study.

The superiority of the EP ligand compared with TOP (and the other ligands tested) is shown in Table 4.15.

4.4.9.3.2 Structural Differences

Clearly from the results presented in Section 4.4.9.3, the results with EP signify a departure from Tucci's inverse relationship between linearity and rate. This relationship is based on ligand basicity. EP probably has more in common electronically with P-i-Pr_3 than the other ligands in Figure 4.15. The electronic differences alone can therefore not adequately explain the superior performance of EP. This implies that the structure of the EP ligand probably also plays an important role.

Table 4.15 Qualitative comparison of ligands studied in Chapter 4 relative to TOP.

Ligand	TOP	TBP	bis-PPB	EP
	"relative" value *			
Rates (relative to TOP)	(1)	(0.83)	(1.41)	(2.09)
% 1-decene product linearities (relative to TOP)	(1)	(0.99)	(0.91)	(1.01)
%*(Aldehyde + Alcohol) selectivities (relative to TOP)	(1)	(0.99)	(1.06)	(1.08)
%Paraffin selectivities (relative to TOP)	(1)	(1.11)	(0.53)	(0.30)
%HOF selectivities (relative to TOP)	(1)	(1.07)	(0.80)	(0.97)
<u>Notes:</u>				
TOP:	Similar structure to TBP.			
TBP:	Not suitable for recycling using distillation.			
bis-PPB:	Has aryl character (less basic than linear alkyl phosphines).			
EP:	Cyclic alkyl phosphine: Overall hydroformylation superiority is evident.			

*For example: A value of say, (0.5), represents half the the value obtained with TOP (1).

In order to more effectively "picture" differences between the linear and cyclic alkylphosphines, various 3-D ligand and catalyst complex structures were constructed with Biosym® molecular modelling software. See Figures 4.21 to 4.25.

The catalyst complexes having two carbonyls attached to the Co atom are assumed to be "active" for hydroformylation [Falbe, 1980][Chern and Helfferich, 1990]. In order to highlight the structural differences more clearly, shorter alkyl chains, having four methylene groups were used for the structures. "Ball and stick" structures are also shown, in which the atoms are given the same size.

Atoms in the structures were given the following colours:

Phosphorous : Purple
Carbon : Green
Hydrogen : White / blue
Oxygen : Red
Cobalt : Yellow

Figure 4.21 Structure of $HCo(CO)_3TBP$ complex. "Ball and stick" as well as "actual" representations.

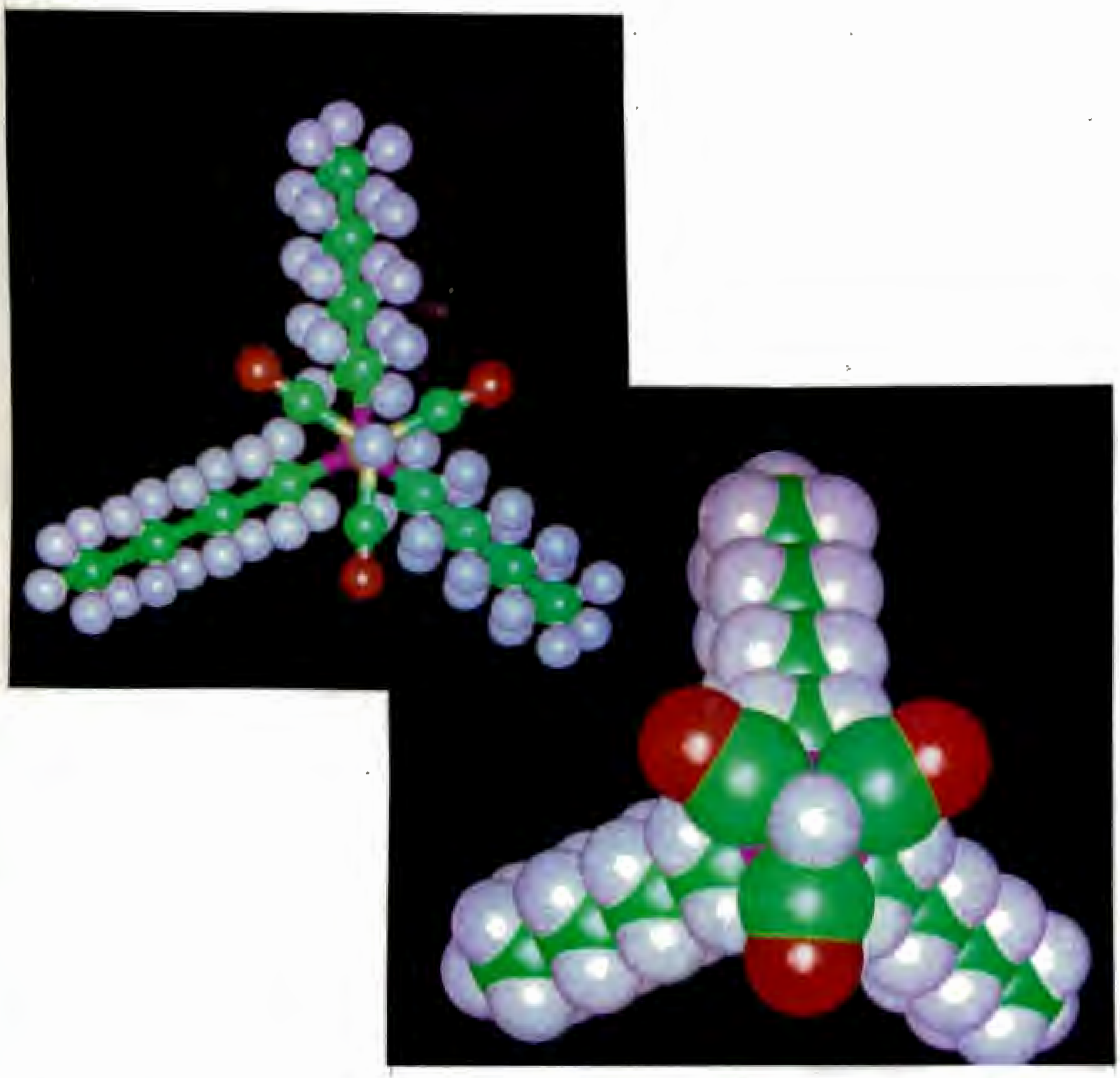

Figure 4.22 Structure of $HCo(CO)_2TBP$ complex.

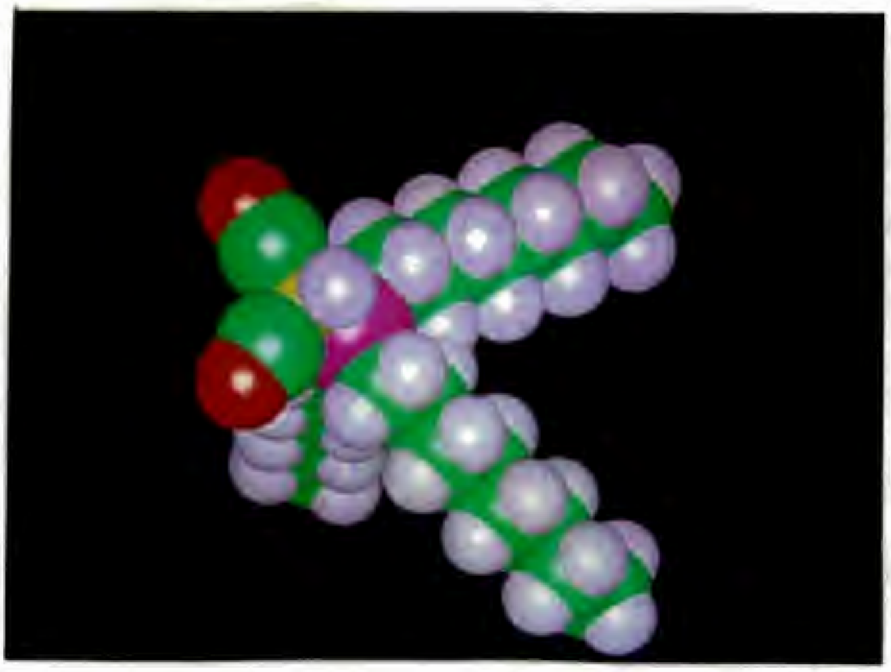

Figure 4.23 Structure of "EP". (Alkyl chainlength shortened to four carbons).

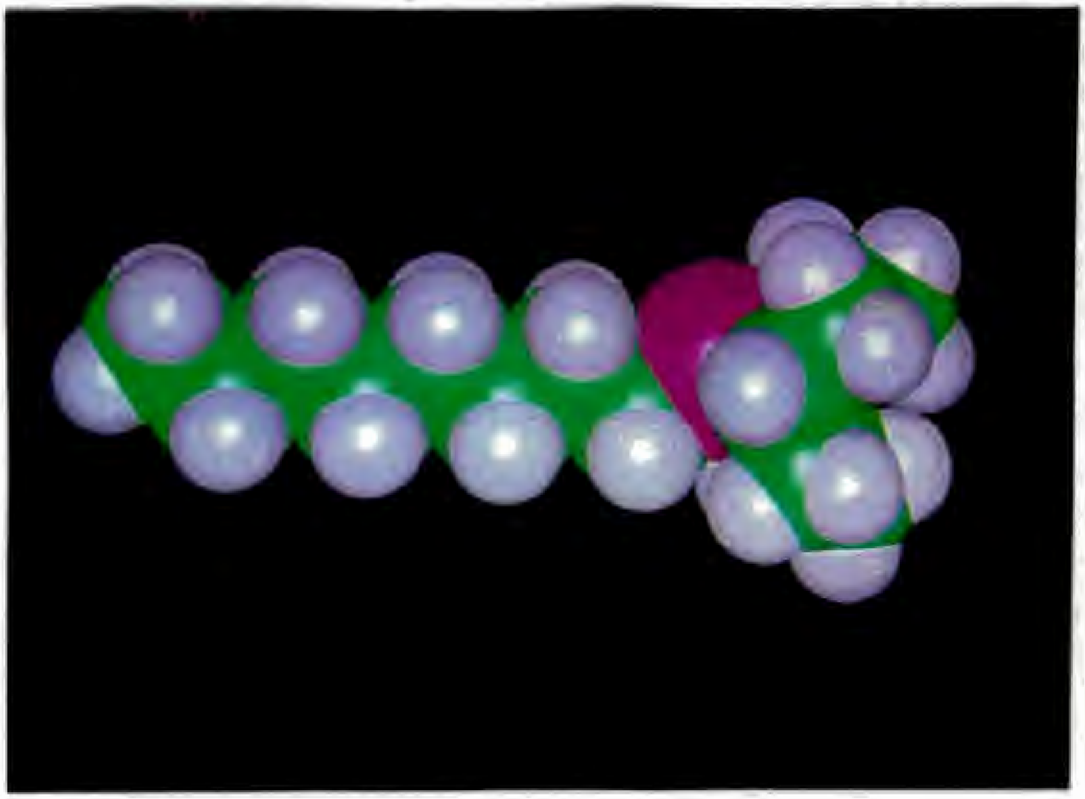

Figure 4.24 Structures of $HCo(CO)_2$Phosphine complexes. Comparison of cyclic and linear alkyl phosphine modified hydrocarbonyls.

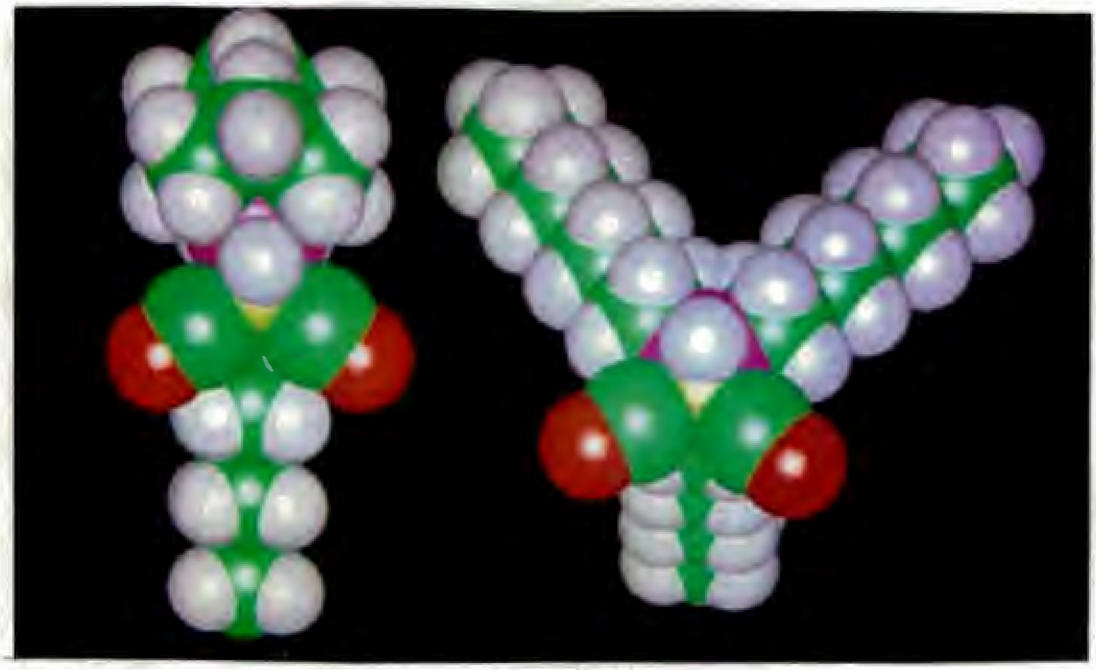

Figure 4.25 Structure of $HCo(CO)_2$"EP" complexes. "Ball and stick" as well as "actual" representations.

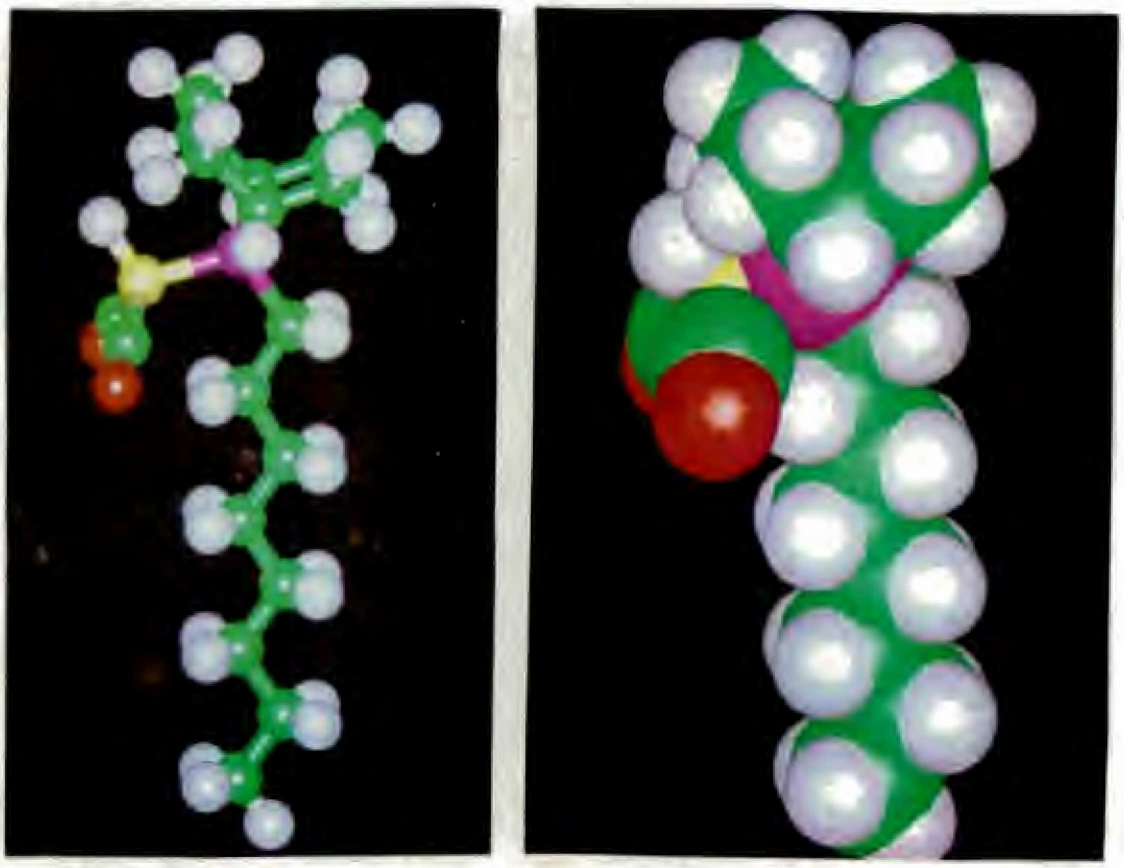

In Figure 4.21 which represents a $HCo(CO)_3TBP$ complex, the Co atom is completely obscured. For an olefin to co-ordinate to the Co, at least one of the carbonyls would have to be dislodged. This may serve as confirmation that the corresponding "active" catalyst complex is more likely to be of the form $HCo(CO)_2TBP$, as represented in Figure 4.22.

From Figure 4.24, it is evident that the catalyst complexes with "EP" do not appear to pose a higher steric constraint than those employing the linear alkyl phosphine. Indeed, one would expect more successful collisions between the olefin and the Co with the EP catalyst, as the catalyst complex has a more streamlined or compact structure. This may in part explain the higher reaction rate (without sacrificing linearity) observed with EP. It is also possible that the EP complexes are more "rigid" and are also less stable due to "ring stress" associated with the cyclic phosphine structure.

4.5 CONCLUSIONS

Repeatability of data was established early on, which allowed subsequent comparisons to be made with confidence.

The kinetics of olefin consumption were shown to be approximately first order with respect to the total olefin content. This first order relationship was demonstrated to be relatively independent of the olefin distribution in the feed, as it was shown to hold for narrow as well as broad F-T fractions.

Faster reaction rates were obtained when using SLO fractions compared with 1-decene feeds with the Co/TOP catalyst. This may be due to better gas-liquid mixing caused by the more polar SLO reaction medium or "solvent".

The hydroformylation system appears to be relatively insensitive to changes in syngas pressure and composition. This was demonstrated by using commercial syngas. The results demonstrate that the F-T and hydroformylation processes can be integrated, so as to utilize the same syngas source.

No clear link could be ascertained between the presence of alkali (KOH), and base catalyzed condensation products which are often reported in these types of hydroformylation systems. Placing this result in the context of the report by Kummer *et al.*, [1972], which states that KOH can prolong the catalyst lifetime, may be taken to imply that KOH is a suitable additive.

Carboxylic acids were demonstrated to contribute to a larger HOF, which indicated that they should be removed from F-T products before use as hydroformylation feeds.

Due to the fact that "washing" with aqueous caustic is an effective way of removing carboxylic acids, the effect of water on hydroformylation was screened. It was demonstrated that the presence of water (10% by volume) gave beneficial results in terms of hydroformylation rates and product selectivities. This indicates that feed "drying" is not an important parameter for these hydroformylation systems.

TBP, bis-PPB and EP ligands were compared with the TOP ligand.
Of these, EP gave superior results in terms of rate and selectivity. This was achieved without compromising the product linearity. The results indicate a departure from previous theories which linked increased product linearity with a decrease in the reaction rate. These differences can be ascribed to the physical structure of the EP ligand and resultant catalyst complex structure.

The results presented in this chapter may be taken to imply that the Co/TOP systems tested were fairly insensitive to the changes made, which is indicative of a robust catalyst and good F-T feed-catalyst compatibility. The EP ligand did however give markedly better results. It was therefore decided to undertake further work with this ligand.

CHAPTER 5

EP MODIFIED Co SYSTEMS

5 EP MODIFIED Co CATALYST SYSTEMS

5.1 INTRODUCTION

From the data presented in Chapter 4, the EP ligand appears to have a more beneficial effect than the n-alkyl phosphines with regards to rates and selectivities. It was therefore decided to further investigate this ligand, and specifically undertake work which was not previously reported for Co/EP systems. Where obvious differences between results obtained with the n-alkyl phosphine (TOP) and EP existed, these are pointed out.

In the constant pressure experiments listed in Table 5.1, the following aspects were investigated:

1) Addition of KOH; 2) EP:Co ratio; 3) Pure 1-decene versus SLO feeds; 4) Testing of C_{10} and various SLO C_{11-12} fractions in order to monitor the effects of, 4.1) olefin chainlength and distribution, 4.2) catalyst concentration, 4.3) reactivity of olefin structures in SLO and 4.4.) formulation of a kinetic expression describing olefin consumption; 5) Temperature study; 6) Syngas composition and pressure.

1-Decene experiments were performed from time to time so that the reactions could be monitored more easily because of the simplified analysis compared to SLO. The effect of changing the above parameters on the reaction kinetics and selectivities was considered. The kinetic expression describing olefin reactivity in these systems was expanded upon to include the effect of olefin chainlength, Co concentration, temperature and syngas composition. This is a common thread throughout this chapter.

Various results are listed in Tables 5.2 to 5.4.2. As undertaken in Chapter 4, various details in these tables are summarized into mini tables which are included in the discussion text. This is to facilitate easier comparisons and assist the reader.

5.2 Co/EP SYSTEMS: CONSTANT PRESSURE RUNS UNDERTAKEN

Table 5.1 Reactions undertaken with Co/EP catalysts.

Run	[Co] g/100ml	L/M Molar ratio	Feed composition (volume/volume)	H_2:CO Molar ratio	Pressure bar (g)	Temp. °C	Additives: KOH/LAS/Co molar ratios
44	0.260	2	SLO C_{10} broad (A)	2	75	170	0.75/ - /1
45	0.250	2	70%1-decene/30% n-octane	2	75	170	0.75/ -/1
46a	0.21	2	70% 1-decene/ 30% n-hexadecane	2	75	170	0.75/ - /1
46b	0.07	2	46a reactor contents (±67ml) + 100ml 1-undecanal	2	75	170	0.75/ - /1
47a	0.208	2	70% 1-decene/ 30% n-hexadecane	2	75	170	-
47b	0.208	2	70% 1-decene/ 30% n-hexadecane	2	86 (13%CO_2)	170	-
48	0.20	2	70% 1-decene/ 30% n-hexadecane	2	75	170	-
49a	0.104	0.5	70% 1-decene/ 30% n-hexadecane	2	75	170	-
49b	0.104	1	70% 1-decene/ 30% n-hexadecane	2	75	170	-
49c	0.104	2	70% 1-decene/ 30% n-hexadecane	2	75	170	-
50a	0.13	2	SLO C_{11-12} broad (A)	2	75	170	0.75/ - /1
50b	0.170	2	SLO C_{11-12} broad (A)	2	75	170	0.75/ - /1
51	0.100	2	SLO C_{11-12} broad (B)	2	75	170	0.75/ 0.1 /1
52	0.160	2	SLO C_{11-12} broad (C)	2	75	175	-
53	0.260	2	SLO C_{11-12} broad (D)	2	75	170	-
54a-d	Temperature runs with "aged" SLO C_{10} feed: (Detailed data not presented)						
55a	0.160	2	SLO C_{11-12} broad (E)	2	75	155	-
55b	0.160	2	SLO C_{11-12} broad (E)	2	75	165	-
55c	0.160	2	SLO C_{11-12} broad (E)	2	75	175	-
55d	0.160	2	SLO C_{11-12} broad (E)	2	75	185	-
55e	0.160	2	SLO C_{11-12} broad (E)	2	75	195	-
55f	0.61	2	50% of reactor 55b product/ 50% SLO C_{11-12} broad (E)	2	75	165	-
55g	0.061	2	50% of reactor 55e product/ 50% SLO C_{11-12} broad (E)	2	75	195	-
56a	0.208	2	70% 1-decene/ 30% n-hexadecane P_{CO} =30 bar; P_{H_2} =15 bar	0.5	45	170	-
56b	0.208	2	70% 1-decene/ 30% n-hexadecane P_{CO} =30 bar; P_{H_2} =30 bar	1	60	170	-
56c	0.208	2	70% 1-decene/ 30% n-hexadecane P_{CO} =30 bar; P_{H_2} =60 bar	2	90	170	-
56d	0.208	2	70% 1-decene/ 30% n-hexadecane P_{CO} =15 bar; P_{H_2} =30 bar	2	45	170	-
56e	0.208	2	70% 1-decene/ 30% n-hexadecane P_{CO} =60 bar; P_{H_2} =30 bar	0.5	90	170	-
57	0.10	2	70% 1-octadecene /30% n-hexadecane	2	75	170	0.75/0.1/1

5.3 Co/EP SYSTEMS: RESULTS OF CONSTANT PRESSURE RUNS

The results are summarized by way of Tables 5.2, 5.3, 5.4.1 and 5.4.2 below

Table 5.2 Gas breakdown of runs undertaken in Table 5.1.

Run	Gas composition (As supplied/ specified by manufacturer) bar (g)	P_{CO} initial	P_{CO2} initial	P_{CO} final	P_{CO2} final	P_{H2} initial	P_{Ar} initial	P_{H2} final	P_{Ar} final	P(total)
44	±33%CO; ±66%H_2	25	-	*27.8	-	50	-	*47.2	-	75
45	±33%CO; ±66%H_2	25	-	°25.8	-	50	-	°49.23	-	75
46a	±33%CO; ±66%H_2	25	-		-	50	-		-	75
46b	±33%CO; ±66%H_2	25	-		-	50	-		-	75
47a	±33%CO; ±66%H_2	25	-		-	50	-		-	75
47b	±5%Ar; ±10%CO_2; ±28.3%CO; ±56.7%H_2	24.4 *26.0	8.6 *9.7	*24.8	*12.2	48.9 *45.8	4.3 *4.7	*42.8	*5.7	86.3 86.2
48	±33%CO; ±66%H_2	25	-		-	50	-		-	75
49a	±33%CO; ±66%H_2	25	-		-	50	-		-	75
49b	±33%CO; ±66%H_2	25	-		-	50	-		-	75
49c	±33%CO; ±66%H_2	25	-		-	50	-		-	75
50a	±33%CO; ±66%H_2	25	-		-	50	-		-	75
50b	±33%CO; ±66%H_2	25	-		-	50	-		-	75
51	±33%CO; ±66%H_2	25	-		-	50	-		-	75
52	±33%CO; ±66%H_2	25	-		-	50	-		-	75
53	±33%CO; ±66%H_2	25	-		-	50	-		-	75
55a -g	±33%CO; ±66%H_2	25	-		-	50	-		-	75
56a	±66%CO; ±33%H_2	30	-		-	15	-		-	45
56b	±50%CO; ±50%H_2	30	-		-	30	-		-	60
56c	±33%CO; ±66%H_2	30	-		-	60	-		-	90
56d	±33%CO; ±66%H_2	15	-		-	30	-		-	45
56e	±66%CO; ±33%H_2	60	-		-	30	-		-	90
57	±33%CO; ±66%H_2	25	-		-	50	-		-	75

°Calculated on the basis of reaction selectivities and moles of olefin converted.
*Measured (from gas ampule samples).
□Clear blocks in the table assume that final values are ± equal to initial values. Gas passed continuously through the system

Table 5.3 Breakdown of olefins measured in Feed: Runs described in Table 5.1. Measured Rate constants (*k*) from plots of ln(1-C) versus time.

Run	Mass % in Feed								% olefin linearity	Co/ olefin mass ratio	*k*	*k'*
	Total olefin	Total α-olefin	linear α-olefin	br. α-olefin	Total int. olefin	linear int. olefin	br. int. olefin	Inerts				
44 :C_{10}	48.6	46.9	29.9	16.9	1.7	1.7	-	51.4	60.4	0.35	0.98	3.79
45 :C_{10}	69.3	68.7	68.7	-	0.64	0.64	-	30.7	100	0.27	0.88	3.53
46a :C_{10}	66.6	65.5	64.5	0.93	1.2	1.2	-	33.4	98.6	0.24	0.81	3.93
47a :C_{10}	69.5	68.1	67.4	0.68	1.3	1.3	-	30.5	99.0	0.23	1.61	7.74
47b :C_{10}	72.1	70.8	70.1	0.70	1.4	1.4	-	27.9	99.0	0.22	1.45	6.96
48 :C_{10}	69.4	68.0	67.5	0.70	1.2	1.2	-	30.6	98.0	0.29	1.51	7.55
49a :C_{10}	66.5	65.3	64.3	1.0	1.1	1.1	-	33.5	98.5	0.12	1.64	15.79
49b :C_{10}	65.9	64.8	63.7	1.1	1.1	1.1	-	34.1	98.4	0.12	1.59	15.31
49c :C_{10}	71.6	70.3	69.2	1.1	1.3	1.3	-	28.4	98.42	0.11	0.94	8.69
50a :C_{11} 50a :C_{12}	29.0 19.4	27.0 14.1	19.8 7.3	7.3 12.0	2.0 0.12	1.3 0.12	0.68 -	51.5	65.9 38.1	0.37 0.70	0.43 0.35	3.22 2.63
50b :C_{11} 50b :C_{12}	29.0 19.6	26.8 19.0	19.4 7.4	7.4 11.6	2.2 0.57	1.4 0.57	0.84 -	51. 2	71.5 40.8	0.47 0.67	0.56 0.48	3.34 2.83
51 :C_{11} 51 :C_{12}	16.21 28.71	14.04 23.88	8.6 13.9	5.4 1003	2.2 4.8	1.6 2.2	0.56 2.6	55.1	53.1 48.2	0.53 0.31	0.39 0.29	3.87 2.87
52 :C_{11} 52 :C_{12}	27.1 26.2	22.2 17.1	19.6 6.8	2.6 18.5	4.9 9.0	4.7 0.87	0.20	46.7	89.6 29.2	0.54 0.69	1.03 0.55	6.50 3.48
53 : C_{11} 53 : C_{12}	16.7 31.4	12.2 21.6	8.9 13.1	3.3 8.5	4.6 11.4	1.6 2.3	3.1 9.1	48.0	59.9 47.6	1.22 0.71	0.85 0.78	4.09 3.76
55a :C_{11} 55a :C_{12}	30.2 19.4	24.1 14.3	21.4 8.3	2.7 8.1	7.1 3.1	5.9 1.42	1.2 1.7	48.9	87.5 55.8	0.49 0.72	0.36 0.27	2.29 1.72
55b :C_{11} 55b:C_{12}	29.6 20.0	23.4 16.7	20.4 8.8	3.0 7.9	6.3 3.3	5.5 2.4	0.79 0.87	50.4	87.2 56.1	0.50 0.71	0.58 0.46	3.70 2.90
55c :C_{11} 55c :C_{12}	29.7 20.3	24.2 17.1	20.9 8.9	3.3 8.2	5.5 3.2	5.1 2.4	0.40 0.84	50.0	87.6 55.3	0.49 0.69	1.15 0.95	7.34 6.08
55d :C_{11} 55d :C_{12}	29.8 19.5	23.6 16.6	20.4 8.7	3.2 7.9	6.3 2.9	5.5 2.9	0.79 -	50.7	86.6 59.4	0.50 0.71	1.63 1.21	9.37 6.88
55e :C_{11} 55e :C_{12}	31.0 20.1	24.4 16.9	20.6 8.5	3.8 8.5	6.6 3.2	5.7 2.4	0.90 0.78	49.9	84.7 54.7	0.48 0.70	1.78 1.45	11.21 9.24
55f :C_{11} 55f :C_{12}	19.9 13.0	15.7 11.1	13.6 5.8	2.1 5.3	4.2 2.0	3.7 2.0	0.53 -	67.1	86.6 59.4	0.33 0.47	0.22 0.18	3.62 2.95
55g :C_{11} 55g :C_{12}	23.3 16.2	18.0 13.5	16.0 7.6	2.0 5.8	6.3 2.8	5.2 1.6	1.0 1.2	60.5	91.3 56.7	0.33 0.44	0.25 0.14	3.15 1.83
56a :C_{10}	66.7	65.3	64.3	0.98	1.4	1.4	-	33.3	98.5	0.24	0.23	1.1
56b :C_{10}	67.5	66.2	65.1	1.1	1.3	1.3	0.54	32.6	98.4	0.24	0.86	4.62
56c :C_{10}	63.4	62.0	61.0	0.97	1.4	1.4	-	36.6	98.5	0.25	1.21	5.50
56d :C_{10}	67.8	66.6	65.5	1.1	1.3	1.3	-	32.2	98.4	0.23	1.02	4.90
56e	73.7	71.8	71.4	0.63	1.9	1.4	0.54	26.3	98.4	0.22	0.96	4.62
57 :C_{18}	65.6	65.6	64.6	1	-	-	-	34.4	98.5	0.17	0.20	1.97

Table 5.4.1 Conversions and selectivities based on the total olefins converted at time 1 (as indicated below).

Run	Time (hours)	Total olefin converted (%)	% Linear α-olefin product linearity*	% Overall hydroform. product linearity	Paraffin selectivity (%)	Aldehyde selectivity (%)	Alcohol selectivity (%)	HOF selectivity (%)
44 :C_{10}	2.0	88.0	86.1	59.3	4.7	7.5	85.6	2.2
45 :C_{10}	2.08	81.2	94.9	92.0	7.3	7.4	84.3	1.1
46a :C_{10}	2.0	78.7	89.9	89.9	6.9	11.2	78.9	2.9
46b	2.0	-	-	-	-	-	-	-
47a :C_{10}	2.0	96.8	90.8	81.3	7.2	5.1	87.4	0.35
47b :C_{10}	2.0	94.0	93.2	84.1	7.2	0.31	85.6	1.6
48 :C_{10}	2.0	94.5	90.8	83.7	69.6	8.1	83.5	1.5
49a :C_{10}	2.0	94.2	74.8	58.3	6.4	52.3	38.5	2.8
49b :C_{10}	2.0	88.0	82.4	68.5	6.3	41.6	52.1	0
49c :C_{10}	2.0	79.4	91.8	83.8	6.58	17.2	76.2	0
50a :C_{11} 50a :C_{12}	2.0	60.6 59.2	88.3 87.8	51.3 42.7	3.9 2.1	21.4 22.0	73.8 75.1	0.86 0.97
50b :C_{11} 50b :C_{12}	2.0	73.3 62.9	85.6 80.1	56.4 39.5	0.66 2.4	25.7 27.2	72.9 70.1	0.70 0.39
51 :C_{11} 51 :C_{12}	2.0	38.7 28.6	87.8 85.1	46.6 35.3	1.6 1.8	63.0 46.3	34.6 50.8	1.4 1.0
52 :C_{11} 52 :C_{12}	2.25	92.1 79.4	87.2 95.7	71.8 30.6	2.2 3.0	4.6 7.3	92.6 89.5	0.59 0.24
53 : C_{11} 53 : C_{12}	2.0	82.0 78.8	86.8 85.3	59.6 46.7	2.7 2.0	6.5 9.9	90.0 82.3	0.74 0.89
55a :C_{11} 55a :C_{12}	2.0	55.5 46.7	91.5 81.8	67.9 37.5	7.3 8.5	28.9 25.8	63.6 65.5	0.20 0.18
55b :C_{11} 55b:C_{12}	2.0	74.4 67.4	88.4 93.9	71.2 54.1	3.9 5.3	25.1 20.3	70.4 74.2	0.57 0.17
55c :C_{11} 55c :C_{12}	2.0	89.6 84.1	88.2 90.5	68.8 46.8	5.1 4.8	8.9 8.2	85.1 86.8	0.84 0.25
55d :C_{11} 55d :C_{12}	2.0	95.8 91.3	84.9 93.4	72.0 59.0	1.5 1.8	5.5 4.1	92.4 93.6	0.63 0.55
55e :C_{11} 55e :C_{12}	2.0	96.4 93.6	85.5 85.9	63.4 37.7	5.0 5.0	3.9 7.2	88.5 86.6	2.6 1.3
55f :C_{11} 55f :C_{12}	2.0	50.3 49.3	89.3 91.5	73.5 56.12	1.7 2.1	8.9 11.3	88.3 86.3	1.0 0.2
55g :C_{11} 55g :C_{12}	2.0	42.8 33.1	84.06 84.86	57.5 27.3	1.8 2.8	48.6 41.1	47.3 55.2	2.3 0.88
56a	2.0	39.0	87.5	76.1	2.7	25.6	70.4	1.3
56b	2.0	73.2	90.1	82.9	3.3	25.8	70.2	0.69
56c	2.0	85.3	93.54	86.7	8.1	4.5	86.8	0.59
56d	2.0	92.6	92.69	85.2	6.5	7.1	85.8	0.66
56e	2.0	83.6	75.7	59.0	4.2	24.0	71.8	0.00 (tr.)
57 :C_{18}	2.0	37.6	94.3	70.8	-	57.3	38.6	4.1

Table 5.4.2 Conversions and selectivities based on the total olefins converted at time 2 (as indicated below).

Run	Time (hours)	Total olefin converted (%)	%Linear α-olefin product linearity*	% Overall hydroform. product linearity	Paraffin selectivity (%)	Aldehyde selectivity (%)	Alcohol selectivity (%)	HOF selectivity (%)
44 :C_{10}	6.16	99.91	84.6	52.9	2.9	3.6	88.8	4.7
45 :C_{18}	6.08	98.99	94.8	90.6	6.9	0.54	90.5	2.1
46a : C_{10}	6.0	99.87	93.8	88.8	7.3	0.47	90.6	1.6
46b	6.0	-	-	-	-	-	-	-
47a :C_{10}	6.08	100	90.0	80.4	7.0	0.24	92.2	0.60
47b : C_{10}	6.0	100	92.6	84.8	6.0	0.31	93.4	0.31
48	6.0	100	90.2	86.2	8.2	0.0 (tr.)	90.2	1.6
49a : C_{10}	6.0	100	74.0	57.4	6.1	1.1	98.0	4.8
49b : C_{10}	6.0	100	81.3	67.0	5.4	1.1	93.5	0.01
49c : C_{10}	6.0	99.6	90.8	82.0	6.2	0.63	93.0	0.14
50a :C_{11} 50a :C_{12}	6.0	91.6 86.9	89.4 87.6	61.2 43.3	5.8 1.9	3.4 6.8	89.6 90.1	1.2 1.2
50b :C_{11} 50b :C_{12}	5.5	94.7 93.1	84.0 80.1	56.4 37.5	3.1 3.0	6.3 14.2	89.0 82.0	1.6 0.84
51 :C_{11} 51 :C_{12}	6.25	88.8 81.8	90.3 85.3	51.9 39.7	2.1 1.0	21.2 12.2	76.3 86.4	0.40 0.38
52 :C_{11} 52 :C_{12}	6.0	97.6 89.6	87.3 95.1	70.0 27.6	3.2 2.8	1.5 8.0	93.6 88.6	1.7 0.66
53 : C_{11} 53 : C_{12}	6.0	94.1 92.3	85.0 83.7	54.2 42.5	2.4 1.7	2.5 1.0	94.8 96.8	0.42 0.53
55a :C_{11} 55a :C_{12}	6.33	90.3 80.8	90.0 84.8	67.9 37.5	4.5 4.2	7.3 12.8	85.5 81.0	2.6 2.0
55b :C_{11} 55b :C_{12}	6.25	95.6 90.0	86.6 92.0	71.2 54.1	3.1 4.1	5.7 6.8	91.0 89.1	0.19 0.05
55c :C_{11} 55c :C_{12}	6.0	99.9 99.9	86.2 84.2	68.8 46.8	2.8 1.8	3.0 5.4	93.0 92.6	1.2 0.24
55d :C_{11} 55d :C_{12}	6.25	97.9 97.1	85.6 92.9	72.0 59.0	0.91 4.2	5.6 3.5	92.9 91.8	0.6 0.53
55e :C_{11} 55e :C_{12}	6.33	99.8 99.5	85.2 87.1	63.4 37.7	0.34 2.0	4.3 7.3	94.4 90.4	0.94 0.40
55f :C_{11} 55f :C_{12}	6.50	90.4 87.3	87.4 83.9	73.4 53.8	3.1 3.6	6.7 9.4	89.8 86.6	0.34 0.51
55g :C_{11} 55g :C_{12}	6.0	74.3 55.7	83.5 85.3	61.9 26.0	3.2 2.9	23.6 20.1	68.3 75.1	4.9 1.9
56a : C_{10}	6.0	64.2	81.8	69.0	2.7	11.8	82.0	3.6
56b : C_{10}	6.0	99.7	88.8	80.9	2.5	1.5	93.0	3.0
56c : C_{10}	6.0	100	93.3	86.2	7.7	0.53	90.3	1.4
56d : C_{10}	6.0	99.8	92.3	84.4	6.1	0.51	91.1	2.2
56e :	6.0	99.65	84.04	71.0	2.3	2.3	93.8	1.6
57 :C_{18}	6.0	66.9	93.6	80.6	13.4	12.3	74.0	0.34

5.4 DISCUSSION OF RESULTS: Co/EP CONSTANT PRESSURE RUNS

5.4.1 KOH Effects

Mason and van Winkle [1970] used KOH with the EP ligand in the example dealing with EP in their patent. These workers did not give a reason for their use of KOH. It was previously shown, in Chapter 4, that KOH does not markedly effect the kinetics of Co/TOP systems (see Section 4.4.6). Nevertheless, it was decided to check the effect of KOH on Co/EP catalyst systems.

As undertaken previously with the TOP runs, KOH was added as a solid powder (see Section 2.2.3.3) to the reactor prior to starting the reactions.

KOH had a marked effect on the reaction kinetics with the Co/EP system, as demonstrated in Figure 5.1 and Table 5.5.

Figure 5.1 Kinetic effect of ligand type and KOH on a 1-decene feed: TOP and EP ligands.

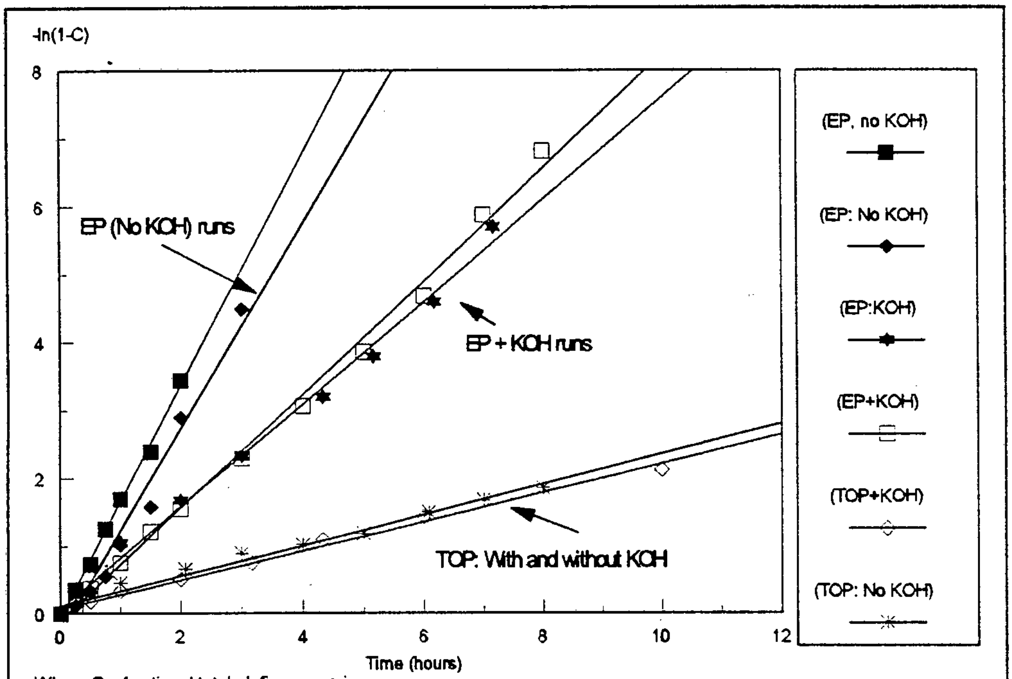

Where C = fractional total olefin conversion
EP sensitive to KOH cf. TOP

Table 5.5 Comparison of linearities and rates for runs as shown in Figure 5.1: Possible effect of KOH on Co/EP systems.

Run	33	36	45	46a	47a	48
Ligand	TOP		EP			
Feed	1-Decene					
KOH:Co molar ratio	0.75 : 1	0 : 1	0.75 : 1	0.75 : 1	0 : 1	0 : 1
k' (hr^{-1}) Rate constant corrected for catalyst concentration	0.90	0.98	3.53	3.93	7.74	7.55
Linearities and Selectivities at 6 hours TOS						
% Linear α-olefin product linearity	90.6	90.5	94.8	93.8	90.0	90.2
% Paraffin selectivity	12.1	13.5	6.9	7.3	7.0	8.2
% Aldehyde selectivity	4.8	3.2	0.54	0.47	0.24	0.0 (tr.)
% Alcohol selectivity	82.1	81.7	90.5	90.6	92.2	90.2
% HOF selectivity	1.0	1.6	2.1	1.6	0.6	1.6

The hydroformylation reaction rates were considerably lower in the presence of KOH for the Co/EP catalyst. The higher reaction rates are associated with somewhat lower alcohol product linearities.

The results obtained with Runs 52 and 53, undertaken in the absence of KOH, confirm that the observations on the effect of KOH on pure C_{10} feeds using the EP ligand, can be extended to SLO fractions. (See Table 5.8 in Section 5.4.4). The reaction rates for these runs are considerably higher (approximately 30%) than for the runs undertaken with KOH. The reactions still remain approximately first order with respect to the total olefin content as observed with previous SLO experiments.

Increased ligand basicity has been linked to lower catalyst activity and increased product linearity (See Figures 4.15 and 4.16). Since KOH is a base, one may speculate that it effectively increases the basicity of the Co/EP system, or the EP ligand, and hence results in lower activity.

5.4.2 Ligand :Co Molar Ratio Effect

The results of Tucci [1970], demonstrated that for linear alkylphosphine ligands (for example TBP), the P:Co molar ratio did not play a significant role between ratios of 1 and 2 (see Figure 4.16). Tucci demonstrated that this was not the case with less basic ligands such as TPP. Given the deviation from expected behaviour observed with EP, it was decided to test the effect of changing the EP:Co molar ratio.

Runs 49a-c were undertaken in this regard. A summary of the relevant reactions and results are listed in Table 5.6 (as well as in Tables 5.4.1 and 5.4.2).

Table 5.6 Summary on the effect of changing the EP:Co molar ratio.

Run	49a	49b	49c
Feed (volume / volume)	70% 1-decene / 30% n-hexadecane		
Initial EP:Co molar ratio	0.5	1	2
k (where $-r_{olefin}=k[olefin]$	1.64	1.59	0.94
Linearities and Selectivities at 6 hours TOS			
% 1-Decene product linearity % Overall linearity of alcohols	74 57	81 67	91 82
% Paraffin selectivity % Aldehyde selectivity % Alcohol selectivity % Heavy selectivity	6.2 1.1 89.4 3.2	5.4 0.3 93.4 0.9	6.4 0.4 93.4 0
% Error in selectivities	4	5	3
[Co] expected in final product (ppm) [Co] measured in final product (ppm)*	1038 407	1038 956	1038 1022

* indication of soluble cobalt

The increase in reaction rates coupled with decreasing product linearity associated with lower EP:Co ratios, are consistent with the trends shown in Figures 4.15 to 4.16.

An additional observation is that these findings are consistent with runs undertaken with "aged" SLO feeds (runs 54a-d in Table 5.1). Feed ageing in the presence of air results in peroxide formation, and these were measured in the "aged" feeds [Kindermans, 1995]. Peroxides would destroy the ligand by oxidation, thus lowering the EP:Co ratio.

The measured cobalt concentration may be taken as an indication of the soluble cobalt content in the reactor liquids after depressurization. This in turn may be taken as an indirect measure of catalyst complex stability *ie.,* less Co deposition would result from more stable EP modified hydrocarbonyls. From Table 5.6, it appears that increasing the EP:Co ratio resulted in less Co deposition after reactor depressurization. Lower amounts of EP ligand therefore give rise to lower overall catalyst stabilities with resultant higher activities. The reliability of cobalt in solution determinations for EP modified Co systems for various runs described in Table 5.1, is illustrated by way of Figure 5.2. Differences in the expected and measured cobalt concentrations can be ascribed to an inaccuracy in the UV-VIS calibration curve.

Surprisingly, and with the exception of the HOF, the reaction selectivities were not markedly affected by changing the EP:Co ratio. If lowering the amount of ligand relative to cobalt had the effect of the system approaching conventional or unmodified catalyst behaviour, then one would expect lower and higher alcohol and aldehyde selectivities for runs 49a and 49b. This however was not the case. Alcohol linearity did follow the expected trend, namely that of lower linearity at higher reaction rates.

Figure 5.2 Cobalt concentration in reactor liquids, for various Co/EP runs.

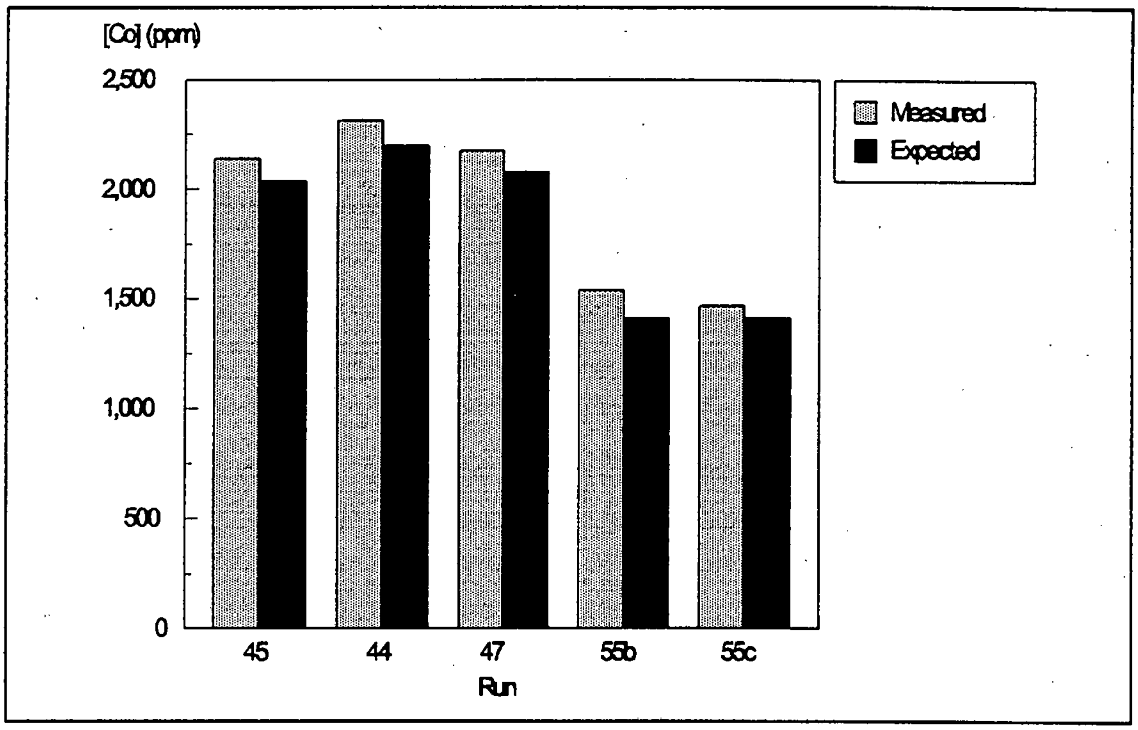

Figure 5.3 First order rate plots at different EP:Co molar ratios (Runs 49a-c).

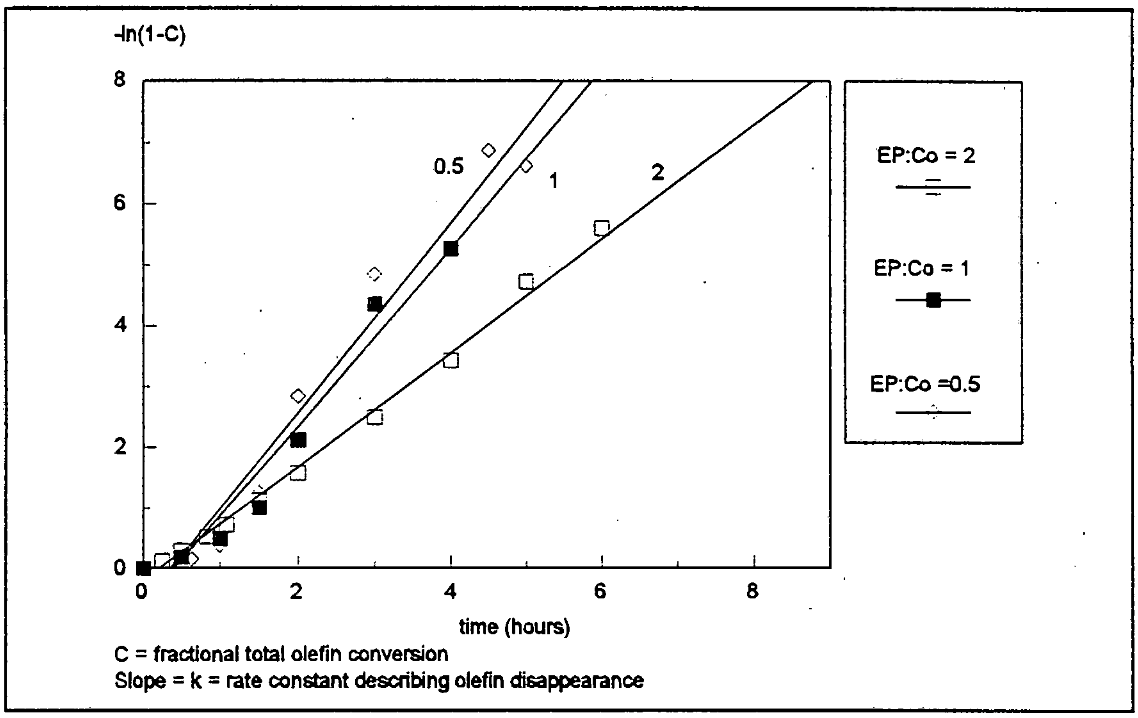

C = fractional total olefin conversion
Slope = k = rate constant describing olefin disappearance

The first order rate constants (in Table 5.6) were calculated from the slopes of the linear plots in Figure 5.3. The lines for the different EP:Co molar ratios do not pass through the origin, which could be taken to imply slower rates of catalyst formation particularly at lower EP levels.

The effect of altering the EP:Co ratio on the alcohol linearity and first order rate constant for olefin consumption (*k*) can also be demonstrated by way of Figure 5.4.

Figure 5.4 Effect of EP:Co ratio on product linearity and olefin reactivity.

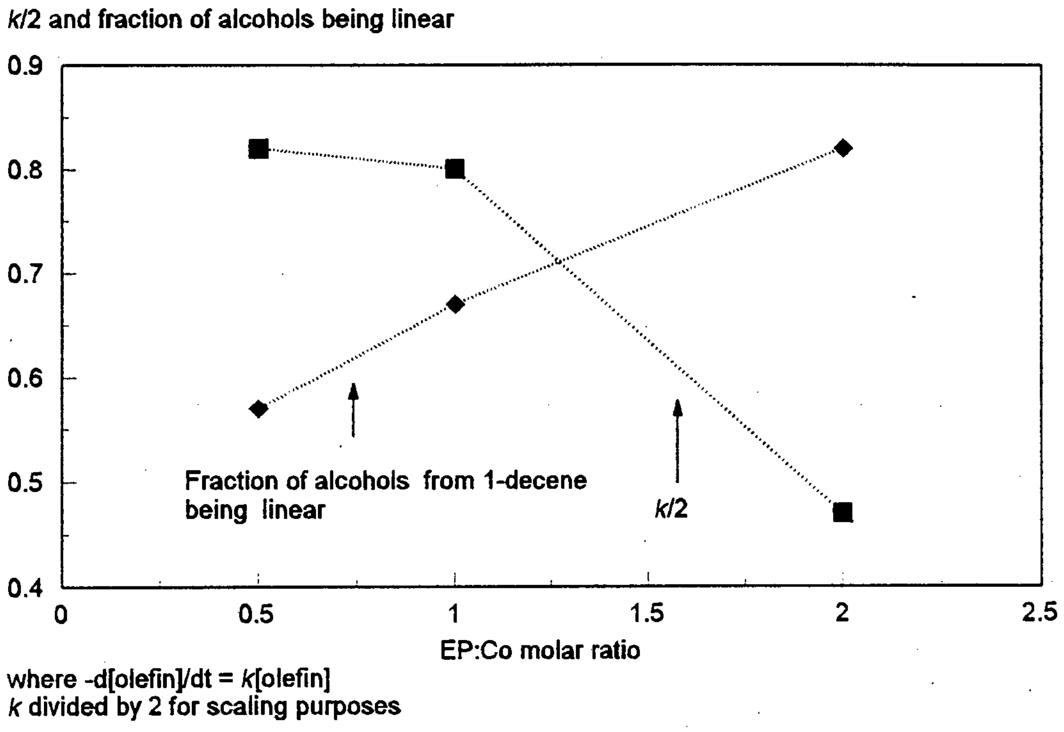

where -d[olefin]/dt = *k*[olefin]
k divided by 2 for scaling purposes

Clearly, the EP:Co molar ratio should be maintained at a value of around 2 or higher if linear products are desired.

Tucci's [1970] reported relationship between ligand basicity, the P:Co ratio, and reaction rates for various phosphine modified systems as discussed in Section 4.9.9, may be relevant in explaining the observations with EP regarding the effect of the Co:EP ratio as well as KOH. By superimposing a Co/TOP catalyst rate constant measured in this study on the Co/TBP values for 1-hexene reported by Tucci (see Figure 4.16), and plotting the Co/EP rate constants for Runs 49a-c relative to the Co/TOP rate constant, one can obtain an approximate comparison between EP and the ligands tested by Tucci. This was undertaken in order to produce Figure 5.5. From Figure 5.5, it is evident that the EP ligand behaves markedly differently to the other alkyl phosphines in terms of the reaction rate and EP:Co ratio. This difference in behaviour is further evident on considering the low product linearity of 67% obtained with a EP:Co molar ratio = 1 which is similar to that obtained by Tucci with the tri-aryl phosphine ligand, TPP of approximately 62%.

As mentioned previously (in Section 1.3.3), higher reaction rates in hydroformylation are generally associated with instability of the carbonyls attached to the central metal atom. This in turn is affected by the amount of electron donation from the ligand (*ie.* basicity of the ligand). It can therefore be argued that the EP ligand behaves as if it has low basicity, and gives rise to a less stable carbonyl complex than the other alkylphosphine ligands. It may further be argued that KOH addition effectively increases the basicity of the EP ligand thereby stabilizing the Co/EP hydrocarbonyl catalyst complex. This in turn has a similar effect to increasing the EP:Co molar ratio.

Figure 5.5 EP (and TOP) data superimposed on Tucci's [1970] results: Effect of P:Co ratio on rate.

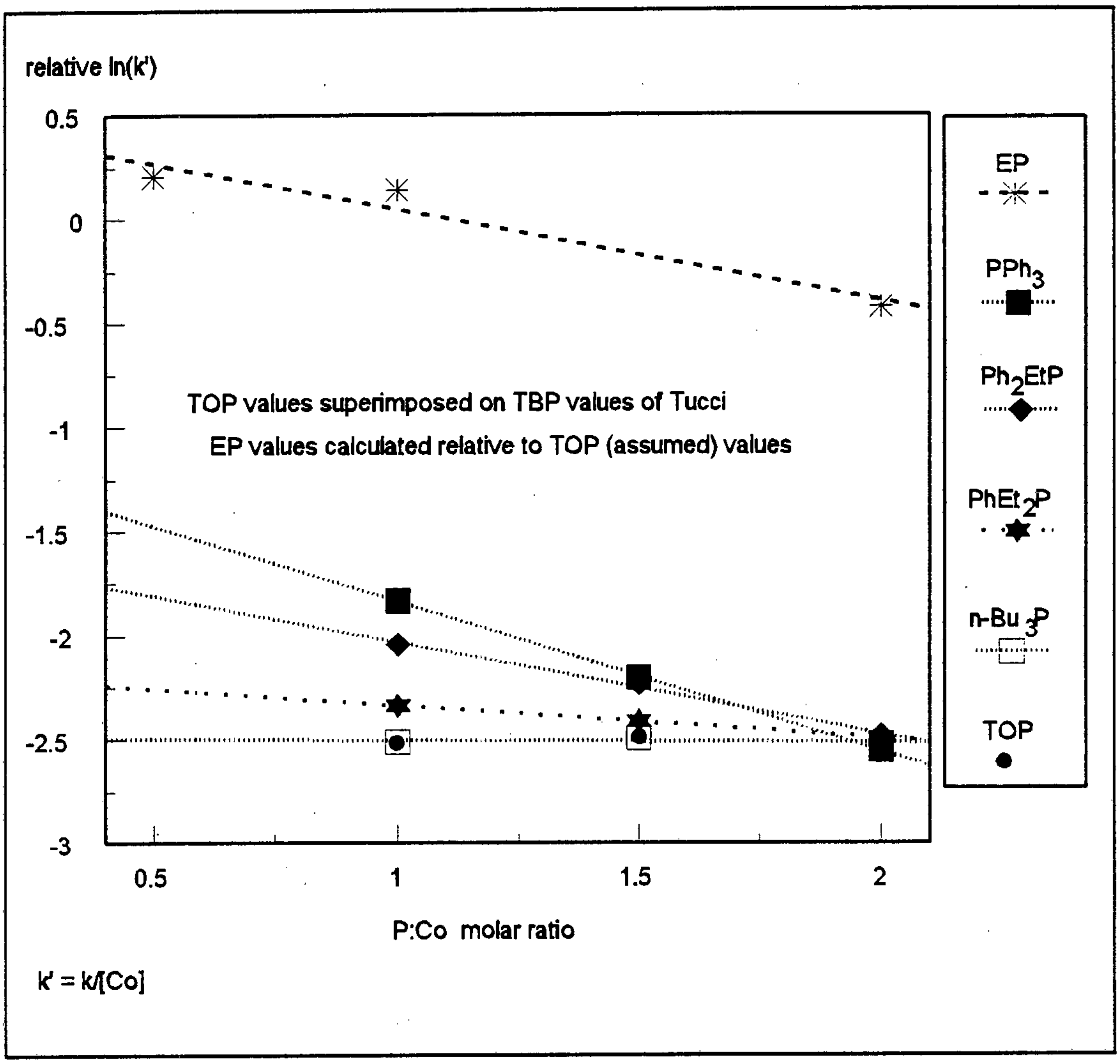

Since product linearity is linked to ligand basicity, and reaction rate is also linked to basicity, it follows that linearity and rate should be linked. This is demonstrated in Figure 5.6 which was generated from various data for runs with 1-decene and Co/EP catalyst in the presence and absence of KOH.

Figure 5.6 Effect of reaction rate on hydroformylation product linearity (at various KOH:Co and EP:Co ratios).

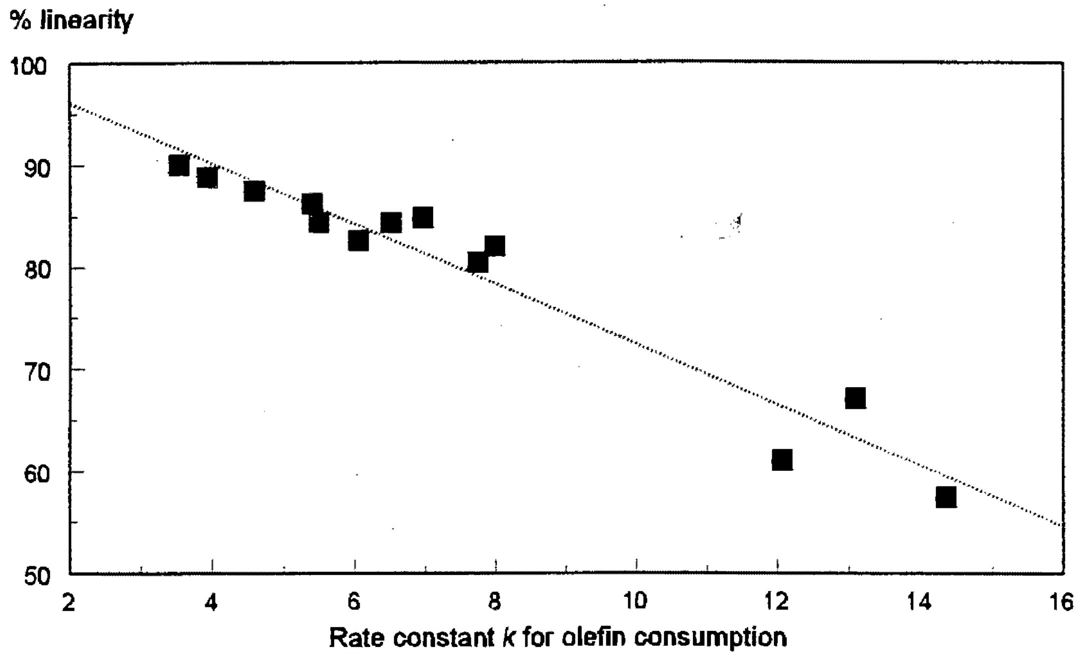

Rate is highly dependant on Co/EP ratio

% linearity: Denotes overall linearity of alcohol products

Given the above observations and arguments, it is tempting to propose a relationship between the role of KOH and the EP:Co molar ratio on hydroformylation performance. This is difficult given the limited number of experiments undertaken in this regard. It can however be stated that the EP:Co ratio is an important parameter in these systems, and the presence of KOH can ensure that these systems behave in a manner such that the apparent EP:Co ratio is high. These higher ratios give rise to higher product linearity. Furthermore, indirect evidence was obtained for improved catalyst stability at higher EP:Co ratios. These observations could prove useful in a continuously operated reactor.

5.4.3 Pure Versus SLO Feeds

The results obtained with 1-decene and a C_{10} SLO broad fraction in runs 45 and 44 respectively, are shown in Table 5.7 and Figure 5.7.

Table 5.7 Comparison of Co/EP catalyst performance in 1-decene and C_{10} SLO.

Run	45	44
Feed (volume / volume)	70% 1-decene / 30% n-octane	SLO C_{10} broad fraction (unwashed)
EP:Co:KOH molar ratio	2 : 1 : 0.75	2 : 1 : 0.75
Co concentration : g/100ml	0.250	0.260
k' (hr^{-1}) corrected for catalyst conc.	3.53	3.79
% Alcohol selectivity at hours TOS	84.3	85.6
% 1-decene hydroformylation product linearity at 2 hours TOS	94.9	86.1
% Overall hydroformylation product linearity at 2 hours TOS	92.0	59.3

Figure 5.7 First order rate plots for 1-decene and C_{10} SLO with the Co/EP catalyst (corrected for catalyst concentration).

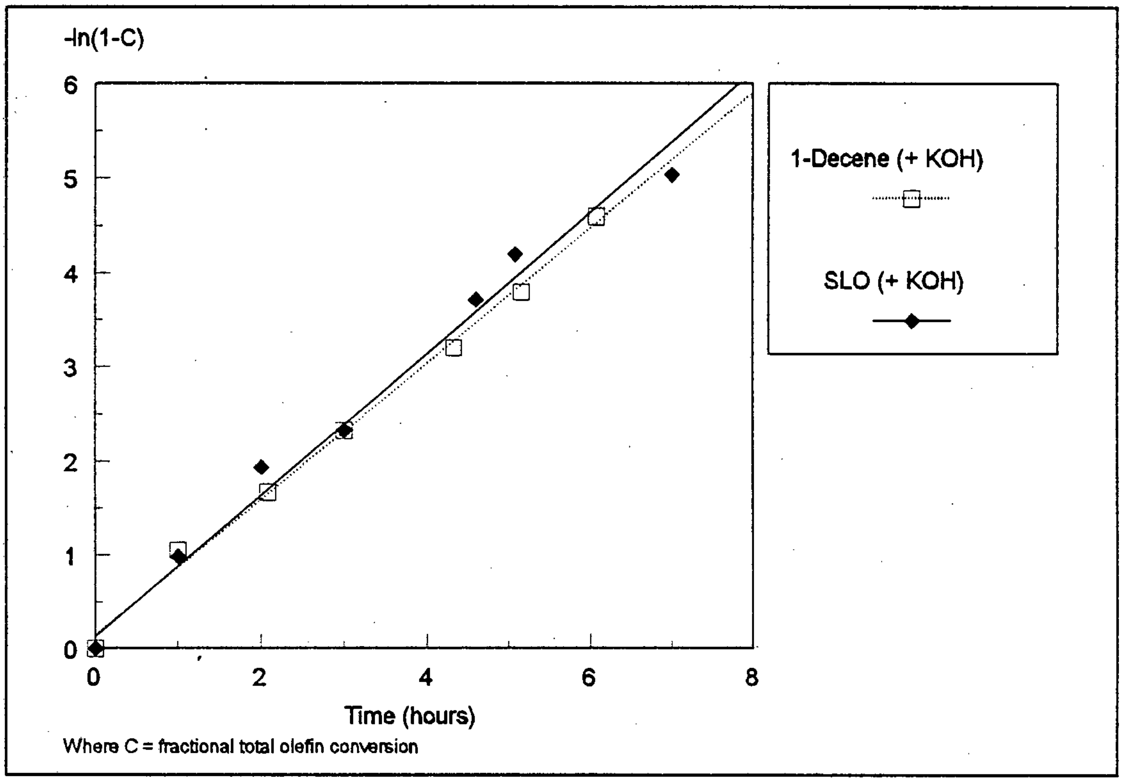

Where C = fractional total olefin conversion

Similar reaction kinetics are evident with the two feeds (see Figure 5.7 and Table 5.7). However, after correcting for catalyst concentration, the reaction kinetics in SLO appear to be marginally faster. This is in contrast to the Co/TOP system where larger improvements in the reaction rate were observed in C_{10} SLO feeds relative to 1-decene (see Table 4.7). The 1-decene hydroformylation product linearity is lower for the SLO feed, possibly as a result of the slightly higher catalyst concentration and concomitant faster kinetics.

One may deduce that the multitude of other components present in SLO (oxygenates, paraffins and aromatics) did not have a marked effect on the reaction rate. Given the similar reactivities with pure and SLO feeds, it may be fair to assume that factors affecting the hydroformylation kinetics of pure feeds would have a similar effect on SLO feeds.

5.4.4 Testing of C_{10} and C_{11-12} SLO Fractions

A C_{10} and various C_{11-12} SLO fractions having different C_{11} and C_{12} olefin contents and distributions, were tested with the Co/EP catalyst. The aim was to monitor the effect of catalyst concentration, olefin chainlength and distribution as well as double carbon number feeds.

C_{11-12} double carbon number F-T fractions constituted a more complex feed than the other feeds tested. Because of the "broad" nature of the feeds, they are relatively easy (and inexpensive) to prepare using distillation. The exhaustive hydroformylation methodology discussed in Section 2.3.1.2 , was demonstrated to still be reliable in quantifying the olefins. An additional check to test the reliability of olefin assignments was developed by making use of the alcohol assignments and linearity as subsequently demonstrated in Section 5.4.4.3. The value of the results under discussion hinge on the accuracy of the analyses. An example of the speadsheet data and selectivity balances for one of the C_{11-12} feeds under discussion is shown in Appendix 3.

Table 5.8 summarizes the relevant runs undertaken as well as the results to be discussed.

Table 5.8 Reactions and kinetic results for SLO fractions tested with Co/EP.

Run	44	50a	50b	51	52	53
SLO "broad fraction" feed	C_{10}	$C_{11\text{-}12}$ (A)	$C_{11\text{-}12}$ (A)	$C_{11\text{-}12}$ (B)	$C_{11\text{-}12}$ (C)	$C_{11\text{-}12}$ (D)
*Measured olefin breakdown (mass% in feed)						
Linear C_{10} α-olefin	29.9	-	-	-	-	
Branched C_{10} α-olefin	16.9	-	-	-	-	-
C_{10} internal olefin	1.7	-	-	-	-	-
Total C_{10} olefin	48.5	-	-	-	-	-
Linear C_{11} α-olefin	-	19.8	19.4	8.6	19.6	8.9
Branched C_{11} α-olefin	-	7.3	7.4	5.4	2.3	3.3
C_{11} internal olefin	-	2.0	2.2	2.2	4.9	4.6
Total C_{11} olefin	-	29.1	29.0	16.2	26.8	16.7
Linear C_{12} α- olefin	-	7.3	7.4	13.9	6.8	13.1
Branched C_{12} α-olefin	-	12.0	11.6	10.0	18.5	8.5
C_{12} internal olefin	-	0.1	0.6	4.8	0.9	11.4
Total C_{12} olefin	-	19.4	19.6	28.7	26.2	31.4
Total olefin	48.5	48.5	48.6	44.9	53	48.1
g Co/ 100ml of feed	0.26	0.13	0.17	0.10	0.16	0.16
Temperature (°C)	170	170	170	170	175	170
EP:Co:KOH molar ratio	2:1 : 0.75	2:1: 0.75	2:1: 0.75	2:1: 0.75	2:1: -	2:1: -
Rate constants** k' (hr^{-1}) for individual carbon number fractions						
C_{10}	3.79	-	-	-	-	-
C_{11}	-	3.22	3.34	3.87	6.50	4.09
C_{12}	-	2.63	2.83	2.87	3.48	3.76

* Measured using exhaustive hydroformylation

** $k' = k/$ (grams Co per 100 ml) *ie.* rate constant corrected for catalyst concentration

5.4.4.1 Olefin Distribution Effects

$C_{11\text{-}12}$ SLO feeds having different olefin distributions were tested. A breakdown of the olefin distributions as determined by exhaustive hydroformylation is shown in Table 5.8. Despite the differences in olefin content and distribution, the overall reaction rates for the three reactions undertaken with the $C_{11\text{-}12}$ feeds in the presence of KOH (Runs 50a-b and 51), were first order with respect to the total C_{11} and total C_{12} olefin contents in the reactor as demonstrated in Figure 5.8 and 5.9. Runs 52 and 53 undertaken in the absence of KOH were much faster but also first order with respect to the total olefin content. Figures 5.8 and 5.9 demonstrate that the rates for C_{11} olefin hydroformylation are faster than for the C_{12} olefins.

Figure 5.8 First order rate plots: Hydroformylation of a $C_{11\text{-}12}$ SLO fraction (A): EP ligand: Runs 50a and 50b.

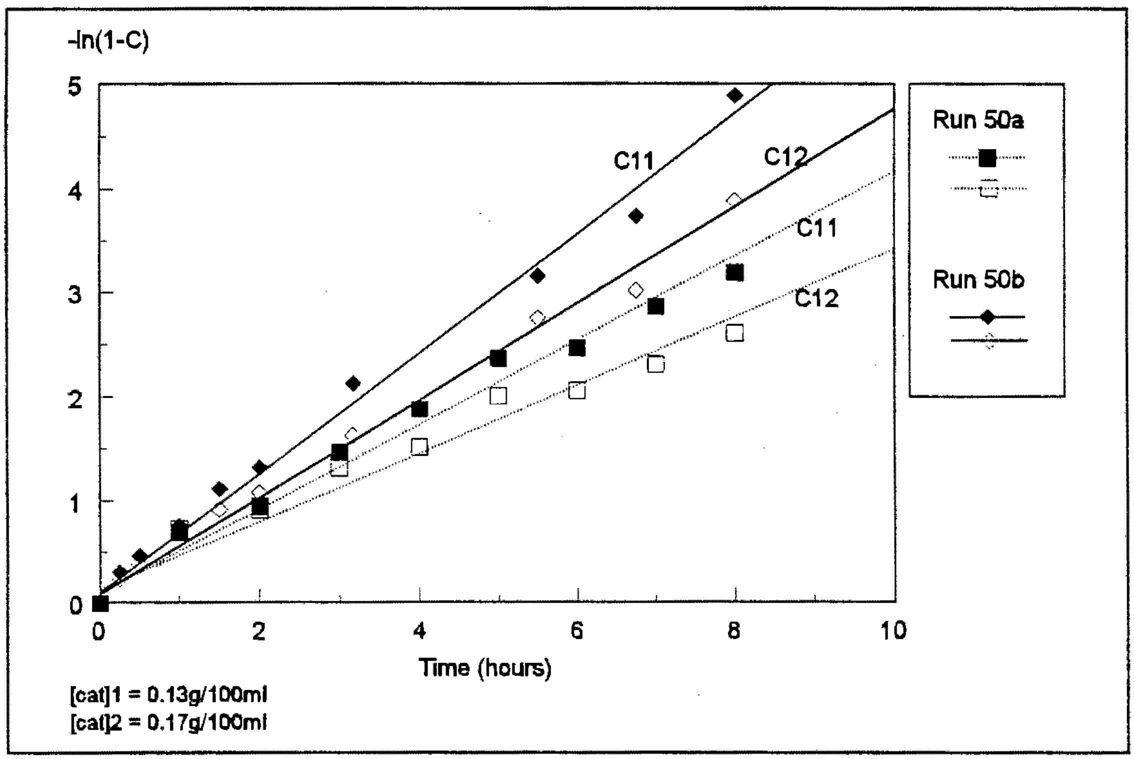

Figure 5.9 First order rate plots: Hydroformylation of a C_{11-12} SLO fraction (B): EP ligand: Run 51.

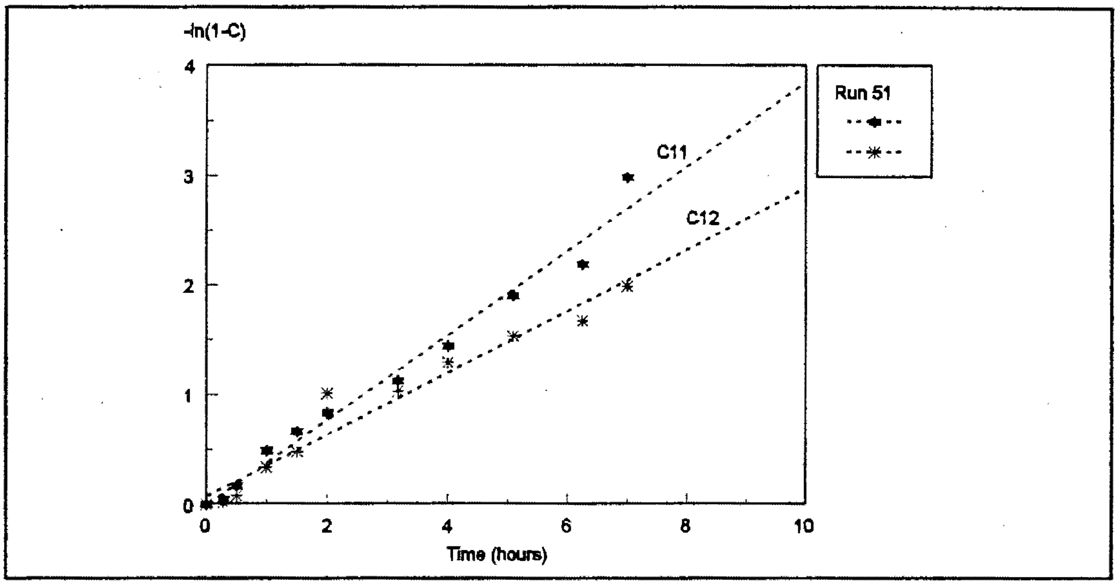

Evidently, the reaction rate is dependent on the olefin chainlength. Correcting for the cobalt concentration, this relationship is approximately linear (for EP as well as TOP modified catalysts) over the range of conditions tested, as evidenced in Figure 5.10.

Figure 5.10 Effect of olefin chainlength on reaction rate using TOP and EP ligands: SLO feeds; various runs.

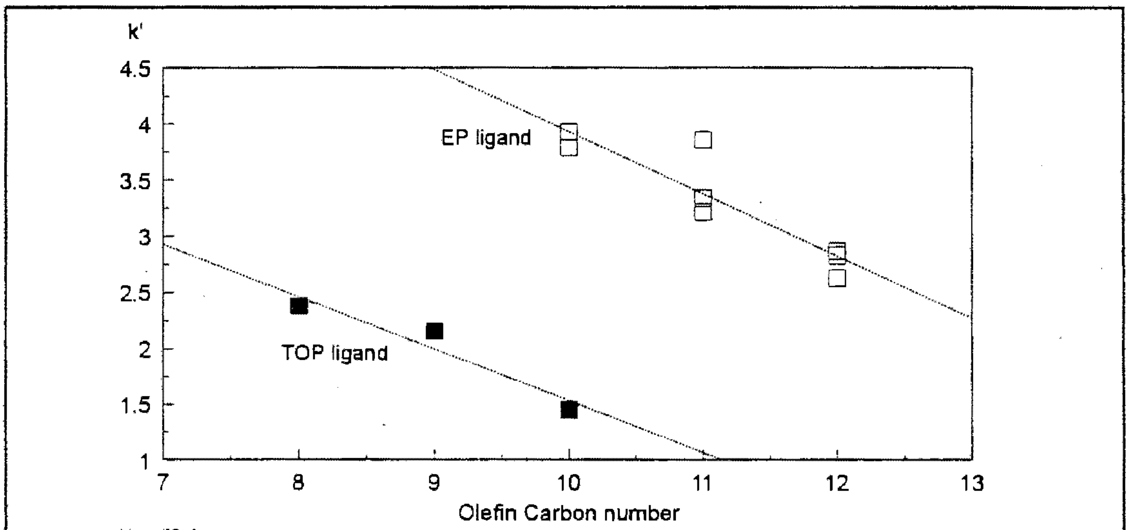

k' = k/[Co]
where k = first order rate constant for olefin consumption
[Co] = g Co per 100ml of feed

5.4.4.2 Catalyst Concentration Effects

Figure 5.11 indicates that for a double carbon number fraction (C_{11} and C_{12}), the rate of olefin hydroformylation for each carbon number appears to be relatively independent of the balance of the adjacent carbon number olefin content. This once more confirms that the olefin distribution (branched and linear) does not markedly affect the reaction rate/s (see Table 5.8). This holds, given that the total olefin contents are similar.

The result suggests that C_{11} olefins do not react preferentially to the C_{12} olefins, (*ie.* there is little competition for active sites), but the C_{11} olefins do react faster, probably due to steric factors (*ie.* more successful collisions) , and the rates are dependent on the catalyst concentration.

Figure 5.11 The effect of $C_{11\text{-}12}$ olefin chainlength and distribution in SLO, and catalyst concentration on hydroformylation kinetics: Co/EP catalysts.

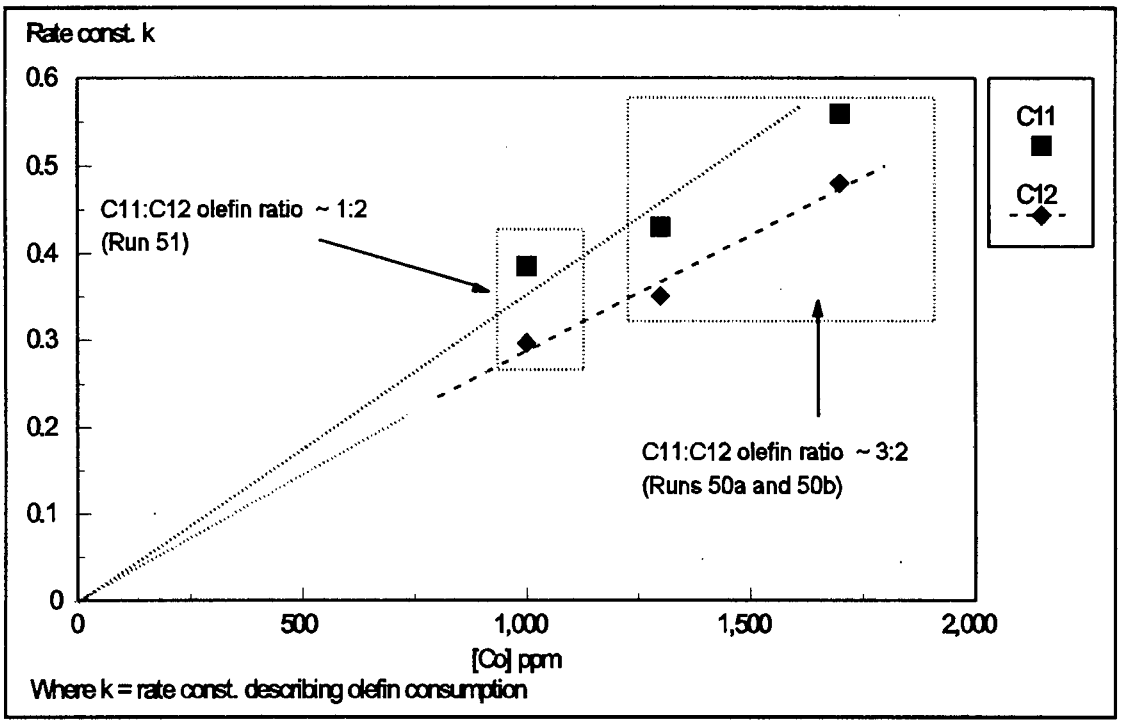

5.4.4.3 Reactivity of Olefin Structures in SLO

For Run 53, a good correlation, and specifically so for the olefin linearity, was obtained between the hydroformylation product distribution and the olefin assignments. This correlation is performed by "back" calculating the expected alcohol linearity (at time = t) from the olefin linearities using the following equation derived (See Appendix 7) for this purpose:

$$(\text{Expected alcohol linearity})_t = \frac{\dfrac{(\text{mass\% linear alcohol})_t \times 100\%}{(\text{mass\% 2-methyl alcohol})_t + (\text{mass\% linear alcohol})_t}}{1 + \dfrac{(\text{mass\% branched olefin})_{t_0} - (\text{mass\% branched olefin})_t}{(\text{mass\% linear olefin})_{t_0} - (\text{mass\% linear olefin})_t}} \tag{5.1}$$

Where t_0 = reaction starting time.

Additional confirmation on the reliability of the analyses, is demonstrated by way of the reaction selectivity results which sum consistently close to values of 100% as indicated in Appendix 3. Table 5.9 indicates the reliability of olefin peak assignments, and specifically as to the linearity or branched nature of the olefins.

Given the satisfactory correlation in the analyses, it may be possible to follow the profile of the different classes of olefins during the course of the reaction. This implies that the linear α, branched α, linear internal and branched internal olefins must be distinguished from each other and quantified. This was attempted for Run 53, and the results are illustrated in Figure 5.12.

Table 5.9 Breakdown of measured and expected C_{11} and C_{12} olefin product linearities from the measured olefin linearity assignments at various reaction times.

Time (hours)	0.75	1	1.5	2	2.75	4	7	24
Product linearity from C_{11} olefins (%):								
Expected:	50.5	55.4	60.2	61.7	61.1	61.3	61.1	60.9
Measured:	50.4	56.3	61.6	61.6	60.6	61.4	60.1	59.6
Product linearity from C_{12} olefins (%):								
Expected:	46.2	49.4	51.8	51.0	49.7	48.9	48.3	47.9
Measured:	44.6	47.6	51.3	53.1	52.1	46.4	46.1	45.4

The apparently lower product linearities observed initially in Table 5.9 are in line with previous observations (see Section 3.4.3.2). The reasons proposed for this are as follows:

The branched α-olefins initially react at the same rate as linear α-olefins (see Figure 5.13). However, isomerization occurs in parallel. Branched internal olefins form more slowly than linear internal olefins, possibly due to steric constraints. This results in a relative build up of branched α-olefins which are "available" for hydroformylation during the initial stages of the reaction. This in turn gives rise to lower initial product linearities. The subsequent build up of branched internal olefins with TOS implies that more linear olefins have reacted, and this is evidenced by the increased product linearity. It appears that when the bulk of the other olefins have reacted, then the remaining branched internal olefins react (via the α-olefin) giving lower linearity. This argument is expanded upon below.

Slopes of the first order rate plots of -ln(1-C) against reaction time (where C = fractional conversion) for the olefin groups in Figure 5.13 can be taken as a measure of the approximate reactivity of each group of olefins.

Figure 5.12 A breakdown of C_{12} olefins in SLO by structural class: Approximate progress of their formation/consumption during hydroformylation with Co/EP (Run 53).

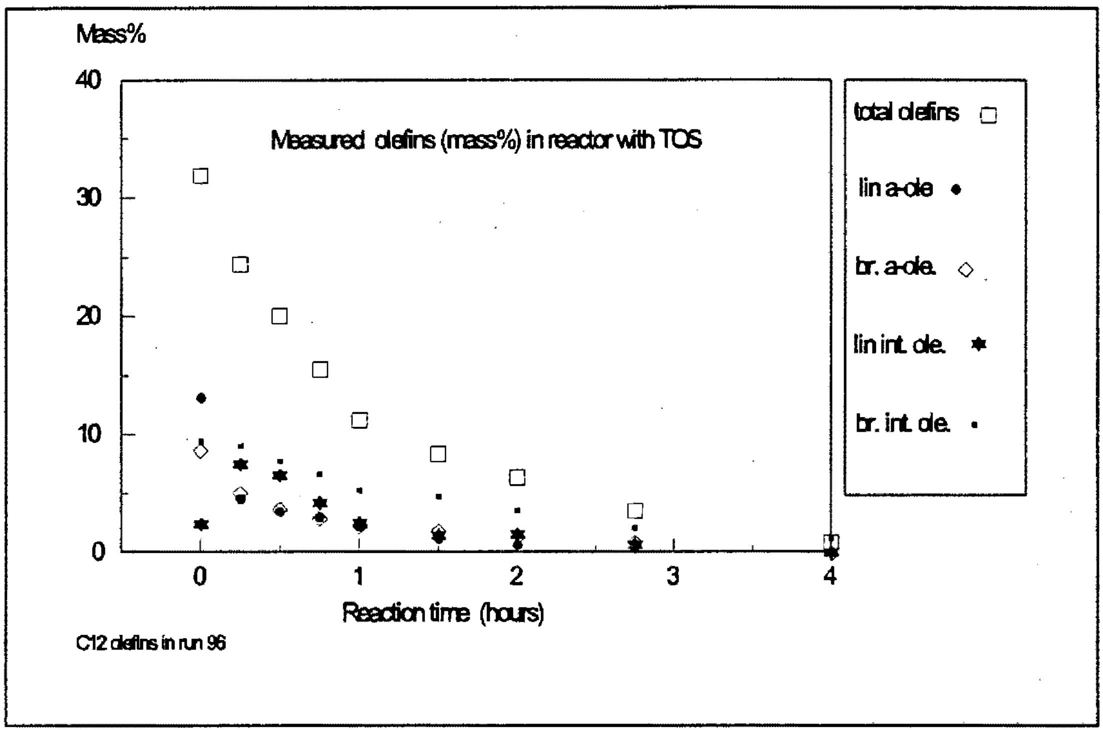

Various subtleties are evident on consideration of Figures 5.12 and 5.13. These are magnified because of the relatively large concentration of branched internal olefins present in the specific $C_{11\text{-}12}$ SLO fraction (D) compared with other SLO fractions tested (see Table 5.8).

It does appear as if the branched internal olefins are less reactive than the balance of the olefins. It is also evident that they are not readily formed during the course of the reaction (they do not increase relative to the branched α-olefins). This contrasts with the observations made with the linear olefins, in that linear internal olefins appear to form more readily. As discussed in Section 3.4.3.2, the internal olefins encountered in SLO during hydroformylation are probably methyl branched, with the double bond adjacent to the point of branching, as this is the thermodynamically preferred structure. Steric factors therefore probably result in their being slow to form by isomerization of the branched α-olefins as well as their being slow to react in these systems (see Figure 3.10). This observation is consistent with the description of the alcohol products in Section 3.4.3.2 (see Figures 3.8), which indicate few products derived from hydroformylation of internal olefins with SLO feeds.

Figure 5.13 Approximate comparison of branched and linear C_{12} olefin reactivities in a $C_{11\text{-}12}$ SLO fraction (Run 53).

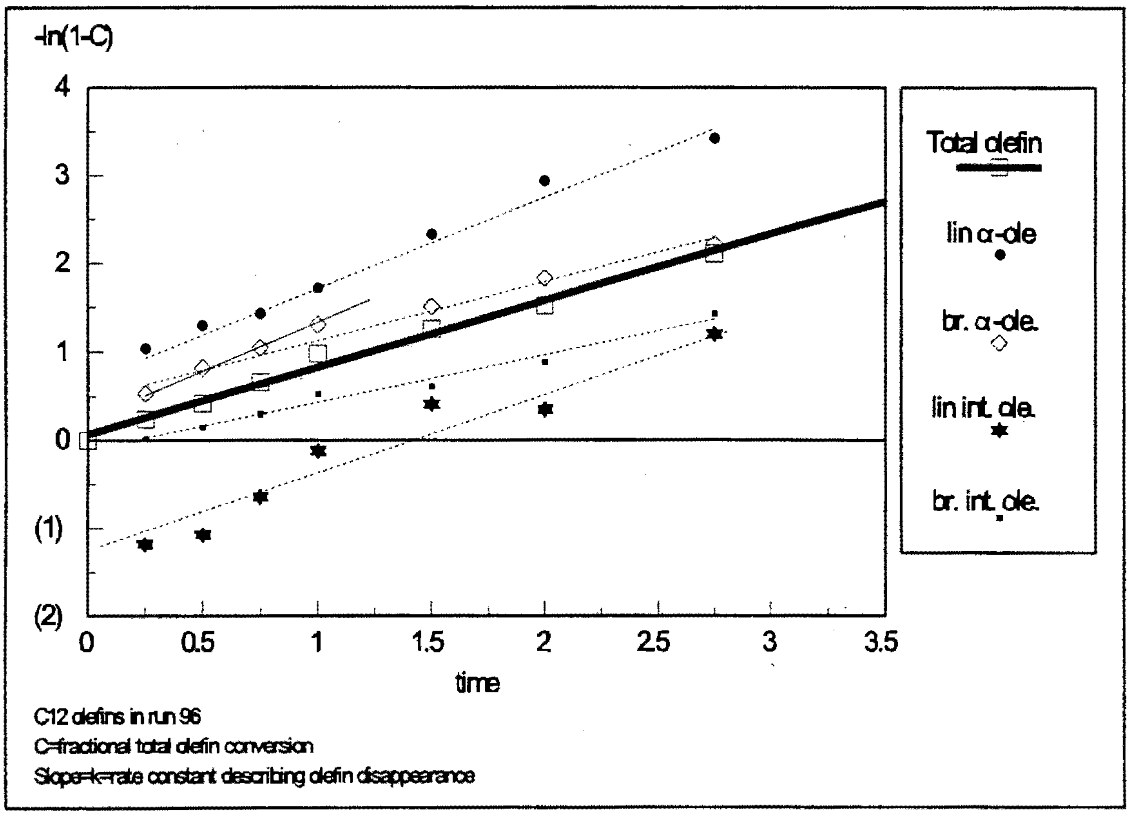

C12 olefins in run 96
C=fractional total olefin conversion
Slope=k=rate constant describing olefin disappearance

Since the fitted lines in Figure 5.13 do not pass through zero, they should be regarded as being "hypothetical". The lines in Figure 5.13 are approximately parallel for the linear olefins, and also parallel for the branched olefins. Indeed, "summing" the curves for the branched olefins would give a resultant "overall branched olefin line" which passes approximately through zero, and similarly for the "linear olefin lines". This may be taken to imply that most hydroformylation takes place via the α-olefin. An insight into the mechanism may also be inferred from the positions at which the lines in Figure 5.13 intersect the y axis. Namely, that re-isomerization of the internal olefins to α-olefins and subsequent hydroformylation probably occur on the same catalyst site/s.

The linearity of the branched α-olefin curve is however questionable, in that a higher initial rate appears to be evident. Although possibly due to experimental error, it does appear to indicate the presence of one, or more, less reactive branched α-olefins. Given the results obtained with the branched internal olefins, this is to be expected if the α-olefinic site is close to the point of branching.

The differences in the slopes of the curves in Figure 5.13 can therefore be used to conveniently explain the observed linearity profile with TOS as demonstrated by the data in Table 5.9. The often observed slight lowering of final product linearity with TOS may be indicative of higher concentrations of less reactive branched olefins at higher overall conversions.

However, given the observation on the differences in reactivities of the olefins, the <u>overall or average</u> reaction of an olefin fraction can still be regarded as being first order with respect to the total olefin in that C_{number} fraction. This is also demonstrated in Figure 5.13. This observation is consistent for the various SLO fractions tested in this study, especially so since they have lower quantities of branched olefins. It may however differ for feeds containing larger amounts of internal branched olefins (as well as 2 and 3-methyl α-olefins). Regarding the reactions as being first order with respect to the total olefin content is however useful in that it can substantially simplify comparisons and it is a satisfactory starting point for kinetic comparisons and modelling.

5.4.4.4 Formulation of an Expression Describing Olefin Reactivity

From the results presented thus far, it can reasonably be stated that the rate of reaction for total olefin consumption in SLO and pure feeds can be described by the term:

$$-d\frac{[\text{total olefin}_{C_x}]}{dt} = k\,[\text{total olefin}_{C_x}] \tag{5.2}$$

In other words, the reaction is first order with respect to olefin for an olefin having a carbon number = C_x.

Given the results on the effects of catalyst concentration and olefin chainlength in Figures 5.10 and 5.11, it may be possible to combine the general term describing the relationship between catalyst concentration and rate of the form

$$k = m_1[\text{Co}] \tag{5.3}$$

(where m_1 is the slope of the curve in Figure 5.11) and the relationship between carbon number and rate of the form:

$$k = -m_2 C_{\text{number}} + \text{constant} \tag{5.4}$$

(where m_2 and the constant are the slopes and intercepts of the curve/s in Figure 5.10 respectively)

to obtain, as a first approximation, an equation of the form:

$$k = (m_1[\text{Co}])(\text{constant} - m_2 C_{\text{number}}) \tag{5.5}$$

Equation (5.5) is simplified, by dividing by the constant term to arrive at an equation having the form:

$$k = m_1 [Co] (1 - \frac{m_2}{constant} C_{number}) \qquad (5.6)$$

which can be simplified to:

$$k = constant_a \; [Co] \; (1 - constant_b \; C_{number}) \qquad (5.7)$$

Regression of equation (5.7) to solve for $constants_{a \text{ and } b}$ using experimental *k*, [Co] and C_{number} values gave a good fit (R square >98.5) to the following expression:

$$k = 8.0435 \; [Co] \; (1 - 0.0537 \; C_{number}) \qquad (5.8)$$

However, the $constant_b$ term in Equation (5.8) implies that at a certain carbon number (around C = 17), the reaction rate becomes negative. This is not possible. Furthermore, a subsequent run with a pure C_{18} feed (Run 57 - see Tables 5.1 to 5.4.2), indicated that hydroformylation took place.

Equation (5.7) was therefore "modified" to:

$$k = constant_a \; [Co] \; (1 - constant_b \; \ln(C_{number})) \qquad (5.9)$$

Regression of equation (5.9) using a Marquardt [1963] routine to obtain values for $constant_a$ and $constant_b$ gave the following equation with a R-square of >98%:

$$k = 11.6797 [Co] (1 - 0.2979 \; \ln(C_{number}))$$

$$= 11.6797 \; [Co] - 11.6797 \; [Co] \; 0.2979 \; \ln(C_{number}) \qquad (5.10)$$

With equation (5.10), it is still possible to predict a negative rate for $C_{numbers} > 29$. This however does not necessarily imply that for longer olefins ($>C_{29}$) the rates will be similar and close to zero when using reaction conditions similar to those used in this study. Similarly, equation (5.10) should not be taken to imply that for shorter olefins ($<C_{10}$) the rate will increase exponentially. The equation is therefore empirical and is only valid over the carbon number range that was actually covered, where it fails is unclear.

Figures 5.14, and 5.15 demonstrate the accuracy of equation (5.10) with experimental data points superimposed.

Figure 5.14 Testing of equation (5.10): *k* versus [Co], experimental and predicted points at various C numbers.

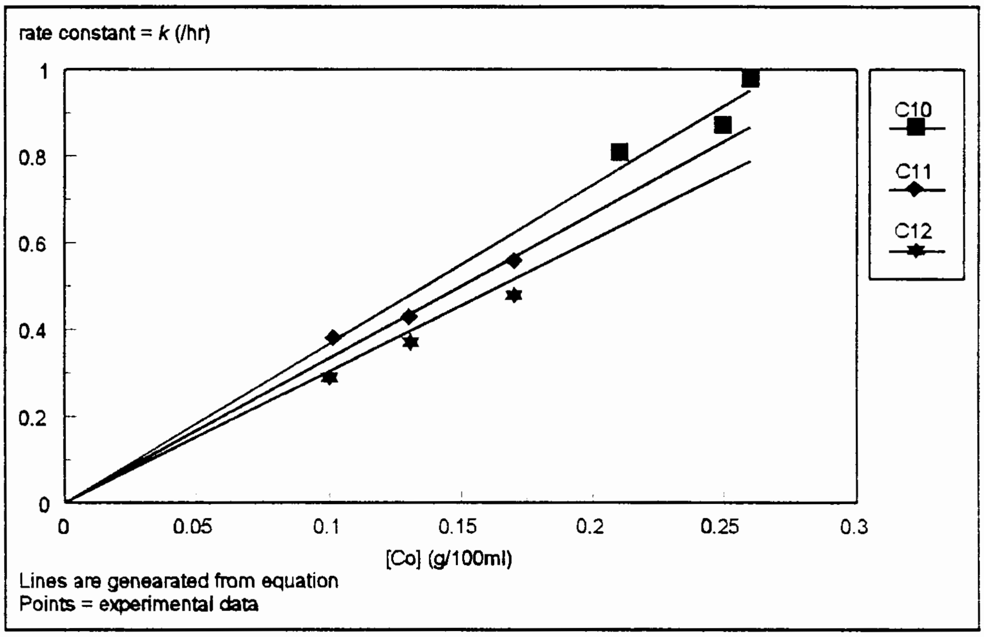

The dependency of the first order rate constant *k* on catalyst concentration <u>and</u> olefin carbon number can be represented by means of three dimensional graphs as in Figures 5.16 and 5.17. The shaded regions (or planes) in the 3-D figures are generated by equation (5.10). Data points □ are superimposed on the region predicted by the equation. Vertical lines drawn above and below the points □ in the graph indicate the respective distance of these points from the "plane " or "surface" described by the equation.

Figure 5.15 Testing of equation (5.10): *k* versus C_{number}, experimental and modelled results, at various catalyst concentrations.

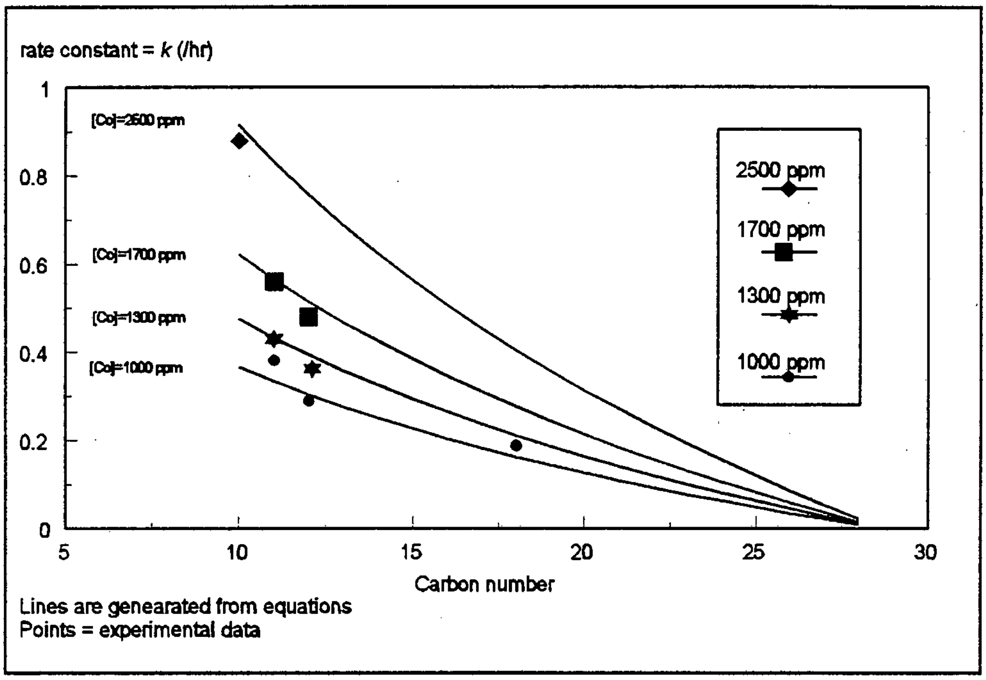

Given the derived relationship between *k*, [Co] and carbon number (C_x), equation (5.2) can therefore be expanded to:

$$-d\frac{[\text{total olefin}_{C_x}]}{dt} = 11.6797(1 - 0.2979\ \ln C_x).[\text{Co}].[\text{total olefin}_{C_x}] \qquad (5.11)$$

Figure 5.16 Dependency of k on Carbon number and catalyst concentration described by the expression: $k = 11.6797\,[\mathrm{Co}]\,(1 - 0.2979 \ln(C_{\mathrm{number}}))$ in the $C_{10\text{-}12}$ region.

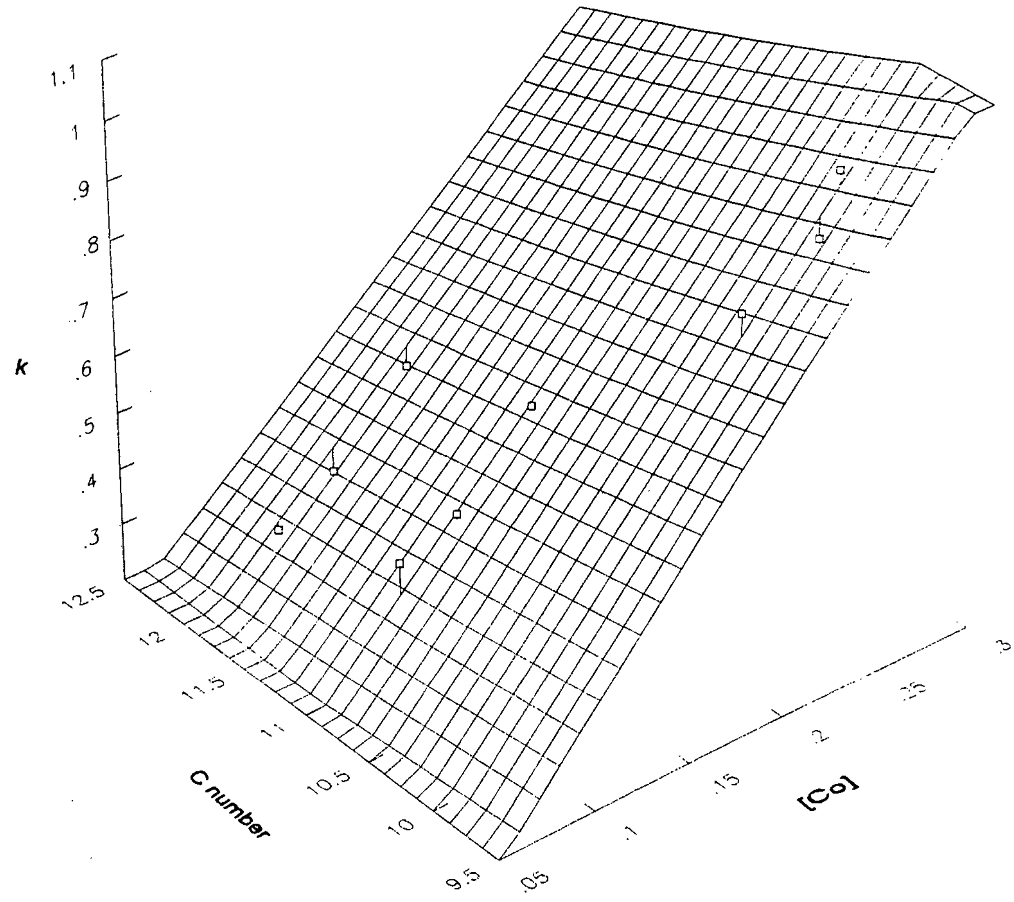

[Co]: units = g/100ml

Figure 5.17 Dependency of *k* on Carbon number and catalyst concentration described by the expression: $k = 11.6797\,[Co]\,(1 - 0.2979 \ln(C_{number}))$ in the $C_{10\text{-}18}$ region.

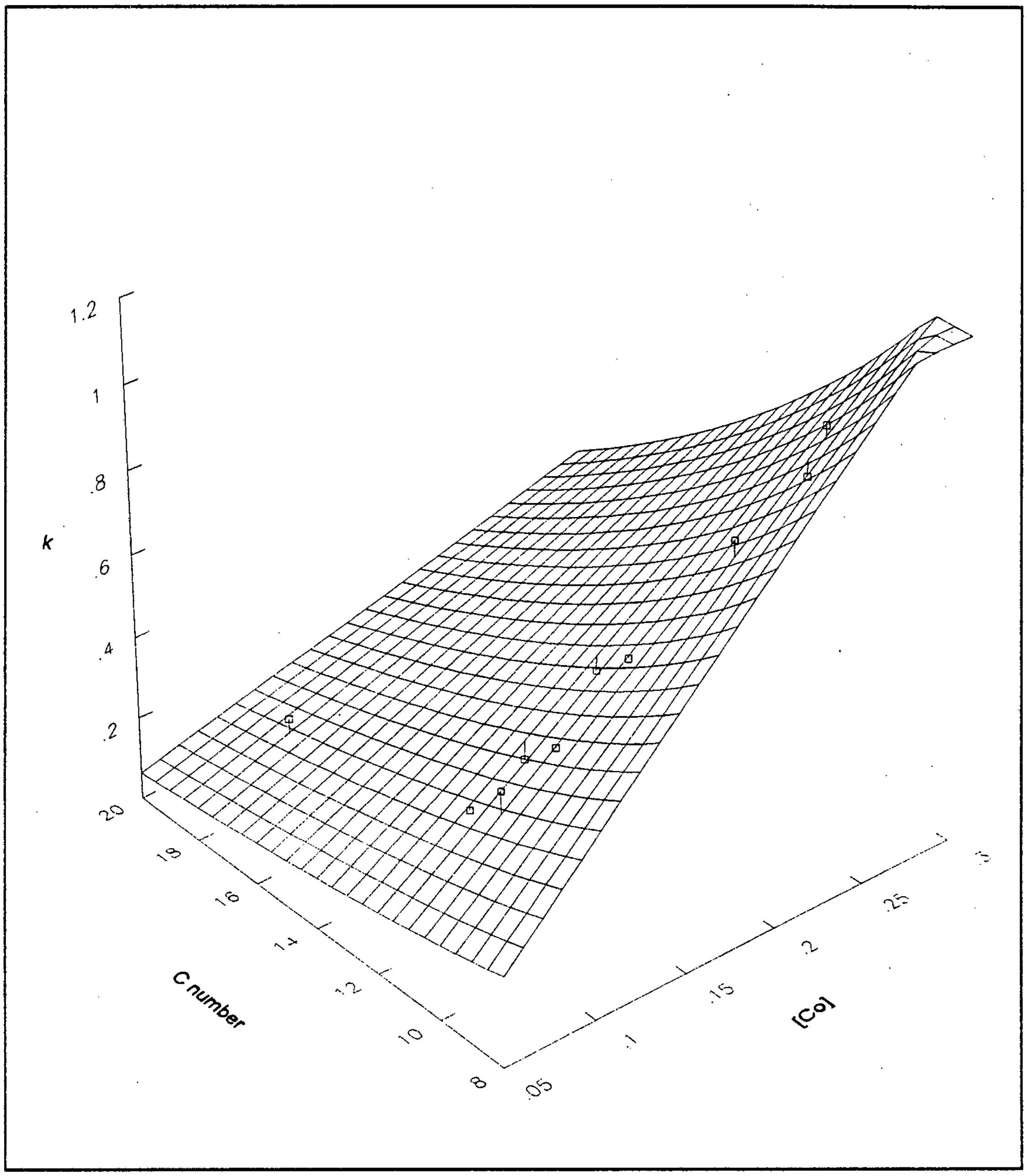

[Co]: units = g/100ml

5.4.5 Temperature Study

The effect of temperature on the hydroformylation of a $C_{11\text{-}12}$ SLO feed (E) was investigated. Reports on the effect of temperature on phosphine modified (specifically EP) Co hydroformylation systems were not sourced in the literature.

Table 5.10 Experiments and results for temperature study.

Run	55a		55b		55c		55d		55e		55f		55g	
Temperature (°C)	155		165		175		185		195		165		195	
Feed	$C_{11\text{-}12}$ SLO : (For composition see Table 5.3)										60% $C_{11\text{-}12}$ SLO 40% 55b product		60% $C_{11\text{-}12}$ SLO 40% 55e product	
[Co] (grams per 100ml of feed)	0.16		0.16		0.16		0.16		0.16		0.061		0.061	
Carbon number	C_{11}	C_{12}	C_{11}	C_{12}	C_{11}	C_{12}	C_{11}	C_{12}	C_{11}	C_{12}	C_{11}	C_{12}	C_{11}	C_{12}
*Initial k (hr^{-1})	0.36	0.27	0.58	0.46	1.15	0.95	1.63	1.21	1.78	1.45	0.22	0.18	0.25	0.14
Initial k' (hr^{-1}) corrected for [Co]	2.29	1.72	3.70	2.90	7.34	6.08	9.37	6.88	11.21	9.24	3.62	2.95	3.15	1.83
Conversions Linearities and Selectivities at 8hours TOS														
% Olefin conversion	93.2	87.3	98.5	98.4	100	100	99.1	97.4	99.5	99.0	91.5	89.3	85.1	62.5
% 1-α olefin prod. lin.	89.4	84.7	86.6	84.6	85.4	80.7	86.3	85.9	85.3	87.2	89.3	90.2	82.7	85.7
% Overall prod. lin	72.8	44.2	69.4	42.5	67.4	39.1	69.7	38.3	64.1	37.7	69.9	43.7	62.0	25.8
% (Aldehyde + Alcohol) selectivity	92.9	93.1	97.9	97.6	92.8	95.1	96.3	98.2	98.4	95.9	94.2	93.8	91.1	95.4

* Slopes of curves for determining *k* deviate from linearity at high temperatures (see Figures 5.18 and 5.19)

No clear trends in the final selectivities were ascertained from the reaction data. This may be taken to imply that the <u>final</u> reaction selectivities were fairly insensitive to temperature differences in the range studied. The alcohol linearities did not always follow the expected trend of lower linearities being associated with higher rates. A possible reason for this may be due to the fact that the <u>overall</u> reaction rates may be slower for reactions undertaken at 185°C and 195°C due to catalyst deactivation (see subsequent discussion). However, there is an indication that the overall product linearities decreased with increasing temperature.

Temperature effects on the reaction kinetics were more evident.

The effect of temperature on the first order rate constants *k* describing C_{11} and C_{12} olefin consumption is evident on comparing the slopes of the plots in Figures 5.18 and 5.19. At high conversions (>95%), a marked deviation from linearity is observed for the experiments undertaken at 185°C and 195°C. This may be ascribed to analysis errors at high conversions. For example, conversions of 99.0% and 99.9 % give -ln(1-C) values of 4.6 and 6.9 respectively.

Figure 5.18 The effect of temperature on the first order rate constant: C_{11} olefins in a $C_{11\text{-}12}$ SLO fraction.

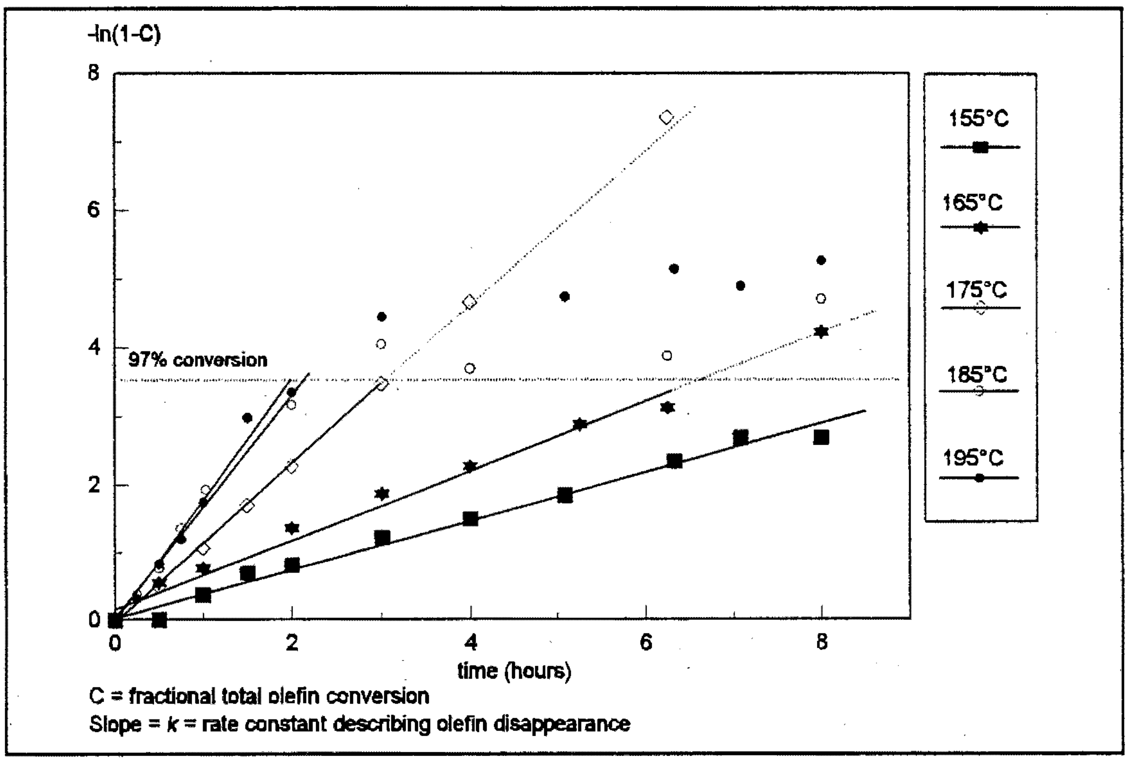

Data points collected at conversions higher than 97% (or values of >3.5 on the y axis in Figures 5.18 and 5.19) were therefore omitted for the purposes of calculating rate constants, *k*.

Figure 5.19 The effect of temperature on the first order rate constant: C_{12} olefins in a $C_{11\text{-}12}$ SLO fraction.

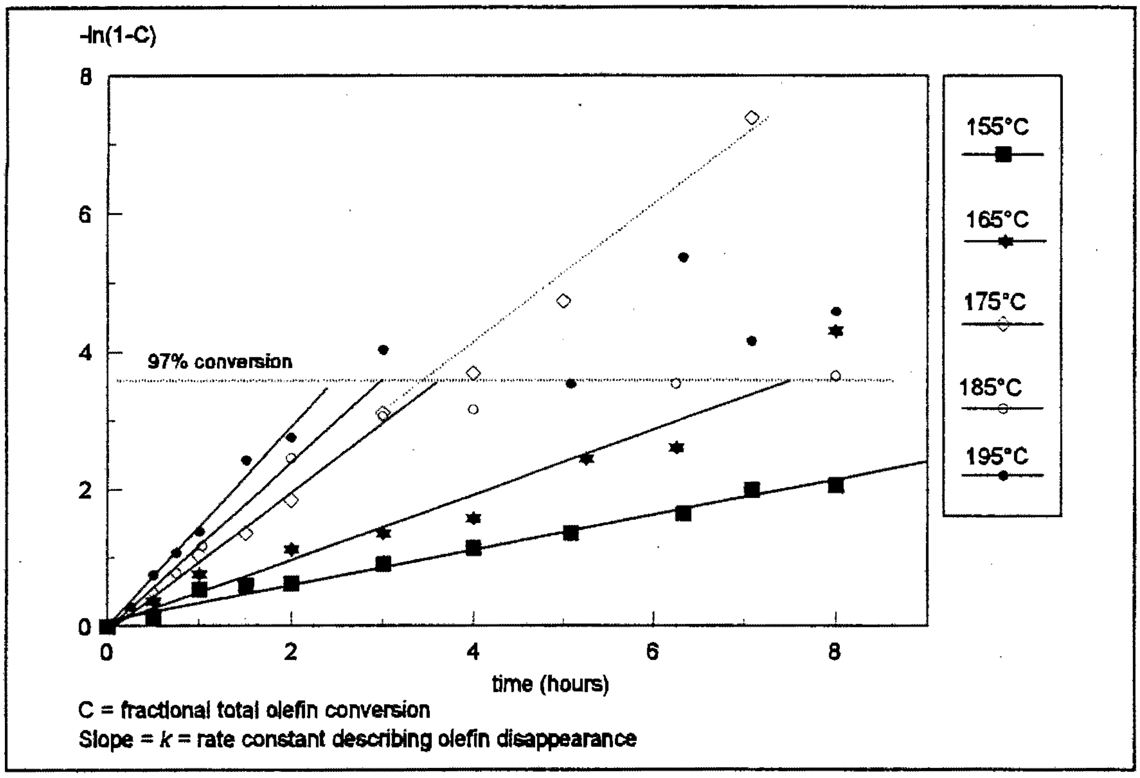

An examination of reactor samples taken from the runs at temperatures above 175°C, indicated that the cobalt readily precipitated out of solution (*ie.* a black precipitate was observed). In order to find a reason for this observation, additional experiments were undertaken. The first experiment entailed addition of 100ml of the $C_{11\text{-}12}$ SLO to the remaining catalyst containing solutions previously used at 165°C (Run 55b), and repeating the reaction under the same conditions of temperature (*ie.* 165°C) and pressure. The progress of the reaction (now termed 55f) was monitored. The lower catalyst concentration attributable to previous sampling and subsequent dilution was taken into account. A similar second experiment was undertaken but with the reactions being undertaken at 195°C (runs 55e and 55g). The kinetic results obtained are shown in Table 5.10, and the results for the high temperature (195°C) runs are illustrated in Figure 5.20.

Figure 5.20 High temperature runs at 195°C; proof of catalyst deactivation; re-used catalyst.

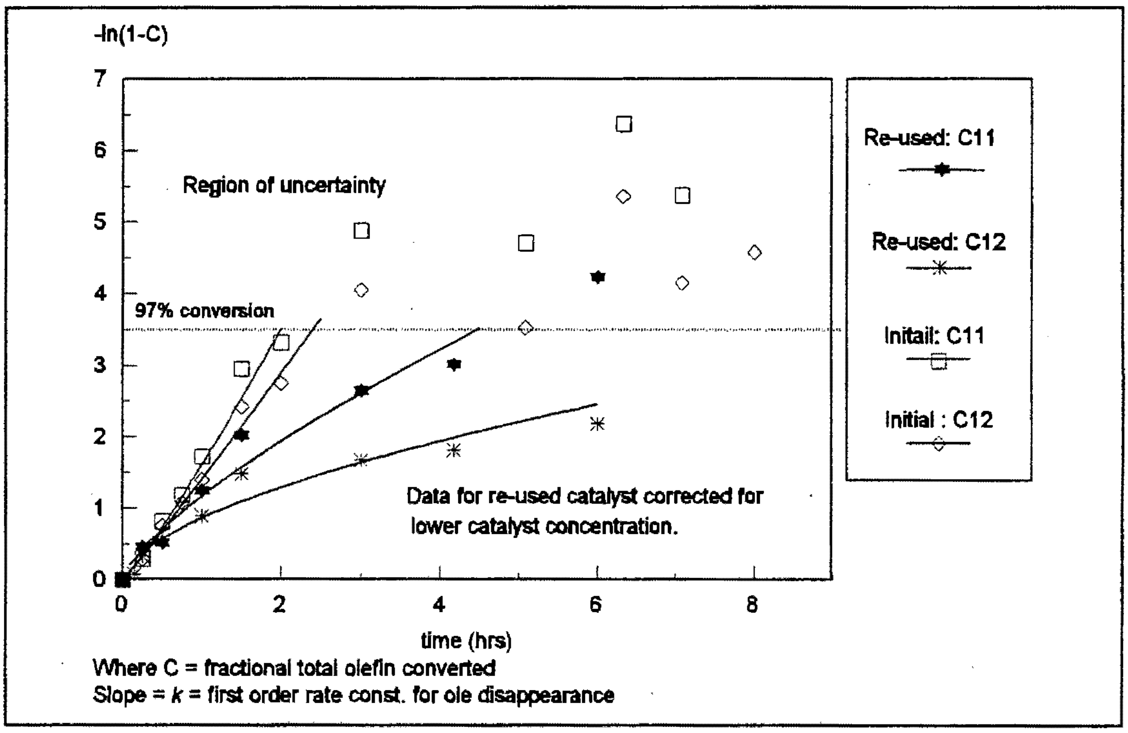

The points above the dotted line in Figure 5.20 are in "a region of uncertainty", wherein small errors in the conversion (*ie.* olefin concentration), are magnified by the natural log function y scale. This can give rise to a large amount of scatter in the data points as evidenced. The curves best fitting all the data in Figure 5.20 are from power series, indicative of a progressive falling off of the reaction rate with time. This indicates that catalyst deactivation may occur from the start of the reactions and not necessarily only at high conversions. Furthermore, the lower reaction rates cannot be ascribed to ligand oxidation at changeover. This would result in a lowering of the EP:Co ratio with concomitant faster reaction rates (see Section 5.4.2). This however was not observed. This result along with the data comparing product linearities and alcohol selectivities for the various runs at different temperatures indicates that the Co concentration apportioned to the active Co/EP complex appears to decreases with time when undertaking reactions at the temperatures above 175°C.

Further evidence of catalyst deactivation and cobalt precipitation at the higher temperatures can be illustrated by way of Figure 5.21 which compares the cobalt concentration of the reactor liquids for Runs 55a-g. This bar graph is meant to convey a qualitative observation, since the actual cobalt concentration attributable to the catalyst complex cannot be accurately quantified using the UV-VIS method described in Section 2.3.3.1, as these determinations are "*ex situ*".

Figure 5.21 Measured cobalt concentration in reactor liquids after 8 hours TOS for runs undertaken at various temperatures.

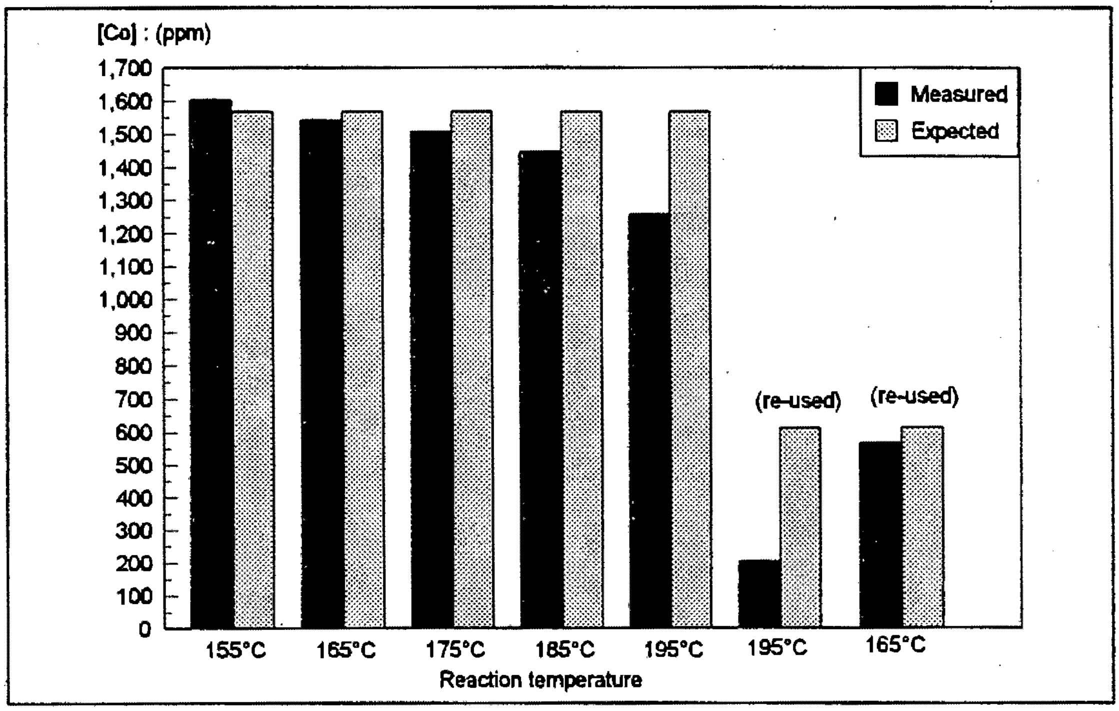

It has been widely reported that conventional hydroformylation catalysts are sensitive to temperature and P_{CO}. This relationship has been plotted [Cornils, Falbe, 1980], and is reproduced in Figure 5.22. This instability was ascribed by Falbe as being due to "gas starvation", specifically CO starvation. This is said to lead to dissociation of the catalyst complex, which gives rise to cobalt precipitation. This starvation has been ascribed to high reaction rates in the mass transfer limited regime. Another argument for deactivation, is the possible inherent instability of the catalyst complex at high temperatures, regardless of the reaction rate. The third explanation for catalyst instability can include components of the two previous arguments, and this is subsequently discussed.

Figure 5.22 Conditions giving rise to Co precipitation with conventional Co hydroformylation catalysts [Falbe, 1980].

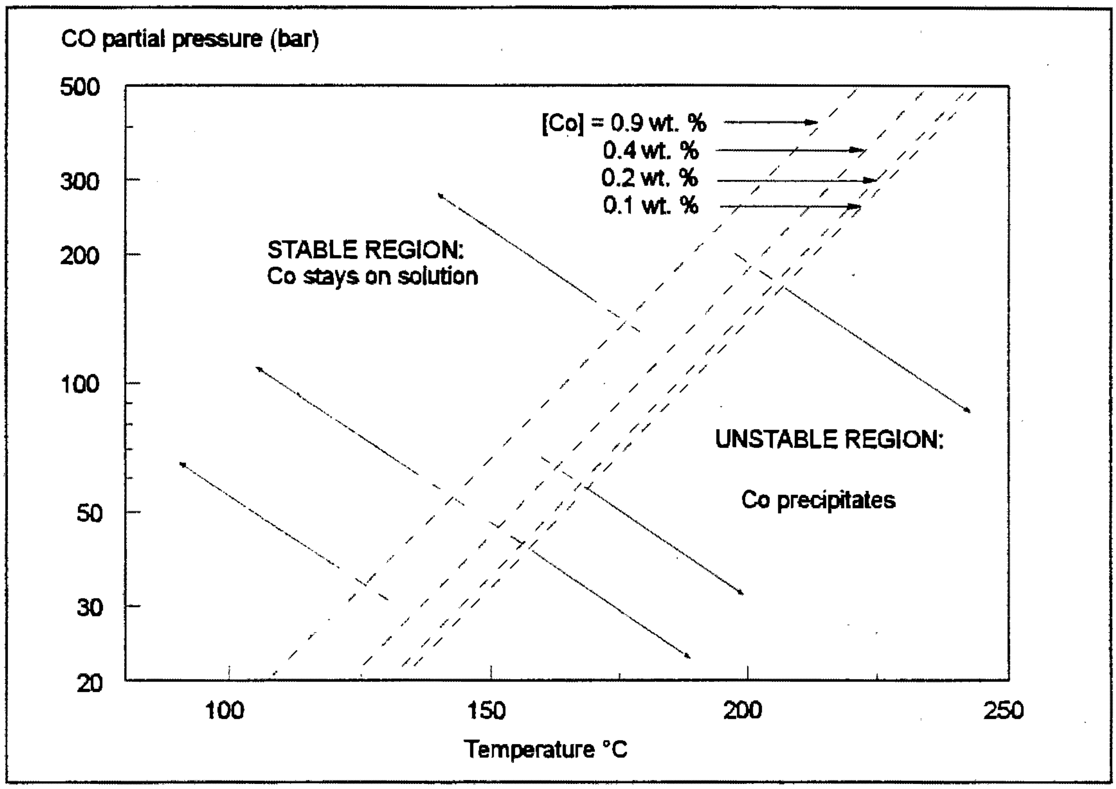

The slopes of the fitted (linear) portions of the curves in Figures 5.18 and 5.19 were used to calculate the values plotted in Figures 5.23 and 5.24. "Region 1" in Figure 5.23 indicates the expected exponential relationship between temperature and the reaction rate. This is not the case for the reactions undertaken at 185°C and 195°C in "Region 2". It is important to note that the rate constant values used for these higher temperatures are derived from the slopes fitted to the initial conversions, and do not take the later points which indicate a deviation from linearity into account. Although these deviations at higher temperatures may have simply been caused by analytical inaccuracies at the low olefin levels or high conversions, mass transfer effects and/or catalyst stability effects may have also played a role. The curvature in the plots at 185 and 195°C in Figures 5.18 and 5.19 as well as the observed darkening of the reactor liquids and precipitation of cobalt, may be taken as evidence of possible catalyst deactivation.

Figure 5.23 Effect of temperature on the first order rate constant for all C_{11} and C_{12} olefins in a SLO $C_{11\text{-}12}$ fraction.

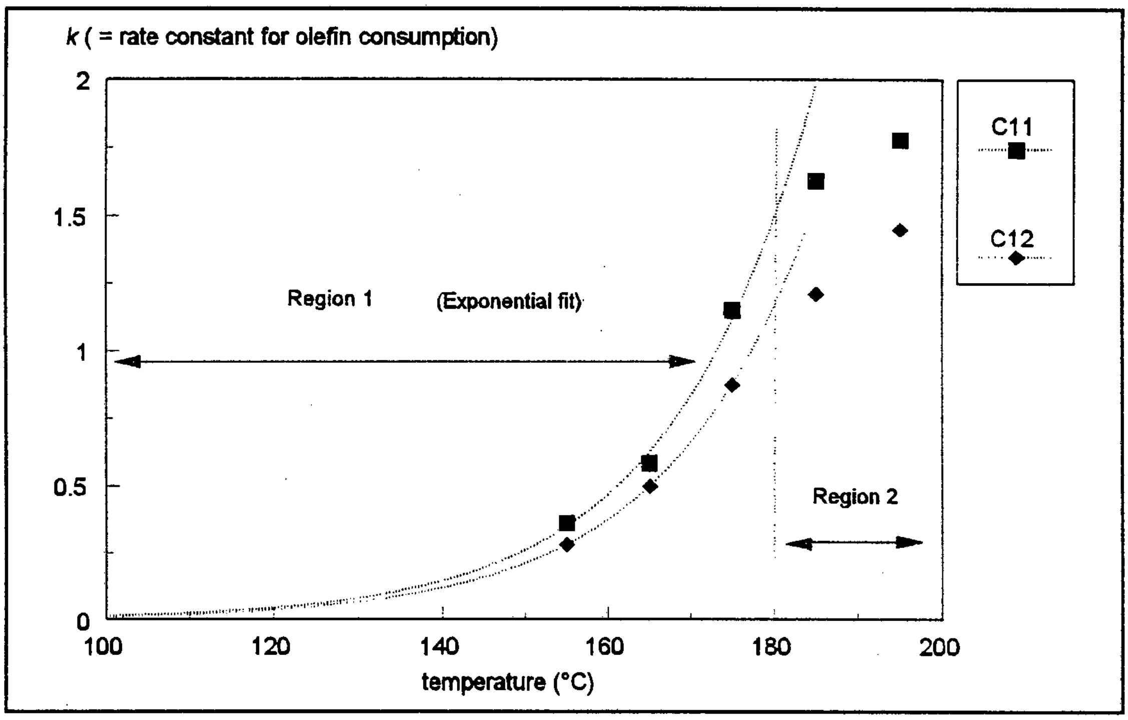

Arrhenius plots of the natural log (ln) of the *k'* values (*k'* = *k*/$[Co]_{in}$ where [Co] is expressed in g/100ml) versus the inverse of the reaction temperatures in Kelvin, are shown in Figure 5.24. Slopes of the curves = E_a/R, where E_a is the activation energy and R is the universal gas constant.

Figure 5.24 Arrhenius Plot of effect of temperature on Co/EP catalyzed hydroformylation of C_{11} and C_{12} olefins in SLO.

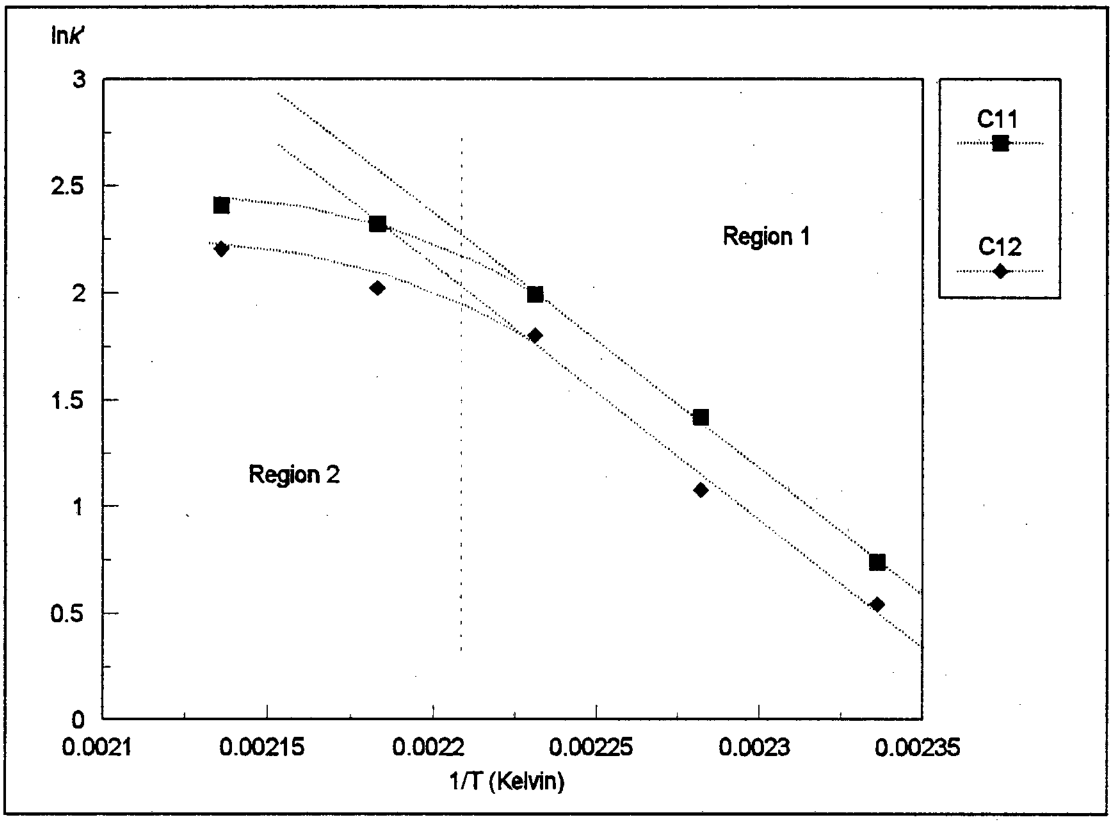

Table 5.11 Activation Energies for C_{11} and C_{12} olefins in SLO.

	Region 1		Region 2	
	C_{11}	C_{12}	C_{11}	C_{12}
y intercept	2.743×10^{12}	2.245×10^{12}	138552	78763
E_a (kJ/mol)	99	99	35	36

The "kinks" in the Arrhenius plots in Figure 5.24 suggest the onset of mass transfer limitations of reactants (CO and H_2) through the liquid phase to the catalyst at temperatures above 175°C and/or early deactivation.

Equation (5.11) describing olefin consumption in these systems can therefore be expanded to:

$$-d\frac{[\mathrm{olefin}]}{dt} = k \cdot e^{-\frac{E_a}{RT}} (1- 0.2979 \ln(C_x)) [\mathrm{Co}][\mathrm{olefin}] \tag{5.12}$$

Where

$E_a \approx$ 99kJ/mol at temperatures ≤ 175°C, and

$E_a \approx$ 36kJ/mol at temperatures ≥ 175°C.

Differences in the rate constants of the C_{11} and C_{12} olefins must be mainly ascribed to a differences in the pre-exponential or "successful collision frequency" factor (see y intercept values in Table 5.11), rather than to differences in the activation energy each one must overcome. (Similar activation energies were calculated for C_{11} and C_{12} olefins). Reports of work undertaken by others appears to confirm this statement as discussed below.

The activation energies of about 99 kJ/mol for the C_{11} and C_{12} olefins in SLO are similar to, but lower than reported values of Voorhies *et al.* [1957] for branched C_7, 1-octene, and C_{12} olefin feeds using unmodified Co hydrocarbonyl catalyst systems. These activation energies were reported to be 115, 118 and 106 kJ/mol respectively by Voorhies *et al.*, who stated that the method of kinetic measurements used for their data was based on the observation of the rate of pressure drop (*ie.* not at constant pressure), exclusive of any induction period. They described their E_a values as being "approximately equivalent in view of the experimental technique".

Other reported activation energies for hydroformylation reactions include the following:

Deshpande and Chaudhari [1989] reported an activation energy of 96 kJ/mol for hydroformylation of allyl alcohol (CH_2=CH-CH_2OH) with a phosphine modified Rh catalyst (HRh(CO)(PPh_3)$_3$) in the temperature range of 60 to 80°C. These workers also reported an activation energy of 117kJ/mol for 1-hexene hydroformylation, also with a HRh(CO)(PPh_3)$_3$ catalyst [Deshpande and Chaudhari, 1988].

The above mentioned results, are in a fairly narrow band, and are in some cases higher than the activation energies reported by Capelli *et al.* [1976] and Gholap *et al.* [1992] who also investigated unmodified cobalt hydroformylation systems. Capelli *et al.* [1976] reported E_a values of 75 kJ/mol and 108 kJ/mol for 1-octene and 2-octene feeds respectively. However, only two temperatures, namely 145°C and 155°C, were used in their study. The work of Gholap *et al.* [1992] involved propylene hydroformylation in the 110 to 150°C temperature range (using three different temperatures) and the 35 to 100 bar pressure range. These workers reported an activation energy of 77kJ/mol. A higher cobalt concentration with respect to the propylene feed of between 0.34 and 0.60 % by mass was used compared with the values reported by Voorhies *et al.* and the ones used in this study.

With the exception of the result of Cappelli *et al.* and Gholap *et al.*, the balance of the reported results encountered, as well as the result generated in this study, appear to indicate that for phosphine modified and unmodified Rh and Co based systems, the activation energy for hydroformylation is fairly independent of the feed composition and reaction conditions. In addition, the results can be taken as confirmation that the experimental data in this study were generated in the correct kinetic regime, (*ie.* the non mass transfer limited regime). The relatively high value of E_a of approximately 99 kJ/mol confirms this. Ligand basicity and steric effects do no appear to effect E_a values, but rather the pre-exponential rate constant. This implies that KOH effects observed in this study would not be expected to effect the reaction activation energy.

The data that Voorhies *et al.* presented used approximately the same catalyst concentration with respect to the cobalt content of 0.2% (*ie.* 0.2 grams of cobalt per 100 grams of feed) as used in this study. This facilitates a direct comparison. This is performed by plotting the present Co/EP results and the hydrocarbonyl results of Voorhies *et al.* in Figure 5.25. Unfortunately Voorhies *et al.* did not specify the syngas composition and pressure.

Figure 5.25 Arrhenius plots for EP modified (this study) and unmodified Co (Voorhies *et al.*) hydroformylation catalysts.

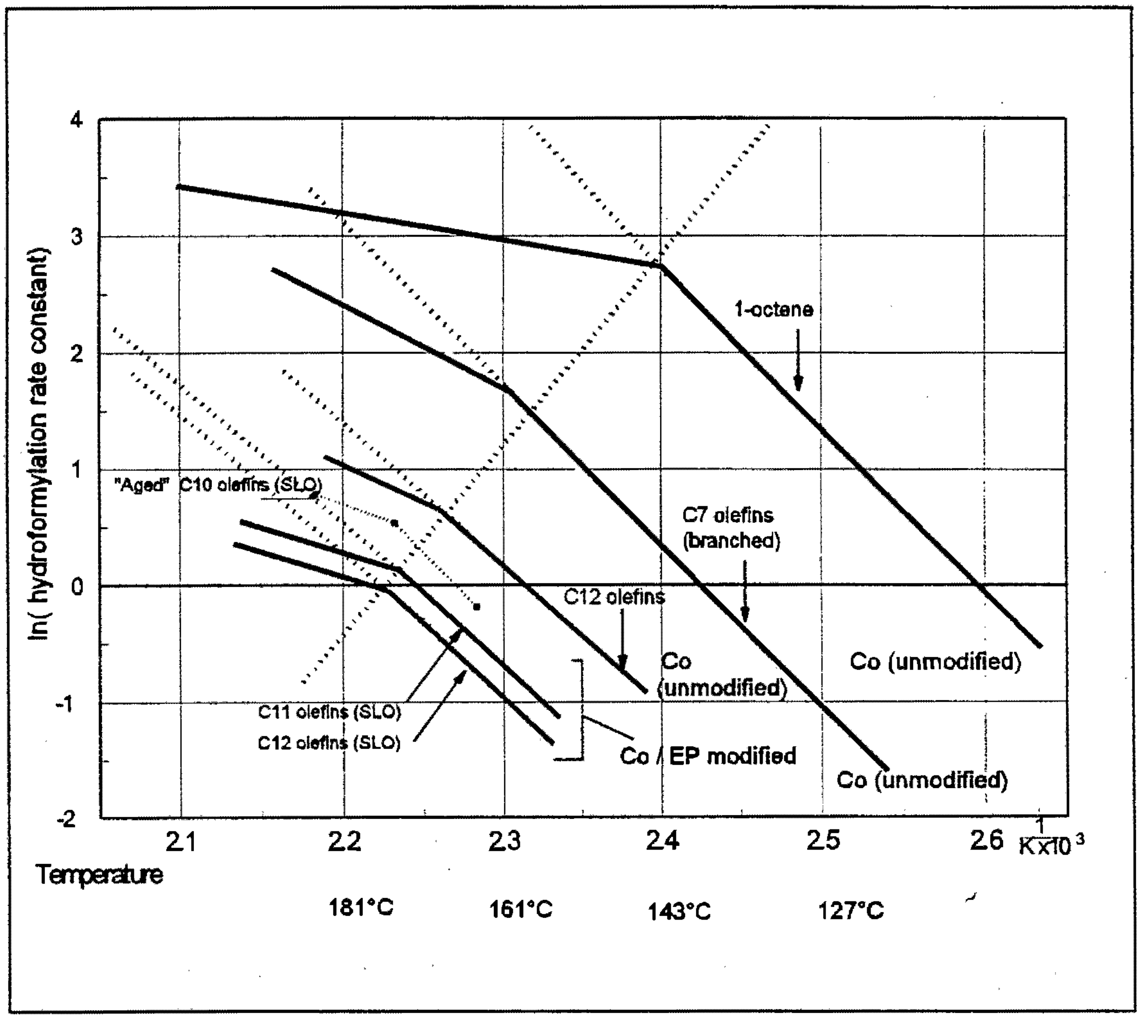

On considering Figure 5.25, various interesting observations can be made.

Three additional points drawn in Figure 5.25 are the rate constants determined from initial measurements of rate for various experiments undertaken with a SLO C_{10} "aged" feed [1]. These points are included, in that they "fit the trend" of the rest of the data in Figure 5.25.

The deviation of the curves in Figure 5.25 from linearity at higher temperatures has been ascribed to "the adverse effect of higher temperatures on catalyst stability" by Voorhies *et al.*. A possible explanation for this deviation would be mass transfer effects. However, if mass transfer (of CO and H_2) alone was the cause for linearity deviations in the curves in Figure 5.25, then one would expect the points of inflection to occur at similar rate constant or ln(k') values, and specifically so for the same catalysts. This however, is not the case.

It is tempting to ascribe the differences in the rate at which the "kink" in the curves occurs to steric factors. That is, when the reaction rate is lower as a result of steric effects, diffusion limitation will appear later (*ie.* at a higher temperature) and visa versa. This argument does however not explain why the "kinks" occur at different reaction rate constants.

An alternative explanation has to do with the effect of temperature on reaction rate and catalyst stability. Thermal decomposition reactions are a function of temperature and time. It can be postulated that at high reaction rates, the cobalt species is exposed to a lower CO co-ordination for longer periods of time due

---

[1] The peroxide content in this feed was shown to be high, and to effect the Co/EP catalyst. Poor linearities were measured, and catalyst deactivation was observed for these experiments. This was ascribed to a lowering of the EP:Co molar ratio caused by ligand oxidation. The data fit the trend in Figure 5.25, notwithstanding the observation that the catalyst system performed markedly differently due to the feed composition/poisons.

to "CO starvation". For the equation;

$$HCoEP(CO)_2 + CO \rightleftharpoons HCoEP(CO)_3$$

more of the "active" $HCoEP(CO)_2$ catalyst will be present at high rates compared to the "inactive" $HCoEP(CO)_3$ complex due to higher rates of CO consumption. If one assumes that the $HCoEP(CO)_2$ complex is less thermally stable, it follows that at high reaction rates the onset of catalyst decomposition or cobalt precipitation is facilitated at a lower temperature.

Bearing in mind that less active Co/P catalysts are used at temperatures in the region of 180°C to 190°C [Falbe, 1980], it may be coincidental, that the regions of inflection for the curves in Figure 5.25, can be joined by an approximately straight line. Given this observation, it is tempting to propose that Figure 5.25 can be used as a screening tool to predict a suitable reaction temperature for a cobalt based hydroformylation catalyst. This can be achieved by using the same catalyst concentration (0.2% by mass as cobalt), measuring the reaction rate constant, and extrapolating (using parallel lines) to the curve predicting the region of inflection, or onset of catalyst deactivation. A recommended operating temperature (to ensure catalyst stability) would then be one that is close to, but below, the temperature in the region of inflection. For the various curves in Figure 5.25, the reaction rate at the region or "point" of inflection, appears to be dependent on the rate at a lower temperature. This is demonstrated by Figure 5.26. Respective regions of catalyst stability and instability may be indicated below and above the line "joining" the regions of inflections in Figure 5.25.

Furthermore, it is interesting that various data points used by Cappelli *et al.* and Gholap *et al.* in determining their lower activation energies of 75-77 kJ/mol can be placed in the "region of instability" in Figure 5.25, thereby explaining the differences in reported activation energies.

Figure 5.26 Possible relationship between catalyst stability and reaction rate.

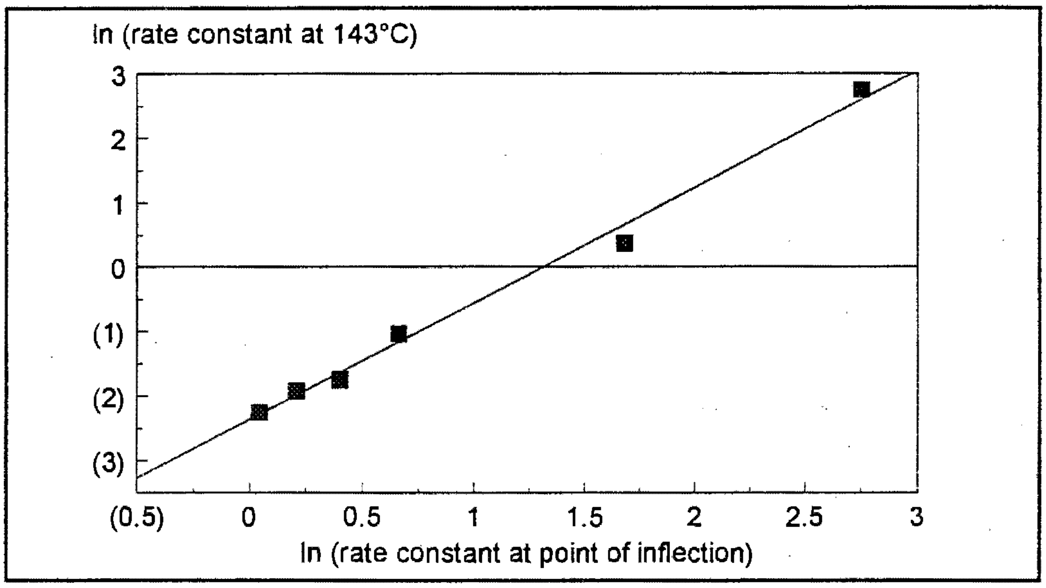

The observations and proposed theory on the effect of temperature on hydroformylation catalyst systems in this study could possibly be confirmed by additional experiments and with other catalysts. For example, a temperature study on other phosphine modified or conventional Co catalysts could be used to test some of the theories. As it was not the intention to study the effect of temperature alone, this may constitute an interesting avenue for further work.

5.4.6 Gas Composition Effects

It was previously demonstrated that similar reaction rates were observed with pure 2:1 H_2:CO syngas and a commercial syngas in experiments using total pressures of 75 bar (g) and 90 bar (g) respectively with TOP modified Co catalysts (see Section 4.4.5). In order to further investigate the effect of feed gas composition and pressure, Runs 47a-b, 56a-e were undertaken. Reaction details and results are summarized in Tables 5.12 and 5.13.

Reactions were undertaken at constant pressure, with the syngas mixtures being passed continuously through the reactor (as described in Section 4.1.1), so that the syngas composition in the reactor remained approximately constant. The effect of syngas composition and pressure was monitored by keeping either the P_{CO} constant and varying the P_{H2}, or keeping the P_{H2} constant and varying the P_{CO}. In addition, the effect of CO_2 was investigated (see Table 5.14).

5.4.6.1 Syngas Effect on Reaction Kinetics

Table 5.12 Kinetic results obtained with various syngas compositions and pressures: 1-Decene feed; Co/EP catalyst.

	Constant P_{CO}; increasing P_{H2} →			Constant P_{H2}; increasing P_{CO} →			
Run	56a	56b	56c	56d	56b	56e	47a
P_{H2} (bar (g))	15	30	60	30	30	30	50
P_{CO} (bar (g))	30	30	30	15	30	60	25
P_{total} (bar (g))	45	60	90	45	60	90	75
H_2:CO ratio	0.5	1	2	2	1	0.5	2
k (hr^{-1})*	0.23	0.86	1.21	1.02	0.86	0.96	1.61
Temperature °C	170						
[Co] g/100ml	0.208						

* Where *k* is the first order rate constant describing olefin consumption.

It is noteworthy that the highest reaction rate in the series of experiments was measured using a 2:1 H_2:CO ratio at 75 bar (Run 47a) . Using a higher total pressure of 90 bar with the same H_2:CO ratio (Run 56c) resulted in a slower reaction. Using a lower pressure of 45 bar, also with a 2:1 H_2:CO ratio (Run 56d) gave a similar reaction rate to the experiment (Run 56c) undertaken at 90 bar. The decrease in reaction rate using 2:1 H_2:CO at 90 bar compared to 75 bar may be speculated as being due to stabilization of the phosphine hydrocarbonyls at higher pressures. This may suggest an optimum reaction pressure.

Figure 5.27 Effect of syngas composition and pressure on the kinetics of Co/EP catalyzed hydroformylation of 1-decene.

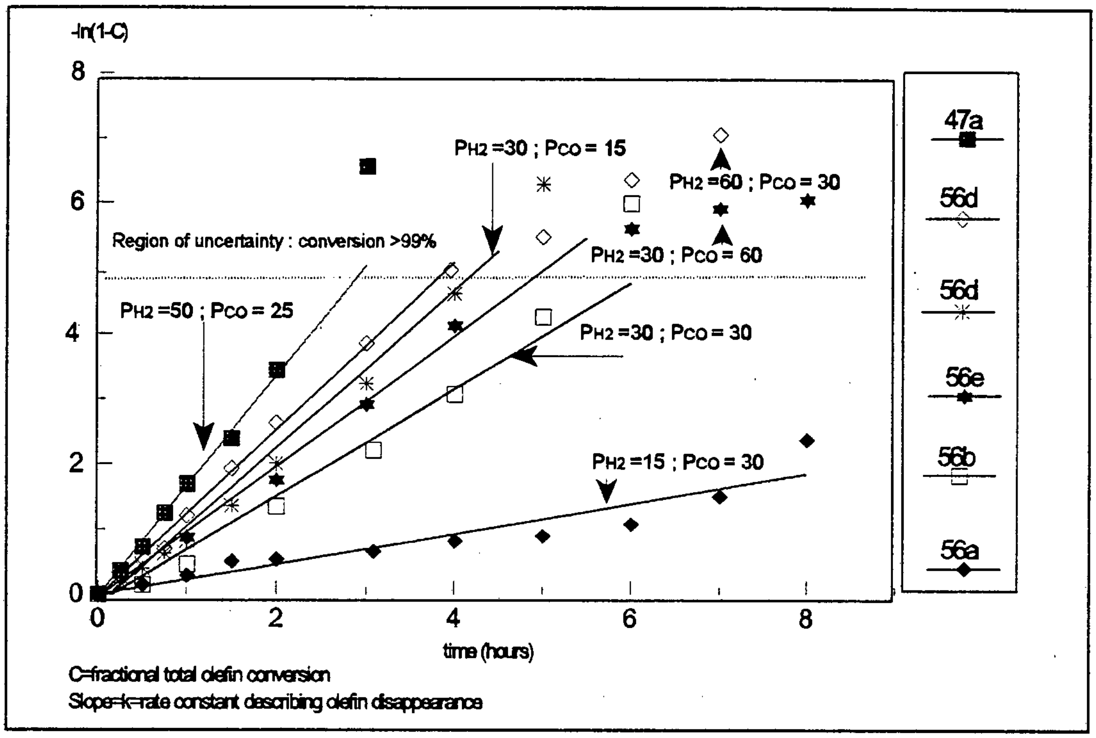

To recap on the effect of syngas, Natta *et al.* [1954] derived the following equation when using unmodified Co catalysts:

$$\frac{-d[\text{olefin}]}{dt} \approx \text{constant}[\text{olefin}][\text{Metal}]\frac{(P_{H_2})}{(P_{CO})} \qquad (5.13)$$

by observing the following:

1) At constant CO pressure, the rate increases greatly with increasing H_2 pressures.
2) At constant H_2 pressure, the rate increases with increasing CO pressure, but only up to 10 atm., and then the rate decreases.

The results in Table 5.12 are in agreement with Natta *et al.*'s statement 1) above. Indeed, the reaction rate appears to be more strongly dependent on the P_{H2} than that of the P_{CO} as demonstrated in Figures 5.28 and 5.29.

Figure 5.28 Plot of rate constant *k* versus P_{H2} , at various P_{CO}; (Runs in Table 5.12).

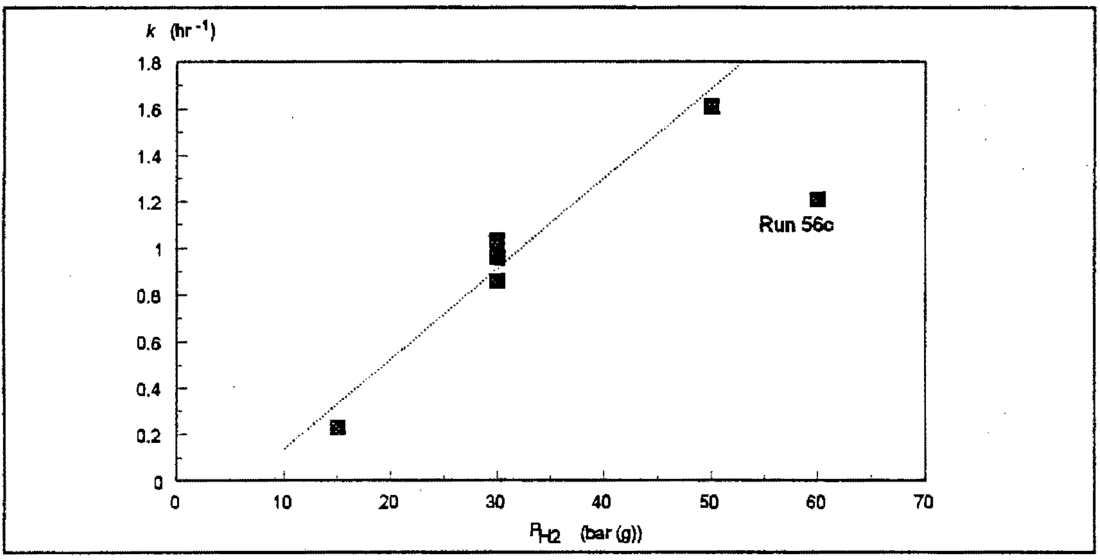

Figure 5.29 Plot of rate constant *k* versus P_{CO}, at various P_{H2}; (Runs in Table 5.12).

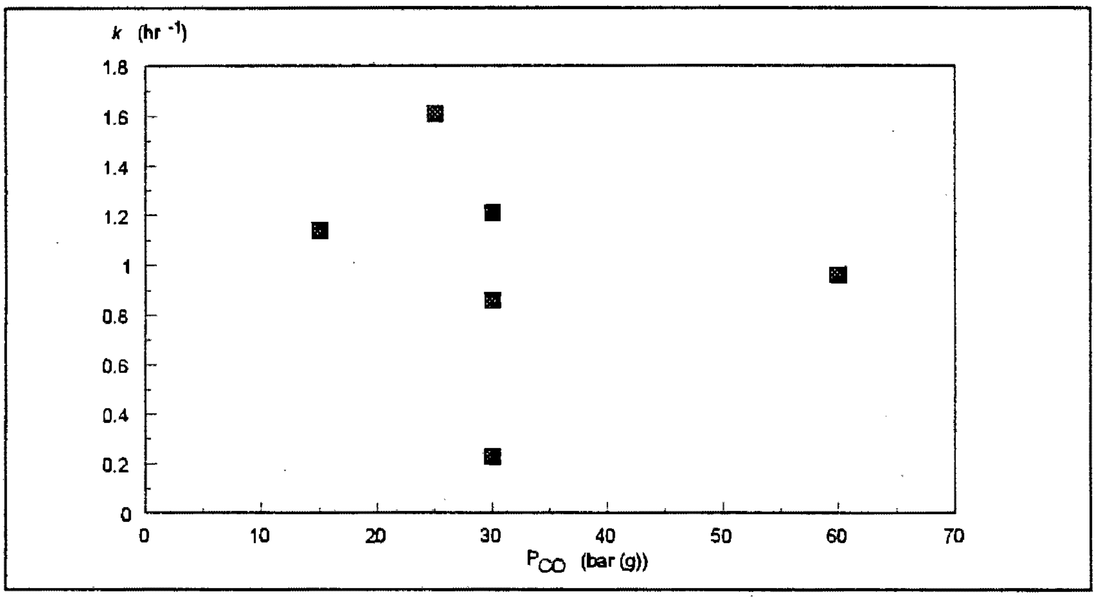

Rate constants determined by the slope of the curves in Figure 5.27 were regressed using a Marquardt [1963] algorithm programmed onto a Fortran fitting routine so as to arrive at an expression (Equation 5.14) which satisfied the rate constants measured for runs 47a, 56a, 56b and 56d and 56e. For reasons that are not clear, Run 56c indicates a deviation from the rest of the data plotted in Figure 5.28, and did not satisfy the equations having the following form:

$$k = k^{\circ}\ e^{-E_a/RT}(1 - 0.2979\ \ln C_{number})[Co](P_{H_2}+P_{CO})(P_{H_2})^x\ (P_{CO})^y \qquad (5.14)$$

Other equations tested in this regard, but which gave larger errors, were of the forms:

$$k = k^{\circ}\ e^{-E_a/RT}(1 - 0.2979\ \ln C_{number})[Co](P_{H_2})^x\ (P_{CO})^y \qquad (5.15)$$

and

$$k = \frac{k^{\circ}\ e^{-E_a/RT}(1 - 0.2979\ \ln C_{number})[Co]}{1 + \dfrac{k'' P_{H_2}}{P_{CO}}} \qquad (5.16)$$

Since equation (5.14) was found to be the most satisfactory (R-squared values ≥90 compared with values of ≤85 for equations (5.15) and (5.16)), and given the results obtained previously on studying the effect of temperature, and cobalt concentration, the following equation was shown to predict the experimental data:

$$\text{rate} = k\ [\text{olefin}] = k''e^{\frac{-E_a}{RT}}\ (1 - 0.2979 \ln C_{number})[Co](P_{H_2}+P_{CO})(P_{H_2})^x(P_{CO})^y[\text{olefin}] \qquad (5.17)$$

Values for x, y and k" were regressed in order to obtain the best fit. R-square values of approximately 90 and 95 were obtained depending on whether the data for run 56e (P_{CO} = 60 bar (g); P_{H2} = 30 bar (g)) was included or excluded (see Figure 5.30).

The respective modelled values are 1.03; -1.09 and 1.49×10^{11} when using the following values and units: E_a =99 000 J mol^{-1}; R = 8.314 J $K^{-1}mol^{-1}$; T = 446.16K; [Co] = 0.2077 gCo/100ml; units of pressure =bar. Given the EP:Co molar ratio is around 2.

The accuracy of the fit (albeit with limited data) is illustrated in Figure 5.30.

Figure 5.30 Modelled and experimental k values: Various H_2:CO ratios, and P_{H2} and P_{CO}. Accuracy test of equation (5.17).

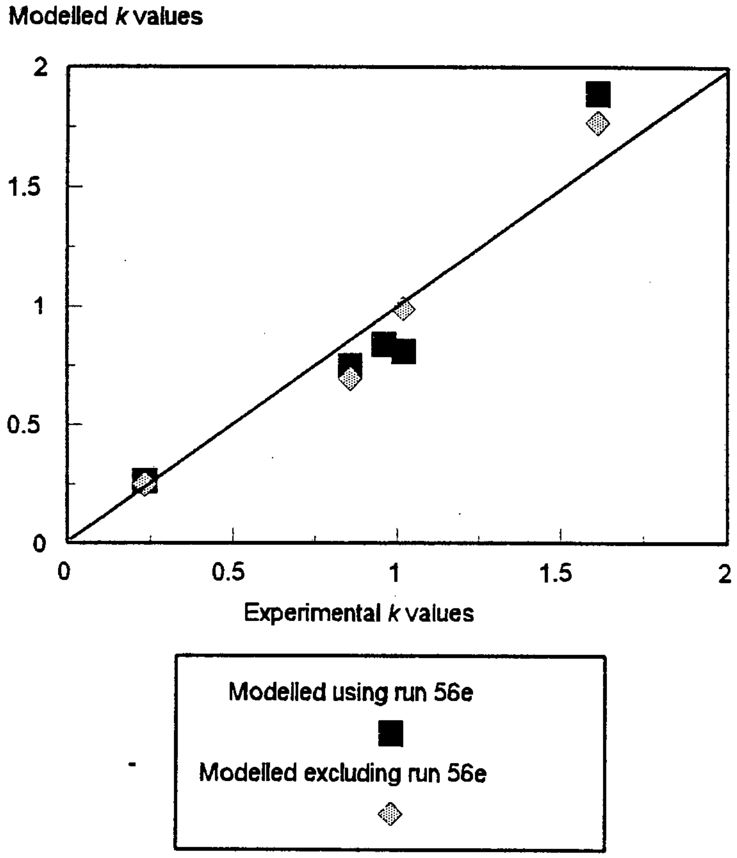

Equation (5.17) can therefore be taken to serve as a general term describing olefin disappearance in the systems under investigation, given that the total syngas pressure is $\leq$ 75 bar (g). The pre-exponential rate constant, k", can be determined experimentally and depends on the EP:Co ratio and alkali (KOH) concentration. The values of x and y can probably be rounded off to +1 and -1 respectively.

Reasons why H_2 enhances the reaction rate whilst CO retards it can be explained in terms of the mechanism described in Figure 1.14 which has been re-represented in Figure 5.31 to include the EP ligand in the catalyst complexes.

Figure 5.31 Multistep hydroformylation pathways using an EP modified Co catalyst.

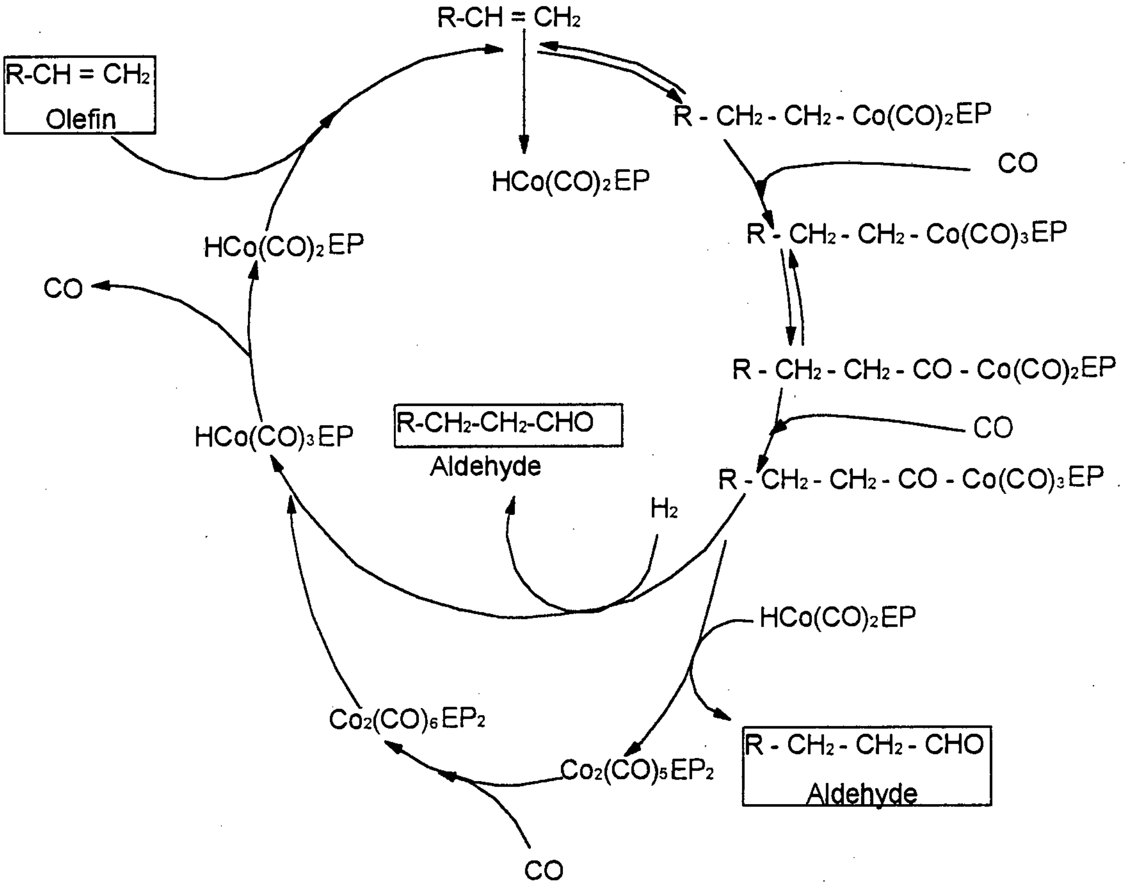

In Figure 5.31, product formation is a result of hydrogenation of a R-CH_2-CO-$Co(CO)_3EP$ intermediate. This may be facilitated either by H_2 or a $HCo(CO)_2EP$ complex. This results in $Co_2(CO)_5(EP)_2$ and $HCo(CO)_3EP$ complexes. Before ending up as the $HCo(CO)_3EP$ complex, the $Co_2(CO)_5(EP)_2$ complex undergoes CO insertion followed by hydrogenation. The $HCo(CO)_3EP$ complex must then "lose" a CO in order to become an "active" $HCo(CO)_2EP$ species.

Overall, hydrogenation therefore facilitates "reactivation" of the catalyst, and CO inhibits this process:

$HCo(CO)_3EP \rightleftharpoons HCo(CO)_2EP + CO$
(inactive) (active)

However, this is only one step in the mechanism. The rest of the cycle includes various steps involving the incorporation of CO. These steps are necessary for the cycle to be completed. Therefore, although CO may slow the reaction rate, there would be no rate at all were it not present. Natta *et al.*'s equation (5.13) does not take this into account and may be taken to imply that as the P_{CO} tends to zero, the rate tends to infinity.

The form of equation (5.17) differs from other reported equations by the fact that it incorporates a total pressure (P_{H2} + P_{CO}) term. In this term, the P_{CO} has a positive effect on the rate. In the P_{CO}^{-1} term, CO has a negative effect. These "opposing" effects may be taken as correcting for the anomaly that if there was no, or little CO present, the hydroformylation rate would tend to infinity.

5.4.6.2 Syngas Effect on Reaction Selectivities

Table 5.13 Selectivity results obtained with various syngas compositions and pressures: 1-Decene feed; Co/EP catalyst.

	Constant P_{CO}; increasing P_{H2} →			Constant P_{H2}; increasing P_{CO} →			
Run	56a	56b	56c	56d	56b	56e	47a
P_{H2} ($bar_{(g)}$)	15	30	60	30	30	30	50
P_{CO} ($bar_{(g)}$)	30	30	30	15	30	60	25
P_{total} ($bar_{(g)}$)	45	60	90	45	60	90	75
H_2:CO ratio	0.5	1	2	2	1	0.5	2
Conversions, Linearities and Selectivities at 2 hours TOS							
% Olefin converted	39.0	73.2	85.3	92.6	73.2	83.6	96.8
% 1-Decene product linearity	87.5	90.1	93.5	92.7	90.1	75.7	90.8
% Overall product linearity	76.1	82.9	86.7	85.2	82.9	59.0	81.3
% Paraffin selectivity	2.7	3.3	8.1	6.5	3.3	4.2	7.2
% Aldehyde selectivity	25.6	25.8	4.5	7.1	25.8	24.1	5.1
% Alcohol selectivity	70.4	70.2	86.8	85.8	70.2	75.8	87.4
% HOF selectivity	1.3	0.7	0.6	0.7	0.7	<0.1	0.4
Conversions, Linearities and Selectivities at 6 hours TOS							
% Olefin converted	64.2	99.8	100	99.8	99.8	99.3	100
% 1-Decene product linearity	81.8	88.8	93.3	92.3	88.8	84.0	90.0
% Overall product linearity	69.0	80.9	86.2	84.4	80.9	71.0	80.4
% Paraffin selectivity	2.7	2.5	7.7	6.1	2.5	2.3	7.0
% Aldehyde selectivity	11.8	1.5	0.5	0.5	1.5	2.3	0.2
% Alcohol selectivity	82.0	93.0	90.3	91.1	93.0	93.8	92.2
% HOF selectivity	3.6	3.0	1.4	2.2	3.0	1.6	0.6

The effects of pressure and syngas composition on the product selectivities and linearities with TOS, are compared in Table 5.13. The following general observations are:

The hydrogenation activities, as evidenced by the alcohol, aldehyde and paraffin selectivities are higher when H_2 rich syngas with a H_2:CO ratio = 2 is employed. Differences in the general selectivity trends during runs undertaken with similar syngas compositions can often be ascribed to differences in the reaction rates or olefin conversion. It is noteworthy that reactions undertaken with the same H_2:CO ratio of 2 (different total pressures) gave rise to similar selectivities. A similar trend was obtained in experiments using a H_2:CO ratio of 0.5. The higher aldehyde selectivity of 11.8% at 6 hours TOS for the H_2:CO = 0.5 run (56a) undertaken at 45 bar should be seen in the context of the low conversion.

There is too much scatter in the Heavy Oxo Fraction (HOF) selectivity data to draw firm conclusions regarding the effect of pressure and syngas composition on heavy oxygenate formation.

Using a 1:1 H_2:CO ratio at a total pressure of 60 bar (g) in run 56b appears to give a favourable result with respect to hydroformylation selectivity. For the final selectivities, a low paraffin value is coupled to a high alcohol value, and the product linearity is not compromised to a great extent. The data indicate that hydrogenation of olefins to paraffins may not always be taken as a measure of expected hydrogenation of aldehydes to alcohols. This appears to be a consistent observation with the EP ligand (see Section 4.4.9.3).

Consideration and comparison of the overall and 1-decene product linearities gives an indication not only as to the effect of syngas pressure and composition on linearity, but also on the reactivity of internal olefins. The somewhat lower linearities obtained with Run 47a compared with the other runs which used a 2:1 H_2:CO ratio may probably be ascribed to the higher reaction rate. However, the overall impression is that the linearity increases as the H_2:CO ratio increases. Low final linearities were obtained for Runs 56a and 56e with the H_2:CO = 0.5. This may in part be ascribed to reactivity of internal olefins under these conditions. In addition, the linearity profiles of Runs 56a and 56e are seen to change significantly with TOS. A possible explanation for this observation could in part lie in the isomerization activity of these systems. Namely, that "re-isomerization" of internal olefins back to α-olefins prior to their being hydroformylated may have been inhibited in Run 56e (90 bar (g) total pressure). However, reactivity of the feed alone cannot explain the lower linearity given the low 1-decene product linearities also observed for these runs. Studies on the effect of syngas composition on the structure of the working catalyst complex could possibly shed more light on this subject.

In summary, the H_2:CO ratio appears to be a more important parameter in determining <u>final</u> selectivities than the H_2 and/or CO partial pressures.

5.4.6.3 Effect of CO_2

Due to the presence of CO_2 in commercial syngas, albeit at low concentration (approximately 1%), its effect was reviewed previously in Section 4.4.5. Although no clear effect could be ascertained, this was probably due to the low levels that were present. It was therefore decided to test the effect of a significant quantity of CO_2 (13% by volume).

Table 5.14 Results obtained with CO_2: 1-Decene feed; Co/EP catalyst.

Run	47a		47b	
Partial Pressures (bar (g))				
P_{H2}	50		50	
P_{CO}	25		25	
P_{CO2}	-		11	
P_{total}	75		86	
k (hr^{-1})	1.61		1.45	
k' (hr^{-1})	7.74		6.96	
Conversions, Linearities and Selectivities : TOS (Time on Stream)	2 hours	6.08 hours	2 hours	6 hours
% Olefin converted	96.8	100	94.0	100
% 1-Decene product linearity	90.8	90.0	93.2	92.6
% Overall product linearity	81.3	80.4	84.1	84.8
% Paraffin selectivity	7.2	7.0	7.2	6.0
% Aldehyde selectivity	5.1	0.2	0.3	0.3
% Alcohol selectivity	87.4	92.2	85.6	93.4
% HOF selectivity	0.4	0.6	1.6	0.3

On comparing the results of Runs 47a-b, it appears that the P_{CO2} of 11 bar (g) had little effect on the hydroformylation performance of the Co/EP catalyst in a batch reactor. It is difficult to ascribe the small differences observed to either the P_{CO2} or the higher total pressure of 86 bar used in Run 47b. From Figure 5.32 it is evident that the rates of olefin consumption were slightly altered by CO_2 addition, and were somewhat lower.

Figure 5.32 Effect of CO_2 on reaction rate: Comparison of Runs 47a-b.

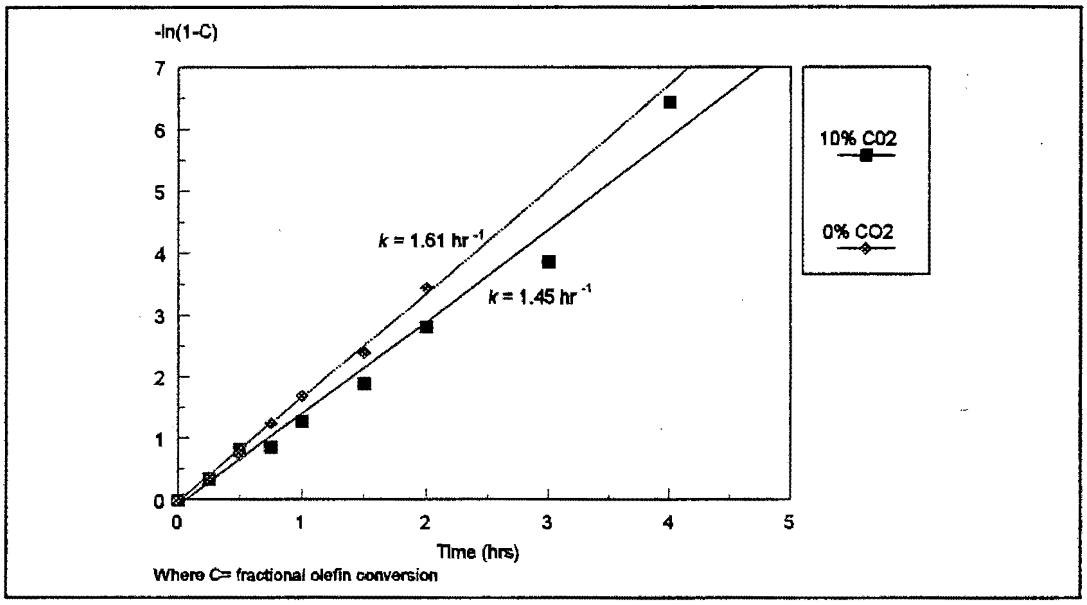

The levels of CO_2 did not alter the reaction selectivities markedly. Also, the HOF did not increase significantly in the presence of CO_2 thereby indicating that CO_2 incorporation did not appear to occur - additional acids were not observed in the product. The results in this study therefore could not substantiate those of Massie and Vasely [1974] (reviewed in Section 4.4.5). These workers advocated the use of large quantities of CO_2 (typically P_{CO2} = 20 atm.) to enhance the reaction selectivity to alcohols, at the expense of olefin conversion for alkyl phosphine modified Co catalyst systems.

5.5 CONCLUSIONS

The results obtained with KOH demonstrate that this (and possibly other) alkali plays an important role in the Co/EP system. Using Co:KOH molar ratios of 1:0.75 gave rise to slower reaction rates compared to systems wherein KOH was omitted. The presence of KOH has a similar effect to increasing the EP:Co ratio, and increasing the ligand basicity. The use of KOH could therefore be advantageous in a continuously operated process wherein catalyst stability and maintaining a fixed EP:Co ratio are important for maintaining long catalyst lifetimes.

Maintaining the EP:Co molar ratio >1, but preferentially around values = 2 is important to ensure catalyst stability, and high selectivities to linear alcohols. If product linearity is not considered to be an important parameter, then the reaction rate can be improved considerably by using lower EP:Co molar ratios. This could however lead to Co deposition or catalyst losses in a reactor.

Similar reaction rates and selectivities were obtained with pure 1-decene and "broad" SLO C_{10} material. This again demonstrates the suitability of HTF-T SLO material as a hydroformylation feedstock.

The results of testing 1-decene, 1-octadecene, a C_{10} and various C_{11-12} SLO fractions were used to quantify the effect of olefin chainlength on reaction kinetics. The speed of collective olefin disappearance being: $C_{10} > C_{11} > C_{12} >> C_{18}$. It was demonstrated that for the SLO fractions tested, the α-olefin distribution (branched : linear and C_{11}:C_{12} ratios) did not have a marked effect on the first order kinetics of overall olefin consumption.

A linear relationship existed between catalyst concentration (measured in terms of the cobalt concentration =[Co]) and reaction rate. This was demonstrated in the range of [Co] =1000ppm to 2600ppm. The effect of [Co] was combined with the effect of olefin chainlength to derive an expression describing olefin reactivity in pure linear and SLO feeds. This expression was expanded to include the effect of reaction temperature as well as syngas composition and pressure.

As regards temperature, a deviation in the reaction kinetics possibly as a result of the onset of Co/EP catalyst changes occurred at temperatures between 175 and 185°C. This was ascribed to mass transfer limitations caused by higher rates of reaction and the inherent catalyst instability at the higher temperatures. The results were compared to those of others. An activation energy of approximately 99 $kJmol^{-1}$ was measured for C_{11} and C_{12} olefins with the Co/EP catalyst. This is comparable to activation energies reported by other workers, but with other catalysts (unmodified Co and TPP modified Rh). The results in this study were superimposed onto those of other workers [Voorhies *et al.*, 1957]. The resultant Arrhenius plots indicates that an approximately linear trend exists between the onset of mass transfer limitation and reaction temperature regardless of the feed and cobalt catalyst.

It was proposed that additional work (with different catalysts and reaction conditions) should be undertaken to verify and expand on this theory linking reaction rates to catalyst deactivation and temperature.

There was little evidence to indicate that changing the temperature in the 155°C to 195°C range affected the reaction selectivities at high conversions.

On changing the syngas composition and pressure, it was demonstrated that a 2:1 H_2:CO ratio employed at a total P_{H2+CO} of around 75 bar (g) gave the best combination in terms of reaction selectivities, conversion and rates. Runs undertaken at a total pressures of 45, 60 and 90 bar (g) wherein the H_2:CO ratio was varied between 0.5 and 2 were used as "yardstick" in this regard.

The presence of a significant quantity of CO_2 (11 bar (g)) in the syngas, did not appear to markedly affect the reaction rate and selectivities. Given the relatively low quantities of CO_2 in commercial F-T syngas, and the findings on the effect of CO_2, it is tentatively suggested that it is not necessary to remove it from syngas that is fed to a continuous process. This recommendation is based on the use of a Co catalyst with the EP ligand, and similar reaction conditions to those used in this study. In addition, it is further recommended that KOH be used in a continuous system - KOH is basic and CO_2 is acidic. The report by Kummer *et al.* [1972] that alkali can stabilize alkylphosphine Co catalysts at low CO_2 levels, and the effect of KOH shown in this study are cited as reasons for this.

The results of experiments undertaken in this chapter, indicated a suitable combination of reaction conditions for ensuring a combination of catalyst stability; high reaction rate and high selectivities to alcohol. The following set of "standard" conditions are therefore proposed:

Co:KOH molar ratio: approximately 0.75:1 (not necessarily optimum).
EP:Co molar ratio: approximately 2:1 (but definitely >1).
Cobalt concentration: 1000 to 2600ppm (mg/litre) range is acceptable (in batch).
Temperature : 170°C.
Syngas composition : H_2:CO ratio of approximately 2:1.
Syngas pressure : approximately 75 bar(g).
Stirrer speed: $\geq$500rpm (to ensure results in the correct kinetic regime).

Various of the above reaction conditions are in agreement with reported ranges of conditions employed (in patents and Falbe's review/s) with phosphine modified Co hydroformylation catalysts.

Having determined suitable reaction conditions, compatibility of the SLO feeds with the Co/phosphine catalysts and extracted kinetic data, it was decided to investigate the following:
Extrapolation of batch reactor conditions and results to a continuously operated reactor unit, and development of a model to achieve this.

CHAPTER 6

MODEL DEVELOPEMENT FOR SCALE-UP

6 MODEL DEVELOPMENT FOR SCALE-UP OF HYDROFORMYLATION SYSTEMS

6.1 THE REACTION SCHEME

The kinetics of olefin consumption evaluated in the previous chapter, is in itself insufficient for determining or predicting the performance of a continuous reactor system as described in Chapter 2 (Section 2.1.3 and Figure 2.7). This is due to other reactions occurring in sequence or in parallel to hydroformylation. These "additional" reactions also have to be modelled, based on a suitable reaction scheme.

Profiles of the reactor contents, as for example in Figure 4.2, may be used to describe the general pathway of the hydroformylation and associated reactions in SLO and pure feeds as follows:
It appears that during the initial stages of the reaction, most α-olefins in the feed are isomerized to internal olefins prior to being hydroformylated and/or hydrogenated. Analysis of the hydroformylation products, *viz.*, aldehydes and alcohols, indicates very few of these are derived from the internal olefins in SLO. This implies that "re-isomerization" back to the α-olefin occurs prior to hydroformylation. This re-isomerization also occurs in 1-decene feeds, but to a lesser extent (see Section 3.4.3.2). Aldehydes formed by hydroformylation of the α-olefins are subsequently hydrogenated to alcohols. The major side reactions which result in lower hydroformylation product yields are olefin hydrogenation and heavy ends formation. Ignoring the effects of carboxylic acids in the feed, most of the heavy oxygenates have been identified as formic acid esters which are derived from reaction of CO with aldehyde (see Section 4.4.7). Using these observations, the general reaction pathway shown in Figure 6.1 is proposed.

Figure 6.1 General pathway of reactions as deduced from the experimental data.

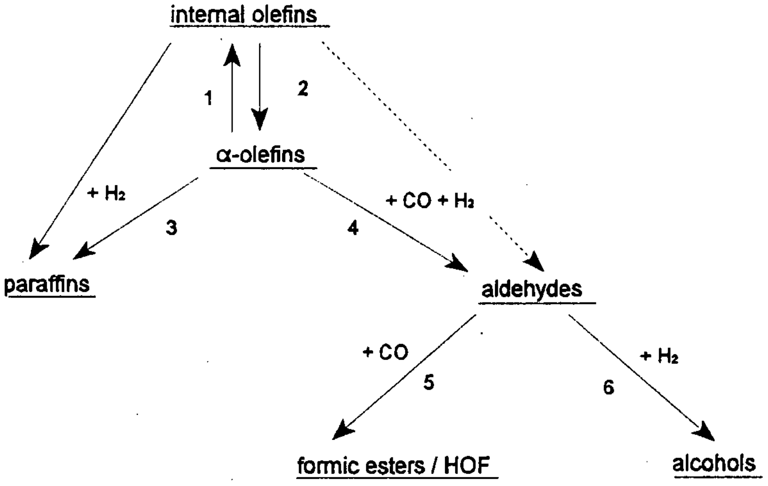

The large amounts of internal olefins formed from α-olefins initially under reaction conditions, implies that coordination and re-coordination of α and internal olefins to the catalyst complexes readily occurs. This is presumably because of internal olefins being thermodynamically favoured over α-olefins. Since these reactions take place at a higher rate than hydroformylation, this implies that a higher activation energy for hydroformylation needs to be overcome compared with isomerization. This isomerization does not appear to influence the reaction rate of olefin consumption (and hydroformylation) which remains first order with respect to the total olefin concentration.

The aldehyde profiles of all the constant pressure runs undertaken in Chapters 4 and 5 appear to indicate that the aldehydes disengage from the catalyst, and subsequently re-engage in order to be hydrogenated to corresponding alcohols. Furthermore, aldehydes are postulated as giving rise to formic acid esters, *ie.* a larger HOF (see discussion in Section 4.4.7). It has been noted that base catalyzed aldol condensation products were difficult to detect in the micro-reactor products.

In order to check the foregoing concepts, Runs 46a-b were undertaken (see Table 5.1). A mixture of 70ml 1-decene and 30ml hexadecane internal standard, 0.876g $Co(OOCCH_3)_2.4H_2O$, 0.344g EP ligand, and 0.159g KOH, was pressurized to 75 bar with 2:1 H_2:CO syngas at 170°C in Run 46a. After 8 hours, approximately all the 1-decene had been consumed. The reaction mixture was cooled to ambient temperature, and 100ml of 1-undecanal was added to the remaining reactor contents. The reaction mixture was subsequently heated to 170°C under N_2, and re-pressured with 2:1 H_2:CO to 75 bar at time zero. The system was then stirred for another 8 hours (Run 46b).

Heavy products different to those measured in routine micro-reactor runs (presumably aldol condensation products) formed during the heating up period for Run 46b at low pressure under N_2, and prior to the introduction of syngas. This is illustrated by way of Figure 6.2 a-b. Subsequent syngas introduction did not result in additional heavy aldol product formation, but did result in hydrogenation of the original condensation products (see Figure 6.2 b-c). However, the light ester component (formates) did increase. In addition to the small increase in esters, the linear aldehyde was converted to the corresponding linear alcohol under hydroformylation conditions. These results are demonstrated by way of Figures 6.2 and 6.3.

Figure 6.2 GC traces of a) Run 46b feed before heating (Run 46a product); b) After heating (low pressure of N_2); c) After 8 hours TOS (high pressure of syngas).

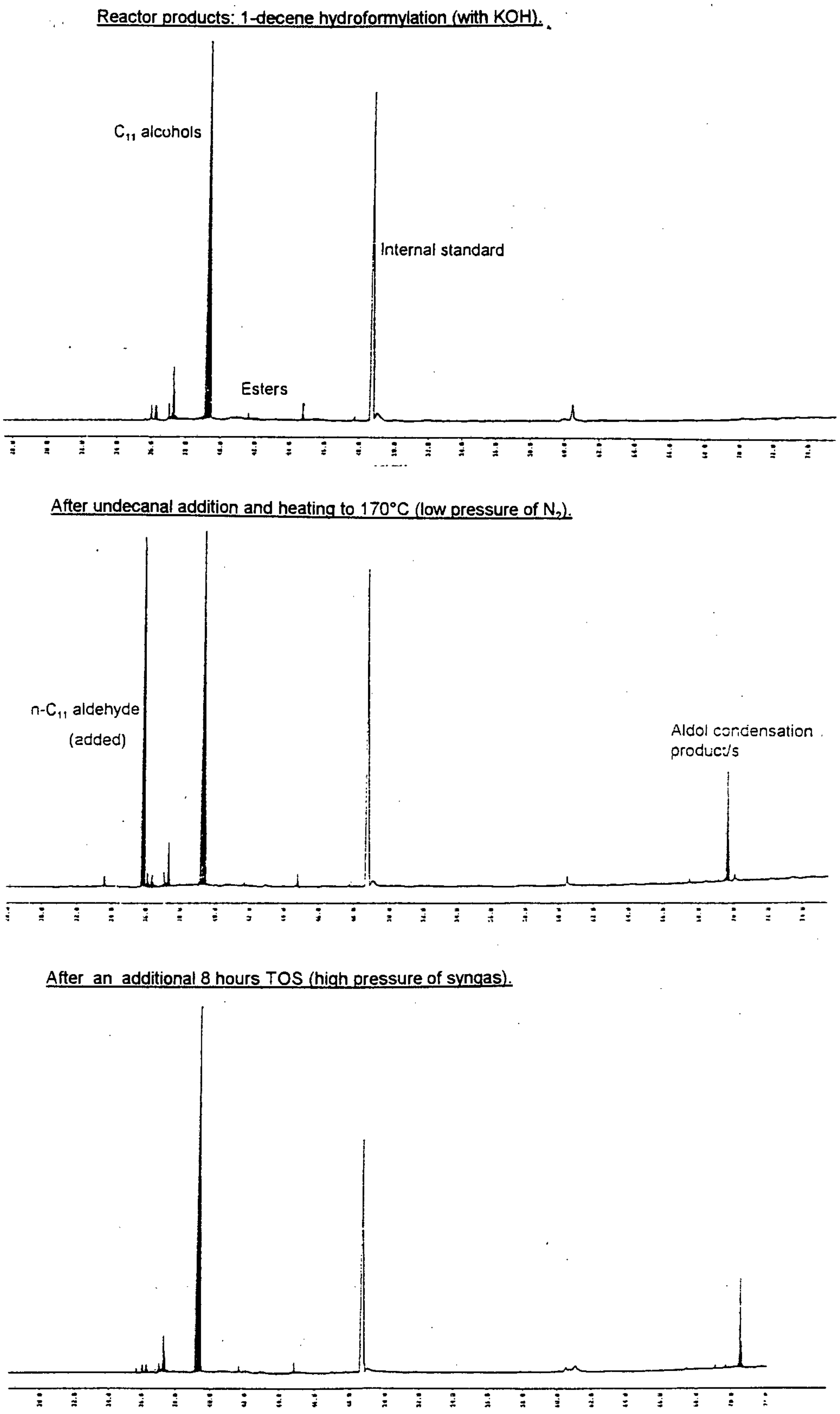

Reactor products: 1-decene hydroformylation (with KOH).

After undecanal addition and heating to 170°C (low pressure of N_2).

After an additional 8 hours TOS (high pressure of syngas).

Figure 6.3 Effect of feeding aldehyde to a Co/EP system under hydroformylation conditions.

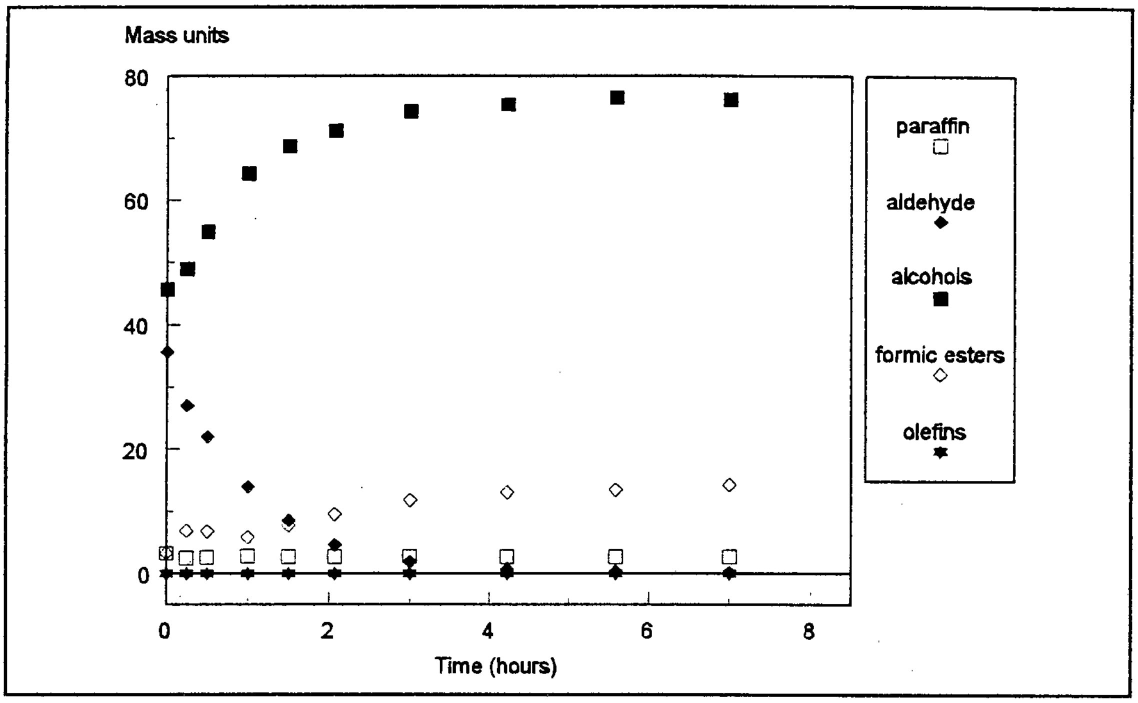

Figure 6.4 First order rate plot describes aldehyde conversion to alcohol and esters.

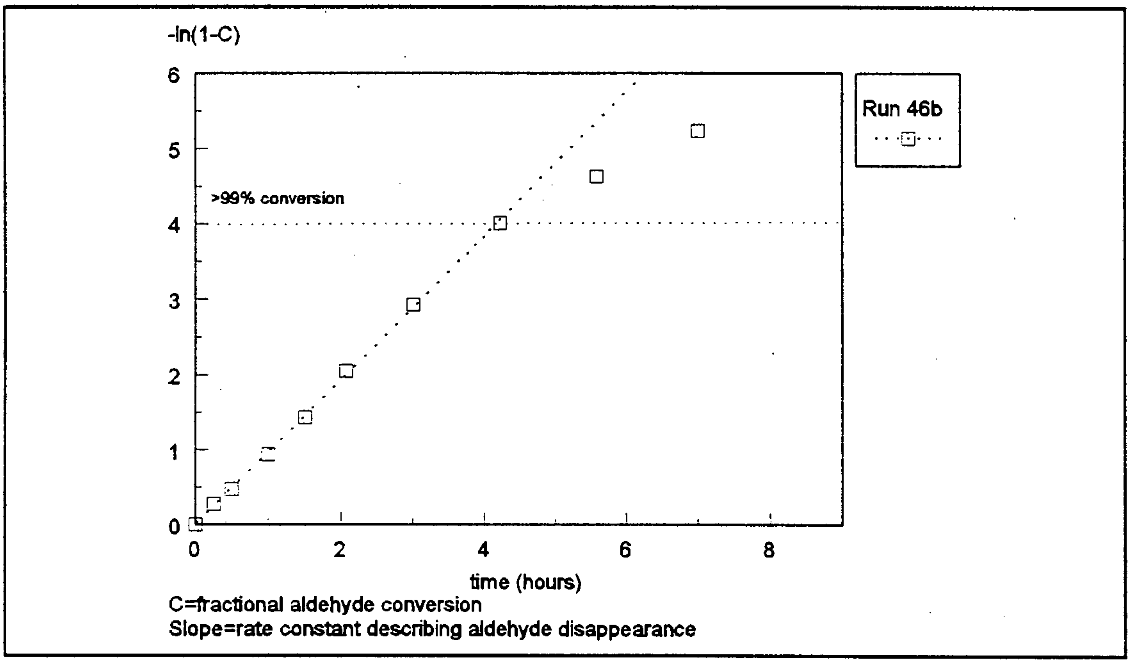

The above findings indicate that KOH probably does catalyze the formation of aldol products, but this reaction is not apparent under hydroformylation conditions. This has important consequences for a continuous process, and indicates that aldehyde recycle in the presence of KOH (and absence of syngas) may be deleterious to such a system if heating in the recycle stream occurs. Aldol condensation products were indeed identified by GC-MS in the recycle stream (heated) of the continuous reactor system.

As expected, aldehydes were readily converted to alcohols under hydroformylation conditions. This reaction is first order with respect to the aldehyde (see Figure 6.4), and confirms subsequent kinetic modelling results, discussed in Section 6.3.

The foregoing experiments prove that after aldehyde formation (*ie.* hydroformylation of the olefin), the aldehyde probably disengages from the active Co site and subsequently has to re-coordinate in order to be hydrogenated to the alcohol.

The above work confirms details of the general pathway of reactions proposed in Figure 6.1 and paves the way for kinetic modelling of the experimental data based on a simplified reaction sequence wherein the internal and α-olefins can be grouped. This is demonstrated in Figure 6.5.

Figure 6.5 Simplified reaction sequence of liquid components (excluding CO and H_2) as deduced from the experimental data.

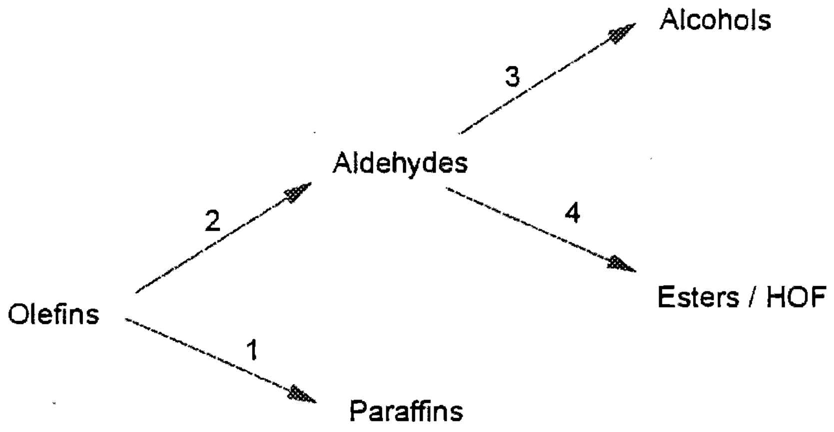

6.2 MODELLING OF THE REACTION NETWORK

6.2.1 Background and Approach

Many references for hydroformylation kinetics appear in the literature. These are listed and in some cases reviewed by Cornils in Falbe's Review [1980] - see additional references at the end of the reference list. However, only two subsequent articles by Helfferich [1989] and Chern and Helfferich [1990], were sourced that deal in some detail with modelling of Co/P systems. (The work by Tucci [1970] is limited to kinetic comparisons of the first order rate constant describing olefin disappearance). Chern and Helfferich presented a theoretical paper based on assumptions of reaction orders, in which the rate equations are derived mathematically, using a Co/P catalyzed hydroformylation system as an example. In the article, emphasis is placed on the reduction of the mathematical complexity of proposed system/s as described by Figure 6.6, so as to "reduce the set of rate equations for all the participants to just the end members (products) and non-trace intermediates". The paper does not include discussions on uniqueness, techniques for parameter fitting, reversibility, thermodynamic constraints [Sorenson and Stewart, 1980], or experimental data validating the authors' equations and model.

Figure 6.6 Reaction network for olefin hydroformylation including reactions to paraffin, alcohol and condensation product as proposed by Chern and Helfferich [1990].

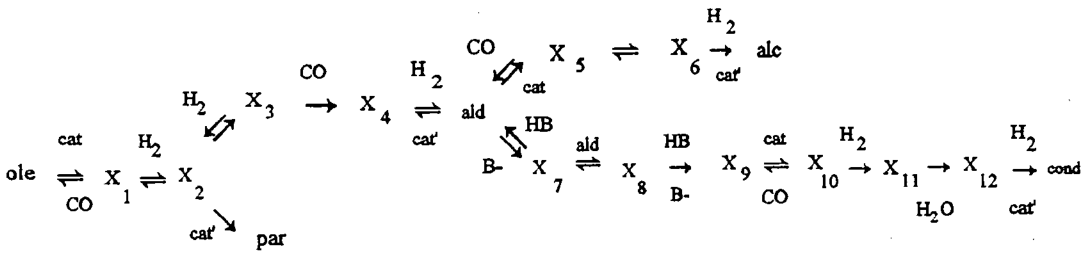

alc = alcohol
ald = aldehyde
cond = condensation product (alcohol)
cat = $HCo(CO)_3\ PR_3$
cat' = $HCo(CO)_2\ PR_3$ CO deficient hydroformylation catalyst
ole = olefin
par = paraffin
B- = base catalyst
HB = conjugate acid
X = intermediates

In essence, the authors [Chern and Helfferich, 1990] present a mathematical model in which the rate equations can be simplified to the following expressions:

$$- r_{ole} = r_{ald} + r_{par} \qquad (6.1)$$

$$-r_{olefin} = \frac{k\,[\mathrm{cat}][\mathrm{ole}]}{1+k'[\mathrm{H_2}]/[\mathrm{CO}]} \tag{6.2}$$

$$r_{par} = \frac{\dfrac{k_{ole}k_{par}[\mathrm{cat}][\mathrm{ole}]}{1+k_a[\mathrm{CO}]/[\mathrm{H_2}]}}{\dfrac{k_{21}}{1+[\mathrm{H_2}]/k_a[\mathrm{CO}]}+\dfrac{k_{23}}{1+k_b[\mathrm{H_2}]/[\mathrm{CO}]}+k_{par}} \tag{6.3}$$

$$r_{alc} = \frac{k_A[\mathrm{cat}][\mathrm{ald}]}{1+k_B[\mathrm{CO}]+k_C[\mathrm{CO}]/[\mathrm{H_2}]} \tag{6.4}$$

$$r_{cond} = \frac{2\,k_f[\mathrm{B^-}][\mathrm{ald.}]^2}{1+k_g[\mathrm{ald.}]+k_h[\mathrm{HB}]} \tag{6.5}$$

$$r_{ald} = \frac{\dfrac{k_{ole,k_{23}}[\mathrm{cat}][\mathrm{ole}]}{1+k_ak_b+k_a[\mathrm{CO}]/[\mathrm{H_2}]+k_b[\mathrm{H_2}]/[\mathrm{CO}]}}{\dfrac{k_{21}}{1+[\mathrm{H_2}]/k_a[\mathrm{CO}]}+\dfrac{k_{23}}{1+k_b[\mathrm{H_2}]/[\mathrm{CO}]}+k_{par}} - \frac{k_A[\mathrm{cat}][\mathrm{ald}]}{1+k_B[\mathrm{CO}]+k_C[\mathrm{CO}]/[\mathrm{H_2}]} - \frac{2k_f[\mathrm{B^-}][\mathrm{ald.}]^2}{1+k_g[\mathrm{ald.}]+k_h[\mathrm{HB}]} \tag{6.6}$$

Equations (6.1) to (6.6) above were derived from Chern and Helfferich's article.

The numerous *k*-values for the above equations were derived mathematically by the authors. The theoretical basis for the derivation of the values is not relevant for the purposes of this thesis. The general form of the equations are of more concern. With the exception of the equation describing the rate of condensation/heavies formation, (for which an alternative mechanism of formation has been postulated - see section 4.4.7) the above equations were simplified by taking the temperature, CO and H_2 and catalyst concentrations as being constant and assuming no mass transfer limitations, to give the following first order expressions:

$$-r_{ole} = r_{ald} + r_{par} \tag{6.7}$$

$$-r_{olefin} = k' \,[cat][ole] \tag{6.8}$$

$$r_{parr} = k_1' \,[cat][ole] \tag{6.9}$$

$$r_{alc} = k_3' \,[cat][ald] \tag{6.10}$$

$$r_{ald} = k_2' \,[cat][ole] - k_3' \,[cat][ald] - \frac{2k_f[B^-][ald.]^2}{1+k_g[ald.]+k_h[HB]} \tag{6.11}$$

Where for consistency with rate data presented in Chapters 4 and 5 (see Tables 4.3 and 5.3);.

$$k_x = k_x' \,[cat] \tag{6.12}$$

Furthermore, the [cat] or catalyst concentration term, can be replaced by the cobalt concentration [Co], which is easier to measure.

Equation (6.11) indicates that the rate of aldehyde appearance is a function of the rate that it forms minus the rate at which it is hydrogenated to alcohol and minus the rate at which it is removed to form heavies. The subscripts for k values in equations (6.7) to (6.11) denote the various reaction steps indicated in Figure 6.5 such that;

k_1 is the rate constant for paraffin formation from olefins.
k_2 is the rate constant for aldehyde formation from olefins.
k_3 is the rate constant for alcohol formation from aldehydes.
k_4 is the rate constant for formic ester /HOF formation from aldehydes.

Analyses of heavy components in the products indicated the presence of formic acid esters. These form as a result of the reaction of syngas with aldehydes, and therefore as previously discussed (see Section 4.4.7), a different mechanism of heavies formation to that proposed by Chern and Helfferich [1990] appears to occur. The experimental results confirmed heavy oxygenate formation in the presence and absence of base B^- (see Section 4.4.6). This contradicts Chern and Helfferich's proposed mechanism for heavies formation as a result of base catalyzed condensation of aldehydes in these types of systems.

For modelling purposes, the reaction rate terms in equations (6.14) - (6.18) which follow, are similar to equations (6.1) - (6.11) with the exception of the r_{heavy} term in equation (6.18) which replaces the r_{cond} term in equation (6.5). The MW_{heavy} term in equation (6.18) is taken to be the molecular weight of the relevant formic acid ester.

6.2.2 Equations For Proposed Kinetic Model

Based on the above simplification of the Chern and Helfferich's [1990] theoretical proposal, the following equations may be used to describe appearance or disappearance of classes of compounds in the batch reactor and by so doing obtain a kinetic model.

In order to utilize the discussed equations, the reaction rates still need to be defined. The governing equation for a species *j* (where *j* can represent any of the liquid components) can be written as follows:

$$\frac{d(M_j/f)}{dt} = r_j/f \tag{6.13}$$

where M_j refers to the mass fraction of component *j* in the reactor, r_j the formation rate of component *j*, *t* represents time and *f*, the dilution factor (see Section 2.3.1.2).

More specifically, based on the suggested kinetic model using equations (6.7) to (6.12) the reaction rates can be expressed as follows[1]:

$$-r_{\text{olefin}} = r_{\text{ald}} + r_{\text{par}}$$

hence,

$$r_{\text{olefin}} = -(k_1 + k_2)M_{\text{olefin}} \tag{6.14}$$

$$r_{\text{aldehyde}} = k_2\ [\text{ole}] - k_3\ [\text{ald}] - k_4\ [\text{ald}]$$

hence[1],

$$r_{\text{aldehyde}} = k_2\left(\frac{MW_{\text{aldehyde}}}{MW_{\text{olefin}}}\right)M_{\text{olefin}} - (k_3 + k_4)M_{\text{aldehyde}} \tag{6.15}$$

---

[1] *MW* refers to the molecular weight of the components in the batch reactor. This is built into the rate equations to reflect the changes in the mass of the measured compenents as a result of the reactions. *ie*., the mass of <u>all</u> the reactants (including H_2 and CO, the concentrations of which are constant) are thereby taken in account.

$$r_{\text{paraffin}} = k_1 \text{ [ole]}$$

hence,

$$r_{\text{paraffin}} = k_1 \left(\frac{MW_{\text{paraffin}}}{MW_{\text{olefin}}} \right) M_{\text{olefin}} \tag{6.16}$$

$$r_{\text{alcohol}} = k_3 \text{ [ald]}$$

hence,

$$r_{\text{alcohol}} = k_3 \left(\frac{MW_{\text{alcohol}}}{MW_{\text{aldehyde}}} \right) M_{\text{aldehyde}} \tag{6.17}$$

$$r_{\text{heavy}} = k_1 \text{ [ald]}$$

hence,

$$r_{\text{heavy}} = k_4 \left(\frac{MW_{\text{heavy}}}{MW_{\text{aldehyde}}} \right) M_{\text{aldehyde}} \tag{6.18}$$

For a given set of kinetic constants (i.e. k_1, k_2, k_3 and k_4) the above equations can be solved to give the mass fractions of the respective species as a function of time. This is done numerically by using the Gear method [Hindmarch, 1989] in IMSL [1989] Math/Library Fortran Subroutine, IVPAG.

6.2.3 Fitting of Kinetic Rate Constants

The aim is to select the kinetic rate constants (*ie.* k_1, k_2, k_3 and k_4) in such a way that the numeric results (which are obtained by methods as discussed above) will approach the experimental results. In other words, if the mass fraction of component *j* observed experimentally at time *t* is represented by M_j and the mass fraction predicted numerically at the same time is represented by $\underline{M}_j$, it is necessary that $\underline{M}_j$ has to approach M_j. In order to ensure this, one of the following error functions was minimized:

$$e_1 = \sum_{i=1}^{m}\sum_{j=1}^{n}(M_j(t_i) - \underline{M}_j(t_i))^2 \qquad (6.19)$$

and

$$e_2 = \sum_{i=1}^{m}\sum_{j=1}^{n}(\ln M_j(t_i) - \ln \underline{M}_j(t_i))^2 \qquad (6.20)$$

where *m* refers to the number of experimental points and *n* to the number of liquid species. The first error function is sensitive to large differences while the second error function amplifies differences which occur at low concentration levels. Consequently, if the minimization of the two error functions predict similar kinetic constants one would expect the model to be valid over a wide range of concentration levels. This serves as a check for the validity of the model. A mathematical advantage of the second error function is that the log of the conversion varies linearly with time for a first order reaction. This simplifies the optimization to the fitting of a straight line. In order to minimize the first error function a quasi-Newton method [Deuflhard, 1974] with a finite-difference gradient as employed by the IMSL [1989] routine UMINF, was used.

6.3 MODELLING RESULTS

All the experiments undertaken in Chapters 4 and 5 were modelled using equation (6.19) as the goal function, as this places less emphasis on the data collected at high conversions (see the previous description of equations (6.19) and (6.20)). The results are listed in Appendices 8 and 9. To demonstrate the effectiveness of the modelling approach, various results are also listed in Table 6.1.

In Table 6.1, the k values are the first order rate constants of olefin consumption experimentally determined from the slopes of -ln(1-C) plots versus time from equation (6.21).

$$-\ln(1-C) - kt \qquad (6.21)$$

Values for $k_1 \ldots k_4$ were calculated using the modelling approach discussed. k'_x values are the rate constant values after correction for the cobalt concentration using equation (6.12) above.

The results listed in Table 6.1 are illustrated graphically (for various feeds and catalysts) in Figures 6.7 to 6.20. These are plots of the modified mass percentage (*ie.* $100M_t\,/\,f_t$ % where M_t is the mass fraction of a species measured at time = t) of components in the reactor (expressed as mass units) versus time (see Section 2.3.1.2). The lines in the plots are generated from the model, and the experimental data are represented by points.

Table 6.1 Table of modelling results: Various runs with TOP and EP modified Co catalysts.

Rate const. (hr^{-1})	k	(k_1+k_2)	k_1	k_2	k_3	k_4	k'	$(k'_1+k'_2)$	k'_1	k'_2	k'_3	k'_4
	Measured and calculated values at various catalyst concentrations						Correcting for catalyst concentration using equation (6.12)[2]					
Run	Meas. value	Calculated values					Meas. value	Calculated values				
TOP ligand : Various runs (shown in Figures 6.7 - 6.11)												
32	0.37	0.43	0.09	0.34	2.29	0.21	1.14	1.32	0.27	1.04	7.05	0.65
33	0.23	0.25	0.03	0.22	1.27	0.03	0.90	1.01	0.13	0.88	5.11	0.11
31	0.51	0.53	0.07	0.46	1.72	0.08	1.98	2.03	0.26	1.77	5.87	0.56
29b	0.26	0.26	0.03	0.23	1.78	0.01	1.15	1.18	0.15	1.03	8.00	0.06
EP ligand : Various runs (shown in Figures 6.12 - 6.20)												
46a	0.81	0.77	0.05	0.73	2.31	0.03	3.93	3.72	0.22	3.50	11.16	0.16
46b	-	-	-	-	0.77	0.05	-	-	-	-	11.14	0.72
44	0.98	1.02	0.02	1	3.16	0.14	3.79	3.93	0.09	3.84	12.21	0.52
50b:C_{11}	0.56	0.73	0.02	0.71	1.35	0.02	3.34	4.34	0.11	4.23	8.00	0.10
C_{12}	0.48	0.59	0.02	0.57	1.28	0.05	2.83	3.50	0.14	3.36	7.60	0.29
51:C_{11}	0.39	0.39	0.001	0.39	0.43	0.001	3.87	3.87	0.01	3.86	4.30	0.01
C_{12}	0.29	0.32	0.001	0.31	0.96	0.001	2.87	3.14	0.01	3.13	9.61	0.01
[3]53:C_{11}	0.85	0.96	0.03	0.93	3.53	0.10	4.09	4.64	0.16	4.49	17.04	0.47
C_{12}	0.78	0.90	0.03	0.87	3.54	0.07	3.76	4.33	0.12	4.21	17.05	0.36

[1] k values should be similar to (k_1+k_2) - see Section 6.4.

[2] Rate constant values were rounded off to the second decimal place, hence the occasional discrepancies after correcting for catalyst concentration.

[3] Run 53 undertaken in the absence of KOH, thereby explaining the higher reaction rates.

Figure 6.7 Modelled and Experimental Data: C_{10}: 1-Decene feed; Co/TOP catalyst (with KOH); Run 32.

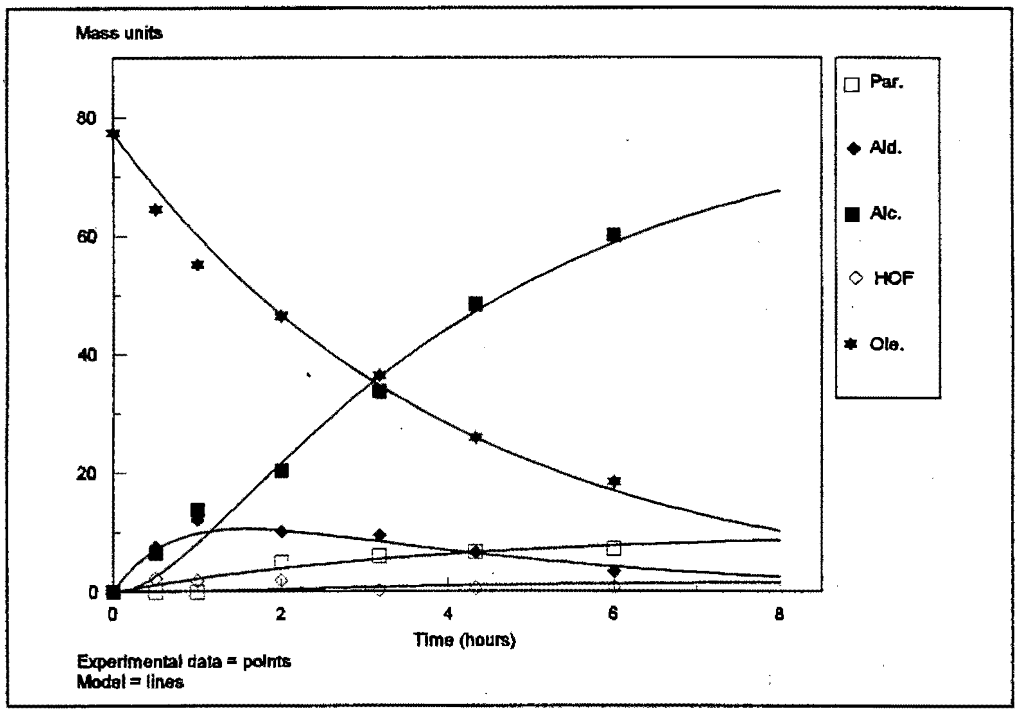

Figure 6.8 Modelled and Experimental Data: C_{10} SLO narrow fraction(A); Co/TOP catalyst (with KOH); Run 33.

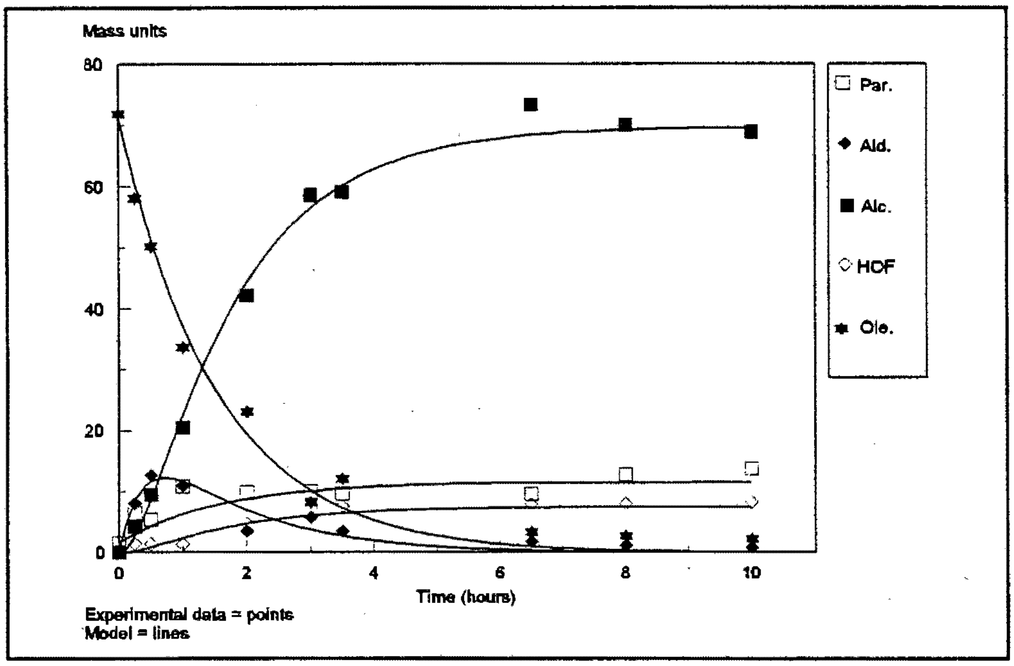

Figure 6.9 Modelled and Experimental Data: C_{10} SLO narrow fraction(A); Co/TOP catalyst (without KOH) ; Run 31.

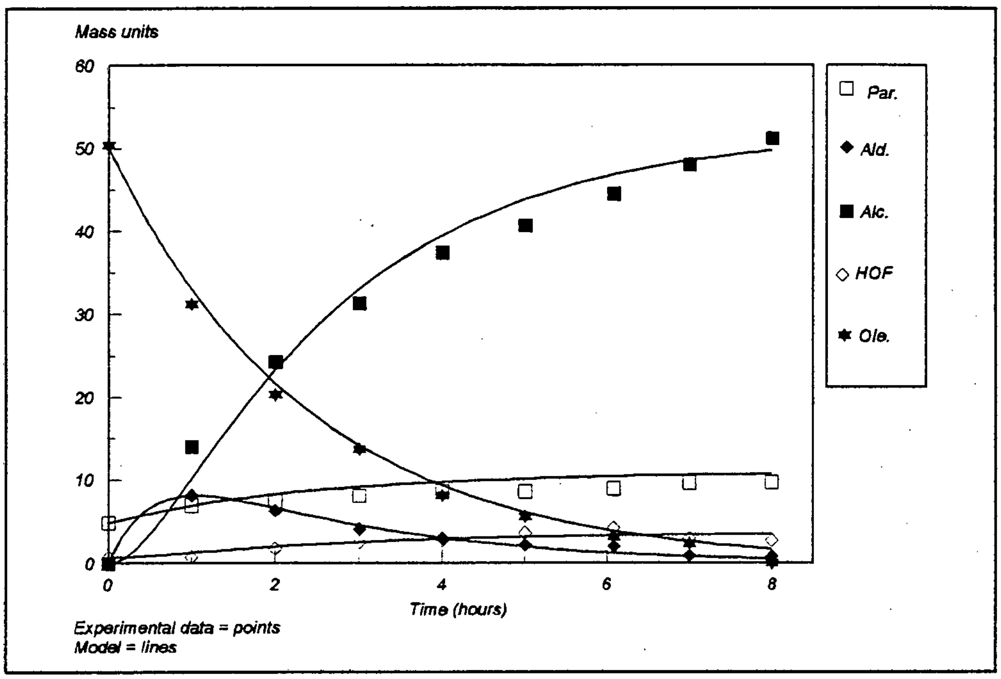

Figure 6.10 Modelled and Experimental Data: C_{10} SLO broad fraction (B); Co/TOP catalyst (without KOH); Run 29b.

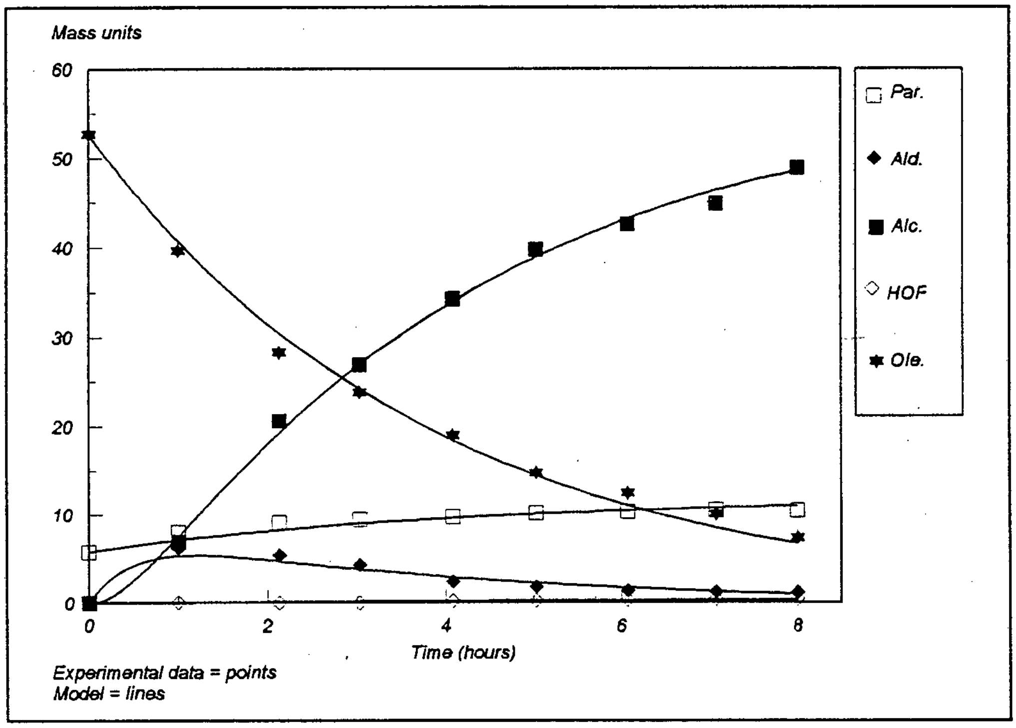

Figure 6.11 Demonstration of experimental and modelling repeatability for four runs undertaken with a C_{10} SLO broad fraction (C); Co/TOP catalyst (without KOH);Runs 29a-d.

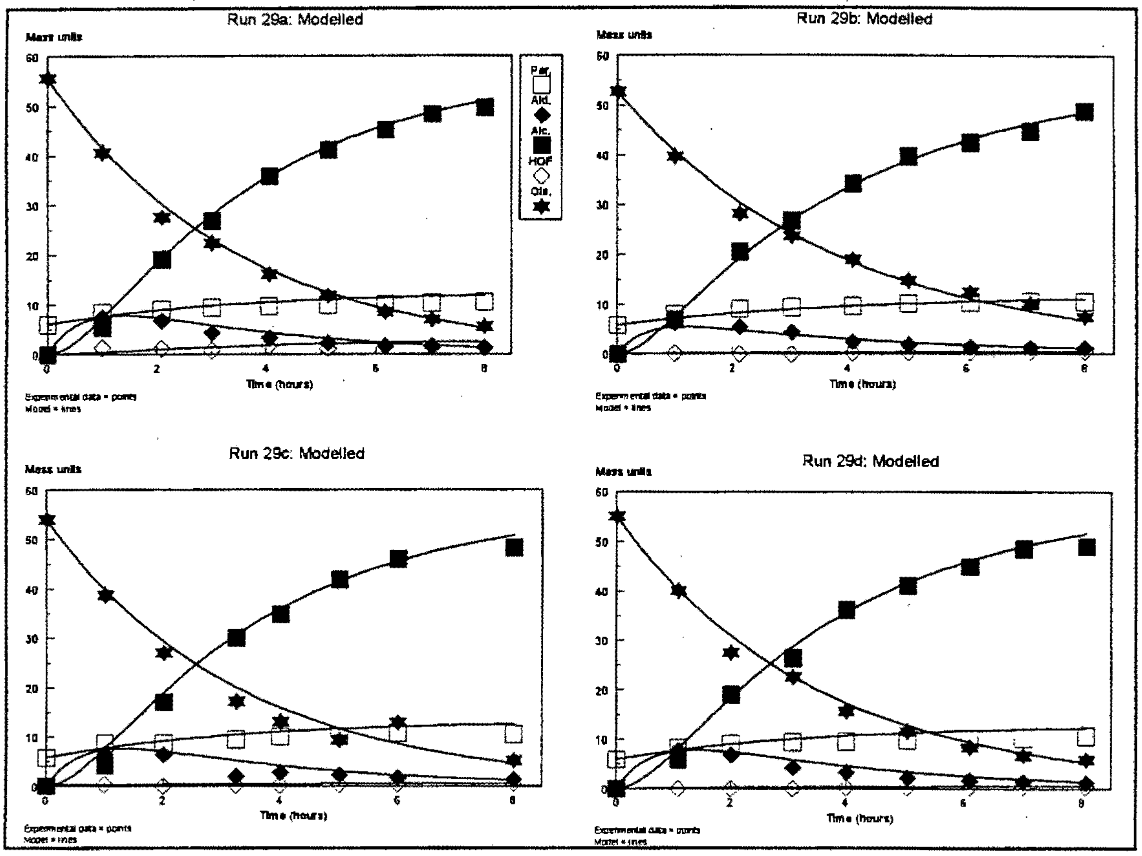

The results in Figure 6.11 and Table 6.2 (4 runs undertaken under the same conditions) demonstrate repeatability.

Table 6.2 Results of 4 repeated runs undertaken with a C_{10} SLO broad fraction; Co/TOP catalyst (without KOH); Runs 29a-d.

	Meas.	Modelled values					Meas.	Modelled values (corrected for catalyst conc.)				
Run	k	(k_1+k_2)	k_1	k_2	k_3	k_4	K	(K_1+K_2)	K_1	K_2	K_3	K_4
29a	0.3	0.29	0.03	0.26	1.43	0.01	1.33	1.31	0.15	1.16	6.45	0.05
29b	0.26	0.26	0.03	0.23	1.78	0.01	1.15	1.18	0.15	1.03	8	0.06
29c	0.29	0.29	0.04	0.26	1.62	0.01	1.29	1.32	0.16	1.16	7.29	0.04
29d	0.3	0.29	0.03	0.26	1.46	0.01	1.33	1.32	0.15	1.17	6.55	0.05

Where $k_x = K_x/[Co]$

[Co] = g/100ml

Figure 6.12 Modelled and Experimental Data: "Feed preparation for Run 46b": 1-Decene feed; Co/EP catalyst (with KOH) ; Run 46a.

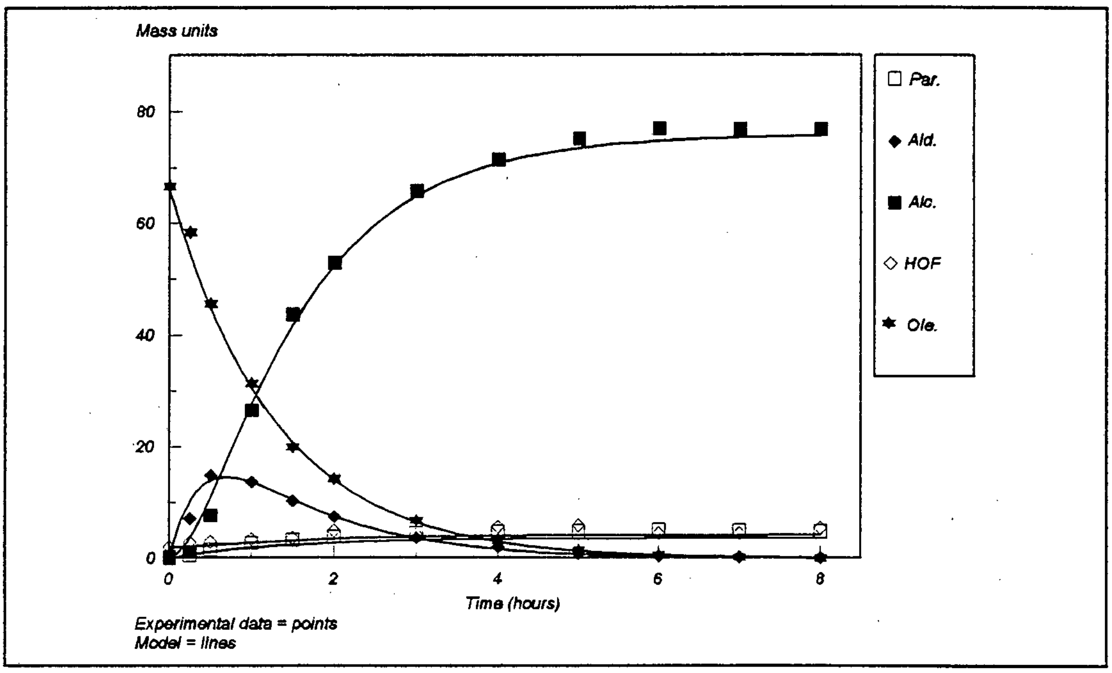

Figure 6.13 Modelled and Experimental Data: Effect of aldehyde addition to Run 46a (above) reactor products; Co/EP catalyst (with KOH) ; Run 46b.

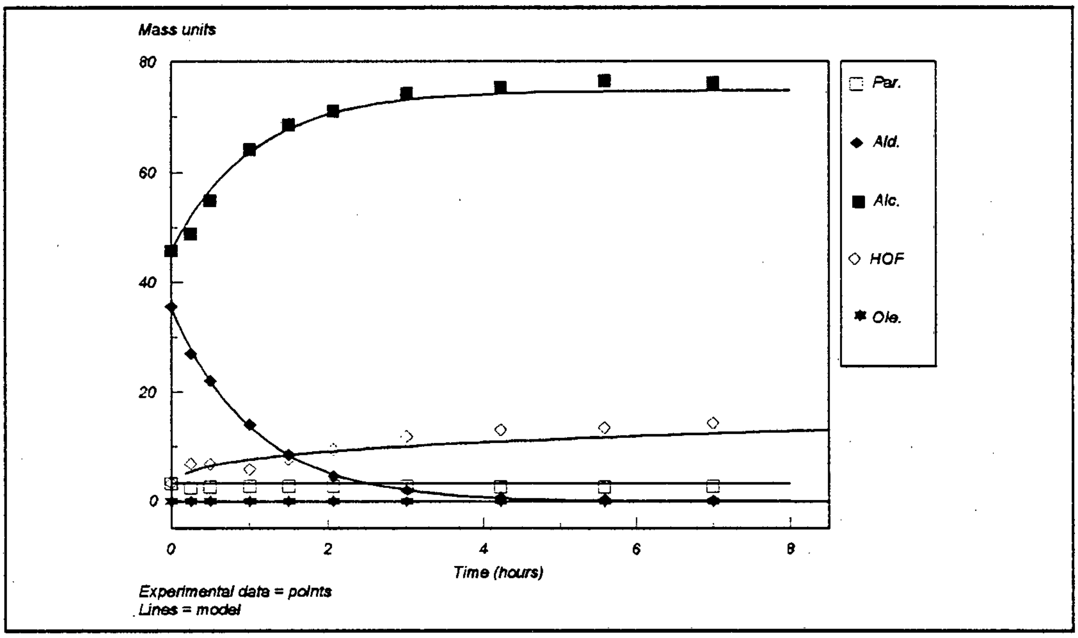

Figure 6.14 Modelled and Experimental Data: C_{10} olefins: C_{10} SLO broad fraction (A); Co/EP catalyst (with KOH) ; Run 44.

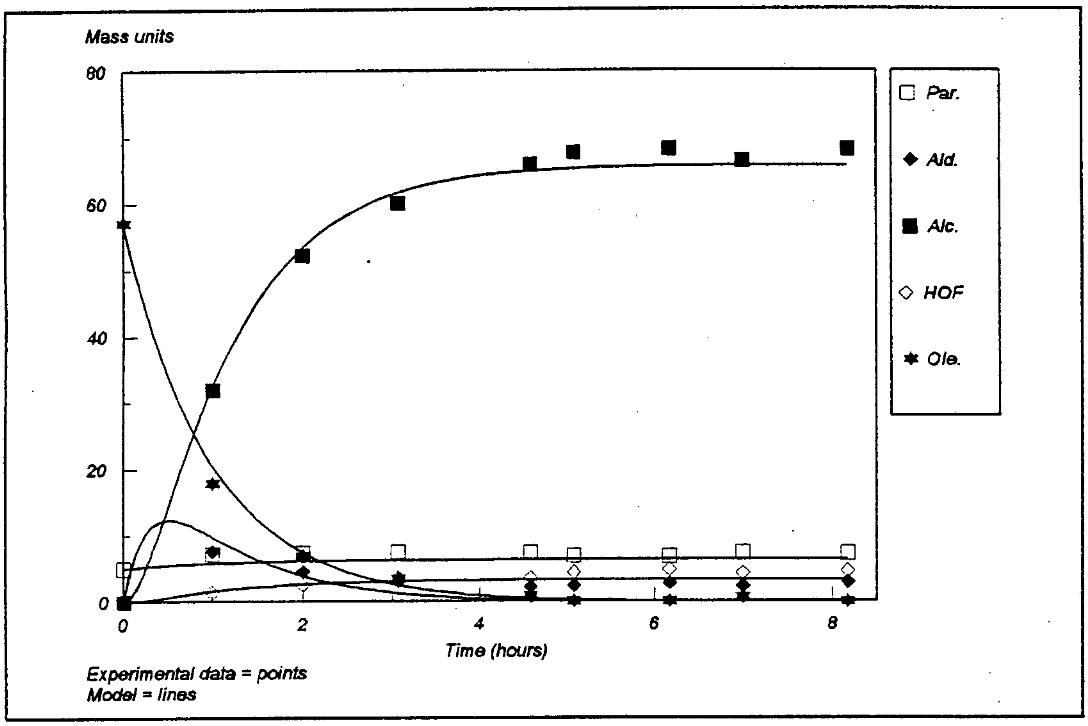

Figure 6.15 Modelled and Experimental Data: C_{11} olefins: $C_{11\text{-}12}$ SLO broad fraction (A); Co/EP catalyst (with KOH) ; Run 50b.

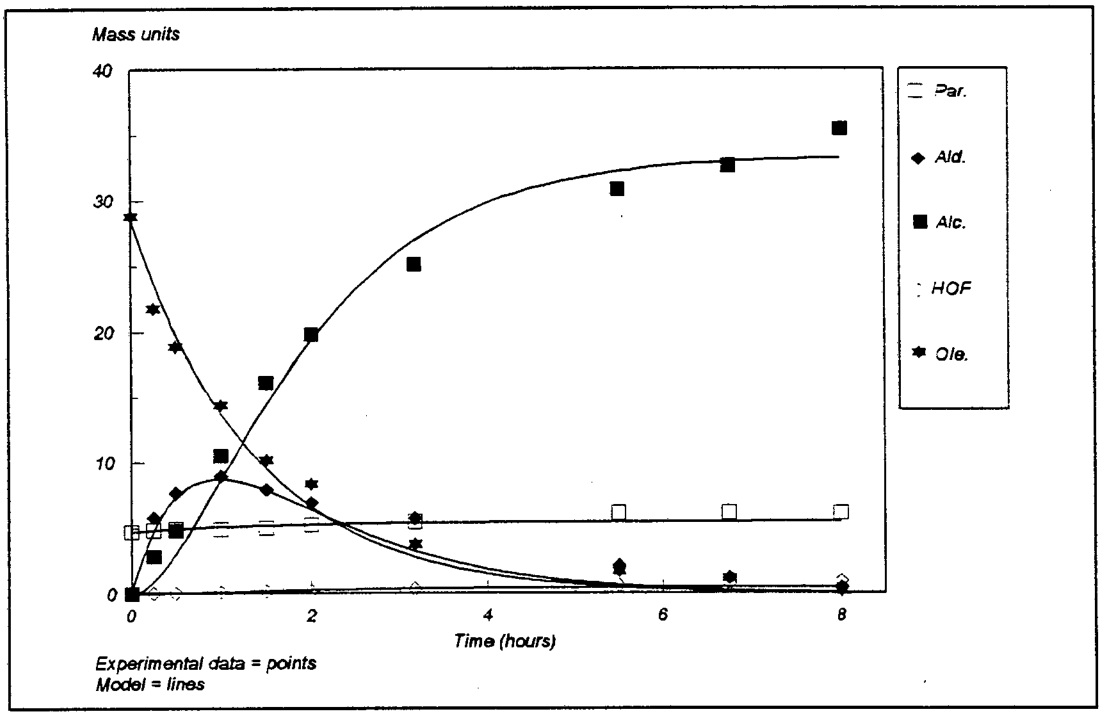

Figure 6.16 Modelled and Experimental Data: C_{12} olefins: $C_{11\text{-}12}$ SLO broad fraction (A); Co/EP catalyst (with KOH) ; Run 50b.

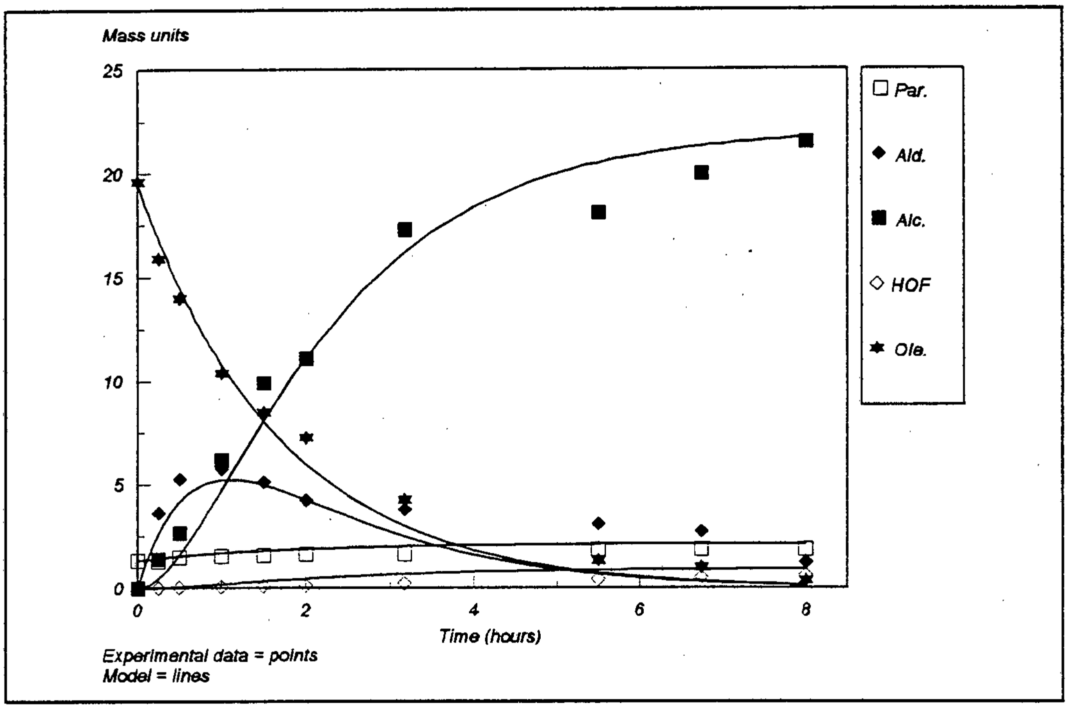

Figure 6.17 Modelled and Experimental Data: C_{11} olefins: $C_{11\text{-}12}$ SLO broad fraction (B); Co/EP catalyst (with KOH) ; Run 51.

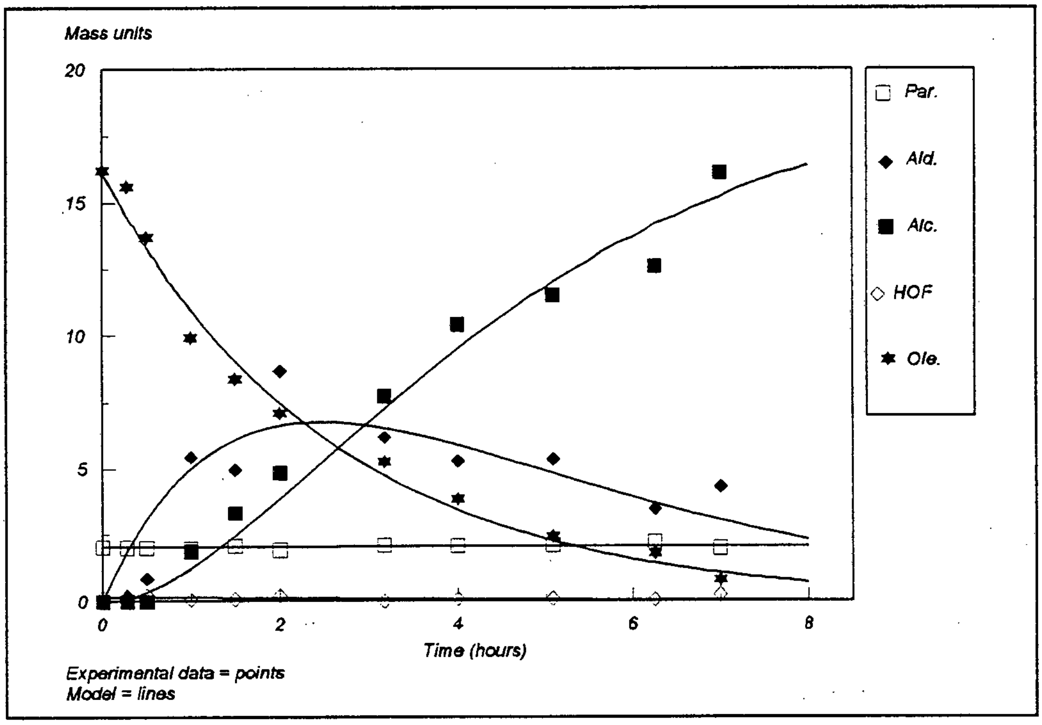

Figure 6.18 Modelled and Experimental Data: C_{12} olefins: $C_{11\text{-}12}$ SLO broad fraction (B); Co/EP catalyst (with KOH) ; Run 51.

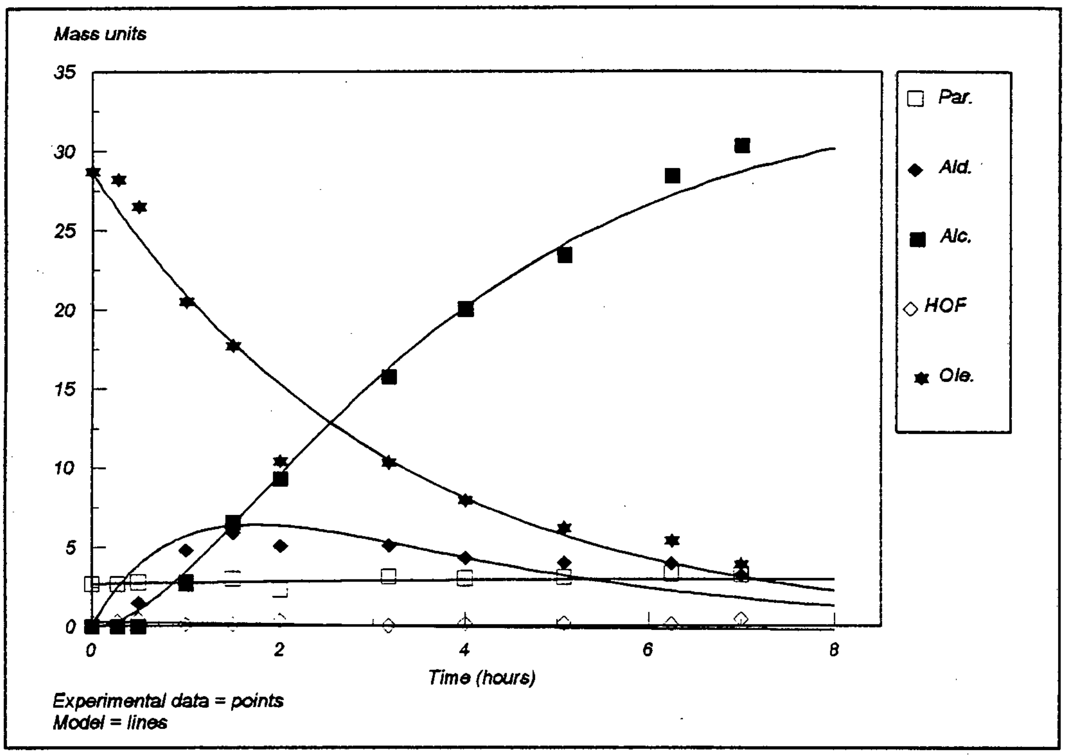

Figure 6.19 Modelled and Experimental Data: C_{11} olefins: $C_{11\text{-}12}$ SLO broad fraction (D); Co/EP catalyst (without KOH) ; Run 53.

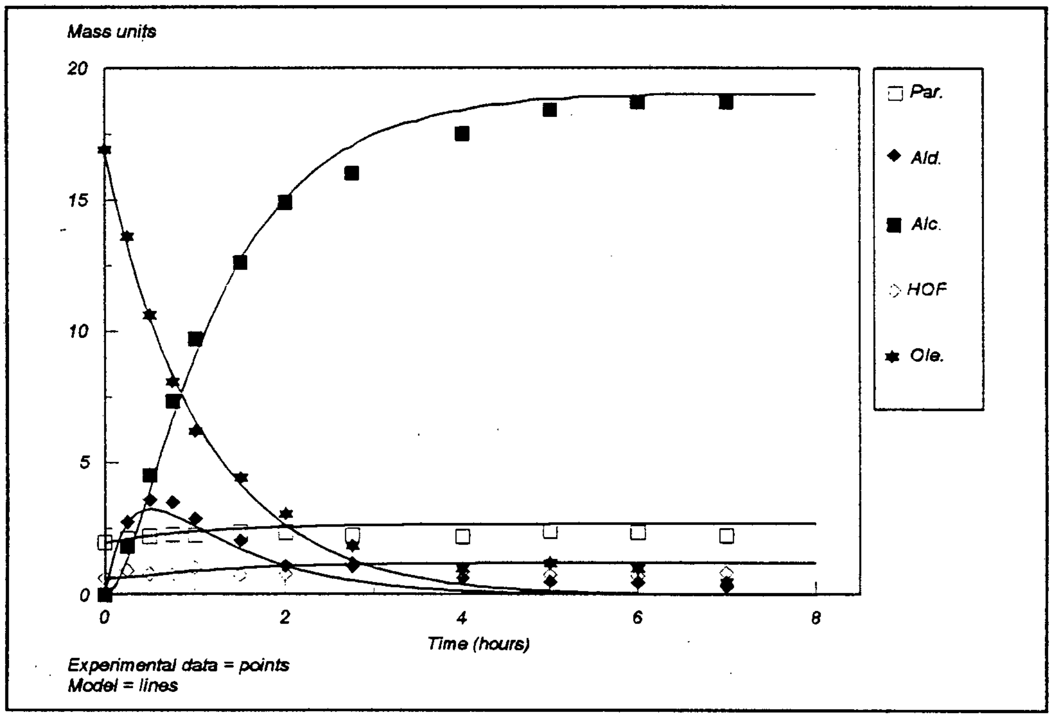

Figure 6.20 Modelled and Experimental Data: C_{12} olefins: $C_{11\text{-}12}$ SLO broad fraction (D); Co/EP catalyst (without KOH) ; Run 53.

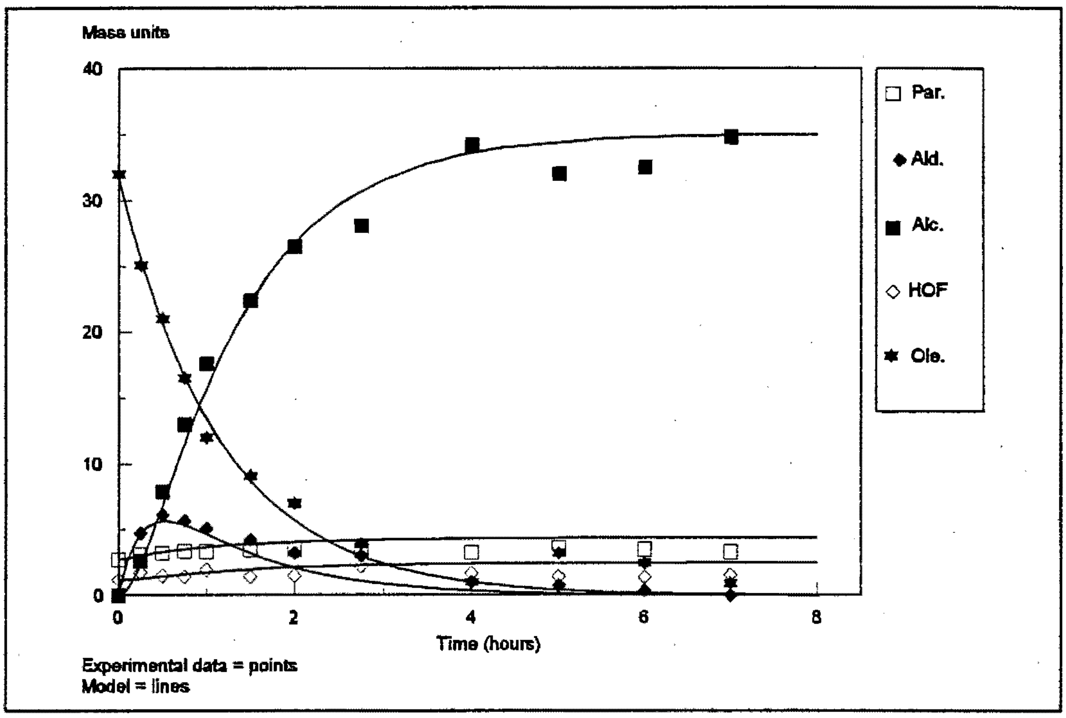

6.4 DISCUSSION OF MODELLING RESULTS

From the previous sections it follows that the experimental *k* values derived from the slopes of the first order plots of -ln(1-C) versus reaction time as represented by equation (6.21), should correspond with (k_1 + k_2) values from equation (6.14). The *k* and (k_1 + k_2) values were derived by effectively minimizing the natural log (see equation (6.19)) and the absolute squared error (see equation (6.20)) functions respectively. Using equation (6.20), the model places emphasis on data collected at the beginning of the experiments, whilst the *k* values derived from the ln(1-C) versus time plots emphasize data collected at low olefin concentrations. This is because at high conversions (*ie.* low olefin concentration), small differences in conversion give rise to large differences in the ln(1-C) values on the y axis of these plots. Only olefin concentrations are used in equation (6.21) to calculate *k*, whilst all the component concentrations are used in the calculations of k_1 and k_2 with the second (modelling) approach. It is noteworthy that when the second error function (equation (6.20)) is used, and the olefin error is weighed more heavily, the k values obtained by measuring the slopes of the first order rate plots can be reproduced by modelling. Differences between the k and $(k_1 + k_2)$ values are shown in Table 6.1 and in Appendices 8 and 9.

There is generally a good correlation between the k and $(k_1 + k_2)$ values for the runs with TOP and EP ligands under "standard" reaction conditions of Co:P molar ratio (Co:P≈1:2), temperature (≈170°C), as well as syngas pressure and composition (total pressure ≈75 bar (g), H_2:CO ≈2:1). Figure 6.21 graphically compares modelling results using the k and (k_1+k_2) approaches. Where large differences exist, these are pointed out. The differences are indicative of uncertainties in the values of the kinetic constants. The scatter of data points on both sides of the central (expected) line in Figure 6.21 indicate that where differences between the k and $(k_1 + k_2)$ exist, these differences are not necessarily due to a deficiency in the model caused by "less reactive olefins" remaining in the batch reactor toward the end of the experiments. If this was the case, then all the data points would lie above the median. That is, k values would be lower than $(k_1 + k_2)$ values due to the emphasis placed on the olefins at low concentrations as discussed above.

Where large differences between the k and $(k_1 + k_2)$ values exist, these are often for runs undertaken at "non standard" conditions - see key to notes in Figure 6.21. These "non standard" conditions appear to indicate changes in reactivity of olefins in the systems with TOS, and are indicative of conditions under which the model may break down. This may be taken to imply that the model is a "narrow" one.

Figure 6.21 Comparison of olefin consumption predictions using modelling approach (k_1+ k_2) and the measurement of k from plots of -ln(1-C) versus time: TOP and EP ligands.

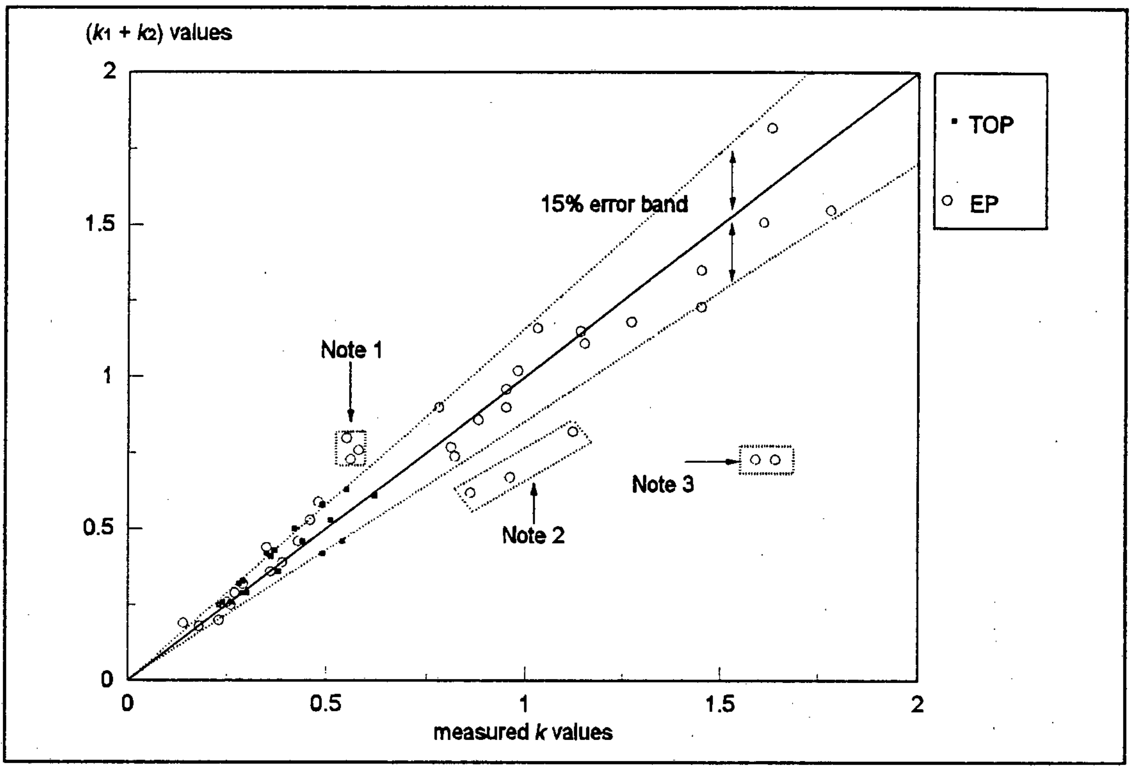

Key to Notes in Figure 6.21:

Note 1: Data collected under "non-standard" conditions of temperature (indicates various runs not undertaken at 170-175°C).

Note 2: Data collected under "non standard" syngas pressure and composition (*ie.*, 75 bar (g) and H_2:CO ratio not 2:1).

Note 3: Data points were collected using starting EP:Co molar ratios of 0.5 and 1, compared with a "standard" ratio of 2.

If one discards the data points collected using temperatures $\geq$175°C; syngas compositions not close to P_{H2} = 50 bar and P_{CO} = 25 bar; and P:Co molar ratios < 1, the accuracy of the model/s can be ascertained. Student's t-tests (Clarke and Cook [1977]) were undertaken in this regard. Assuming the null hypothesis, *ie.*, that the difference between the mean (k_1+k_2) and k values should equal zero; the results indicated that there were not significant differences at the 99% and 95% confidence levels for the TOP and EP ligands respectively.

This correlation is indicative of a satisfactory mass balance as well as a satisfactory model based on the proposed reaction pathway. This is because measured products and olefins are used in the (k_1+k_2) approach, whilst only olefins are made use of in determining k.

In addition, Figure 6.13 illustrates that the model accurately predicts aldehyde conversion to alcohols from the batch experimental data. For Runs 46a and 46b (where aldehyde was added to the system in Run 46b) k_3' values of 11.16 and 11.14 hr^{-1} were obtained respectively. These values therefore appear to indicate that most (if not all) the aldehyde desorbs from the catalyst complex before re-adsorption prior to hydroformylation. Measurement of the slope of the curve of -ln(1-(fractional aldehyde conversion)) against time in Figure 6.4 gave a value of 0.786 which after correcting for cobalt concentration (dividing by [Co]), gives a value of 11.23 hr^{-1} . This is similar to the k_3' values and may be taken to serve as additional confirmation of the model accuracy.

6.5 CONTINUOUS CATALYST TESTING

In order to test the validity of the results generated in the micro-reactor, continuous testing of the catalyst/s were undertaken with a larger reactor system as described in Section 2.1.3.

The primary function of the continuous reactor was to test catalyst lifetime in order to evaluate catalyst - feed compatibilities. The reactor was operated continuously for periods of time up to 2 months without instability using SLO feeds similar to the ones tested in this study *ie.*, there was no unexpected catalyst deactivation or build-up of a HOF. Termination of continuous runs were usually necessitated by changes to the feed and/or catalyst. Reaction selectivities and product linearities were the same as those measured in the constant pressure micro-reactor batch experiments. These values, as well as the measured olefin conversions (see Figure 6.24) remained approximately constant during periods of continuous testing.

The success of the operation demonstrated the suitability of HTF-T feeds (SLO) for use as a hydroformylation feedstock.

The kinetic model was verified on the continuous reactor system. This was performed by combining the kinetic results derived in the current study with the following mass balance describing the performance of the continuous reactor system:

$$M_j^{in} - (M_j^{out}/f) + (rate_j t/f) = 0 \qquad (6.22)$$

Equation 6.22 represents the mass balance for a species "j" over the reactor (where "j" can represent any of the liquid components). M_j^{in} and M_j^{out} refer to the mass fraction of component j at the inlet and the outlet of the reactor, $rate_j$ is the formation or consumption rate of component j evaluated at the outlet conditions, and t represents the residence time. The dilution factor f, is defined as the mass of liquid entering the reactor divided by the mass of liquid leaving the reactor.

As the work on the continuous reactor system is still ongoing, these results will be published at a later date.

6.6 CONCLUSIONS

A kinetic model for the multistep hydroformylation reaction catalyzed by alkylphosphine modified Co catalysts was developed and successfully tested. This model is based on a proposed reaction pathway and "batch" micro-reactor data obtained using pure and SLO feeds.

Continuous operation of the larger reactor system further demonstrated that SLO feeds are compatible with phosphine modified Co catalysts. After pre-treating the feed with aqueous NaOH, no gross poisons could be identified. This confirmed earlier theories on the "cleanup" of feed being limited to carboxylic acid removal.

CHAPTER 7

CONCLUDING REMARKS AND RECOMMENDATIONS

7 CONCLUDING REMARKS AND RECOMMENDATIONS

The original objectives of the study as set out in Section 1.4 of Chapter 1, were met. These were; i) to identify a suitable hydroformylation catalyst system for HTF-T feeds; ii) characterization and quantification of such a hydroformylation system whilst; iii) testing the effects of reaction variables, including feed composition and ligand variants and; iv) a kinetic investigation incorporating; v) modelling for scale-up of a selected system based on micro-reactor results. These objectives are reviewed in the Synopsis as well as in the conclusions of Chapters 3-6.

In addition to the conclusions already made in the previous chapters, the following general remarks and recommendations are made:

Although the study was limited to testing feed fractions giving rise to products in the C_{9-13} range, it is conceivable that lighter and heavier fractions would also be suitable feedstocks. Indeed, the lighter fractions in HTF-T products contain more olefins in relation to "inerts", and this would yield more productive hydroformylation systems.

Distillation, and removal of carboxylic acids were identified as the only pre-requisite steps in the feed preparation for phosphine modified cobalt systems. Since no continuous test with a Rh catalyst system was performed, additional purification of the feed <u>may</u> be necessary with Rh-based catalysts. The linearity of the feed, and therefore the products, can be enhanced by refractionating the feed so as to concentrate the linear α-olefin. The additional cost in the feed preparation has to be weighed up against the potential benefits of a more linear product.

Due to reported difficulties associated with efficient rhodium catalyst recovery in the hydroformylation of higher olefins, it is recommended that Co based catalysts be employed with these feeds. Recent 2-phase systems which make use of modified ligands such as those developed at Hoechst [Kühlein, 1994] and Union Carbide [Abatjoglou *et al.,* 1995] which are proposed as being suitable for rhodium catalyst recovery in long chain olefin hydroformylation, may hold promise. However, the complicated and polar nature of SLO feeds may pose problems in a system employing phase separation as a method of catalyst recycle.

In situ characterization of the hydroformylation catalyst complexes is recommended in order to more accurately quantify and qualify the effect of reaction variables on the "working" catalyst. Computer-based molecular modelling of the catalyst complexes, would also be useful. Such a study, in which molecular orbital theory plays an important role, can be used to determine the energetic states of reaction intermediates. The results could be used to determine the most suitable metal/ligand combination for a catalyst, as well as the desired olefin distribution in a SLO feed. In this manner, the system could be "tailored" to give the best combination of performance and product characteristics.

Hydroformylation feedstock "ageing" should be avoided due to the formation of oxidizers/ peroxides [Kindermans, 1994][Wood and Garrou, 1984]. SLO feeds may be particularly sensitive to these problems because of oxygenates already present. A feed "ageing" study, or investigation into a suitable oxygen "scavenger" may therefore be of use. Alternatively, this issue would be largely negated on integration of F-T and Oxo process in that immediate use of the F-T streams would be facilitated.

A proposed integration of HTF-T Synthol and Oxo processes is illustrated in Figure 7.1. This could hold the following advantages:

- Integration of the gas streams.
- Decreased capital costs for a hydroformylation plant, because of existing facilities and infrastructure.
- All the feedstocks for a hydroformylation process are essentially sulphur free.
- Apart from acting as a solvent, the inert components in SLO have alternative synthetic fuel value and can be routed to existing oil work-up facilities.
- Minimal "cleanup" of the feed.
- Value addition or beneficiation of HTF-T products.

Figure 7.1 Schematic representation of incorporation of an Oxo process into an existing Synthol plant.

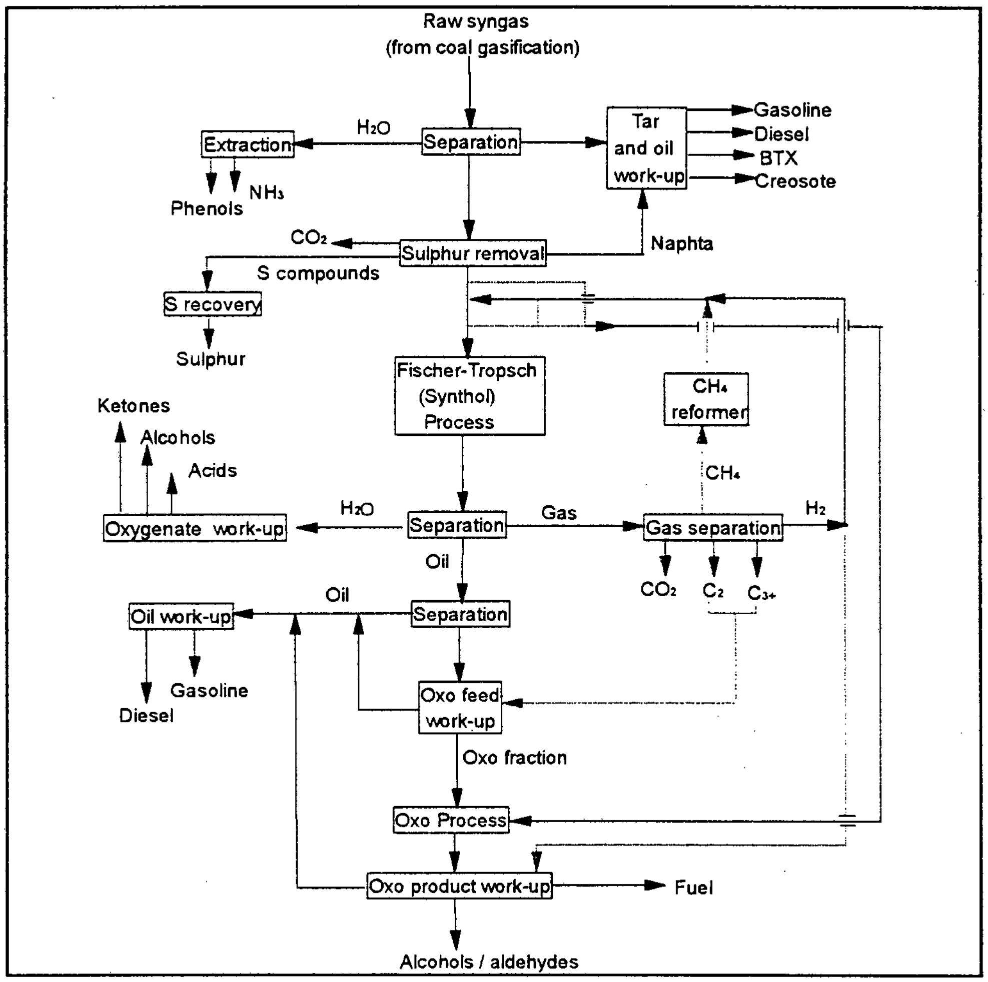

A unique mix of hydroformylation products is obtained due to the structure of the mono-methyl branched olefins in SLO. Making use of Rh and Co based catalysts, it was demonstrated that the branched hydroformylation products were mainly mono-methyl branched primary aldehydes and/or alcohols with the methyl branch being at any position along the linear molecular "backbone". The smaller quantities of di-methyl branched products may be characterized by the fact that they also have methyl branches at any one position along the linear molecular "backbone", but the second methyl branch is the 2-methyl one. In contrast, the only methyl alcohols obtained with pure linear feeds are of the 2-methyl variety, with the balance of the branched material resulting from hydroformylation of internal olefins.

The various mono and di-methyl branched hydroformylation products described can therefore be considered exclusive to high temperature F-T feeds. The chainlength of the branched side "groups" are generally of the same length or shorter than branched side-chains obtained with pure linear olefin feedstocks. It can be speculated that detergents containing these mono and di-branched species may be superior, as they contain a unique combination of linear and branched character. Linearity is associated with natural and high value products, whilst branched detergents are reportedly stronger or more active surfactants. This represents an opportunity.

It is worth mentioning that the SLO derived alcohols were purified by conventional methods of 1), distillation, 2) caustic treatment for ester removal, and 3) hydrogenation, were demonstrated [Betts *et al.*, 1996] to be as biodegradable as commercially available detergent alcohols which are approximately 85% linear. Further comparative tests should shed light on the surfactant performance characteristics. These are expected to be superior.

Finally, it can be concluded that a technical and commercial opportunity exists that the findings in this thesis can be used to add value to synthetic fuel feedstocks.

REFERENCES

REFERENCES

Abatjoglou, A.G., Peterson, R.R., Bryant D.R., *in Proc. of 209th ACS National Meeting*, Anaheim, USA (1995).

Adkins, H., Krsek, G., *J. Am. Chem. Soc.*, **70**, 383 (1948).

Adkins, H., and Krsek, G., *J. Am. Chem. Soc.*, **71**, 3051 (1949).

Ainsworth, S.J., *C&EN*, p34, Jan. (1994).

Ainsworth, S.J., *C&EN*, p30, 23 Jan. (1995).

Aldridge, C.L., Jonassen, H.B., *J. Am. Chem. Soc.*, **85**, 886 (1963).

Alvila, L., Pakkanen, T.A., Pakkanen, T.T., *J. Mol. Cat.*, **73**, 325-334 (1992).

Anderson, R.B., in "Advances in Catalysis" Vol. 5, Eds.,Frankenberg, Komarewsky, Rideal, Academic Press Inc., New York (1953).

Anderson, R.B., in "Catalysis" Vol. IV, Ed. P.H. Emmett, Reinhold, New York (1956).

Avey, A., Schut, D.M., Weakley, T., Tyler, D.R., *Inorg. Chem.*, **32**, 233 (1993).

Bahrmann, H., Haubs, M., Kreuder, W., Müller, T., EP 0 374 615 to Hoechst AG (1989).

Bartik, T., Bartik. B., Hanson, B.E., *J. Mol. Catal.*, **85**,121 (1993).

BASF, German Patent., 293, 787 (1913).

Bauer, R.S., Chung, H., Keim, W., van Zwet, H., DE Patent 2101391, to Shell Internationale Research Maatschappij N.V., (1972).

Bauer, R.S., Chung, H., Canell, L.G., Keim, W., van Zwet, H., DE Patent 2101422, to Shell Internationale Research Maatschappij N.V., (1972).

Beller, M., Cornils, B., Frohning, C.D., Kohlpainter C.W., *J. Mol. Catal.*, **104**, 17 (1995).

Beck, K., Diploma Thesis, Karlsruhe University, Ch. 5, 68 (1967).

Betts, M.J., Dry, M.E., Geertsema, A., Rall, G.H., RSA Patent Appln. No. 96/5545 (1996).

Billing, E., Abatjoglou, A.G., Bryant, D.R., US Patent 4 668 651, Union Carbide Corp. (1987).

Billing, E., Abatjoglou, A.G., Bryant, D.R., US Patent 4 748 261, Union Carbide Corp. (1988).

Billing, E., Abatjoglou, A.G., Bryant, D.R., US Patent 4 769 498, Union Carbide Corp. (1988).

Billing, E., Abatjoglou, A.G., Bryant, D.R., US Patent 4 885 401, Union Carbide Corp. (1989).

Braca, G., Sbrana, S., Piancenti, F., Pino, P., *Chim. Ind.* (Milan), **52**, 1091 (1970).

Brady, R.C., and Petit, R., *J. Am. Chem. Soc.*,**102**, 6182 (1980).

Brady R.C., and Petit, R., *J. Am. Chem. Soc.*,**103** (5), 1289 (1981).

Breslow, D.S., Heck, R.F., *Chem. Ind.* (London), 467 (1967).

Brown, S.K., Wilkinson, G., *J. Chem. Soc. A*, 2753 (1970).

Bruanstein, P., Rose, J., in "Stereochemistry of Organometallic and Inorganic Compounds", Vol. 3, Ed. I. Bernal, Elsevier, Amsterdam (1988).

Bryant, D.R., US Patent 4 143 075, Union Carbide Corp. (1979).

Buhling, A., Kamer, P.C.J., van Leeuwen, P.W.N.M., *J. Mol. Catal. A.:Chem.*, **98**, 69-80 (1995).

Burnham-Tinker, H., Morris, D.E., US Patent 4 052 461, to Monsanto (1977).

Cappelli, A., D'Angeli, C., Andreetta, A., Capparella, G., Chem. React. Eng. Proc. Int. Symp. 4th. (1976).

Chern, J-M., Helfferich, F.G., *AIChE Journal,* **36** No.8, 1200-1208 (1990).

Clarke, G.M., Cooke, D., "A Basic Course in Statistics", 2nd Ed. p235, Edward Arnold (Publishers) Ltd., London (1981).

Cornils, B., Förster; I., *Chem.-Ztg.*, **97**, 374 (1973).

Cornils, B., Payer R., Traenckner, K.C., *Hydrocarbon Process.*, No. **6**, 83 (1975).

Cornils, B., in "New Syntheses with Carbon Monoxide", Ed. J. Falbe, Springer-Verlag, Berlin (1980).

Cornils, B., Rottig, W., in "Chemical Feedstocks from Coal" (Translated from "Chemierohstoffe aus Kohle" originally published in 1977), Ed. J. Falbe, Chp.10. pp 467, John Wiley and Sons inc., New York (1982).

Cornils, B., Herrmann, W.A., Rasch, M., *Agnew. Chem.* (Int. Ed. Engl.), **33**, 3144, (1994).

Davidson, P.J., Hignett, R.R.,Thompson, D.T., in "Catalysis", 1, Special Periodical Reports V, The Chemical Society, Burlington House, London (1977).

Demianiw, D.G. , in Kirk-Othmer; Encycl. Chem. Tech. 3rd Ed. Vol. **16**, p480, Wiley Interscience (1981).

Deshpande, R.M., Chaudhari, R.V., *Ind. Eng. Chem. Res.*, **27**, 1996-2002 (1988).

Deshpande, R.M., Chaudhari, R.V., *J. of Catal.*, **115**, 326-336 (1989).

Deshpande, R.M., Divekar, S.S., Gholap, R.V., Chaudhari, R.V., *J. Mol.Catal.*, **67**, 333-338 (1991).

Desphpande, R.M., Bhanage, B.M., Divekar, S.S., Chaudhari, R.V., *J.Mol. Catal.*, **78**, L37-L40 (1993).

Deuflhard P., "A Modified Newton Method for the Solution of Ill -Conditioned Systems of Nonlinear Equations with Application to Multiple Shooting.", Numer. Math. 22, 289-315 (1974).

Dietz, W.A., *J. Gas Chrom.*, **5 (2)**, 68 (1967).

Dry, M.E., in "Catalysis Science and Technology", Vol. 1,Eds. J.R. Anderson and M.Boudart, Springer, Berlin, (1981).

Dry, M.E., " Conversion of Syngas to Fuels and Chemicals" in *Proc. of the Int. Conf. on Cat. and Catal. Proc.,* Cape Town, South Africa (1993).

Dry, M.E., Personal Communications with the author (1993).

Ekstroom, A., and Lapszewics, J.A., *J. Phys. Chem.*, **91**, 4514 (1987).

Evans, D., Osborn, J.A., Jardine, F.H., Wilkinson, G., *Nature*, **208**, 1203 (1965).

Falbe, J., "Synthesen mit Kohlenmonoxyd, Organische Chemie i. E., p19, Springer Berlin-Heidelberg-New York (1967).

Falbe, J., Tummes, H., Meis, J., German Patent Appl. 1295537 for Rührchemie AG (1969).

Falbe, J., "Oxosynthese. In: Ullmann's Encyklopädie der technischen Chemie, Ergänzungsband, p87 (1969), München-Berlin: Urban & Schwarzenberg (1969).

Falbe, J., Ed., in "Carbon Monoxide in Organic Synthesis" - Translated by C.R. Adams, Springer-Verlag, Berlin-Heidelberg-New York (1970).

Falbe, J., "Fischer-Tropsch- Synthese, Chemierohstoffe aus Kohle", Wiley Interscience; Stuttgart (1977).

Falbe, J. Ed., in "New Syntheses with Carbon Monoxide", Springer-Verlag, Berlin, (1980).

Fell, B., Boll, W., Hagen, J., *Chem.-Ztg.*, **99**, 452, 485 (1975).

Fell, B., *Chem.-Ztg.*, **101**, 343 (1977).

Fell, B., Papadogianakis, G., *J. Mol. Catal.*, **66**, 143-154 (1991).

Fiato, R.A., Soled, S.L., US 4 621 102, to Exxon Research and Engineering Co. (1986).

Fiato, R.A., Gates, W.E., US 4 639 431, to Exxon Research and Engineering Co. (1987).

Fischer, F., and Tropsch, H., *Brenst. Chem.* **4**, 276 (1923).

Fischer, F., and Tropsch, H., *Brenst. Chem.* **7**, 97 (1926).

Flory, P.J., *J. Am. Chem. Soc.*, **58**, 1877 (1936).

Freitas, E.R and Gum, C.R., *Chem. Eng. Prog.*, **75** (1), 73 (1979).

Frohning, C.D., Kölbel, H., Ralek, M., Rottig, W., Schnur, F., and Schulz, H., "Chemical Feedstocks from Coal" (Translated from "Chemierohstoffe aus Kohle" originally published in 1977), Ed. J. Falbe, Chp.8.4 pp 392-421, John Wiley and Sons Inc., New York (1982).

Fuggle,J.C., *J. Elec. Spectrosc. Rel. Phenom.*, **21**, 275 (1980).

Garlasschelli, L., Marchionna, M., Lapalucci, M.C., Longoni, G., *J. Mol. Catal.*, 68, 7- 21, (1991).

Garrou, P.E., Hartwell, G.E, US Patent 4 262 147 to Dow Chemical Co. (1981).

Gholap, R.V., Kut, O.M., Bourne, J.R., *Ind. Chem. Res.*, **31**, 1597-1601 (1992).

Glockner, P.W., Keim, W., Mason, R.F., Bauer, R.S., DE Patent 2053758, "Catalytic Oligomerization of Ethylene" to Shell Internationale Research Maatschappij N.V., 13 May (1971).

Greene, C.R., Meeker, R.E., US Patent 3 274 263, to Shell Oil Co. (1966).

Gregor, J.H., *Catal. Letters*, **7**, 317 (1990).

Grosser, L.W., Knoth, H.W., Parshall, G.W., *J. Mol. Catal.*, **2**, 253 (1977).

Haggin, J., *C&EN*, 25 April (1995).

Hamai, S., *J. Chem. Soc. Jpn.*, **62**, 516 (1941).

Hargis, D., US Patent 4 261 865, to Ethyl Corporation (1981).

Healy, F.J., Livingston, J.R., Mozeleski, E.J., Stevens , J.G., Sartori, G., to Exxon , US 5 288 818 (1991), US 5 298 669 (1993).

Hecht, O., Kröper, H., in "Naturforschung und Medizin in Deutschland 1939-1946", 36, pp115, Ed. K. Ziegler, Dieterich'sche Verlagsbuchhandlung Wiesbaden (1948).

Heck , R.F., and Breslow, D.S., Actes congr. Int. Catalyse 2^e, Paris (1960).

Heck, R.F., Breslow, D.S., *J. Am.Chem. Soc.*, **83**, 4023 (1961).

Heck, R.F.J., *J. Organomet. Chem.*, **2**, 195 (1964).

Heck, R.F., *Advanc. Organometal. Chem.*, **4**, 243 (1966).

Heckel, H., Martin, F., Roelen, O., DE Patent 902,851, to Ruhrchemie (1943).

Heil, B., Marko, L., *Chem. Ber.*, **102**, 2238 (1969).

Helfferich, F.G., *J. Phys. Chem.*, **93**, 6676-6681 (1989).

Helfferich, F.G., Chern, J.M., *AIChE.J*, **36** (8) 1200 (1990).

Henderson, W.A., Streuli, C.A., *J. Am. Chem. Soc.*, **82**, 5791 (1960).

Henrici-Olivé, G., and Olivé, S., in "The Chemistry of the Hydrogenation of Carbon Monoxide", Springer, New York (1984).

Henrici-Olivé, G. and Olivé, S., in "The Chemistry of the Metal-Carbon Bond, Vol. 3", pp 391, Eds. Hartley and Patai, John Wiley and Sons, New York (1985).

Herrmann, W.A., *Agnew. Chem. Int. Ed.* Engl., **21**, 117 (1982).

Herrmann, W.A., Elison, M., Köcher, C., Fischer, J., Öfele, K., DE Patent Appl. 4,447,066 (1995).

Herrmann, W.A., Elison, M., Köcher, C., Fischer, J., DE Patent Appl. 4,447,067 (1995).

Herrmann, W.A., Fischer, J., Elison, M., Köcher, C., DE Patent Appl. 4,447,068, (1995).

Hidai, M., Matsuzaka, H., *Polyhedron*, **7**, 2369 (1988).

Hindmarsh AC, GEAR: Ordinary Differential Equation Solver, Lawrence Livermore Laboratory Report UCID-30001, Revision 3 (1989).

Hjortkjaer, J., *J. Mol. Catal.*, **17**, 1 (1979).

Hölderich, W.F., "New Developements in the use of Microporous Materials in Organic Synthesis" in *Proc. of Int. Con. on Cat. and Catal. Proc.,* Cape Town, South Africa (1993).

Hunter, D.L., Moore, S.E., Garrou, P.E., Dubois, R.A., *Appl. Catal.*, **19**, 259 (1985).

IMSL Math Library, Users Manual., Vol 1. , Ver 1.1., January (1989).

Ishii, Y., M. Sato, M., Matsuzaka, H., Hidai, M., *J. Mol. Catal.*, **54**, L13 (1989).

Jager, B., Dry, M.E., Shingles, T., Steynberg, A.P., *Catal. Letters*, **7**, 293-302 (1990).

Jager, B., Dry, M.E., Shingles, T., Steynberg, A.P., Yukawa, Y., "A new more efficient Synthol Reactor for Fischer-Tropsch Synthesis", in *Proc. of 6th National Meeting of SAICE*, Durban, August (1991).

Jager, B and Espinoza, R., *Catal. Today*, **23** , 17-28 (1995).

Johnson, J and Raghuram, S., in *Proc. of AIChE National Meeting*, Minneapolis, Minnestota, Aug.16-19 (1987).

Jongsma, T., Challa, G., van Leeuwen, P.W.N.M., *J. Organomet. Chem.*, **421**, 128, (1991).

Karandikar, B.M., Morsi, B.I., Shah, Y.T., Carr, N.L., *Canadian J. Chem. Eng.*, **65**, 973 (1987).

Keim, W., *Chem. -Ing.-Tech.*, **56** (11), 850-853 (1984).

Kindermans S., Personal Communication with the author (1995).

Kirshenbaum, I., Inchalik, E.J., in "Chemical Technology Encyclopaedia", Kirk-Othmer, p637, (1981).

Kohl, G., Schroeder, L., Fischer, H., Kinne, M., Schmuck, R., Bethke, H.J., Vysotskii, M.P., Imyantov, B.E., Kuvaev, B.E., Monakhova, N.E., East German Patent DD 206, 374 , CA 101,151,400 (1984).

Kosswig, K., Personal Communication, "Head-Technical Surfactant Applications" Huls AG, Marl, Germany August (1994).

Kröper, H., in " Anlagerung von Kohlenmonoxyd und Wasserstoff an Olefine (Hydroformylierung). In: Houben-Weyl, Vol. IV/2. pp 367. Georg Thieme, Stuttgart (1995).

Kühlein, K., "Recent developements in catalyst research at Hoechst AG" in *Proc. of 9th Int. Symp. on Hom. Catal.*, K4, P11, Jerulasem, Israel, August (1994).

Kummer, J.T., and Emmet, P.H., *J.Am. Chem. Soc.*, **75**, 5177 (1953).

Kummer, R., Nienburg H.J., Kniese W., German Patent 2045169 , to BASF (1972).

Kuntz, E., US Patent 4 248 802 to Rhone-Poulenc Industries (1981).

Kuntz, E.G., *Chemtech*, **17**, 570 (1987).

Lof, P., in Elseviers Periodic Table of Elements, Elsevier Science Publishers, B.V., (1987).

Macho, V., *Chem. Zvesti,* **15**, 181 (1961).

Macho, V., Mistrik, J., Ciha, *M., Chem. Commun.*, **29**, 826 (1964).

Macho, V., *Chem. Zvesti,* **25**, 49 (1971).

Maitlis, P., Long, H., Wang, Z-Q., Turner, M.L., *Proc. of 9th Int. Sym. Hom. Cat.*, p11, Jerusalem, Israel (1994).

Markó, L., P. Szabo, P., *Chem. Technol.* (Berlin), **13**, 482 (1961).

Markó, L., Bor, G., Almasy, G., Szabo, P., *Brennstoff-Chem.*, **44**, 184 (1963).

Markó, L., Kovács, I., Sisak, A., Sóvágó, J., Ungváry, F., *Proc. of 9th Int. Sym. Hom. Cat.,* p340, Jerusalem, Israel (1994).

Marquardt, D.W., *J. Soc., Indust. Appl., Math.*, Vol **II**, No. **2**., 43 (1963).

Mason, R.F., van Winkle, J.L., US Patent 3 400 163, " Bicyclic Heterocyclic Sec- and Tert-Phosphines", Shell Oil Co. (1968).

Mason, R.F., van Winkle, J.L., US Patent 3 527 818, "Oxo Alcohols Using Catalysts Comprising Ditenary Phosphines", Shell Oil Co. (1970).

Massie, S.N.P., Vesely, J.A., German Patent 2 415 902 ; to UOP (1974).

Matsuzaka, H., Kodama, T., Uchida, Y., Hidai, M., *Organometallics*, **7**, 1608 (1988).

McGrath, H.G., US 2 543 327 for M.W. Kellog Co. (1951).

Mieczyńska, E., Trzeciak, A.M., Ziółkowski, J.J., *J. Mol. Catal.*, **73** 9 (1992).

Mieczyńska, E., Trzeciak, A.M., Ziółkowski, J.J., *J. Mol. Catal.*, **80**, 189 (1993).

Milstein, D., Huckoby, L.J., *J. Am. Chem. Soc.* , **104**, 6150 (1982).

Mirbach, M.J., Mirbach, M.F., Saus, A., Topalsavoglou, N., Nhu Phu, T., *J. Am.Chem. Soc.*, **103**, 7590 (1981).

Morris, R.C., Bauer, R.S., Chung, H., Keim, W., and van Zwet, H., DE Patent 2062335, "Ethylene polymerization catalysts", to Shell Internationale Research Maatschappij N.V. (1971).

Muetterties, E.L., and Stein, J., *Chem. Rev.* **79** (6), 479 (1979).

Nagel U., Kinzel, E., *Chem. Ber.*, **119**, 1731 (1986).

Natta, G., Ercoli, R., Castellano, S., *Chim. Ind.*, **34**, 503 (1952).

Natta, G., Ercoli, R., Castellano, S., *J. Amer. Chem. Soc.*, **76**, 4049 (1954).

Natta, G., Ercoli, R., Castellano, S., *Brennstoff-Chem.*, **36**, 176 (1955).

Nieuwenhuis, R.A., *Pet. Tech.*, **268**, 46-50 (1980).

Onoda, T., *Chemtech*, p34-37, September (1983).

Orchin, M., Kirch, L., Goldfarb, J., *J. Am. Chem. Soc.*, **78**, 5450 (1956).

Orchin, M., Kirch, L., *J. Am. Chem. Soc.*, **80**, 4428 (1958).

Orchin, M., *J. Am. Chem. Soc.*, **81**, 3597 (1959).

Orchin, M., Karapinka, G., Abstracts 137th A.C.S. Meeting, Cleaveland, Ohio, pp 92-100, April (1960).

Orchin, M. and Rupilius, W., *Catal. Rev.* **6**, 85 (1972).

Osborn, J.A., Wilkinson, G., Young, J.F., *J. Chem. Soc., Chem. Commun.*, 17 (1965).

Oswald, A.A., Hendricksen, D.E., Kastrup, R.V., Merola, J.S., Reish, J.C., in Proc.of the 1982 Lubrizol Award Symposium of the Petroleum Chem. Div. Inc., National Meeting of the Am. Chem. Soc., Las Vegas, Nevada (1982).

Oswald, A.A., Hendricksen, D.E., Kastrup, R.V., Mozeleski, E.J., in Homogeneous Transition Metal Catalyzed Reactions:- Electronic Effects on the Synthesis" Chp. 27, p395, Am. Chem. Soc. (1992).

Ozaki, A., and Aika, K., in "Catalysis Science and Technology, Vo1", Eds. J.R. Anderson and M. Boudart, Springer, Berlin (1981).

Paulik, F.E., *Catal. Rev.* **6**, 49 (1972).

Pichler, H., Ziesecke, K-H., *Brenst. Chem.*, **30**, 333, (1939).

Pichler, H., *ibid.* Vol. **4** (1952).

Pichler, H., in "Advan. Catal. Vol. 4", Eds. Frankenburg, Komarewsky and Rideal, Academic Press Inc., New York, (1952).

Pichler, H., Schulz, H., Elstner, M., *Brennstoff-Chemie*, **48**, 78-87 (1967).

Pichler, H., Schulz, H., Kühne, D., *Brennst. Chem.*, **45** (11), 344 (1968).

Pichler, H and Schulz, H., *Chem. Ing. Tech.*, **42,** 1162, (1970).

Pino,P., Pucci, S., Piacenti, F., *Chem. Ind.* (London), 294 (1963).

Pino, P., Piacenti, F., Pucci, S., Bianchi, M., Lazzaroni, R., *J. Am. Chem. Soc.*, **90**, 6847 (1968).

Pino, P., Piacenti, F., and Bianchi, M., in "Organic Syntheis via Metal carbonyls, Vol. 2, p43, John Wiley and Sons, Inc., New York (1977).

Polievka, M., Mistrik, E.J., *Chem. Zvesti*, **26** (2), 149 (1972).

Pruett, R.L., Smith, J.A., *J. Org. Chem.*, **34** No. 2, 327-330 (1969).

Pruett, R.L., Smith, J.A., US Patent 3 527 809, Union Carbide Corp. (1970).

Pruett, R.L., Smith, J.A., US Patent 3 527 809, Union Carbide Corp. (1970).

Pruett, R.L., Smith, J.A., UK Patent 1 338 237, Union Carbide Corp. (1973).

Pruett, R.L., in "Advances in Organometallic Chemistry", Hydroformylation, pp1-60, Vol 17, Academic Press (1979).

Pryde, E.H., Frankel, E.N., Cowan, J.C., *Am. J. Oil Chem. Soc.*, **49**, 451 (1972).

Renaud, E., Russel, R.B., Fortier, S., Brown, S.J., Baird, M.C., *J. Organomet. Chem.*, **419**, 403 (1991).

Roberts, D.A., Geoffrey, G.L., in "Comprehensive Organometallic Chemistry", Eds. G.A. Wilkinson, F.G.A. Stone, E.W. Abel, Vol. 6, Pergamon, Oxford (1982).

Roder, K., and Werner, H., *Agnew. Chem. Int. Ed.* Engl., **26** (7), 686 (1982).

Roelen, O., German Patent, 849 548 (1938).

Roelen, O., U.S. Patent, 2 317 066 (1943).

Roelen, O., in "Naturforschung und Medizin in Deutschland 1939-1946", **36**, 166, Ed. K. Ziegler, Dieterich'sche Verlagsbuchhandlung, Wiesbaden (1948).

Rofer-De Poorter, C.K., *Chem. Rev.*, **81**, 447 (1970).

Rogier, E.R., US Patent 4 216 343, to Henkel Corp. (1980).

Ross, J., *Appl. Catal.* (A.Gen.), **125**, No.1, N3 (1995).

Rottig, W., DE 897,698 to Ruhrchemie (1948).

Rylander, P.N., "Organic Synthesis with Nobel Metal Catalysts", Academic Press, New York and Londodn, 215 (1973).

Sabatier, P., and Senderens, J.B., *Hbd. Seances Acad. Sci.*, **134,** 514 (1902).

Sadtler and Heyden; The Sadtler Standard Gas Chromatography Retention Index Library; Vol. 4 (1986).

Sanchez-Delgado, R.A., Bradley, J.S., Wilkinson, G., *J. Chem. Soc., Dalton Trans.*, 399 (1976).

Sanger, A., *J. Mol. Catal.*, **3**, 221 (1977/78).

Schultz, H.S., Bellstedt, F., *Ind. Eng.Prod. Res. Dev,* **12**, 176 (1973).

Schulz, G.V., *Z. Phys. Chem. Abt. B.*, **30**, 379 (1975).

Schulz, H., in ""Chemical Feedstocks from Coal" (Translated from "Chemierohstoffe aus Kohle" originally published in 1977), Ed. J. Falbe, Chapter 8.4 pp 392-421, John Wiley and Sons inc., New York (1982).

Schulz, H., Geertsema,A., *Erdöl und Kohle*, **39**, 93 (1977).

Schulz, H., Erdöl und Kohle-Erdgas-Pertochemie vereinigt mit Brennstoff Chemie; **30**, Nr.3, p123-131 (1977).

Schulz, H., Erich, E., Gorre,H., van Steen,E., *Catalysis Letters,* **7**, pp157-168 (1990).

Schulze J., in "Chemical Feedstocks from Coal" (Translated from "Chemierohstoffe aus Kohle" originally published in 1977), Ed. J. Falbe, Chapter 12. pp 512-584, John Wiley and Sons inc., New York (1982).

Sie, T., Senden, M.M.G., van Wechem, H.M.H., *Catalysis Today*, **8**, 371-394, (1991).

Singleton, D.M., Glockner, P.W., Keim, W., DE Patent 2159370 to Shell Internationale Research Maatschappij N.V., June (1972).

Slaugh, L.H., Mullineaux, R.D., US Patent 3 239 566, to Shell Oil Co. (1966).

Slaugh, L.H., and Mullineaux, R.D., US Patent 3 239 569, Shell Oil Co. (1966).

Slaugh, L.H., Mullineaux, R.D., US Patent 3 239 570, to Shell Oil Co. (1966).

Slaugh, L.H., Mullineaux, R.D., US Patent 3 239 571, Shell Oil Co. (1966).

Slaugh, L.H., Mullineaux R.D., US Patent 3 448 157, to Shell Oil Co. (1969).

Slaugh, L.H., Mullineaux, R.D., US Patent 3 448 158, to Shell Oil Co. (1969).

Slaugh L.H., Mullineaux, R.D., *J. Organometal. Chem.*, **13**, 469 (1986).

Sofianos, A., *Catalysis Today*, **15**, 149 (1992).

Soled, S.L., Miseo, S., Iglesia, E., Fiato, R.A., US 5 100 856, to Exxon Research and Engineering Co. (1992).

Sorenson, J.P.,Stewart, W.E., *AIChE. J.*, **26**, 98 (1980).

Spitzer, E.L.T.M., *Siefen, Oele, Fette, Wacshe*, **107** (6), 141-143 (1981).

Storch, H.H., Golumbic, N., and Anderson, R.B., in "The Fischer-Tropsch and Related Syntheis", John Wiley, New York (1951).

Streitwieser, A., Heathcock, C.H., "Introduction to Organic Chemistry", 2nd Ed., p516, p613, MacMillan Publishing Co. Inc., New York (1981).

Tannenbaum, I., *Proc. of 9th Int. Sym. Hom. Cat.,* p375 Jerusalem, Israel (1994).

Thayer, A.M., *C&EN*, p26, 25 Jan. (1993).

Trzeciak, A.M., Ziółkowski, J.J., *J. Mol. Catal.*, **43,** 105 (1988).

Trzeciak, A.M., Ziółkowski, J.J., *J. Organomet. Chem.*, **390,** 105 (1990).

Trzeciak, A.M., Ziółkowski, J.J., *J. Organomet. Chem.*, **464,** 107 (1993).

Trzeciak, A.M., Szterenberg, L., Wolszczak, E., Ziółkowski, J.J., *J. Mol. Catal.* A: Chem., **99,** 23-28 (1995).

Tucci, E.R., *Ind. Eng. Chem. Prod. Res. Dev.*, **7**, 31, (1968).

Tucci, E.R., *Ind. Eng.Prod. Res. Dev.*, **7**, 32, 227 (1968).

Tucci, E.R., *Ind. Chem. Prod. Res. Develop.*, **9** No.4, 516-521 (1970).

Tummes, H., US 3 993 695 , to Ruhrchemie AG (1976).

Tummes, H., Heim, W., DE 1937 662 , to Ruhrchemie AG (1981).

Ungvary, F., Markó, L., *J. Organomet. Chem.*, **20**, 205-209 (1969).

van Berge, P.J., in *Proc. of the Int. Conf. on Cat. and Catal. Proc.*,Cape Town, South Africa (1993).

van Winkle, J.L., Morris, R.C., Mason, R.F., US Patent 3 440 291, Shell Oil Co. (1969).

van Winkle, J.L., Morris, R.C., Mason, R.F., US Patent 3 420 898, Shell Oil Co. (1969).

van Winkle, J.L., Morris, R.C., Mason, R.F., UK Patent 125403, to Shell International Research Maatschappij (1971).

van Vliet, A., US Patent 4 647 707, to Exxon Research and Engineering Co. (1987).

Vines, G., *New Scientist*, p 22, 26 August (1995).

Voevodski, V.V., Volkenshtein F.F., and Semenov, N.N., Proc. All Union Conf.-Probl. Chem. Catal. and Reactiv., Izd. Akad. Nauk. USSR, Moscow, pp 423 (1955).

Voorhies, A., Owen, J.J., Johnson, J.F., "The Oxo Process" in Advances in Petroleum Chemistry and Refining", Volume 1., Interscience, New York, 500-501 (1957).

Weber, J., German Patent Appl. 1290535 for Ruhrchemie AG (1968).

Wender, I., Orchin, M., and Storch, H., *J. Am. Chem. Soc.*, **72**, 4842 (1950).

Wender, I., Sternberg, H.W., Orchin, M., *J. Am. Chem. Soc.*, **75**, 3041 (1953).

Wender, I., Metlin, S. Erqun, S., Sternberg H.W., Greenfield, H., *J.Am. Chem. Soc.* **78**, 5401 (1956).

Wenzel, W., *Agnew. Chem.*, **B20**, 225 (1948).

Wiebus, E., Cornils, B., *Chem.-Ing.-Tech.* , **66**, Nr. 7 p916-923 (1994).

Wilkes, J.B., US Patent 3 928 232, to Chevron Res. Co. (1975).

Wood, C.D., Garrou, P.E., *Organometallics*, **3**, 170-174 (1984).

Kinetic References in Falbe, J., in "New Syntheses with Carbon Monoxide", Springer-Verlag, Berlin, (1980):

Alekseeva K.A. *et al.* C.A. 88, 5850 d (1978).

Cappelli, A., D'Angeli, C., Andreetta, A., Capparella, G., *Chem. React. Eng. Proc. Int. Symp. 4th,* p186 (1976).

Cavelien d'Oro, P., *et al.*; Paper presented at Symp. on Rhodium in Homog. Catalysis; Veszprenn, p76, Sept (1978).

Happel, J., Csuha, R.S., *J. Catal.*, **20,** 132 (1971).

Happel, J., Csuha, R.S., *Al ChE. J.*, **17**, 927 (1971).

Heil, B., Marko, L., *Chem. Ber.*, **104**, 3418 (1991).

Heil, B., Marko, L., *Chem. Ber.* **102**, 2238 (1969).

Hignett, R.R., Davidson, P.J., DE-OS Patent 2 827 301 to Johnson Matthey and Co Ltd. (1979).

Angelici, R.J., *J. Organomet. Chem. Rev.* **3**, 173 (1968).

Hignett, R.R., Davidson, P.J., DE-OS Patent 2 827 300 to Johnson Matthey and Co Ltd. (1979).

Marko, L., *Acta Cient,* Venez. Supl. **24** (2), 49 (1973).

Marko, L., Ugo, R., Aspects of Homogeneous Catalysts, D. Riedel Publ. Comp., Dortrecht (1974).

Oliver, K.L., Booth, F.B., *Erdöl und Kohle*, **24**, 346 (1971).

Orchin, M., Rupilius, W., *Catal. Rev.* **6** (1), 85 (1972).

Polyakov, A.A., Gankin, W. Yu., Rybakov, V.A., Fuks, I.S., *Int. Chem. Eng.*, **16**, 518 (1976).

Thompson, D.T., Whyman, R., In: Schrauzer, GN (Ed): "Transition Metals in Homogeneous Catalysis", New York, Marcel Dekker (1971).

Tjan, P.W.H.L., Scholten, J.F., Proc. Int. Congr. Catal. 6th (1976).

Wender, I., Pino, P., "Organic synthesis via Metal Carbonyls", Vol. **2**, Wiley-Interscience Publ. (1976).

Whyman, R., *J. Orgomet. Chem.*, **94**, 303 (1975).

Wysokinskii, G.P., Gankin, Yu. W., Rudkowskii , D.M., (Ed.), in "Carboxylation of Unsaturated Hydrocarbons", Allunions Sci. Res., Inst. for Petrochem Proc., Leningrad, Chem. Dep. p27f (1968).

Wysokinskii, G.P., Gankin, W. Yu., Rudkowskii, D. M., Katal. Reakts. Zhidk. Faze, Tr. Vses. Konf. 2nd. (1966); C.A. 69, 18 367j (1968).

APPENDICES

APPENDIX 1

Example of 1-Decene Hydroformylation

GC trace of reactor liquids at intermediate conversion:
1-Decene feed : Run 36.

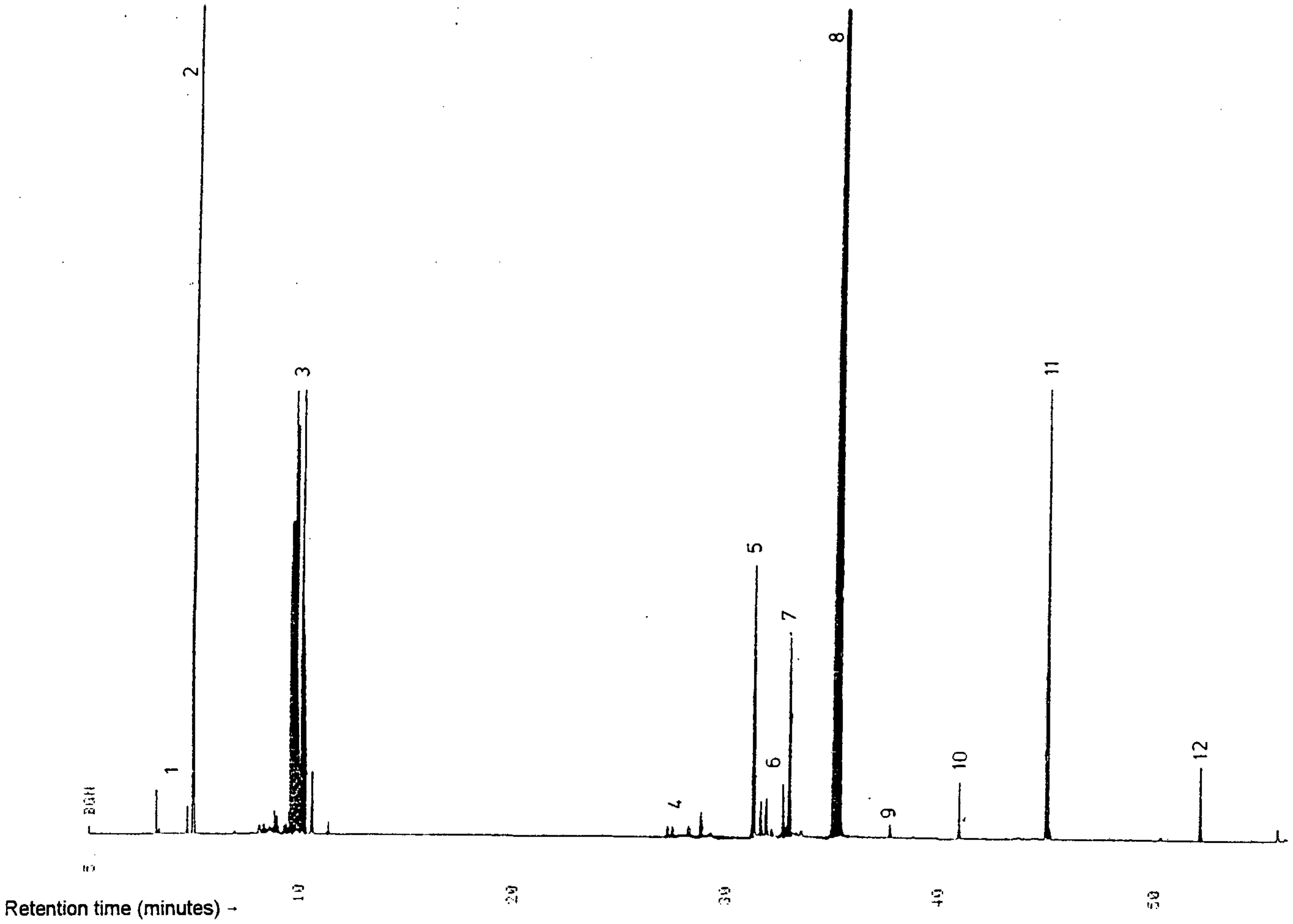

Key to the numbered peaks (MS identification):

1	n-Octane impurities.
2	n-Octane.
3	Region of remaining decene (internal olefins) and n-decane.
4	Branched aldehydes (formed by hydroformylation of internal olefins).
5	1-Undecanal.
6	Branched alcohols (formed by hydrogenation of branched aldehydes).
7	2-Methyl decanol.
8	1-Undecanol.
9	Ester (formate).
10	Ester (decyl acetate).
11	Hexadecane.
12	Phthalate impurity.

GC trace of reactor liquids after 100% conversion:
1-Decene feed : Run 36.

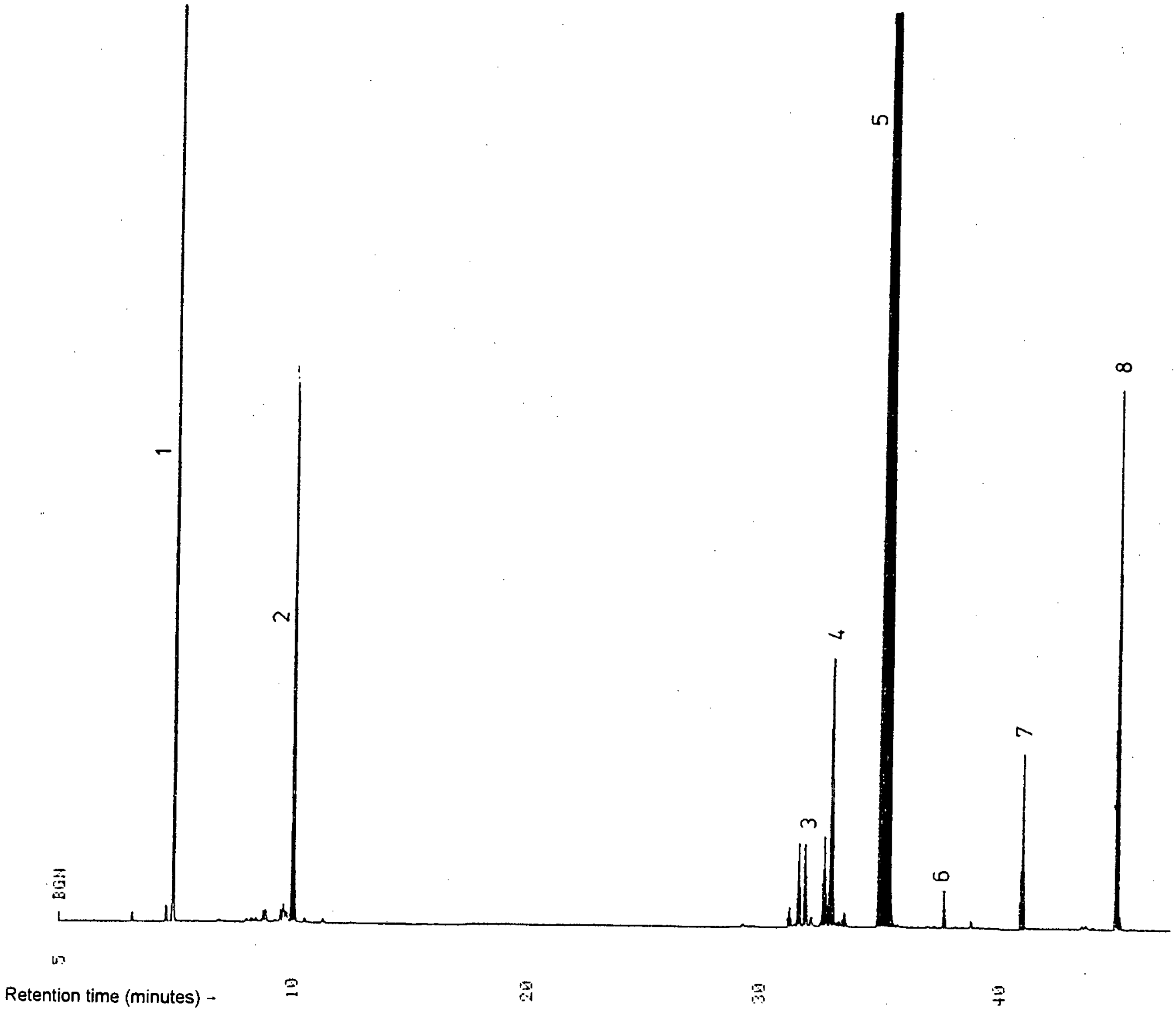

Key to the numbered peaks:

1	n-Octane.
2	n-Decane.
3	Branched alcohols.
4	2-Methyl decanol.
5	1-Undecanol.
6	Ester (formate).
7	Ester (decyl acetate).
8	Hexadecane.

Spreadsheet results of GC data workup: 1-Decene feed; Co/TOP catalyst: Run 36.

		TOS (hours)	0.00	1.00	2.00	3.00	4.00	5.00	6.17	7.00	8.00
Resp. Fac.	Ret. time	SPECIES	mass%	mass%	mass%	mass%	mass%	mass%	mass%	mass%	mass%
1.00	3.63		0.25								
1.00	2.98						0.30	0.51			0.37
1.00	4.93	n-octane	18.16	18.34	15.31	15.08	19.84	19.39	20.23	19.81	17.14
1.00	8.07	alpha olefin	0.26								
1.00	9.28	int olefin	0.00	0.26							
1.00	9.45	alpha olefin	0.42								
1.00	9.68	int olefin	0.00								
1.00	9.79	1-decene	72.19	4.40	1.77	0.91	0.72	0.78	0.58	0.61	0.35
1.00		int olefin		7.94	11.33	11.89	10.12	8.59	6.54	5.36	4.68
1.00	9.93	int olefin	0.29	9.94	9.58	7.92	6.21	5.21	3.83	3.19	2.69
1.00		int olefin			2.13	1.63	1.22	0.99	0.73	0.60	0.51
1.00	10.22	n-decane	0.72	2.62	4.89	6.11	6.27	6.65	6.84	6.76	6.03
1.00	10.22	int olefin	0.00	19.27	9.65	5.66	3.87	3.08	2.20	1.87	1.45
1.00	10.64	*	0.37	6.84	3.93	2.33	1.61	1.29	0.93	0.77	0.64
0.80	16.78	*						0.26			
0.80	28.17	aldehyde		0.27	0.33	0.30				0.24	1.17
0.80	28.77	*		1.13	0.88	0.58	0.39	0.31		0.24	0.98
0.80	29.25	2me-decanal					0.25			0.30	
0.80	31.28	1-undecanal		9.25	6.60	4.28	2.68	2.20	1.66	1.48	
0.80	31.60	alcohol				0.29	0.36	0.54	0.67	0.79	
0.80	31.87	*				0.37	0.46	0.61	0.74	0.85	0.99
0.80	32.66	*			0.46	0.72	0.68	1.00	1.16	1.27	1.45
0.80	32.99	2me-decanol		1.00	2.17	3.11	3.44	3.79	4.26	4.50	4.92
0.80	35.24	1-undecanol									28.46
0.80	35.28	*		11.02	21.19	30.87	33.78	27.66	40.84	43.37	8.15
0.80	35.33	*						9.52			12.29
0.80	37.86	Ester								0.27	0.30
0.80	38.94	*			0.31				0.32		
0.80	40.93	*			0.33	0.36	0.45	0.54	0.67	0.69	0.85
0.80	44.59	*	0.43								
0.80	45.04	n-hexadecane	6.91	6.60	6.75	6.60	6.19	6.17	6.18	6.17	6.15
0.80	46.24	Heavy Oxo Fraction	0.00						0.26		
0.80	51.24	*	0.00						0.25		
0.60	52.14	*	0.00	1.12	2.19	1.00	0.91	0.90	0.84	1.04	0.43
0.80	52.98	*	0.00						0.25		
			100.00	100.00	84.69	84.92	100.00	100.00	100.00	100.00	100.00
0.80	68.35	TOP	3.85	3.51	2.19	1.64	0.72	0.52	0.53		0.76
0.80	76.37	TOP=O	1.02	1.73	2.77	4.90	4.42	4.17	6.44	4.58	3.40

Using Dilution Factor

Results	0.00	1.00	2.00	3.00	4.00	5.00	6.15	7.00	8.00
Based on a-olefin:									
% 1-decene conversion		93.58	97.34	98.61	98.89	98.78	99.09	99.03	99.45
% alpha decene conversion		93.96	97.50	98.70	98.95	98.88	99.14	99.09	99.48
% total decene conv.		30.31	43.28	54.45	64.13	69.21	77.09	80.70	83.79
% 1-decene product linearity		95.31	92.75	91.86	90.81	91.23	90.88	90.32	90.50
% overall product linearity		89.43	67.83	86.73	86.23	86.32	86.14	84.54	83.17
Based on a-olefin converted:									
% decane selectivity		2.99	6.28	8.01	8.88	9.54	10.04	9.93	11.55
% aldehyde selectivity		13.68	9.69	8.30	4.37	3.33	2.25	3.08	2.77
% alcohol selectivity		15.26	29.22	42.80	50.75	58.56	63.62	67.87	69.69
% internal olefin selectivity		68.07	54.56	42.89	35.93	30.37	22.38	18.42	14.67
% heavy oxygenate selectivity		0.00	0.28	0.00	0.07	0.19	1.71	0.72	0.92
Normalized Total		100.00	100.00	100.00	100.00	100.00	100.00	100.00	100.00
Correction factor		1.01	0.99	0.97	1.04	1.04	1.04	1.04	0.99
Based on TOTAL olefin converted:									
% decane selectivity		9.52	15.45	15.30	13.64	13.81	13.14	12.43	13.98
% aldehyde selectivity		41.45	21.84	11.68	6.43	4.55	2.75	3.59	3.29
% alcohol selectivity		46.23	85.84	79.37	74.62	77.23	77.88	79.71	82.89
% heavy oxygenate selectivity		0.00	1.81	0.78	0.80	0.90	2.66	1.40	1.62
Normalized Total		97.21	104.74	107.11	95.49	96.30	98.44	97.13	101.75
Correction factor		1.00	1.00	1.00	1.00	1.00	1.00	1.00	1.00
Dilution factor	1.00	0.95	0.93	0.91	0.90	0.89	0.88	0.87	0.87
-ln(1-C)	0.00	0.38	0.57	0.79	1.03	1.18	1.47	1.64	1.82
a-ole: -ln(1-C)	0.00	2.81	3.69	4.34	4.56	4.47	4.78	4.70	5.26
Time (hours)	0.00	1.00	1.00	1.00	1.00	1.00	1.00	1.00	1.00
Mass%									
alpha-olefin	72.87	4.40	1.77	0.91	0.72	0.78	0.58	0.61	0.35
internal olefins	0.66	44.25	36.82	29.43	23.04	19.43	14.23	11.79	9.97
total olefin	73.52	48.65	38.59	30.34	23.77	20.21	14.81	12.40	10.32
decane	0.72	2.62	4.89	8.11	6.27	6.65	6.84	6.76	6.03
aldehydes	0.00	10.65	7.81	5.14	3.32	2.51	1.86	2.28	2.13
alcohols	0.00	12.01	23.82	35.36	38.95	43.12	47.68	50.79	54.29
heavies	0.43	0.00	0.63	0.36	0.45	0.54	1.76	0.98	1.15
other	25.32	26.06	24.25	22.68	27.24	26.97	27.25	26.82	24.09

APPENDIX 2

Example of SLO C_{10} Broad Fraction Hydroformylation

SLO C_{10} broad fraction (as used in run 29a): Expanded GC trace at zero conversion; Co/TOP catalyst.

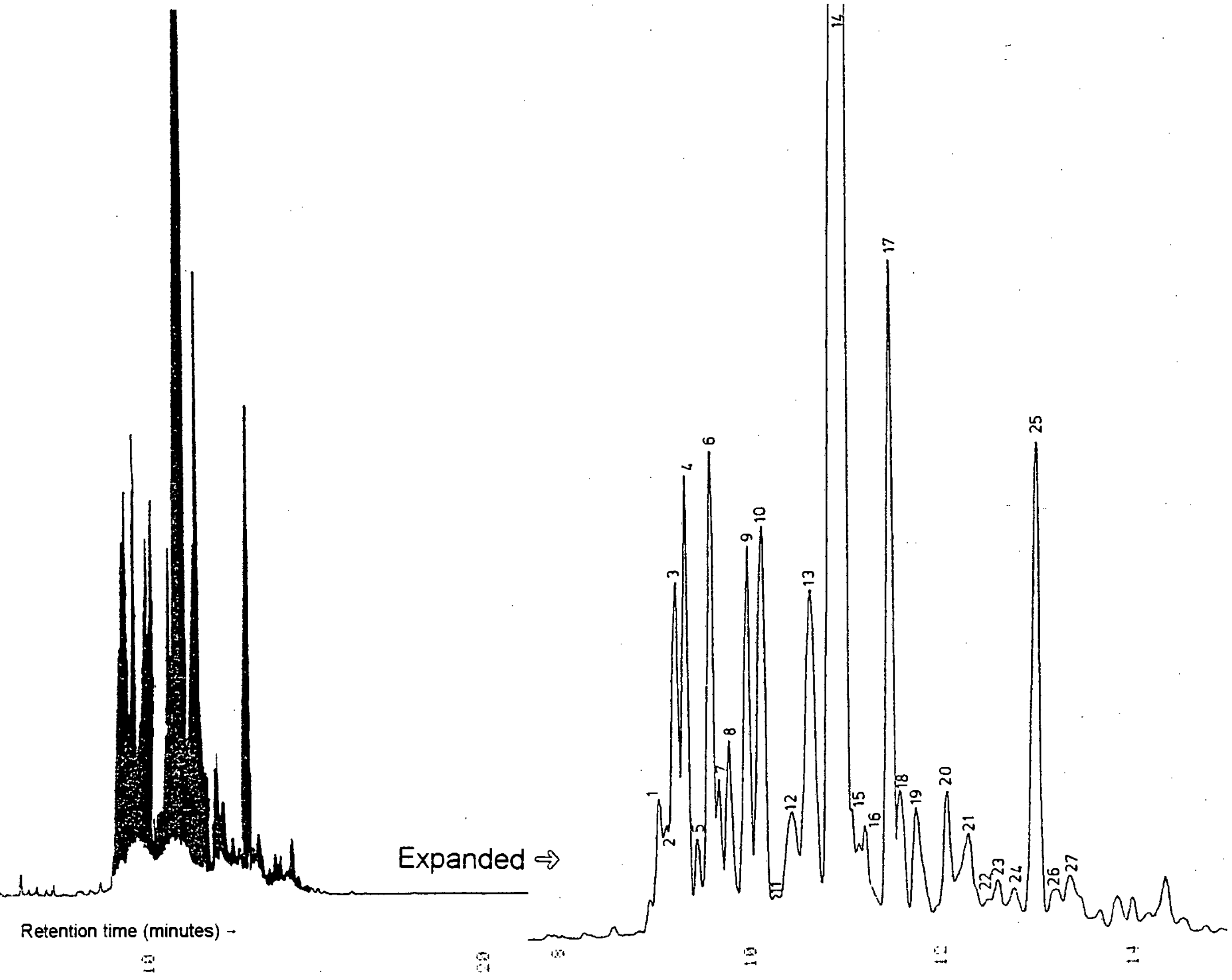

Key to GC-MS main peak identifications of numbered peaks: (Probable components in brackets)

1	C_{10} olefin
2	Oxygenate + internal olefin
3	C_{10} olefin
4	C_{10} olefin + aromatic
5	Aromatic + paraffin/olefin
6	C_{10} olefin
7	Paraffin + aromatic + C_{10} olefin
8	" " " "
9	Oxygenate + C_{10} olefin
10	Aromatic+ C_{10} olefin + paraffin
11	C_{10} internal olefin
12	Diene + cyclic olefin
13	C_{10} olefin + low aromatic
14	<u>1-Decene</u>
15	Internal olefin
16	Internal olefin
17	n-Decane
18	Internal olefin + aromatic
19	Aromatic
20	Internal olefin + unknown
21	Olefin / Aromatic
22	Aromatic + cyclic olefin
23	" " "
24	" " "
25	Aromatic
26	Aromatic + paraffin
27	Aromatics

SLO C_{10} broad fraction (as used in run 29a): Expanded GC trace at intermediate conversion; Co/TOP catalyst. Demonstrates isomerization.

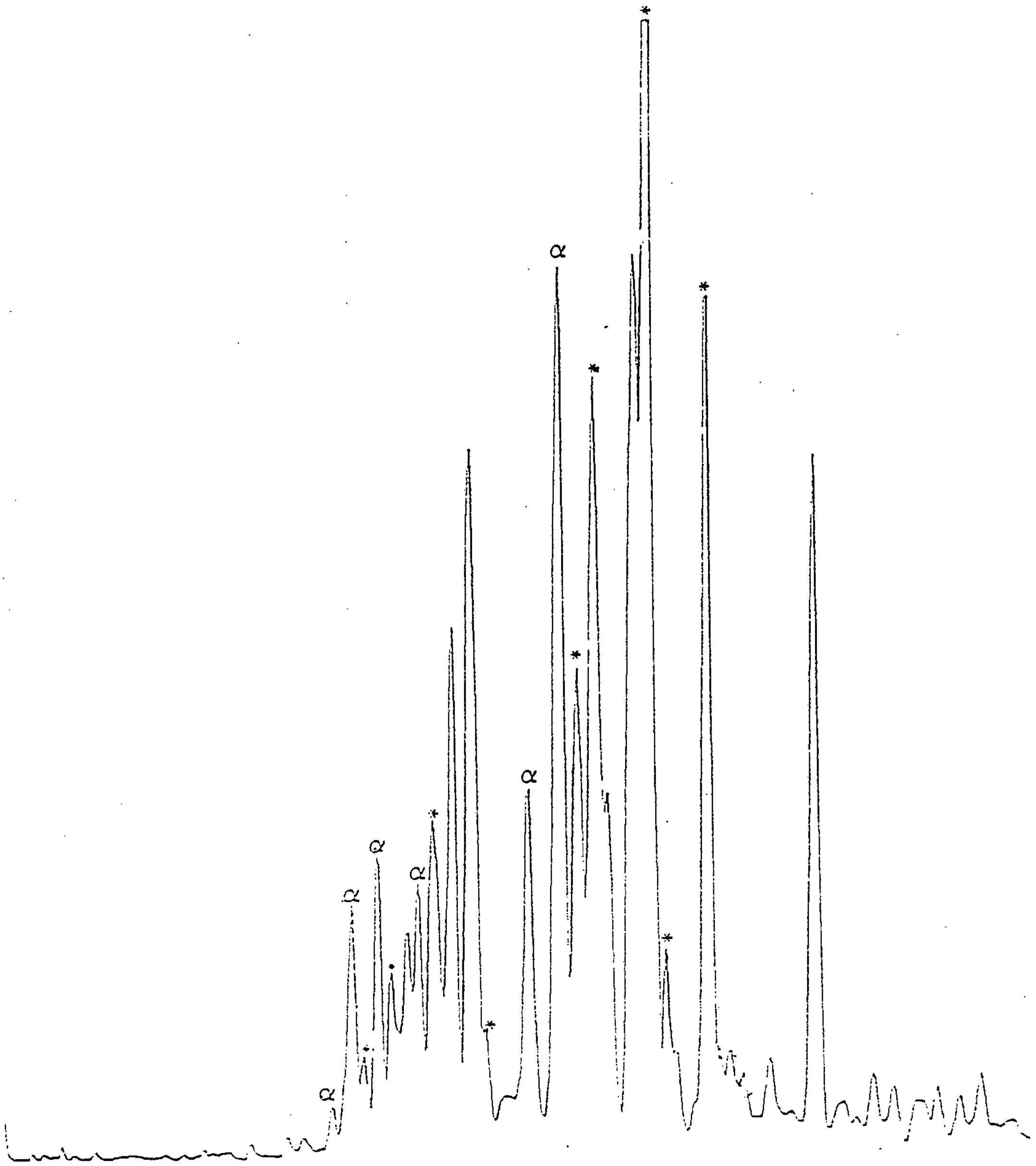

Isomerization in SLO: Composition at intermediate conversion

α Represents alpha olefins (remaining after isomerization to internal olefins).

✳ Represents internal olefins (mainly from α-olefin isomerization).

● Represents n-decane.

Balance of peaks (unmarked) represent F-T components (inert to hydroformylation).

SLO C_{10} broad fraction (as used in run 29a) remaining after exhaustive hydroformylation: Expanded GC trace; Co/TOP catalyst.

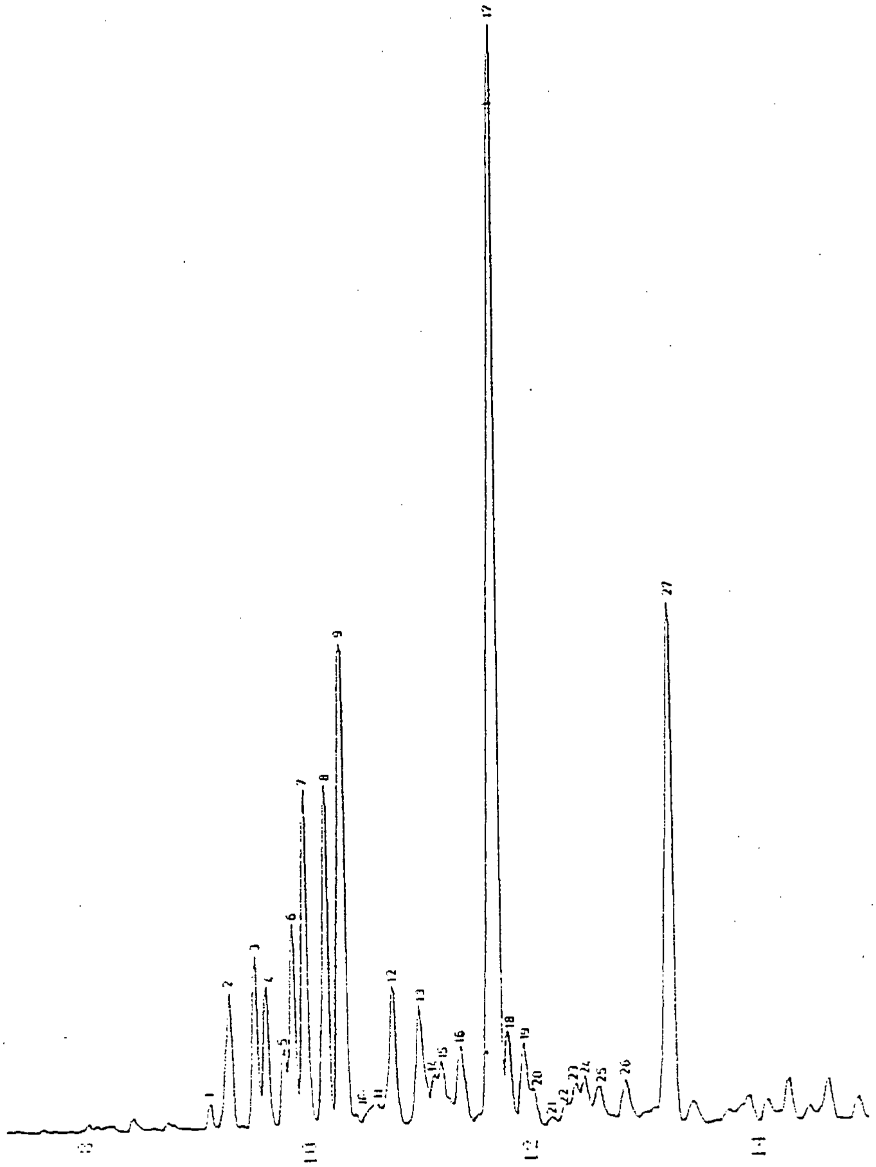

Key to GC-MS main peak identifications of numbered peaks:

1	Oxygenate
2	Oxygenate + aromatic
3	Aromatic
4	"
5	Paraffin
6	Paraffin
7	Paraffin + di-olefin
8	Oxygenate + low di-olefin
9	Aromatic + paraffin
10	Cyclic paraffin / olefin
11	Diene / cyclic olefin
12	Oxygenate + olefin (low)
13	Aromatic
14	Olefin/cyclic paraffin
15	" " "
16	Internal olefin
17	n-Decane + low diene
18	Aromaric + low diene
19	" " "
20	" " "
21	Diene /aromatic
22	"
23	"
24	Cyclic diene
25	Aromatic + diene
26	Aromatic
27	Aromatic + diene +paraffin
28	Aromatic

GC trace of reactor liquids at high conversion:
SLO C_{10} feed : Co/TOP catalyst; Run 29a.

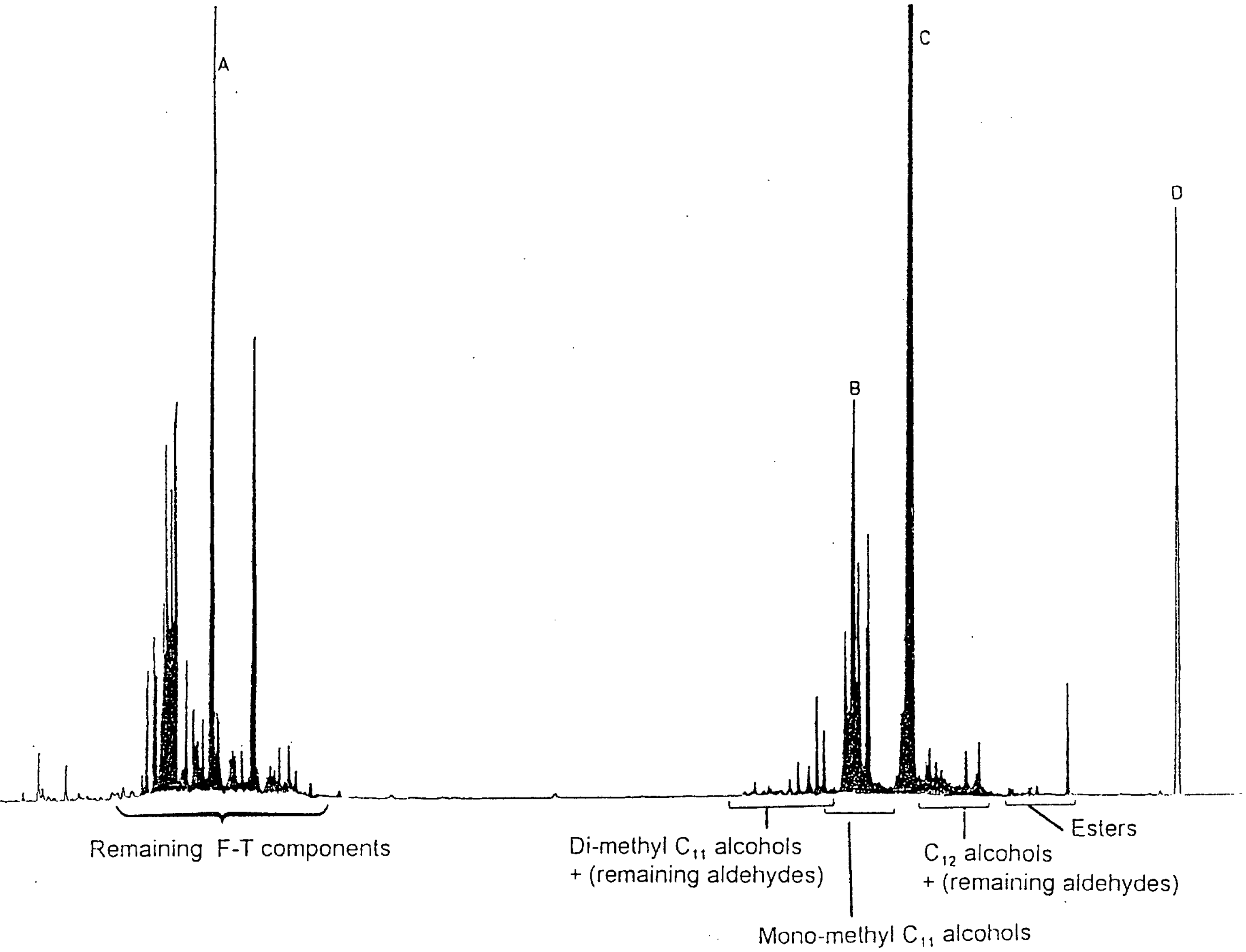

Key to main peaks:

A	n-Decane.
B	2 Methyl-decanol.
C	1-Undecanol.
D	Hexadecane internal standard.

Spreadsheet results of GC data workup: SLO C_{10} fraction feed; Co/TOP catalyst; Run 29a. Data breakdown and calculated results with TOS.

TOS (hours)	0.00	1.00	2.08	3.00	4.05	5.12	6.17	7.03	8.00	23.00
Mass% of component groups										
Olefins:										
a-olefin (6)	1.12	0.00	0.00	0.00	0.00	0.00	0.00	0.00	0.00	0.00
a-olefin (5)	3.20	0.55	0.13	0.69	0.00	0.00	0.00	0.00	0.00	0.00
a-olefin (4)	2.32	0.61	0.38	0.47	0.20	0.22	0.11	0.07	0.07	0.00
a-olefin (3)	3.35	0.93	0.30	0.21	0.08	0.06	0.04	0.02	0.02	0.00
a-olefin (2)	3.91	1.70	0.41	0.18	0.07	0.05	0.01	0.01	-0.03	0.00
1-decene (1)	36.04	9.27	7.50	5.15	6.17	4.92	3.94	3.32	2.72	0.00
int. branched (2-7)	0.00	4.16	2.54	2.11	0.87	0.92	0.39	0.22	0.37	-0.00
int. linear (1)	2.78	20.47	15.55	10.56	8.14	5.34	4.04	3.49	2.73	0.00
total br. a-olefin	13.90	3.80	1.22	1.55	0.36	0.33	0.16	0.09	0.06	0.00
total br. olefin	13.90	7.96	3.75	3.66	1.23	1.25	0.55	0.31	0.43	-0.00
total lin. olefin	38.82	29.75	23.05	15.71	14.31	10.25	7.98	6.81	5.45	0.00
total a-ole	49.94	13.08	8.72	6.70	6.53	5.25	4.09	3.41	2.78	0.00
tot int-ole	2.78	24.63	18.08	12.67	9.01	6.25	4.43	3.71	3.10	-0.00
total C10 olefin	52.72	37.71	26.80	19.37	15.54	11.50	8.53	7.12	5.88	-0.00
Aldehydes: from:										
a-olefin (6)	0.00	0.18	0.25	0.20	0.18	0.14	0.00	0.00	0.00	0.00
a-olefin (5)	0.00	0.46	0.43	0.28	0.22	0.16	0.10	0.00	0.00	0.00
a-olefin (4)	0.00	0.39	0.34	0.20	0.15	0.00	0.00	0.00	0.00	0.00
a-olefin (3)	0.00	0.48	0.41	0.25	0.17	0.00	0.00	0.00	0.00	0.00
a-olefin (2)	0.00	0.17	0.14	0.00	0.00	0.00	0.00	0.00	0.00	0.00
1-decene (1)	0.00	5.51	4.84	3.11	2.32	1.75	1.44	1.31	1.11	0.72
total br. a-olefin	0.00	1.68	1.57	0.94	0.72	0.30	0.10	0.00	0.00	0.00
total C11 aldehyde	0.00	7.19	6.41	4.04	3.04	2.05	1.54	1.31	1.11	0.72
Alcohols: from:										
a-olefin (6)	0.00	0.00	0.28	0.33	0.50	0.62	0.58	0.88	0.78	1.29
a-olefin (5)	0.00	0.40	1.27	1.74	2.32	2.60	2.90	3.02	3.64	3.55
a-olefin (4)	0.00	0.50	1.22	1.51	1.88	2.08	1.89	2.36	2.04	2.96
a-olefin (3)	0.00	0.37	1.29	1.76	2.33	2.85	3.14	3.27	3.31	3.90
a-olefin (2)	0.00	0.00	0.89	1.18	1.46	1.66	1.73	1.80	1.33	2.48
1-decene (1)	0.00	3.58	12.43	17.50	23.33	26.69	29.48	30.99	32.02	35.56
total int. olefin	0.00	0.38	0.58	1.00	1.00	0.74	0.80	0.81	1.16	1.14
total br. a-olefin	0.00	1.27	4.95	6.52	8.48	9.80	10.24	11.32	11.09	14.19
total C11 alcohols	0.00	5.23	17.97	25.03	32.81	37.23	40.52	43.12	44.27	50.89
total C12 alcohols	0.00	0.00	1.96	2.47	3.53	3.98	4.18	4.35	4.46	5.15
Paraffin:										
n-decane	6.03	8.17	8.58	8.82	8.89	9.03	9.19	9.29	9.49	9.86
Heavy oxygenates:										
ester a	0.00	0.00	0.00	0.00	0.24	0.29	0.36	0.39	0.44	0.80
ester b	0.00	1.24	1.13	0.75	1.36	0.82	1.06	1.18	0.81	0.38
total	0.00	0.00	0.00	0.00	0.24	0.29	0.36	0.39	0.44	0.80
SLO: (balance)	41.25	41.71	40.24	42.74	39.49	39.90	39.87	38.77	38.80	37.74
dilution factor	1.00	0.97	0.94	0.93	0.92	0.91	0.90	0.90	0.89	0.88
-ln(1-C)	0.00	0.31	0.62	0.93	1.14	1.43	1.72	1.89	2.08	
Conversions + linearity:										
1-decene con. %		73.54	77.97	84.70	81.33	84.99	87.89	89.74	91.55	100.00
a-decene con. %		73.07	81.53	85.64	85.75	88.44	90.92	92.39	93.77	100.00
overall decene con. %		26.44	46.20	60.65	67.87	76.00	82.07	84.95	87.53	100.00
%1-decene prod. linearity		85.90	86.80	86.58	86.42	86.25	86.06	85.87	85.67	84.52
% overall product linearity		61.04	60.05	59.34	60.15	61.30	62.08	61.30	60.99	58.13
% Selectivities:										
Based on a-olefin:										
Paraffin/octane		6.62	7.98	8.53	8.47	8.88	9.22	9.24	9.63	10.08
Aldehyde		17.22	14.79	9.02	6.40	4.27	3.16	2.59	2.19	1.33
ALcohol		12.38	41.01	55.17	68.21	76.88	82.21	84.58	85.98	92.82
Int. olefin		63.78	36.22	27.29	16.50	9.45	4.79	2.93	1.45	-5.48
Heavies		0.00	0.00	0.00	0.42	0.52	0.62	0.66	0.74	1.25
Normalized total		100.00	100.00	100.00	100.00	100.00	100.00	100.00	100.00	100.00
correction factor (multiplied selectivites by for total =100%)		1.03	1.08	1.08	1.00	1.02	1.02	1.00	1.00	0.98
Based on total olefins :										
Paraffin/octane		18.29	12.51	11.73	10.14	9.81	9.68	9.52	9.78	9.56
Aldehyde		47.55	23.19	12.40	7.66	4.72	3.32	2.67	2.22	1.26
ALcohol		34.17	64.31	75.67	81.69	84.90	86.34	87.13	87.25	88.00
Heavies		0.00	0.00	0.00	0.51	0.57	0.65	0.68	0.75	1.18
Normalized total		100.00	100.00	100.00	100.00	100.00	100.00	100.00	100.00	100.00
correction factor		1.09	1.01	1.11	1.00	1.02	1.02	1.00	1.00	0.98
Corrected masses (mass units for modelling)										
par	6.03	8.40	9.08	9.45	9.69	9.93	10.18	10.36	10.60	11.22
ald	0.00	7.39	6.78	4.33	3.31	2.25	1.71	1.46	1.25	0.82
alc	0.00	5.38	19.02	26.80	35.76	40.95	44.90	48.08	49.50	57.89
heavy	0.00	0.00	0.00	0.00	0.26	0.32	0.39	0.44	0.49	0.90
olefin	52.72	38.78	28.37	20.75	16.94	12.55	9.45	7.94	6.58	-0.00

APPENDIX 3

Example of SLO $C_{11\text{-}12}$ Broad Fraction Hydroformylation

Spreadsheet results of GC data workup: SLO $C_{11\text{-}12}$ fraction feed; Co/EP catalyst; Run 53: Breakdown of components by structural class.

TOS (hours)	0 hrs	15 min	30 min	45 min	1 hr	1 hr 30	2hr	2 hr 45 min	4hr	5hr	6hr	7hr	24 hr
Mass% of component groups													
C11 Olefins:													
a-olefin (7)	0.20	0.02	0.10	0.01	0.01	0.09	0.02	0.14	0.09	0.10	0.08	0.05	0.00
a-olefin (6)	0.63	0.24	0.19	0.27	0.24	0.15	0.16	0.00	0.00	0.00	0.00	0.00	0.00
a-olefin (5)	0.74	0.38	0.22	0.12	0.08	0.06	0.05	0.03	0.02	0.04	0.03	0.01	0.00
a-olefin (4)	0.78	0.25	0.14	0.14	0.13	0.11	0.08	0.06	0.04	0.05	0.03	0.02	0.00
a-olefin (3)	0.09	0.14	0.06	0.00	0.00	0.00	0.00	0.00	0.00	0.00	0.00	0.00	0.00
a-olefin (2)	0.85	0.61	0.31	0.27	0.22	0.19	0.14	0.10	0.06	0.06	0.06	0.03	0.00
1-undecene (1)	8.87	3.55	1.44	1.35	0.99	0.55	0.29	0.37	0.20	0.19	0.17	0.14	-0.00
int. branched (2-5)	3.01	2.70	2.15	1.47	1.20	1.05	0.84	0.45	0.25	0.37	0.34	0.11	0.00
int. linear (1)	1.57	5.29	5.57	3.99	2.95	1.91	1.23	0.54	0.24	0.25	0.18	0.07	0.00
total br. a-olefin	3.28	1.64	1.01	0.82	0.68	0.59	0.45	0.32	0.21	0.28	0.20	0.12	0.00
total br. olefin	8.29	4.34	3.18	2.30	1.88	1.64	1.29	0.77	0.45	0.63	0.53	0.23	0.00
total lin. olefin	10.44	8.83	7.01	5.34	3.94	2.48	1.52	0.81	0.44	0.44	0.38	0.21	-0.00
total C11 olefin	16.73	13.17	10.17	7.64	5.82	4.11	2.81	1.68	0.89	1.06	0.89	0.44	-0.00
C12 Olefins:													
a-olefin (7)	0.50	0.42	0.31	0.17	0.15	0.16	0.12	0.08	0.05	0.11	0.09	0.03	
a-olefin (6)	1.11	1.10	0.98	0.92	0.74	0.60	0.47	0.34	0.19	0.19	0.14	0.07	
a-olefin (5)	1.89	-0.28	0.45	0.53	0.42	0.39	0.29	0.23	0.13	0.13	0.09	0.06	0.00
a-olefin (4)	1.57	2.10	1.04	0.65	0.54	0.32	0.21	0.11	-0.05	0.09	0.03	-0.04	0.00
a-olefin (2)	2.03	0.63	0.13	0.05	-0.07	0.01	-0.02	-0.04	-0.50	0.07	0.13	0.01	0.00
a-olefin (3)	1.41	0.91	0.68	0.52	0.39	0.28	0.20	0.13	0.05	0.09	0.08	0.03	0.00
1-dodecene (1)	13.11	4.53	3.47	3.00	2.21	1.19	0.64	0.39	0.05	0.10	0.02	-0.05	0.00
int. branched (2-6)	9.06	8.76	7.57	8.50	5.20	4.70	3.55	2.06	1.18	1.78	1.32	0.49	0.00
int. linear (1)	2.30	7.46	6.58	4.24	2.51	1.46	1.53	0.65	0.00	0.59	0.51	0.29	0.00
total br. a-olefin	8.51	4.90	3.59	2.84	2.17	1.76	1.28	0.85	-0.14	0.70	0.56	0.16	0.00
total br. olefin	15.97	12.14	9.88	8.25	6.48	5.71	4.23	2.49	0.80	2.18	1.65	0.55	0.00
total lin. olefin	15.41	11.99	10.05	7.24	4.72	2.65	2.17	1.04	0.05	0.69	0.53	0.24	0.00
total C12 olefin	31.38	24.13	19.92	15.49	11.21	8.35	6.41	3.53	0.85	2.86	2.17	0.80	0.00
total (C11+C12) olefin	48.11	37.30	30.09	23.13	17.02	12.46	9.22	5.22	1.74	3.93	3.07	1.24	0.00
Aldehydes: from:													
1-undecene (1)	0.00	1.86	2.31	2.18	1.64	1.11	0.74	0.54	0.15	0.13	0.15	0.05	0.13
total C12 aldehyde	0.00	2.70	3.47	3.34	2.73	1.92	1.03	1.01	0.59	0.45	0.44	0.29	0.13
1-dodecene (1)	0.00	2.70	3.40	3.09	2.66	2.11	1.85	1.74	0.00	0.00	0.00	0.00	1.90
total C13 aldehyde	0.00	4.35	5.56	5.11	4.55	3.76	2.84	2.34	0.57	0.33	0.32	0.00	1.90
C12 Alcohols: from:													
a-olefin (6)	0.00	0.14	0.24	0.31	0.33	0.43	0.47	0.55	0.52	0.54	0.62	0.57	0.73
a-olefin (5)	0.00	0.32	0.55	0.84	0.95	0.71	0.79	0.81	0.97	0.94	0.92	0.95	1.00
a-olefin (4)	0.00	0.00	0.00	0.00	0.00	0.00	0.58	0.71	0.68	0.75	0.72	0.73	0.76
a-olefin (3)	0.00	0.10	0.27	0.44	0.53	0.68	0.73	0.76	0.80	0.94	0.95	1.03	1.05
a-olefin (2)	0.00	0.19	0.35	0.52	0.62	0.72	0.76	0.82	0.98	0.95	1.08	0.96	1.21
1-undecene (1)	0.00	0.63	2.08	3.97	5.60	7.81	8.93	9.37	10.03	10.60	10.54	10.48	10.89
other*	0.00	0.37	0.98	1.01	1.24	1.70	1.72	1.89	2.10	2.08	2.18	2.29	2.18
total C12 alcohols	0.00	1.75	4.45	7.09	9.27	12.05	13.95	14.91	15.87	16.70	17.01	16.98	17.91
C13 Alcohols: from:													
a-olefin (7)	0.00	0.11	0.19	0.13	0.14	0.18	0.34	0.35	0.43	0.33	0.31	0.59	1.02
a-olefin (6)	0.00	0.13	0.40	0.51	0.54	0.78	0.89	1.05	1.20	1.06	1.07	1.25	1.27
a-olefin (5)	0.00	0.00	0.00	0.32	0.44	0.60	0.78	0.39	0.98	0.82	0.91	0.92	1.09
a-olefin (4)	0.00	0.15	0.33	0.48	0.61	0.77	0.95	1.14	1.15	1.29	1.22	1.35	1.31
a-olefin (3)	0.00	0.15	0.46	0.73	1.01	1.19	1.37	1.35	1.88	1.57	1.58	1.88	1.82
a-olefin (2)	0.00	0.12	0.50	0.73	1.00	1.23	1.41	1.59	1.94	1.92	1.63	1.85	1.84
1-dodecene (1)	0.00	0.97	3.43	6.44	8.86	11.65	13.98	14.66	15.72	15.84	15.79	15.64	16.17
other*	0.00	1.24	2.84	3.63	4.67	5.36	5.84	6.91	9.66	7.99	9.59	9.92	10.43
total C13 alcohols	0.00	2.97	8.16	12.97	17.37	21.77	25.54	27.45	33.07	30.53	31.11	33.60	34.95
tot C12+C13 alcohol	0.00	4.62	12.61	20.06	26.65	33.82	39.49	42.36	48.94	47.23	48.12	50.58	52.76
Paraffin:													
n-undecane	1.95	2.07	2.12	2.16	2.14	2.23	2.20	2.10	2.03	2.22	2.17	2.05	2.01
n-dodecane	2.70	3.00	3.08	3.21	3.16	3.27	3.29	3.16	3.01	3.33	3.22	3.03	3.05
Heavies:													
From Co(acetate)	1.55	1.51	1.48	1.46	1.45	1.43	1.42	1.41	1.40	1.40	1.40	1.39	1.38
Total Heavy oxygenates:	1.38	2.44	2.07	1.95	2.63	1.90	2.03	2.99	2.25	1.91	1.93	2.08	1.82
heavies from ole	0.14	0.93	0.59	0.49	1.19	0.47	0.51	1.58	0.85	0.51	0.43	0.59	0.44
SLO:													
(balance)	45.55	43.51	41.00	41.03	41.12	40.64	39.90	40.83	40.85	40.50	40.83	40.73	38.32
mass% added													
C12 products	-0.00	0.01	0.02	0.02	0.02	0.03	0.03	0.03	0.03	0.04	0.04	0.04	0.04
C13 products	-0.00	0.01	0.03	0.03	0.04	0.05	0.05	0.06	0.06	0.06	0.06	0.06	0.07
dilution factor	1.00	0.98	0.96	0.94	0.93	0.92	0.92	0.91	0.90	0.91	0.90	0.90	0.99

GC trace of reactor liquids at high conversion: SLO $C_{11\text{-}12}$ feed : Run 53; Co/EP catalyst.

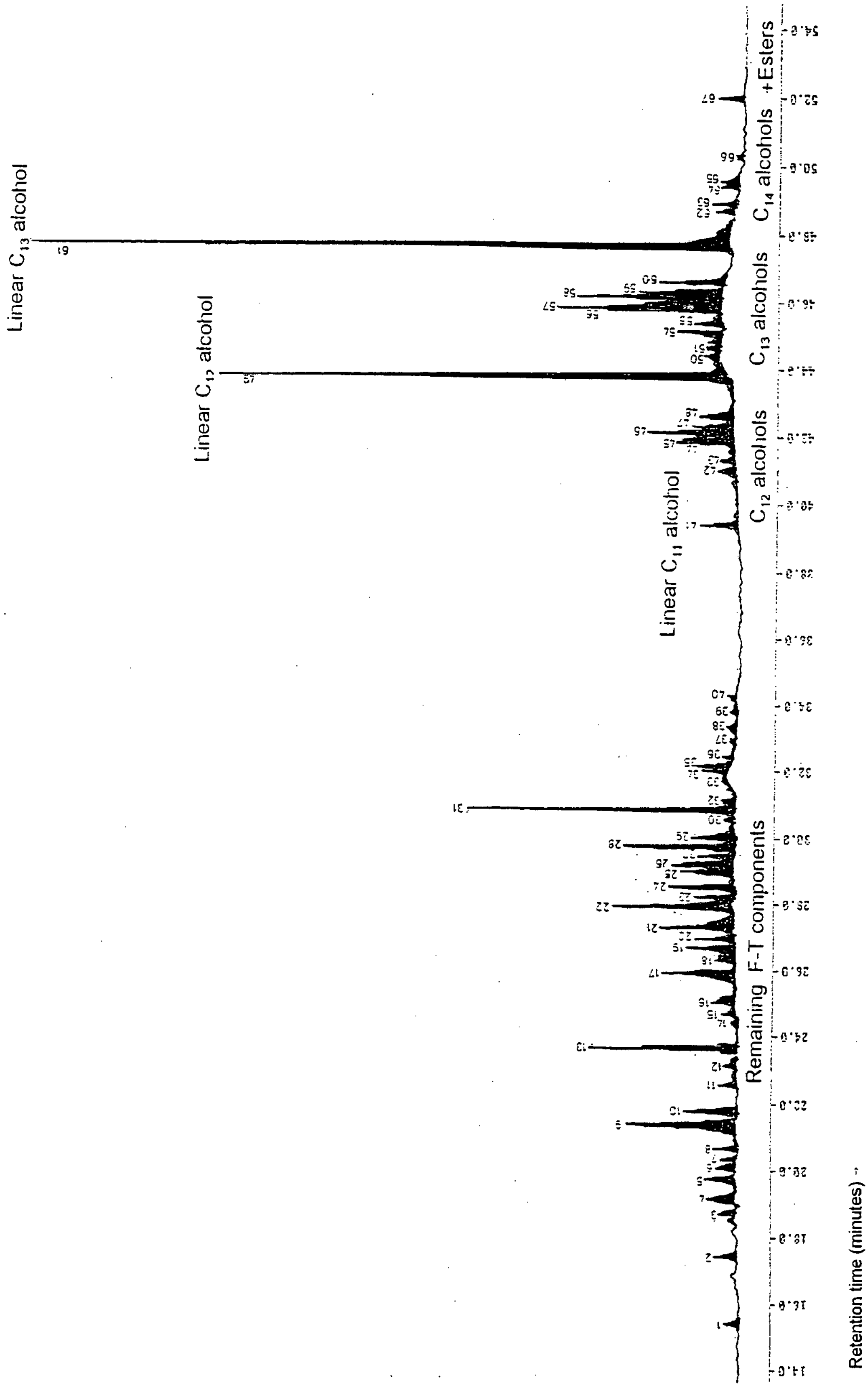

Key to GC-MS main peak identifications (numbered peaks):

1	Paraffin
2	Aromatic
3	Oxygenate + cyclic olefin/diene
4	Aromatic
5	Oxygenate + aromatic
6	Aromatic + paraffin
7	Paraffin
8	Paraffin
9	Aromatics + Oxygenates
10	Aromatic
11	Cyclic paraffin + cyclic olefin/diene
12	Aromatics + cyclic olefin /diene
13	n-Paraffin
14	Aromatic
15	Aromatic
16	Cyclic olefin /diene
17	Aromatics (various) + oxygenate
18	Oxygenate + aromatic
19	Aromatic + cyclic olefin
20	Oxygenate + aromatic
21	Aromatic
22	Oxygenate
23	Paraffin + aromatic
24	Paraffin
25	Paraffin + diene
26	Paraffin + oxygenate + aromatic
27	Aromatics
28	Aromatic +aromatic oxygenate
29	Oxygenate
30	Cyclic paraffin
31	n-Paraffin
32	Aromatics
33	Cyclic olefin/paraffin + aromatic
34	Aromatic + paraffin
35	Aromatics
36	"
37	"
38	"
39	"
40	Oxygenate
41	1-Undecanol
42-43	C_{12} alcohols (probably di-methyl branched)
44-45	C_{12} alcohols (mono-methyl branched)
46	2-Methyl undecanol
47-48	C_{12} alcohols(mono-methyl branched)
49	1-Dodecanol
50-56	C_{13} alcohols (mono and di-methyl branched)
57	2-Methyl dodecanol
58-60	C_{13} alcohols (mono -methyl branched)
61	1-Tridecanol
62-66	C_{14} branched alcohols + esters
67	Tridecyl acetate

Spreadsheet results of GC data workup: SLO $C_{11\text{-}12}$ fraction feed; Co/EP catalyst; Run 53: Various results including conversions; linearities and selectivities

TOS (hours)	0 hrs	15 min	30 min	45 min	1 hr	1 hr 30	2hr	2 hr 45 min	4hr	5hr	6hr	7hr	24 hr
Conversions + linearity:													
1-undecene con.%		59.09	83.05	83.87	88.04	93.27	96.43	95.39	97.54	97.61	97.83	98.21	100.00
a-undecene con.%		22.18	39.57	54.33	64.22	72.93	80.50	88.27	93.51	91.89	93.14	96.79	100.00
overall undecene con.%		19.47	36.57	51.69	62.78	73.40	81.63	88.95	94.08	92.98	94.10	97.09	100.00
1-undecene prod. linearity		88.25	88.23	88.65	88.29	84.57	86.10	84.93	84.91	85.12	84.97	85.55	85.10
overall C12 oxo product linearity		49.43	48.94	52.30	53.28	53.95	55.51	52.86	54.70	55.42	54.24	54.37	54.51
1-dodecene con.%		64.63	72.38	75.74	81.93	90.18	94.66	96.72	99.61	99.19	99.85	100.41	100.00
a-dodecene con.%		21.05	33.75	46.31	59.38	67.21	74.93	85.54	95.71	87.95	90.83	96.70	100.00
overall dodecene con.%		21.35	33.76	47.75	61.77	71.16	77.89	87.63	96.99	89.93	92.33	97.18	100.00
1-dodecene oxo prod. linearity		83.44	85.91	86.86	86.49	85.68	85.25	84.48	83.86	83.77	83.71	83.25	83.25
overall C13 oxo product linearity		28.16	36.12	43.14	44.12	45.84	46.66	45.12	39.86	43.47	42.50	39.24	38.52
average conversion		20.70	34.74	49.12	62.12	71.94	79.06	88.09	95.98	90.99	92.95	97.15	100.00
average linearity		35.55	40.58	46.32	47.31	48.66	49.74	47.81	45.02	47.63	46.58	44.50	44.09
Selectivities:													
Based on overall C11 olefin:													
Paraffin/undecane	0.00	2.52	2.76	2.87	2.43	3.03	2.76	1.89	1.53	2.69	2.35	1.58	1.40
Aldehyde	0.00	56.72	42.20	31.06	21.87	13.35	6.71	6.14	3.53	2.59	2.47	1.67	0.71
Alcohol	0.00	36.44	53.62	65.23	73.50	83.01	89.73	89.68	93.82	94.17	94.76	95.93	97.13
Heavies	0.00	4.32	1.42	0.85	2.20	0.61	0.80	2.29	1.12	0.55	0.42	0.81	0.75
total	0.00	100.00	100.00	100.00	100.00	100.00	100.00	100.00	100.00	100.00	100.00	100.00	100.00
correction factor	1.00	0.80	0.85	0.91	0.94	0.94	0.97	0.98	1.01	0.96	0.96	1.00	0.98
Based on overall C12 olefin:													
Paraffin/dodecane	0.00	0.30	1.28	2.03	1.58	2.04	1.98	1.43	0.88	2.08	1.68	0.98	1.08
Aldehyde	0.00	56.62	39.48	27.59	20.01	14.43	9.80	7.59	1.69	1.05	1.00	0.00	0.00
Alcohol	0.00	36.98	57.35	69.27	75.66	82.78	87.26	88.19	96.18	96.18	96.78	98.06	98.41
Heavies	0.00	6.10	1.89	1.12	2.75	0.76	0.96	2.79	1.25	0.69	0.53	0.96	0.50
total	0.00	100.00	100.00	100.00	100.00	100.00	100.00	100.00	100.00	100.00	100.00	100.00	100.00
correction factor	1.00	1.01	0.85	0.90	0.94	0.93	0.91	0.96	0.95	0.96	0.97	0.95	0.94
Summary of reactor contents (mass %)													
C11 olefins													
linear (alpha and int.)	10.44	8.83	7.01	5.34	3.94	2.46	1.52	0.81	0.44	0.44	0.36	0.21	-0.00
branched	6.29	4.34	3.16	2.30	1.88	1.64	1.29	0.77	0.45	0.63	0.53	0.23	0.00
C12 olefins													
linear (alpha and internal)	15.41	11.99	10.05	7.24	4.72	2.85	2.17	1.04	0.05	0.69	0.53	0.24	0.00
branched	15.97	12.14	9.88	8.25	6.48	5.71	4.23	2.49	0.80	2.18	1.65	0.55	0.00
C12 aldehydes													
linear (alpha and internal)	0.00	1.88	2.31	2.18	1.64	1.11	0.74	0.54	0.15	0.13	0.15	0.05	0.13
branched	0.73	1.43	1.71	1.72	1.58	1.28	0.59	0.74	0.65	0.54	0.48	0.42	0.15
C13 aldehydes													
linear (alpha and internal)	0.00	2.70	3.40	3.09	2.66	2.11	1.85	1.74	0.00	0.00	0.00	0.00	1.90
branched	0.00	1.65	2.16	2.02	1.88	1.65	0.99	0.60	0.57	0.33	0.32	0.00	0.00
C12 alcohols													
linear (alpha and internal)	-0.12	0.40	1.76	3.57	5.22	7.43	8.59	9.03	9.74	10.29	10.24	10.20	10.62
branched (from linear)	0.12	0.23	0.32	0.40	0.38	0.38	0.34	0.34	0.29	0.31	0.31	0.28	0.27
branched (from branched)	0.00	1.12	2.37	3.12	3.67	4.25	5.03	5.54	5.84	6.10	6.47	6.50	6.92
linear selectivity from linear olefins	ERR	63.19	84.73	89.94	93.25	95.17	96.24	96.39	97.11	97.06	97.09	97.34	97.51
C13 alcohols													
linear (alpha and internal)	0.00	0.40	2.72	5.78	8.26	11.16	13.57	14.29	15.35	15.52	15.48	15.48	15.88
branched (from linear)	0.00	0.57	0.71	0.66	0.60	0.48	0.41	0.37	0.35	0.33	0.32	0.38	0.29
branched (from branched)	0.00	1.90	4.73	6.53	8.51	10.12	11.56	12.79	17.35	14.69	15.32	17.78	18.78
linear selectivity from linear olefins	ERR	41.48	79.44	89.73	93.23	95.85	97.09	97.48	97.58	97.93	97.98	97.71	98.22
Product linearity from C11													
'linear ole reacted per 100 mass units fed		1.61	3.43	5.10	6.50	7.98	8.92	9.53	10.00	10.00	10.08	10.23	10.44
'branched ole reacted per 100 mass units fed		1.95	3.13	3.99	4.41	4.64	4.99	5.51	5.83	5.66	5.75	6.06	6.29
Expected linearity from olefin composition		28.59	44.32	50.46	55.54	60.16	61.71	61.08	61.34	61.98	61.82	61.13	60.86
linear prod. pre 100 mass units fed		0.40	1.76	3.57	5.22	7.43	8.59	9.03	9.74	10.29	10.24	10.20	10.62
branched prod. pre 100 mass units fed		1.35	2.69	3.52	4.05	4.62	5.36	5.88	6.13	6.41	6.78	6.78	7.19
Measured prod linearity		22.80	39.60	50.38	56.29	61.64	61.55	60.59	61.38	61.60	60.17	60.09	59.61
Product linearity from C12													
'linear ole reacted per 100 mass units fed		3.42	5.36	6.17	10.68	12.76	13.23	14.36	15.36	14.72	14.88	15.16	15.41
'branched ole reacted per 100 mass units fed		3.83	8.10	7.72	9.49	10.26	11.74	13.48	15.17	13.80	14.32	15.42	15.97
Expected linearity from olefin composition		29.81	39.65	46.23	49.38	52.75	51.00	49.72	48.85	50.11	49.47	49.27	47.89
linear prod. pre 100 mass units fed		0.40	2.72	5.78	8.26	11.16	13.57	14.29	15.35	15.52	15.48	15.48	15.88
branched prod. pre 100 mass units fed		2.47	5.43	7.19	9.11	10.60	11.97	13.16	17.72	15.02	15.63	18.12	19.07
Measured prod linearity		14.00	33.39	44.56	47.56	51.29	53.14	52.06	46.43	50.82	49.74	46.06	45.44
Mass units for modelling													
C11	0.00	0.25	0.50	0.75	1.00	1.50	2.00	2.75	4.00	5.00	6.00	7.00	24.00
par	1.95	2.12	2.21	2.29	2.29	2.41	2.41	2.30	2.25	2.45	2.40	2.27	2.25
ald	0.00	2.76	3.62	3.53	2.92	2.08	1.13	1.11	0.66	0.50	0.49	0.32	0.14
alc	0.00	1.79	4.64	7.50	9.93	13.06	15.25	16.37	17.50	18.44	18.82	18.86	19.95
heavy	0.59	0.87	0.75	0.72	0.98	0.72	0.77	1.14	0.87	0.73	0.70	0.80	0.71
ole	16.73	13.47	10.61	8.08	6.23	4.45	3.07	1.85	0.99	1.17	0.99	0.49	-0.00
C12	0.00	0.25	0.50	0.75	1.00	1.50	2.00	2.75	4.00	5.00	6.00	7.00	24.00
par	2.70	3.07	3.21	3.39	3.38	3.55	3.59	3.47	3.34	3.87	3.56	3.37	3.42
ald	0.00	4.45	5.80	5.41	4.87	4.07	3.10	2.57	0.64	0.38	0.35	0.00	2.13
alc	0.00	2.93	8.51	13.73	18.60	23.58	27.90	30.14	36.67	33.72	34.42	37.33	39.15
heavy	1.10	1.63	1.41	1.35	1.84	1.35	1.45	2.14	1.63	1.38	1.32	1.51	1.33
ole	31.38	24.68	20.78	16.40	12.00	9.05	7.00	3.88	0.94	3.16	2.41	0.89	0.00

APPENDIX 4

Comparison of Results: "Internal standard" Versus Calculated "Dilution Factor" Methods

Calculated results for the same set of reactor contents. Run 36.

Using Dilution Factor

Results	0.00	1.00	2.00	3.00	4.00	5.00	6.15	7.00	8.00
Based on a-olefin:									
% 1-decene conversion		93.58	97.34	98.61	98.89	98.78	99.09	99.03	99.45
% alpha decene conversion		93.98	97.50	98.70	98.95	98.88	99.14	99.09	99.48
% total decene conv.		30.31	43.28	54.45	84.13	69.21	77.09	80.70	83.79
% 1-decene product linearity		95.31	92.75	91.86	90.61	91.23	90.88	90.32	90.50
% overall product linearity		89.43	87.83	86.73	86.23	86.32	88.14	84.54	83.17
Based on a-olefin converted:									
% decene selectivity		3.00	8.28	8.01	8.88	9.54	10.04	9.93	11.55
% aldehyde selectivity		13.75	9.69	8.30	4.37	3.33	2.25	3.08	2.77
% alcohol selectivity		15.33	29.22	42.82	50.75	56.56	63.62	67.87	69.89
% internal olefin selectivity		68.40	54.58	42.90	35.93	30.37	22.38	18.42	14.87
% heavy oxygenate selectivity		-0.49	0.28	-0.03	0.07	0.19	1.71	0.72	0.92
Normalized Total		100.00	100.00	100.00	100.00	100.00	100.00	100.00	100.00
Correction factor		1.02	0.99	0.97	1.04	1.04	1.04	1.04	0.99
Based on TOTAL olefin converted:									
% decane selectivity		9.52	15.45	15.30	13.84	13.61	13.14	12.43	13.96
% aldehyde selectivity		41.45	21.84	11.68	6.43	4.55	2.75	3.59	3.29
% alcohol selectivity		46.23	85.84	79.37	74.62	77.23	77.88	79.71	82.89
% heavy oxygenate selectivity		0.00	1.61	0.76	0.80	0.90	2.66	1.40	1.62
Normalized Total		97.21	104.74	107.11	95.49	96.30	98.44	97.13	101.75
Correction factor		1.00	1.00	1.00	1.00	1.00	1.00	1.00	1.00
Dilution factor	1.00	0.95	0.93	0.91	0.90	0.89	0.88	0.87	0.87
-ln(1-C)	0.00	0.36	0.57	0.79	1.03	1.18	1.47	1.64	1.82
a-ole: -ln(1-C)	0.00	2.81	3.69	4.34	4.56	4.47	4.78	4.70	5.28
Time (hours)	0.00	1.00	1.00	1.00	1.00	1.00	1.00	1.00	1.00
Mass%									
alpha-olefin	72.87	4.40	1.77	0.91	0.72	0.78	0.58	0.61	0.35
internal olefins	0.66	44.25	36.82	29.43	23.04	19.43	14.23	11.79	9.97
total olefin	73.52	48.65	38.59	30.34	23.77	20.21	14.81	12.40	10.32
decane	0.72	2.62	4.89	8.11	6.27	6.85	8.84	6.78	8.03
aldehydes	0.00	10.65	7.81	5.14	3.32	2.51	1.86	2.26	2.13
alcohols	0.00	12.01	23.82	35.36	38.95	43.12	47.68	50.79	54.29
heavies	0.43	0.00	0.83	0.36	0.45	0.54	1.78	0.96	1.15
other	25.32	28.06	24.25	22.68	27.24	26.97	27.25	26.82	24.09

Using Internal Standard

Results	0.00	1.00	2.00	3.00	4.00	5.00	6.15	7.00	8.00
Based on a-olefin:									
% 1-decene conversion		99.87	99.95	99.97	99.98	99.97	99.98	99.98	99.99
% alpha decene conversion		93.98	97.62	98.78	98.94	98.85	99.15	99.10	99.49
% total decene conv.		30.69	46.27	56.78	63.93	89.21	77.47	81.11	84.24
% 1-decene product linearity		95.31	92.75	91.86	90.81	91.23	90.88	90.32	90.50
% overall product linearity		89.43	87.83	88.73	88.23	88.32	86.14	84.54	83.17
Based on a-olefin converted:									
% decane selectivity		2.99	6.23	7.97	8.88	9.54	10.03	9.91	11.53
% aldehyde selectivity		13.75	9.70	8.31	4.37	3.33	2.25	3.06	2.78
% alcohol selectivity		15.34	29.28	42.87	50.74	56.57	63.65	87.91	69.94
% internal olefin selectivity		68.40	54.58	42.91	35.93	30.37	22.37	18.41	14.85
% heavy oxygenate selectivity		-0.49	0.24	-0.05	0.07	0.19	1.70	0.71	0.91
Normalized Total		100.00	100.01	100.00	100.01	100.00	100.00	100.00	100.00
Correction factor		1.02	1.05	1.02	1.03	1.04	1.06	1.06	1.02
Based on TOTAL olefin converted:									
% decane selectivity		9.33	13.57	13.85	13.76	13.61	12.84	12.08	13.46
% aldehyde selectivity		42.87	21.14	10.98	6.77	4.78	2.88	3.73	3.24
% alcohol selectivity		47.80	83.73	74.49	78.82	80.69	81.49	82.75	81.69
% heavy oxygenate selectivity		0.00	1.58	0.71	0.84	0.94	2.79	1.45	1.60
Normalized Total		100.00	100.00	100.00	100.00	100.00	100.00	100.00	100.00
Correction factor		1.05	1.09	1.03	1.04	1.04	1.07	1.07	1.02
-ln(1-C)	0.00	0.37	0.62	0.84	1.02	1.18	1.49	1.67	1.85
a-ole: -ln(1-C)	0.00	2.61	3.74	4.39	4.55	4.47	4.77	4.71	5.28
TIME (HRS)	0.00	2.00	2.00	3.00	4.00	5.00	8.15	7.00	6.00
Mass%									
alpha-olefin	72.87	4.40	1.77	0.91	0.72	0.78	0.58	0.61	0.35
internal olefins	0.86	44.25	36.82	29.43	23.04	19.43	14.23	11.79	9.97
total olefin	73.52	48.65	38.59	30.34	23.77	20.21	14.81	12.40	10.32
decane	0.72	2.62	4.89	8.11	8.27	6.65	6.84	6.76	6.03
aldehydes	0.00	10.85	7.81	5.14	3.32	2.51	1.86	2.26	2.13
alcohols	0.00	12.01	23.82	35.38	38.95	43.12	47.68	50.79	54.29
heavies	0.43	0.00	0.83	0.38	0.45	0.54	1.76	0.98	1.15
other	25.32	26.06	24.25	22.68	27.24	26.97	27.25	26.82	24.09

APPENDIX 5

Mass Balance Example

Hydroformylation of a SLO C_{10} narrow fraction in n-octane solvent (Run 16 described in Chapter 3). Rh TPP catalyzed reaction "1 litre" autoclave reactor.

Physical Constants

Species	Density (g/ml)	Molecular Weight
1-Decene	0.74	140.27
n-Decane	0.73	142.28
C_{11} aldehyde	0.825	170.3
C_{11} alcohol	0.83	172.31

The reactor liquids were weighed before being analyzed by gas chromatography.

Reactant mixture (including catalyst precursors)

Mass of reactant mixture = 157.66 g.
Mass % of decene (olefins) in reactant mixture = 41.93
Mass % of decane (paraffins) in reactant mixture = 1.92

⇒ Moles (olefin) in reactant mixture :

$$- \frac{41.93}{100} \times \frac{157.66}{140.27} - 0.47$$

⇒ Moles (paraffin) in reactant mixture :

$$- \frac{1.92}{100} \times \frac{157.66}{142.28} - 0.02$$

Products mixture (including catalyst)

Mass of product mixture = 162.35 g.
Mass % of decene (olefins) in product mixture = 1.88
Mass % of decane (paraffins) in product mixture = 8.66
Mass% of C_{11} aldehydes in product mixture = 35.47
Mass% of C_{11} alcohols in product mixture = 1.60

⇒ Moles (olefin) in product mixture :

$$- \frac{1.88}{100} \times \frac{162.35}{140.27} - 0.02$$

Similarly:
Moles (paraffin) in product mixture = 0.10
Moles (aldehyde) in product mixture = 0.34
Moles (alcohol) in product mixture = 0.02

Molar Balance

For every mole of olefin reacted, 1 mole of paraffin, aldehyde or alcohol is formed. From the moles calculated previously:

Moles of olefin reacted = 0.47 - 0.02 = **0.45**
Moles of product formed = 0.34+ 0.02 + (0.10 - 0.02) = **0.44**

Gas Uptake / Balance

Aldehyde formation:
$H_2 + CO + R\text{-}CH{=}CH_2 \rightarrow R\text{-}CH_2\text{-}CH_2\text{-}CHO$
2 moles of gas consumed for every mole of product formed.
⇒ 0.34 x 2 = 0.68 moles of gas used.

Alcohol formation:
$2H_2 + CO + R\text{-}CH{=}CH_2 \rightarrow R\text{-}CH_2\text{-}CH_2\text{-}CH_2\text{-}OH$
3 moles of gas consumed for every mole of product formed.
⇒ 0.02 x 3 = 0.06 moles of gas used.

Hydrogenation:
$H_2 + R\text{-}CH{=}CH_2 \rightarrow R\text{-}CH_2\text{-}CH_3$
1 mole of gas consumed for every mole of product formed.
⇒ 1 x (0.10 - 0.02) = 0.08 moles of gas used

Total moles of gas used: = 0.82

Assuming ideal gas behaviour: $PV = nRT$ and $\Delta P = \Delta nRT/V$
Gas volume in the reactor = ±1300ml - 200ml = 1100 ml
$\Delta n = 0.82$; R constant = 8.314

Temperature = (90 + 273.16 K) = 363 K

$$\Rightarrow \Delta P - \frac{0{,}82 \times 8.314 \times 363.16}{1100 \times 10^{-6}} - 22.51 \times 10^{5}\,\text{Pa} - \pm 22.51\ \text{bars(g)}$$

This corresponds closely with the measured pressure drop of 22.6 bar (g) .

APPENDIX 6

GC Analysis Check

GC result of a make-up mixture of pure oxo alcohols derived from SLO and C_{11-12} SLO: Goes to proving reliability of GC analyses.

A sample for GC analysis was made up as follows:

10 ml of C_{11-12} SLO. Measured weight = 7.95 grams.
10 ml of C_{12-13} purified alcohols. Measured weight = 8.20 grams.

ie actual mass percent: C_{11-12} SLO = 49.23%; C_{12-13} alcohols = 50.77%.

The sample was injected onto a GC for analysis as described in Section 2.3.1.

Using GC peak response factors of 1 and 0.845 respectively for the SLO and alcohol portions of the chromatogram, the following results were obtained.

Mass % in sample		Difference
SLO: Measured (GC) Actual (weight)	49.35 49.23	0.12
Alcohols: Measured (GC) Actual (weight)	50.55 50.77	-0.12
Overall error %		0.24

APPENDIX 7

Using Alcohol Linearity to Check Olefin Analyses

Derivation of Equation (5.1) in Section 5.4.4.3.

The expected alcohol linearity of the products is calculated from the n/i ratio (or linear α-olefin product linearity which is measured, and the amount of linear and branched olefins that have reacted.

It is assumed that linear products can only be obtained from linear olefins (internal and α-olefins). Branched products can be obtained from linear and branched olefins. The branching probability of products obtained from linear olefins is assumed to be 100% minus the linear α-olefin product % linearity. The probability of branched products from branched olefins is assumed to be 100%.

Therefore at time = t:

$$(\text{Expected alcohol linearity})_t = \frac{(\text{mass\% linear alcohol})_t \times 100\%}{(\text{mass\% 2-Methyl alcohol})_t + (\text{mass\% linear alcohol})_t} \times \frac{A}{A+B}$$

Where:
$A = (\text{mass\% of linear olefin})_{t0} - (\text{mass\% of linear olefin})_t$
$B = (\text{mass\% of branched olefin})_{t0} - (\text{mass\% of branched olefin})_t$

(t_0 denotes time zero).

Substituting for A and B, and simplification gives equation (5.1)

$$(\text{Expected alcohol linearity})_t = \frac{\dfrac{(\text{mass\% linear alcohol})_t \times 100\%}{(\text{mass\% 2-Methyl alcohol})_t + (\text{mass\% linear alcohol})_t}}{1 + \dfrac{(\text{mass\% branched olefin})_{t0} - (\text{mass\% branched olefin})_t}{(\text{mass\% linear olefin})_{t0} - (\text{mass\% linear olefin})_t}} \qquad (5.1)$$

APPENDIX 8

Modelling results: Runs Undertaken in Chapter 4: TOP ligand.

	Meas.	Modelled values					Meas.	Modelled values (corrected for catalyst conc.)				
Run	k	(k_1+k_2)	k_1	k_2	k_3	k_4	K'	$(K'_1+K'_2)$	K'_1	K'_2	K'_3	K'_4
29a	0.3	0.29	0.03	0.26	1.43	0.01	1.33	1.31	0.15	1.16	6.45	0.05
29b	0.26	0.26	0.03	0.23	1.78	0.01	1.15	1.18	0.15	1.03	8	0.06
29c	0.29	0.29	0.04	0.26	1.62	0.01	1.29	1.32	0.16	1.16	7.29	0.04
29d	0.3	0.29	0.03	0.26	1.46	0.01	1.33	1.32	0.15	1.17	6.55	0.05
30	0.44	0.46	0.05	0.41	2.2	0.04	1.42	1.49	0.17	1.32	7.12	0.13
31	0.51	0.53	0.07	0.46	1.72	0.08	1.98	2.03	0.26	1.77	5.87	0.56
32	0.37	0.43	0.09	0.34	2.29	0.21	1.14	1.32	0.27	1.04	7.05	0.65
33	0.23	0.25	0.03	0.22	1.27	0.03	0.90	1.01	0.13	0.88	5.11	0.11
34	0.38	0.36	0.05	0.31	1.71	0.14	1.22	1.16	0.17	0.99	5.53	0.46
35	0.35	0.42	0.05	0.37	2.97	0.24	1.42	1.68	0.21	1.47	11.94	0.97
36	0.24	0.26	0.04	0.23	1.7	0.03	0.98	1.06	0.15	0.91	6.85	0.13
37	0.28	0.32	0.03	0.29	1.46	0.08	1.11	1.28	0.11	1.17	5.87	0.32
38	0.29	0.33	0.04	0.28	2.83	0.08	1.13	1.27	0.17	1.09	10.92	0.32
39	0.42	0.5	0.06	0.44	2.99	0.5	1.45	1.71	0.22	1.5	6.64	0.32
40:C8 40:C9	0.54 0.49	0.46 0.42	0.07 0.08	0.40 0.34	1.74 2.94	0.04 0.22	2.38 2.16	2.06 1.86	0.29 0.35	1.77 1.51	7.72 13.05	0.16 0.99
41:C8 41:C9	0.62 0.55	0.61 0.63	0.06 0.04	0.55 0.59	3.51 6.71	0.08 0.22	2.52 2.23	2.47 2.55	0.26 0.15	2.21 2.41	14.25 27.2	0.32 0.89
42	0.36	0.41	0.07	0.34	3.03	0.28	1.17	1.33	0.2	1.1	9.33	0.87
43	0.49	0.58	0.05	0.53	1.35	0.1	2.04	2.4	0.21	2.18	5.61	0.4

Where $k_x = K'_x/[Co]$
$[Co]$ = g/100ml

APPENDIX 9

Modelling results: Runs Undertaken in Chapter 5: EP ligand.

Run	k (hr^{-1})	(k_1+k_2)	k_1	k_2	k_3	k_4	k'	$(k'_1+k'_2)$	k'_1	k'_2	k'_3	k'_4
44	0.98	1.02	0.02	1	3.16	0.14	3.79	3.93	0.09	3.84	12.21	0.52
45	0.88	0.86	0.05	0.82	3.41	0.12	3.53	3.48	0.19	3.28	13.71	0.47
46a	0.81	0.77	0.05	0.73	2.31	0.03	3.93	3.72	0.22	3.5	11.16	0.16
46b	-	-	-	-	0.77	0.05	-	-	-	-	11.14	0.72
47a	1.61	1.51	0.1	1.39	2.74	0.02	7.74	7.27	0.46	6.66	13.18	0.11
47b	1.45	1.23	0.08	1.12	2.6	0.03	6.96	5.93	0.4	5.37	12.47	0.13
49a	1.64	0.73	0.02	0.72	0.73	0.02	15.8	7.04	0.18	6.86	7.06	0.16
49b	1.59	0.73	0.01	0.72	1	0.01	15.3	7.03	0.09	6.94	9.61	0.13
49c	0.82	0.74	0.05	0.69	1.79	0.01	7.89	7.1	0.48	6.63	17.22	0.09
50a:C_{11} C_{12}	0.43 0.35	0.46 0.44	0.03 0.01	0.43 0.43	1.82 1.66	0.07 0.05	3.22 2.63	3.50 3.34	0.22 0.09	3.28 3.26	13.75 12.53	0.51 0.37
50b:C_{11} C_{12}	0.56 0.48	0.73 0.59	0.02 0.02	0.71 0.57	1.35 1.28	0.02 0.05	3.34 2.83	4.34 3.50	0.11 0.14	4.23 3.36	8.00 7.60	0.10 0.29
51:C_{11} C_{12}	0.39 0.29	0.39 0.32	0.001 0.001	0.39 0.31	0.43 0.96	0.001 0.001	3.87 2.87	3.87 3.14	0.01 0.01	3.86 3.13	4.30 9.61	0.01 0.01
52:C_{11} C_{12}	1.03 0.55	1.16 0.80	0.08 0.02	1.08 0.78	4.55 6.45	0.15 0.05	6.50 3.48	7.33 5.02	0.52 0.12	6.82 4.91	28.70 40.69	0.94 0.30
53:C_{11} C_{12}	0.85 0.78	0.96 0.90	0.03 0.03	0.93 0.87	3.53 3.54	0.10 0.07	4.09 3.76	4.64 4.33	0.16 0.12	4.49 4.21	17.04 17.05	0.47 0.36
55a:C_{11} C_{12}	0.36 0.27	0.36 0.29	0.02 0.01	0.34 0.28	1.25 1.17	0.05 0.04	2.29 1.69	2.27 1.81	0.10 0.09	2.17 1.79	7.97 7.48	0.29 0.26
55b:C_{11} C_{12}	0.58 0.46	0.76 0.53	0.00 0.03	0.76 0.50	1.23 1.47	0.00 0.01	3.70 2.90	4.84 3.35	0.03 0.20	4.81 3.16	7.81 9.39	0.02 0.05
55c:C_{11} C_{12}	1.15 0.95	1.11 0.90	0.01 0.03	1.09 0.87	2.50 3.22	0.2 0.011	7.34 6.08	7.07 5.74	0.09 0.18	6.97 5.56	15.92 20.50	0.12 0.06
55d:C_{11} C_{12}	1.63 1.27	1.82 1.18	0.05 0.02	1.76 1.16	6.77 8.70	0.03 0.04	10.18 7.93	11.58 7.52	0.34 0.15	11.24 7.37	43.16 55.41	0.17 0.23
55e:C_{11} C_{12}	1.76 1.45	1.55 1.35	0.11 0.09	1.43 1.26	7.37 8.53	0.08 0.07	11.21 9.24	9.86 8.57	0.72 0.57	9.14 8.00	46.98 54.32	0.52 0.47
55f:C_{11} C_{12}	0.26 0.18	0.25 0.18	0.25 0.17	0.002 0.01	0.51 0.52	0.003 0.02	4.26 2.95	4.21 3.02	0.04 0.16	4.17 2.86	8.32 8.56	0.05 0.03
55g:C_{11} C_{12}	0.25 0.14	0.26 0.19	0.00 0.00	0.25 0.19	0.52 0.65	0.04 0.02	3.15 1.83	3.30 2.46	0.06 0.03	3.25 2.43	6.66 8.26	0.57 0.26
56a	0.23	0.2	0.01	0.2	1.24	0.01	1.11	0.99	0.04	0.94	5.95	0.04
56b	0.86	0.62	0.02	0.6	1.37	0.02	4.13	2.98	0.08	2.9	6.62	0.08
56c	1.12	0.82	0.06	0.75	4.11	0.03	5.38	3.93	0.3	3.63	19.8	0.15
56d	1.14	1.15	0.05	1.09	2.7	0.02	5.48	5.52	0.26	5.25	13.01	0.08
56e	0.96	0.67	0.09	0.58	1.29	0.12	4.61	3.24	0.45	2.8	6.21	0.56

APPENDIX 10

Modelling Plots of Key Runs in Chapter 4: TOP ligand.

Modelled and Experimental Data: C_{10} : 1-Decene feed; Co/TOP catalyst (with KOH); Run 33.

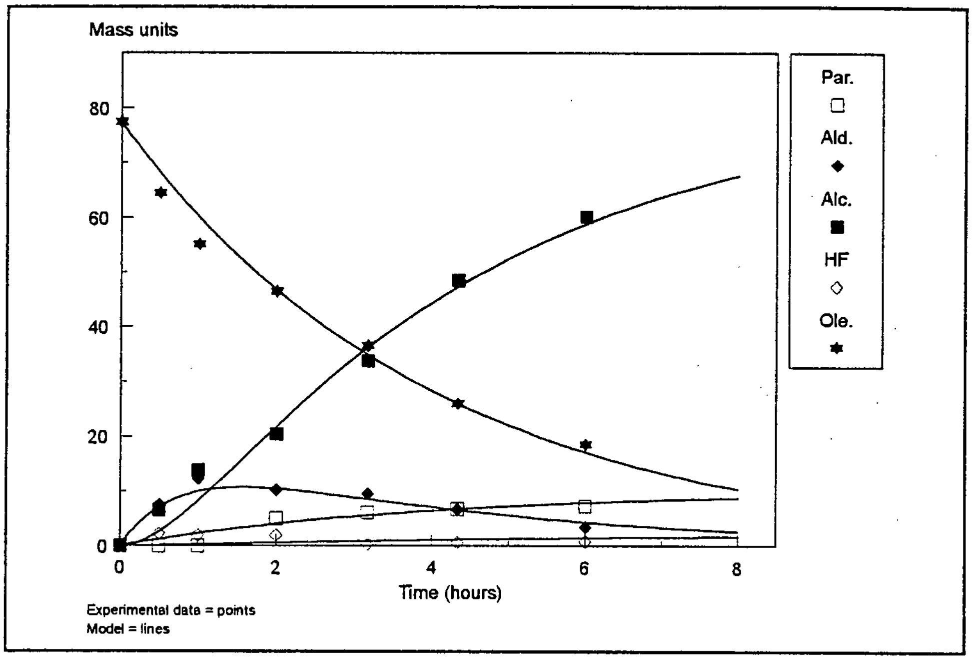

Modelled and Experimental Data: 1-Decene feed; Co/TOP catalyst (with KOH); Run 36.

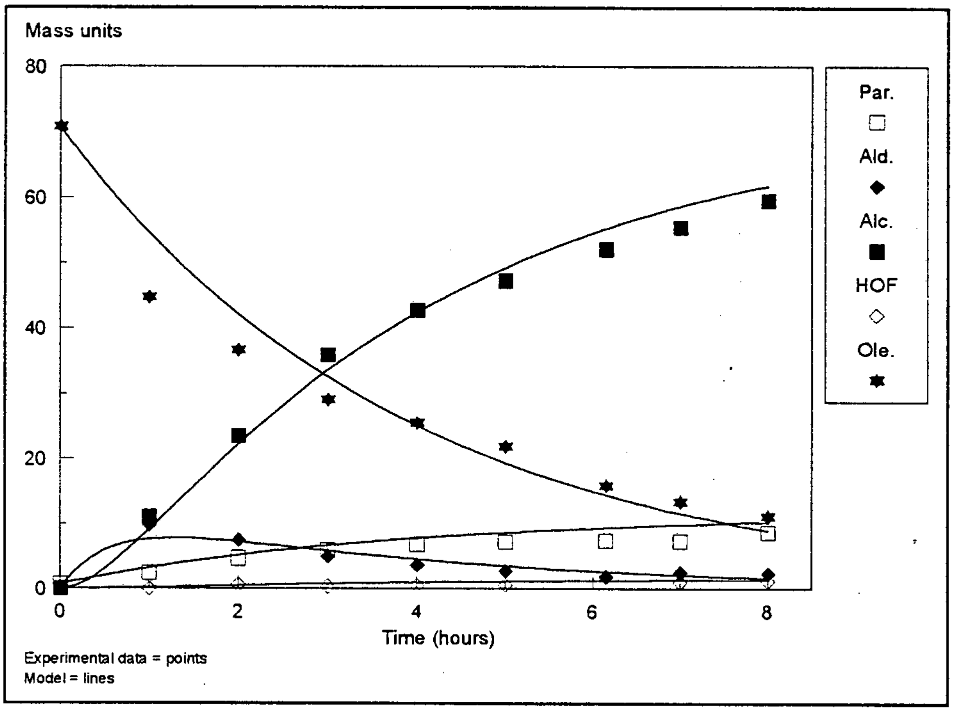

Modelled and Experimental Data: C_{10} SLO narrow fraction(A); Co/TBP catalyst (with KOH); Run 42.

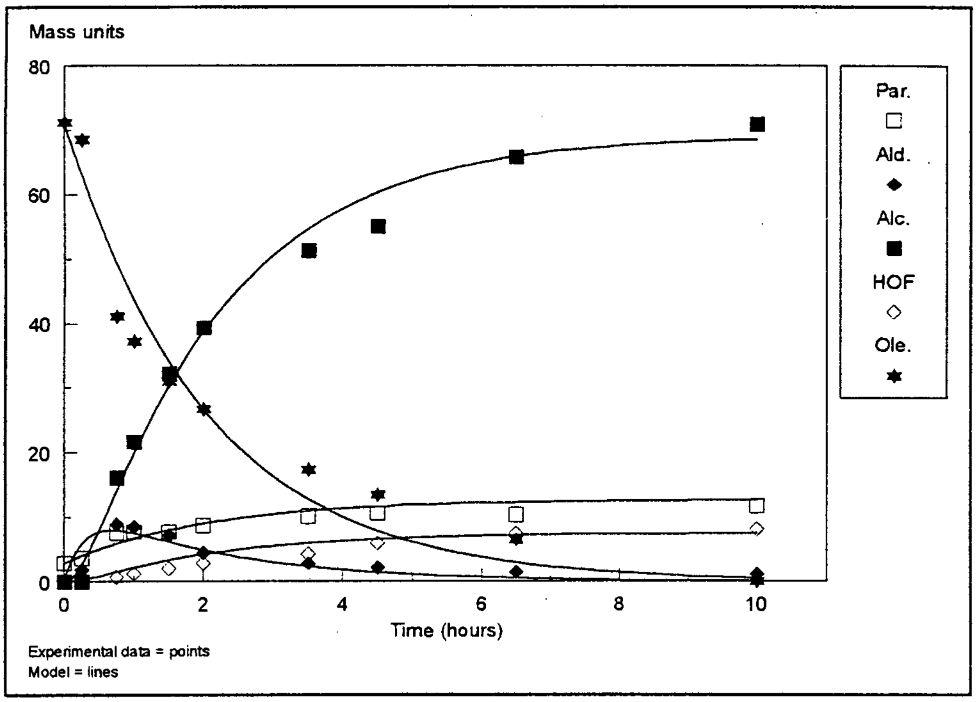

Modelled and Experimental Data: C_{10} SLO narrow fraction(A); Co/TOP catalyst (with KOH); Run 32.

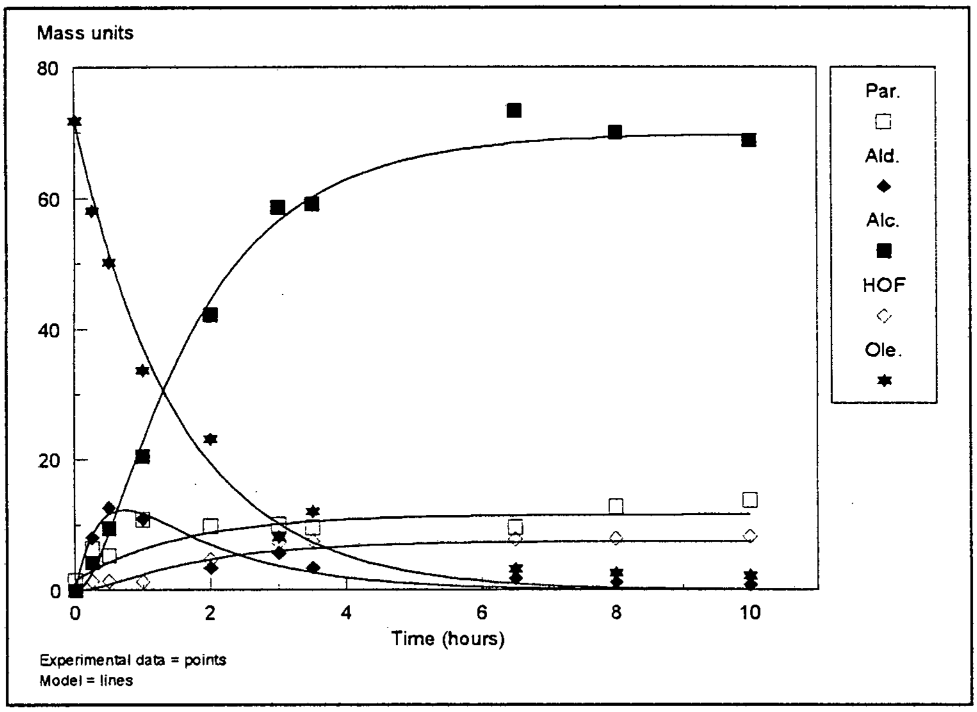

Modelled and Experimental Data: C_{10} SLO narrow fraction(A); Co/TOP catalyst (without KOH) ; Run 31.

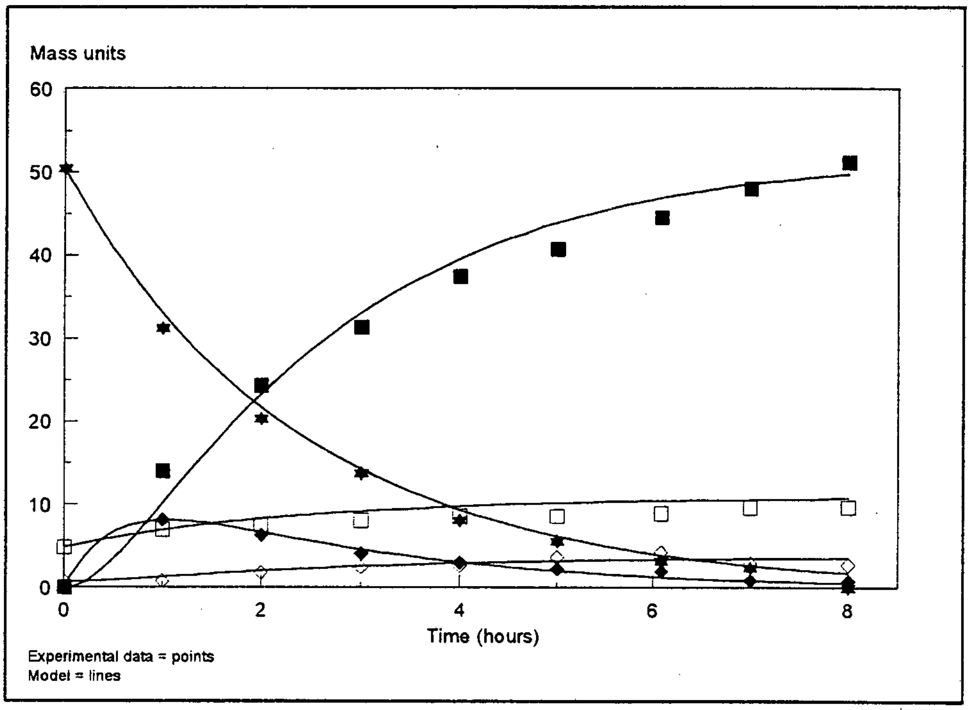

Modelled and Experimental Data: C_{10} SLO broad fraction (C); Co/TOP catalyst (without KOH); Run 29a.

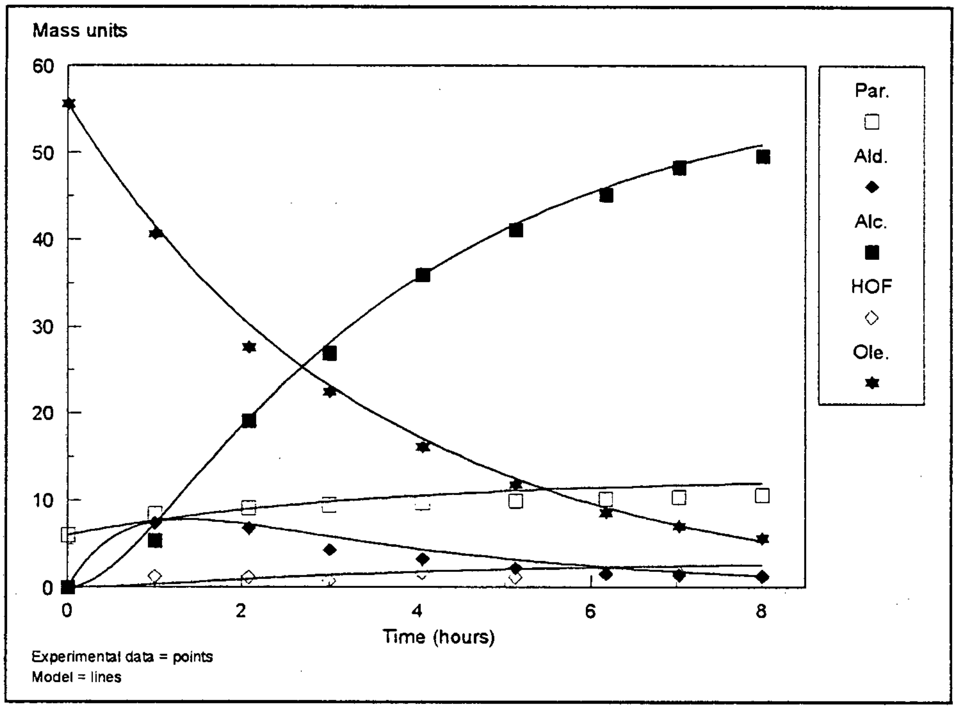

Modelled and Experimental Data: C_8 olefins: C_{8-9} SLO fraction; Co/TOP catalyst (with 10% H_2O) ; Run 41.

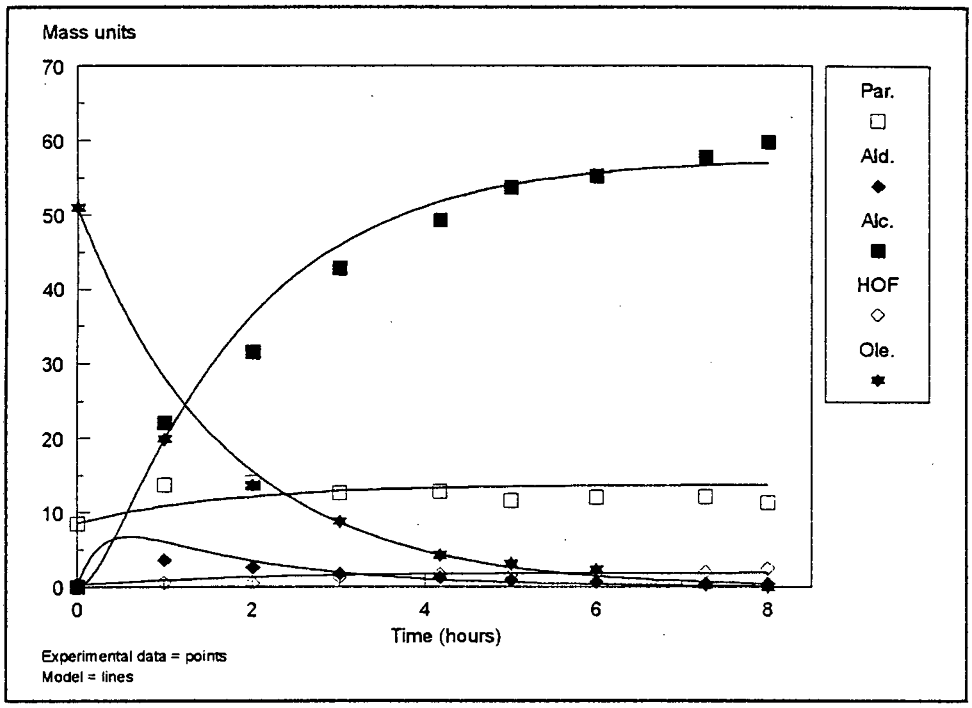

Experimental data = points
Model = lines

Modelled and Experimental Data: C_9 olefins in C_{8-9} SLO fraction; Co/TOP catalyst (with 10% H_2O) ;Run 41

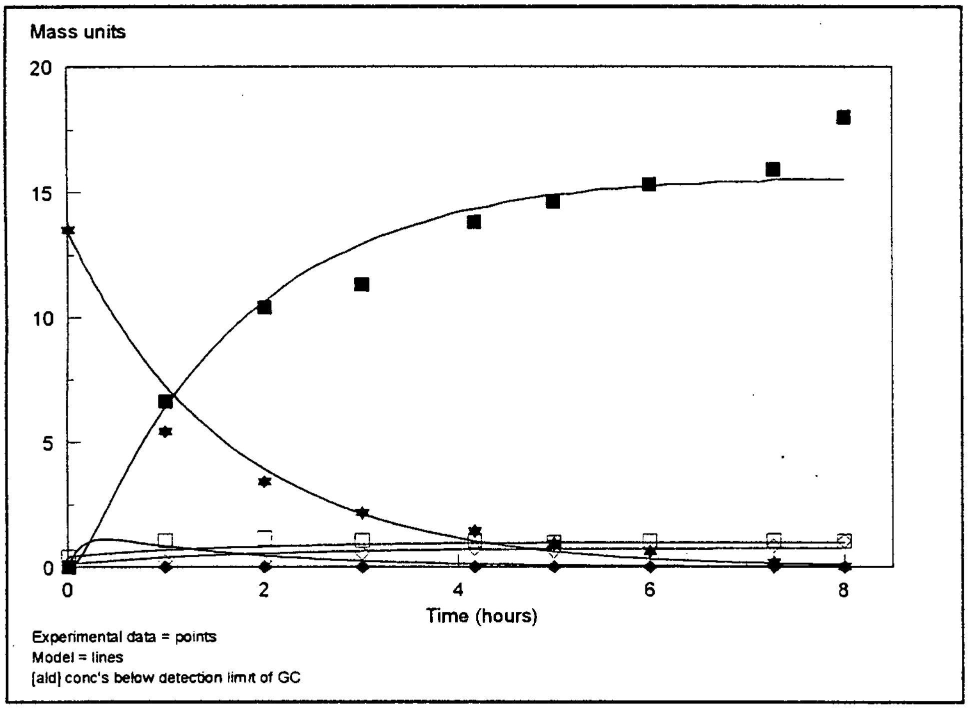

Experimental data = points
Model = lines
[ald] conc's below detection limit of GC

Modelled and Experimental Data: C_8 olefins: C_{8-9} SLO fraction; Co/TOP catalyst (without H_2O) ; Run 40.

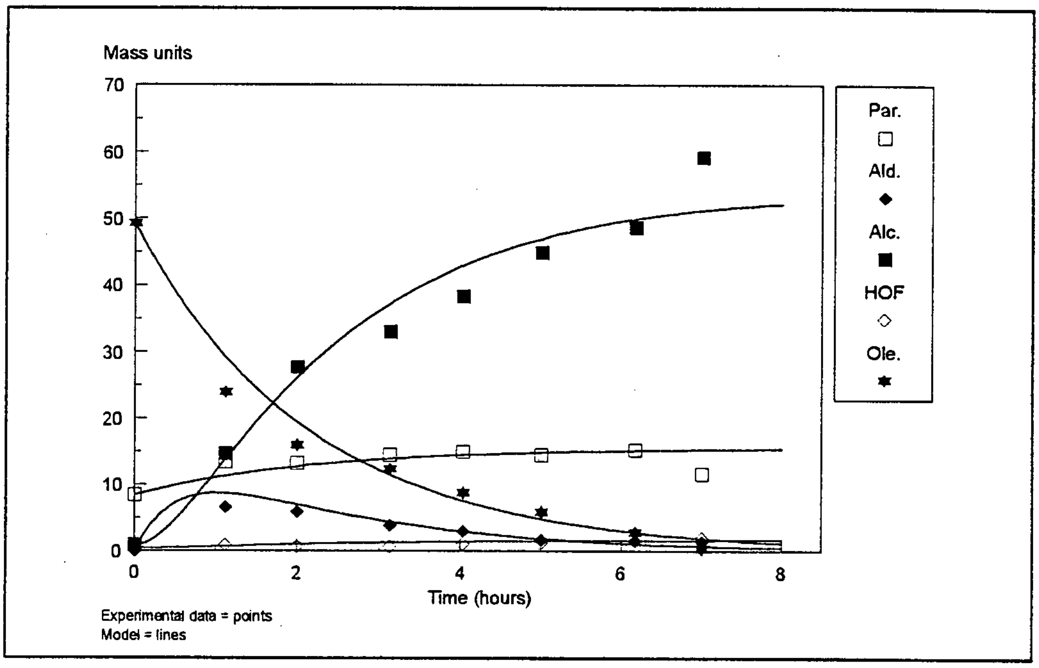

APPENDIX 11

Modelling Plots of Key Runs in Chapter 5

Modelled and Experimental Data: 1-Decene feed; Co/EP catalyst (with KOH); Run 45.

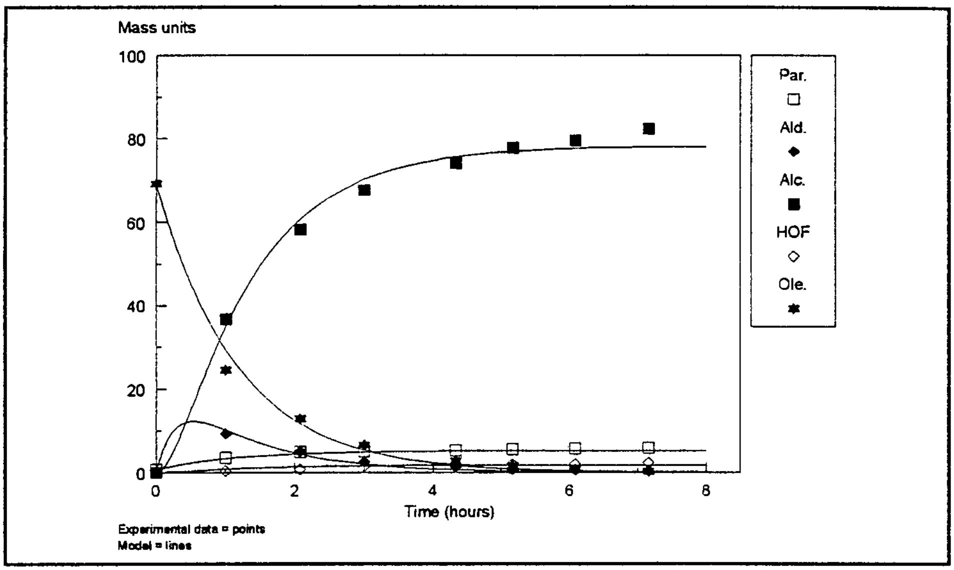

Modelled and Experimental Data: 1-Decene feed; Co/EP catalyst (without KOH); Run 47a.

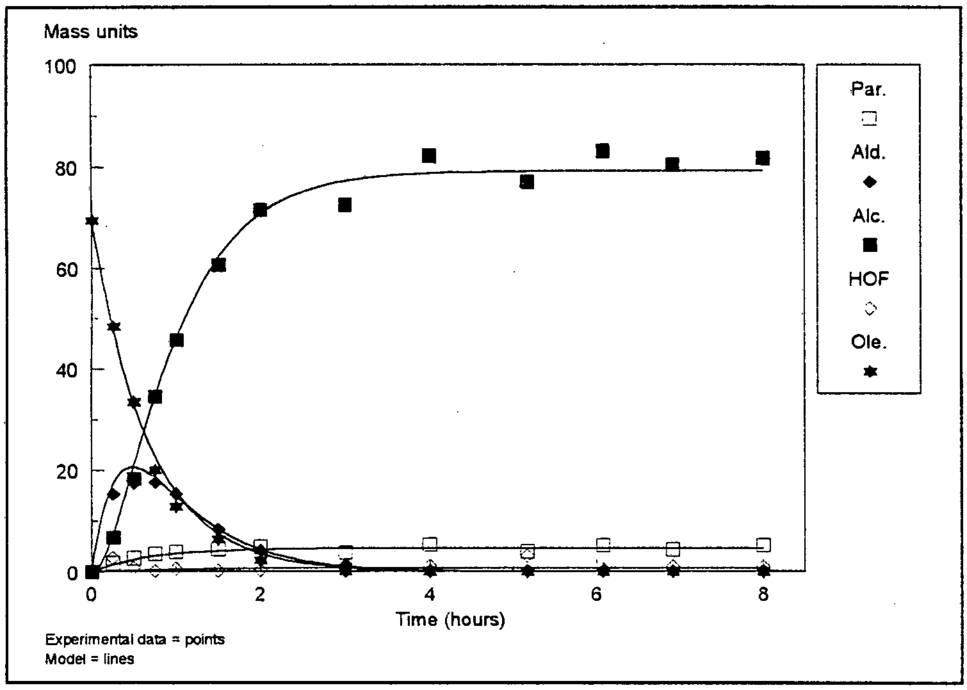

Modelled and Experimental Data: C_{10} olefins: C_{10} SLO broad fraction; Co/EP catalyst (with KOH) ; Run 44.

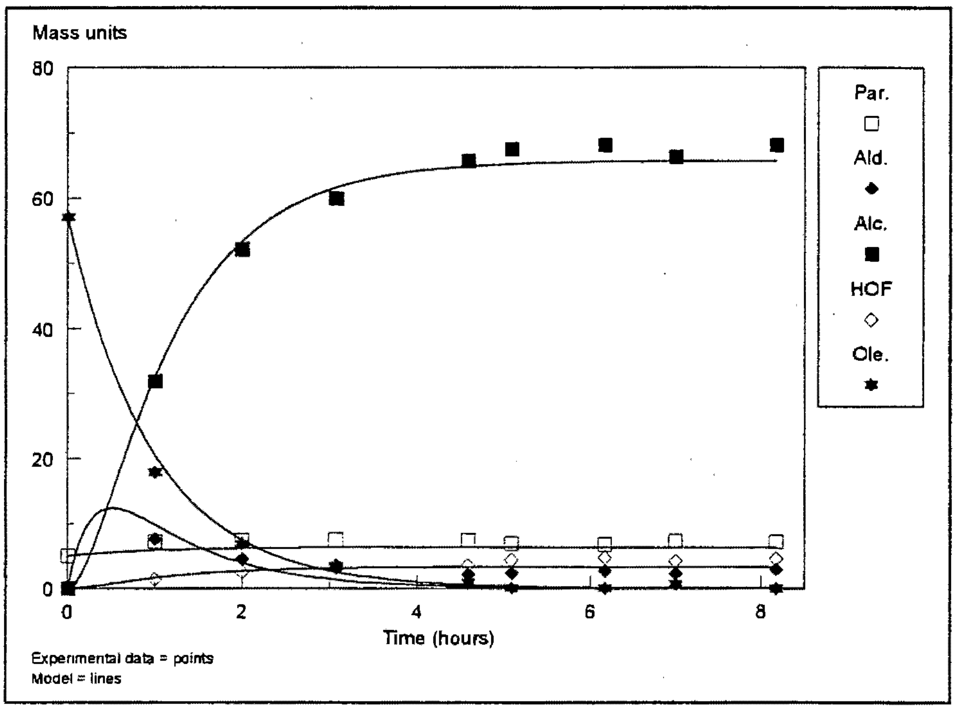

Modelled and Experimental Data: C_{11} olefins: C_{11-12} SLO broad fraction; Co/EP catalyst (with KOH) ; Run 50b.

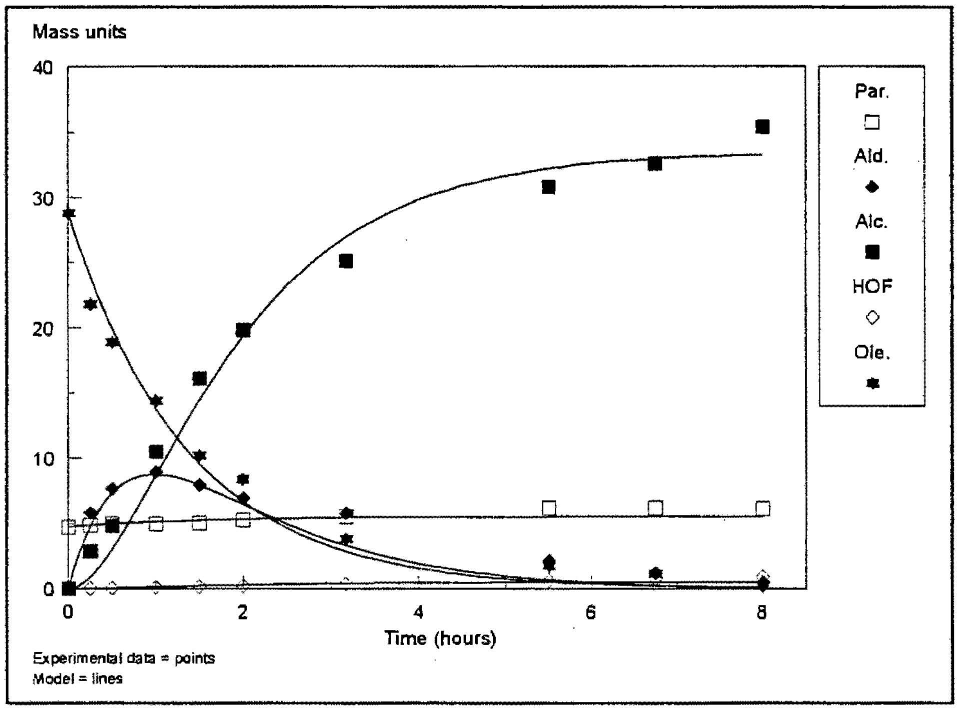

Modelled and Experimental Data: C_{12} olefins: $C_{11\text{-}12}$ SLO broad fraction (A); Co/EP catalyst (with KOH) ; Run 50b.

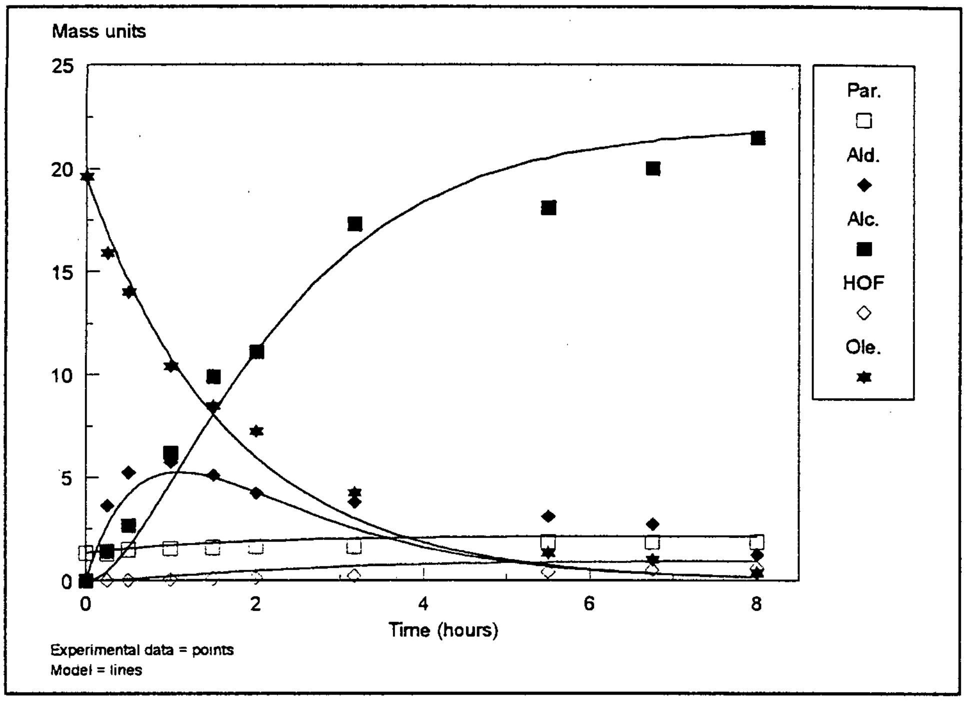

Modelled and Experimental Data: C_{11} olefins: $C_{11\text{-}12}$ SLO broad fraction (E); Co/EP catalyst (without KOH) ; Run 53.

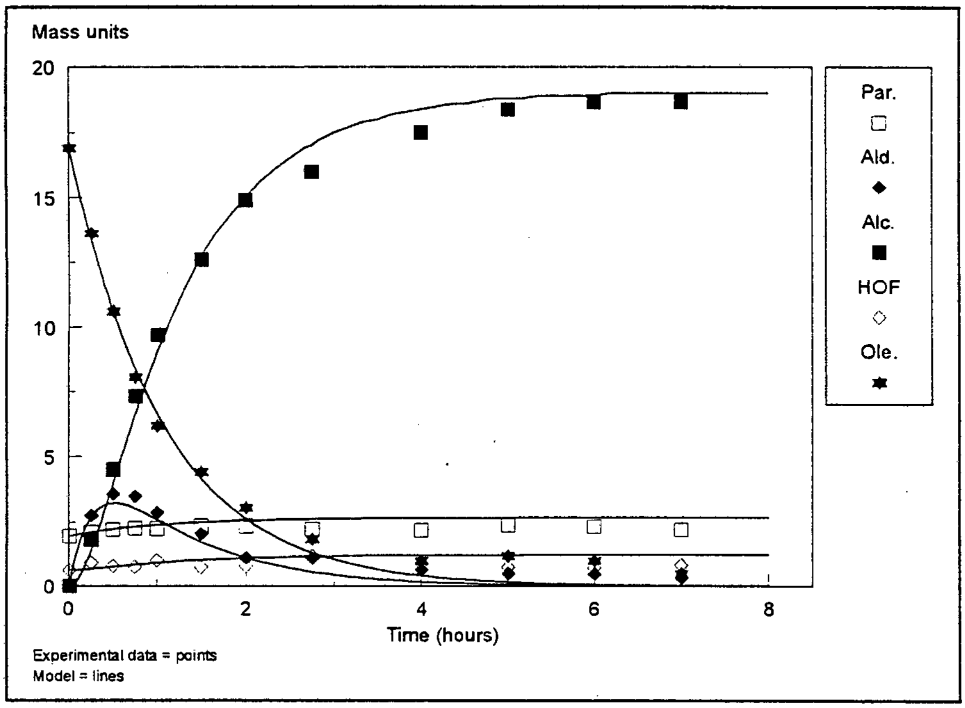

Modelled and Experimental Data: C_{12} olefins: C_{11-12} SLO broad fraction (E); Co/EP catalyst (without KOH) ; Run 53.

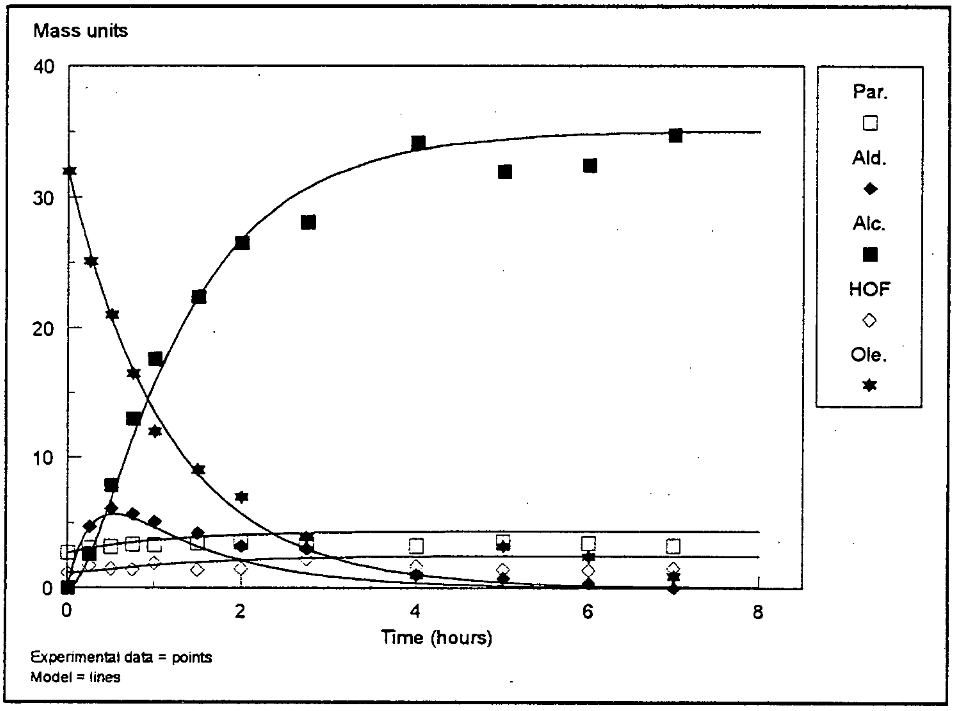

Modelled and Experimental Data: "Feed preparation for Run 46b": 1-Decene feed; Co/EP catalyst (with KOH) ; Run 46a.

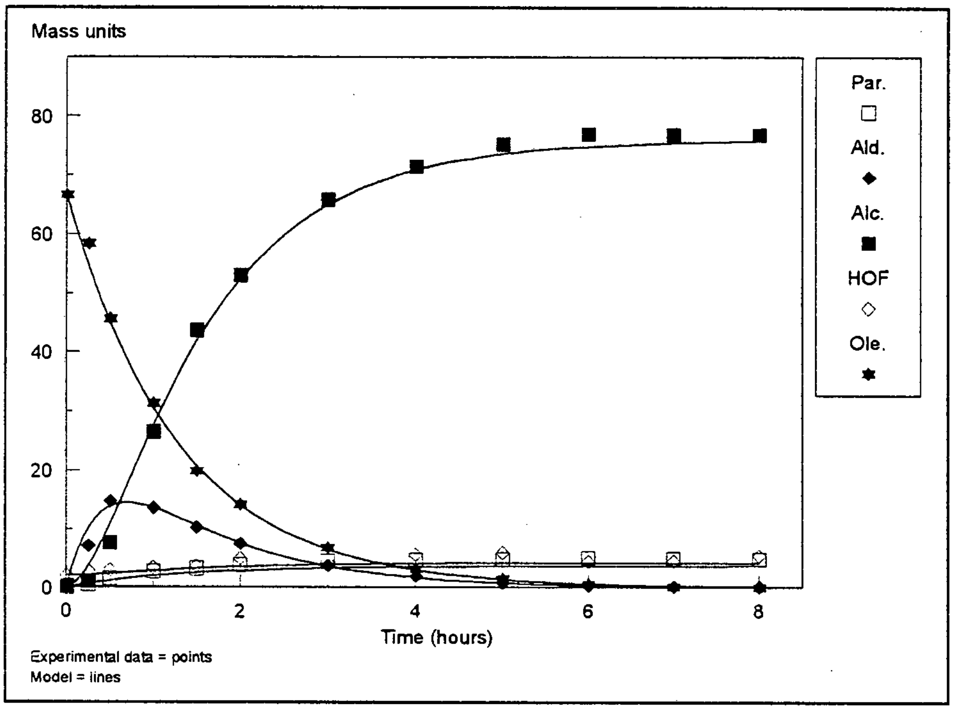

Modelled and Experimental Data: Effect of aldehyde addition to Run 46a (above) reactor products; Co/EP catalyst (with KOH) ; Run 46b